UNIVERSIDADE FEDERAL DO PARÁ
INSTITUTO DE GEOCIÊNCIAS
PROGRAMA DE PÓS-GRADUAÇÃO EM GEOLOGIA E GEOQUÍMICA

TEDE DE DOUTORADO

GEOLOGIA, GEOQUÍMICA, GEOCRONOLOGIA E PETROGÊNESE DAS SUÍTES TTG E DOS LEUCOGRANITOS ARQUEANOS DO TERRENO GRANITO-GREENSTONE DE RIO MARIA, SUDESTE DO CRÁTON AMAZÔNICO

Tese apresentada por:

JOSÉ DE ARIMATÉIA COSTA DE ALMEIDA

BELÉM
2010

Dados Internacionais de Catalogação-na-Publicação (CIP)
Biblioteca Geólogo Raimundo Montenegro Garcia de Montalvão

A447g Almeida, José de Arimatéia Costa de

Geologia, geoquímica, geocronologia e petrogênese das suítes TTG e dos leucogranitos arqueanos do Terreno Granito-*Greenstone* de Rio Maria, sudeste do Cráton Amazônico. / José de Arimatéia Costa de Almeida; Orientador: Roberto Dall'Agnol – 2010

xiii, 208 f. : il.

Tese (Doutorado em Geoquímica e Petrologia) – Programa de Pós-Graduação em Geologia e Geoquímica, Instituto de Geociências, Universidade Federal do Pará, Belém, 2010.

1. Cráton Amazônico. 2. Terreno Granito-*Greenstone* de Rio Maria. 3. Mesoarqueano. 4. Suítes TTG. 5. Suítes de leucogranitos. I. Universidade Federal do Pará. II. Dall'Agnol, Roberto, *orient*. III. Título.

CDD 20ª ed.: 558.115

Universidade Federal do Pará
Instituto de Geociências
Programa de Pós-Graduação em Geologia e Geoquímica

GEOLOGIA, GEOQUÍMICA, GEOCRONOLOGIA E PETROGÊNESE DAS SUÍTES TTG E DOS LEUCOGRANITOS ARQUEANOS DO TERRENO GRANITO-*GREENSTONE* DE RIO MARIA, SUDESTE DO CRÁTON AMAZÔNICO

TESE APRESENTADA POR
JOSÉ DE ARIMATÉIA COSTA DE ALMEIDA

Como requisito parcial à obtenção do Grau de Doutor em Ciências na Área de GEOQUÍMICA E PETROLOGIA

Data de Aprovação: **23/03/2010**

Comitê de Tese:

ROBERTO DALL'AGNOL (Orientador)

JAANA HALLA

LÚCIA TRAVASSOS DA ROSA COSTA

MOACIR JOSÉ BUENANO MACAMBIRA

REINHARDT ADOLFO FUCK

Belém
2010

Dedico este trabalho exclusivamente a minha mãe Zélia Costa de Almeida (in memorian) pelo amor, carinho, confiança e incentivo e por ter me direcionado por caminhos vitoriosos, sempre acreditando e não poupando esforços para construir o melhor futuro para mim. Agradeço a Deus a cada momento que passamos juntos e por ter conhecido a melhor pessoa do mundo. Amarei-te eternamente.

AGRADECIMENTOS

O autor expressa seu sincero e profundo agradecimento a todas as pessoas e entidades que direta ou indiretamente prestaram sua contribuição para que este trabalho fosse concluído com êxito, em especial:

- Ao criador do céu e da Terra, *DEUS*.
- Ao meu pai Manoel Rosa de Almeida pelo amor, respeito e dedicação e por sempre ter desejado o melhor futuro para mim.
- Ao Programa de Pós-Graduação em Geociências da Universidade Federal do Pará (UFPA), pelo fornecimento de infra-estrutura necessária à realização deste trabalho.
- Ao PRONEX/CNPq (Proc. 66.2103/1998-0), CNPq/Universal (Proc. 484524/2007-0) e INCT de Geociências da Amazônia pelo suporte financeiro durante a execução desta pesquisa.
- Ao Conselho Nacional de Desenvolvimento Científico e Tecnológico (CNPq) pela concessão da bolsa de estudo durante o decorrer desta pesquisa.
- Ao Grupo de Pesquisa Petrologia de Rochas Granitóides (GPPG) do Instituto de Geociências (GC) da UFPA, pelo suporte técnico-científico indispensável ao desenvolvimento deste trabalho.
- Ao professor Roberto Dall'Agnol, pela orientação, amizade, paciência e motivação, com inúmeras discussões que foram indispensáveis ao longo deste trabalho.
- Ao Dr. Marcelo A. de Oliveira pela amizade, respeito científico, imensa ajuda e trocas de informações nas etapas de campo, bem como discussões referentes ao tema desta pesquisa.
- Fabriciana V. Guimarães, Samantha B. Dias e Manoel A. Costa são agradecidos pela contribuição substancial no estudo dos granitóides arqueanos do Terreno Granito-*Greenstone* de Rio Maria.
- Agradeço a Gilmara, Fabriciana, Samantha, Manoel, Patrick, Tayla (a galera da "força tarefa") pela ajuda no tratamento das amostras para o estudo de geocronologia.
- Aos Laboratórios de Geologia Isotópica da UFPA e de Estudos Geodinâmicos da Universidade de Brasília pelo suporte na aquisição dos dados isotópicos.
- Ao Dr. Marco A. G. Toro e Cristoferson pela imensa ajuda na obtenção dos dados Pb-Pb por evaporação em monocristais de zircão.

- Elton Dantas, Bárbara Lima and Sérgio Junges pelo apoio e orientação na aquisição dos dados U-Pb por LA-ICPMS em zircão.
- Aos componentes do GPPG (Roberto, Hilton, Albano, Cláudio, Regis, Davis, Marcelo, Carlos Marcello, Gilmara, Antônio, Fabriciana, Samantha, Pablo, Eleilson, Mara, Alice, Rose, Patrick, Nathan, Adriel, Joseanna, Katucha, Gilvana, Jardel, Francisco, P. Henrique, Tayla) pelo companheirismo, críticas, sugestões e contribuições a este trabalho.
- À Cleida e Géssica por todo auxílio junto a secretaria da pós-graduação e pela orientação dos tramites para a entrega deste documento e convocação da banca julgadora.
- Aos funcionários do Instituto de Geociências, em especial os técnicos administrativos Afonso Quaresma e Carlos Alberto pelo apoio e imensa ajuda nas etapas de campo.
- Registro um agradecimento especial a minha futura esposa Angela de Vilhena Ribeiro pelo amor, carinho, compreensão, dedicação, amizade, consideração, confiança, incentivo e principalmente pelo companheirismo nos momentos difíceis.

SUMÁRIO

DEDICATÓRIA..... i
AGRADECIMENTOS..... ii
RESUMO..... 1
ABSTRACT..... 4

1 – INTRODUÇÃO..... 7
1.1 – APRESENTAÇÃO..... 8
1.2 - LOCALIZAÇÃO DA ÁREA..... 11
1.3 - CONTEXTO GEOLÓGICO REGIONAL..... 11
1.4 – GRANITÓIDES ARQUEANOS..... 15
1.4.1 **- Suíte Tonalito-Trondjemito-Granodiorito (TTG)**..... 18
1.4.2 **- Suítes Sanukitóides**..... 20
1.4.3 **– Biotita-granitos e Biotita-granodioritos**..... 20
1.5 – ASSOCIAÇÕES TONALÍTICA-TRONDHJEMÍTICA-GRANODIORITICA (TTG) DO TERRENO GRANITO-*GREENSTONE* DE RIO MARIA..... 22
1.6 – GRANITOS ARQUEANOS ARQUEANOS DO TERRENO GRANITO-*GREENSTONE* DE RIO MARIA..... 23
1.7 - APRESENTAÇÃO DO PROBLEMA..... 24
1.8 – OBJETIVOS..... 28
1.9 - MATERIAIS E MÉTODOS..... 29
1.9.1 – **Pesquisa Bibliográfica**..... 29
1.9.2 – **Mapeamento Geológico**..... 29
1.9.3 – **Petrografia**..... 32
1.9.4 – **Geoquimica**..... 32
1.9.5 – **Geocronologia**..... 33
2 - ZIRCON GEOCHRONOLOGY AND GEOCHEMISTRY OF THE TTG SUITES OF THE RIO MARIA GRANITE-GREENSTONE TERRANE: IMPLICATIONS FOR THE GROWTH OF THE ARCHEAN CRUST OF CARAJÁS PROVINCE, BRAZIL..... 34

José de Arimatéia Costa de Almeida

Roberto Dall'Agnol

Marcelo Augusto de Oliveira

Fabriciana Vieira Guimarães

Moacir José Buenano Macambira

Márcio Martins Pimentel

Osmo Tapani Rämö

Albano Antonio da Silva Leite

Submetido: PRECAMBRIAN RESEARCH

Letter of Submission……..…….... 35

ABSTRACT…….……. 36

1. Introduction…….…. 38

2. Geological setting……..…… 39

3. Geology of the TTG suites of the RMGGT……..….. 43

4. Petrography……..……..….. 45

5. Geochronology……..…… 48

5.1. Sample selection and analytical procedures……...…… 48

5.2. Zircon morphology and internal structure…….. 50

5.3. Results……...…….. 51

5.3.1. Arco Verde tonalite: samples MAR-66, MAR-148, MAR-149, and MAR-111..... 51

5.3.2 - Mogno trondhjemite: samples MFR-53, FMR-98, FMR-87, and AM-03..... 56

5.3.3 –Mariazinha Tonalite: samples FMR-25 and AM-02A..... 59

5.3.4 – Caracol Tonalitic Complex……...……. 61

5.3.5 - Agua Fria Trondhjemite: sample AM-01……...……. 61

6. Geochemistry……...…….…….... 62

6.1. Major elements……...……..... 62

6.2. Trace elements and geochemical signatures……..... 63

6.3. Nd isotopes……..... 71

7. Discussion……..... 74

7.1. Timing of TTG magmatism in the Rio Maria granite-greenstone terrane……..... 74

7.2. Geochemical characteristics as petrogenetic indicators of the RMGGT TTG magmas…..... 76

7.3. Comparison with other TTG series……..... 79

7.4. Possible mantle wedge influence in TTG composition…… 81

7.5. Petrogenesis of the RMGGT TTGs and geodynamic implications……. 82

8. Conclusions……..... 84

Acknowledgements……..……..... 86

Appendix A. Analytical procedures for whole rock chemical analyses…..……..... 86

References……..……..... 87

3 - GEOCHEMISTRY AND ZIRCON GEOCHRONOLOGY OF THE ARCHEAN GRANITE SUITES OF THE RIO MARIA GRANITE-GREENSTONE TERRANE, CARAJÁS PROVINCE, BRAZIL…… 97

José de Arimatéia Costa de Almeida

Roberto Dall'Agnol

Albano Antonio da Silva Leite

Submetido: Journal of South American Earth Sciences

Letter of Submission……..……..... 98

ABSTRACT……...……..... 99

1. Introduction……...……..... 100

2. Geological setting……...……..... 101

3. Geology of the Archean granite suites of the RMGGT……. 104

3.1. Potassic leucogranites……..……..... 104

3.2. Leucogranodiorite-granite group (LGdG) ……..……..... 105

3.3. Granites associated with sanukitoid suites (Rancho de Deus granite) …..……..... 106

4. Petrography……..……..... 106

5. Geochronology……..……..... 109

5.1. Potassic leucogranites……..……..... 109

5.2. Leucogranodiorite-granite group……..……..... 110

5.2.1. Available geochronological data……..……..... 110

5.2.2 - New geochronological data for the Guarantã suite…..……..... 110

5.2.1.1 – Guarantã granite: samples MAR-64 and MAF-33…..……..... 110

5.2.1.2 – Trairão Granodiorite: sample MAR-121…..……..... 114

5.3. Granites associated with sanukitoid suites (Rancho de Deus pluton) …..……..... 114

6. Geochemistry…… 115
6.1. Potassic leucogranites…… 115
6.2. Leucogranodiorite-granite group (LGdG) …… 121
6.3. Granites associated with sanukitoid suites (Rancho de Deus pluton) …… 123
7. Discussion…… 124
7.1. The granites of the RMGGT and their comparison with other Archean granitoids…… 124
7.1.1. Comparison between the granites and other granitoid groups of the RMGGT…… 124
7.1.2. Comparison between the granites of the RMGGT and similar granites of other Archean terranes…… 126
7.2. Petrogenesis of the Archean granites of the RMGGT: A preliminary approach…… 129
7.3. The ages of the Archean granites of the RMGGT and tectonic implications…… 133
8. Conclusions…… 134
Acknowledgements…… 135
Appendix A. Analytical procedures…… 136
References…… 138
4 - PETROLOGY OF THE ARCHEAN LEUCOGRANODIORITE-GRANITE SUITES: IMPLICATIONS FOR THE CRUSTAL EVOLUTION OF THE RIO MARIA GRANITE-GREENSTONE TERRANE, CARAJÁS PROVINCE, BRAZIL…… 147
José de Arimatéia Costa de Almeida
Roberto Dall'Agnol
Samantha Barriga Dias
Fernando Jacques Althoff
Submetido: Lithos
Letter of Submission…… 148
ABSTRACT…… 149
1. Introduction…… 150
2. Geological Setting…… 152
3. Geologic features of the leucogranodiorite-granite (LGdG) suites…… 155
4. Petrography…… 156
5. Geochemistry…… 159
5.1. Major Elements…… 159

5.2. Trace Elements 164
6. Comparison between the LGdG suites and Archean granitoids 166
6.1. Comparison between the LGdG suites and the TTG and sanukitoid suites of the RMGGT 166
6.2. LGdG suites vs. transitional TTG or GG 170
7. Discussion 171
7.1. Petrogenesis of the LGdG suites 171
7.1.1. Magmatic differentiation or partial melting of TTG 171
7.1.2. Mixing between sanukitoids magmas and high-K leucogranite melts 172
7.1.3. Interaction between mantle-derived magmas and TTG continental crust 173
7.1.4. The restite model 173
7.1.5. Partial melting of mafic lithologies 174
7.1.6. Input of LILE-enriched component 175
7.1.7. An alternative model for the origin of the LGdG suites 176
8. Conclusions 181
Acknowledgements 182
Appendix A. Analytical procedures 182
References 183
5 - CONCLUSÕES E CONSIDERAÇÕES FINAIS **192**
REFERÊNCIAS 197

LISTA DE ILUSTRAÇÕES

FIGURAS

1 - INTRODUÇÃO

Figura 1 - Mapa de localização da Província Mineral de Carajás..... 12

Figura 2 - Domínios Arqueanos do Cráton Amazônico..... 13

Figura 2 - Mapa Geológico simplificado do Terreno Granito-Greenstone de Rio Maria 17

2 - ZIRCON GEOCHRONOLOGY AND GEOCHEMISTRY OF THE TTG SUITES OF THE RIO MARIA GRANITE-GREENSTONE TERRANE: IMPLICATIONS FOR THE GROWTH OF THE ARCHEAN CRUST OF CARAJÁS PROVINCE, BRAZIL

Figure 1 - a) Simplified sketch map of the Amazonian craton and b) Geological sketch map of the Carajás province……. 40

Figure 2 - Geological map of the Rio Maria granite-greenstone terrane…….. 42

Figure 3 - QAP and Q-(A+P)-M for the TTG rocks of the Rio Maria granite-greenstone terrane 47

Figure 4 - Diagrams for the dated samples from the Arco Verde Tonalite…….. 55

Figure 5 - Diagrams for the dated samples from Mogno trondhjemite…… 57

Figure 6 - Diagrams for the dated samples from Mariazinha tonalite……. 60

Figure 7 - Concordia diagram of U–Pb zircon analytical results for sample AM-01 from Água Fria trondhjemite……...…..... 62

Figure 8 - (a-h) Major element Harker diagrams (in %wt) for the TTG suites of the Rio Maria granite-greenstone terrane…… 66

Figure 9 - Diagrams showing the distribution of samples of the TTG granitoids of the Rio Maria granite-greenstone terrane…… 67

Figure 10 - Harker plots for selected trace elements (in ppm) for the Rio Maria TTGs……. 68

Figure 11 - Chondrite normalised REE patterns for TTG suites of the Rio Maria granite-greenstone terrane…… 70

Figure 12 - a) La/Yb vs Yb; b) La/Yb vs Sr/Y; c) Sr/Y vs Y; d) Nb/Ta vs Sr/Y; e) Nb/Ta vs La/Yb diagrams used to discriminate the different groups of TTG granitoids of the Rio Maria granite-greenstone terrane…… 72

Figure 13 - εNd vs age diagram showing inicial isotopic composition of TTG granitoids of the Rio Maria granite-greenstone terrane……... 73

Figure 14 - Summary of geochronological data presented in this study for the timing of TTG

magmatism in the Rio Maria granite-greenstone terrane……. 75

Figure 15 - SiO2 vs Sr diagram showing the distribution of samples of the TTG suites of the Rio Maria granite-greenstone terrane and the fields for TTG series of Pilbara craton, Barberton granite-greenstone terrane and eastern Finland. The average composition of TTGs from the western Karelian and Kola cratons is also shown for comparison……... 80

3 - GEOCHEMISTRY AND ZIRCON GEOCHRONOLOGY OF THE ARCHEAN GRANITE SUITES OF THE RIO MARIA GRANITE-GREENSTONE TERRANE, CARAJÁS PROVINCE, BRAZIL

Figure 1 - (a) Location of the studied area in Amazonian Craton. (b) Geological map of the Rio Maria granite-greenstone terrane showing the location of the dated samples……. 102

Figure 2 - Geochonological overview of the previous available data for Archean units of the Rio Maria granite-greenstone terrane and new geochronological data for the Guarantã suite and Rancho de Deus granite obtined in this work…….. 103

Figure 3 - QAP and Q-(A+P)-M for the Archean granite suites of the Rio Maria granitegreenstone terrane……. 109

Figure 4 - Diagrams for the samples dated from the Guarantã suite……... 113

Figure 5 - Harker diagrams for the Archean granite suites of the Rio Maria granite-greenstone terrane……... 118

Figure 6 - Geochemical plot showing the distribuition of the samples of the Archean granite suites of the Rio Maria granite-greenstone terrane…….. 119

Figure 7 - Harker plots for selected trace elements and elemental ratios for Archean granite suites. 120

Figure 8 - REE patterns of Archean granite suites of Rio Maria granite-greenstone terrane (normalized to chondrite after Evensen et al., 1978)……... 122

Figure 9 - Variation diagrams for the Archean granitoids of the Rio Maria granite-greenstone terrane……... 125

Figure 10 - (a) K/Na vs A/CNK or (b) #Mg or (c) TiO2, (d) #Mg vs A/CNK, (e) Ni vs Sr and (f) Y vs Ba diagrams for Archean granitoids of the Rio Maria granite-greenstone terrane…….. 128

Figure 11 - Major element discrimination diagram proposed by Sylvester (1994) for Archean granite suites of the Rio Maria granite-greenstone terrane…….. 130

4 - PETROLOGY OF THE ARCHEAN LEUCOGRANODIORITE-GRANITE SUITES: IMPLICATIONS FOR THE CRUSTAL EVOLUTION OF THE RIO MARIA GRANITE-GREENSTONE TERRANE, CARAJÁS PROVINCE, BRAZIL

Figure 1 - (a) - Location of the studied area in the Amazonian craton. (b) Geological map of the Rio Maria granite-greenstone terrane……... 153

Figure 2 - Geochonological overview of the previous available data for Archean units of the Rio Maria granite-greenstone terrane……. 154

Figure 3 - Features of the Guarantã suite (a) Enclave of the Arco Verde tonalite in Azulona leucogranodiorite; (b) Oriented alkali feldspar phenocrysts defining a WNW–ESE trending subvertical foliation; (c) Hand sample of the foliated porphyritic pink monzogranite from Guarantã pluton; (d) Hand sample of the porphyritic pinkish gray granodiorite from Trairão pluton; (e) K-feldspar phenocrystal in a medium-grained equigranular matrix of quartz, plagioclase, microcline, biotite, epidote, and accessory minerals. (f) Euhedral magmatic epidote enclosed by biotite..... 157

Figure 4 - QAP and Q-(A+P)-M for the leucogranodiorite-granite suites of the Rio Maria granitegreenstone terrane……. 158

Figure 5 - Major element Harker diagrams (%wt) for leucogranodiorite-granite suites from Rio Maria granite-greenstone terrane……. 162

Figure 6 - Geochemical plots showing the distribuition of the samples of the leucogranodiorite granite suites from Rio Maria granite-greenstone terrane……...……. 163

Figure 7 - Harker plots for selected trace elements and elemental ratios for leucogranodioritegranite suites from Rio Maria granite-greenstone terrane……... 166

Figure 8 - Chondrite normalised (Evensen et al., 1978) REE patterns for (a, b, c) Guarantã suite of the Rio Maria granite-greenstone terrane, (d) Transitional TTGs from Yilgarn craton (D. Champion, written communication), (e) Granite-granodiorite suite from Wyoming province (Frost et al., 2006) and (f) Transitional TTGs from Dharwar craton (Jayananda et al., 2006, Prabhakar et al., 2009)……. 167

Figure 9 - a) La/Yb vs Yb and a) Sr/Y vs Y diagrams used to discriminate the different groups of leucogranodiorite-granite suites from of RMGGT. c) K_2O vs Ba/Sr diagram showing the distribution of the samples of the leucogranodiorite-granite suites from Rio Maria granite-greenstone terrane…… 168

Figure 10 - A trace element model for the fractional crystallisation of the Rio Maria Granodiorite…….. 178

Figure 11 - Diagrams showing the result of the mixing between the Ba-Sr enriched granitic from Guarantã suite and trondhjemitic members: a) K_2O/Na_2O vs CaO; b) Sr vs Ba……. 179

TABELAS

1 – INTRODUÇÃO

Tabela 1 - Dados geocronológicos das unidades arqueanas do Terreno Granito-*Greenstone* de Rio Maria..... 16

2 - ZIRCON GEOCHRONOLOGY AND GEOCHEMISTRY OF THE TTG SUITES OF THE RIO MARIA GRANITE-GREENSTONE TERRANE: IMPLICATIONS FOR THE GROWTH OF THE ARCHEAN CRUST OF CARAJÁS PROVINCE, BRAZIL

Table 1 -Geochronological overview of the previous available data for Archean units of the Rio Maria granite-greenstone terrane..... 42

Table 2 - Modal composition (point counting) of representative samples of theTTG units of the RMGGT…… 46

Table 3 - Summary of zircon single-crystal evaporation Pb isotopic data from the TTG suites of the Rio Maria granite-greenstone terrane..... 52

Table 4 - Summary of LA-ICP-MS U–Th–Pb results for zircons from TTG suites of the Rio Maria granite-greenstone terrane..... 53

Table 5 - Representative chemical compositions of the different TTG units of the Rio Maria granite-greenstone terrane…… 64

Table 6 - Geochemical characteristics for the TTG groups discussed in this paper 71

Table 7 - Sm-Nd isotopic data for the TTG granitoids of the Rio Maria granite-greenstone terrane……... 73

3 - GEOCHEMISTRY AND ZIRCON GEOCHRONOLOGY OF THE ARCHEAN GRANITE SUITES OF THE RIO MARIA GRANITE-GREENSTONE TERRANE, CARAJÁS PROVINCE, BRAZIL

Table 1 - Modal compositions (point counting) of representative samples of the Archean granite suites of the Rio Maria granitegreenstone terrane…… 108

Table 2 - Summary of zircon single-crystal evaporation Pb isotopic data from the Guarantã granite of the Guarantã suite……..... 111

Table 3 - Summary of LA-ICP-MS U–Th–Pb results for zircons of the Guarantã granite, Trairão granodiorite and Rancho de Deus granite. 111

Table 4 - Representative chemical compositions of the different Archean granite suites of the Rio Maria granite-greenstone terrane……... 116

4 - PETROLOGY OF THE ARCHEAN LEUCOGRANODIORITE-GRANITE SUITES: IMPLICATIONS FOR THE CRUSTAL EVOLUTION OF THE RIO MARIA GRANITE-GREENSTONE TERRANE, CARAJÁS PROVINCE, BRAZIL

Table 1 - Chemical composition of the leucogranodiorite-granite suites of the Rio Maria granite-greenstone terrane…… 160

Table 2 - Modelling major and trace element compositions, fractionated mineral assemblages for differetiation of the Rio Maria Granodiorite…….. 178

RESUMO

As suítes tonalíticas-trondhjemíticas-granodioríticas (TTG) são os principais granitóides arqueanos, porém os corpos de leucogranitos calcico-alcalinos também possuem distribuição expressiva no Terreno Granito-*Greenstone* de Rio Maria (TGGRM), sudeste do Cráton Amazônico. Mapeamento geológico em áreas chaves e estudos petrográficos e geoquímicos, aliados ao refinamento dos dados geocronológicos utilizando os métodos de datação Pb-Pb por evaporação e U-Pb por LA-ICP-MS em zircão, permitiram concluir que o TGGRM foi palco de, pelo menos, três eventos formadores de TTG durante o Mesoarqueano. O primeiro evento exibe idade de 2,96±0,2 Ga e nele deu-se a geração do Trondhjemito Mogno e das rochas mais antigas do Tonalito Arco Verde. No segundo evento, ocorrido em 2,93±0,1 Ga, deu-se a formação do Complexo Tonalítico Caracol, do Tonalito Mariazinha e das rochas mais jovens do Tonalito Arco Verde. O último evento apresenta idade de 2,86±0,1 Ga e nele foi gerado o Trondhjemito Água Fria, de distribuição areal muito restrita. Comprovou-se que a idade do Trondhjemito Mogno é significativamente maior do que a anteriormente admitida, reduzindo a importância do magmatismo TTG de idade próxima de 2,87 Ga no TGGRM. Além disso, uma nova unidade TTG, denominada Tonalito Mariazinha, foi definida no mesmo e constatou-se que as rochas formadoras do Tonalito Arco Verde exibem idades variáveis no intervalo de 2,98 a 2,93 Ga.

Três grupos de TTGs foram identificados no TGGRM: 1) grupo com alta razão La/Yb, apresentando altas razões Sr/Y e Nb/Ta, originado a partir da fusão de uma fonte de composição máfica, em condições de pressão relativamente elevada (≥1,5 GPa), deixando granada e anfibólio no resíduo; 2) grupo com valor moderado da razão La/Yb, derivado de magmas gerados em condições intermediárias de pressão (~1,0-1,5 GPa), porém ainda no campo de estabilidade da granada; 3) grupo com baixa razão La/Yb, e também baixas razões Sr/Y e Nb/Ta, gerado a partir de magma formado em pressões comparativamente menores (≤1,0 GPa), proveniente da fusão parcial de fonte anfibolítica, tendo plagioclásio como fase residual. Não há nenhuma correspondência temporal entre os diferentes grupos e os três períodos de formação de magmas TTG em Rio Maria. Da mesma forma, não se observa relação direta entre estes grupos e as diferentes unidades, podendo algumas delas, como, por exemplo, o Tonalito Arco Verde, englobar granitóides com alta, intermediária e baixa razão La/Yb.

Os dados geocronológicos demonstram que o magmatismo granítico *stricto sensu* arqueano (2,87- 2,86 Ga) registrado no TGGRM, sucedeu o principal evento de geração de TTGs (2,98- 2,92 Ga), sendo contemporâneo ou ligeiramente posterior à colocação da suíte sanukitoíde Rio Maria (~2,87 Ga). Com base em dados petrográficos e geoquímicos, foram distinguidas três suítes de leucogranitos arqueanos: a) leucogranitos potássicos (granitos Xinguara e Mata Surrão), compostos dominantemente por biotita-monzogranitos com alto conteúdo de SiO_2, K_2O e Rb, mostrando enriquecimento em elementos terras raras leves em relação aos pesados e moderada a pronunciada anomalia de Européio. Esses granitos são similares aos granitos baixo-CaO do Cráton Yilgarn e aos granitos calcico-alcalinos CA2, assumindo-se que seus magmas foram produzidos a partir da fusão parcial de TTGs; b) Anfibólio-biotita monzogranitos, representados pelo Granito Rancho de Deus, cuja gênese deveu-se à diferenciação por cristalização fracionada de magmas sanukitóides afins aos da suíte Rio Maria, com a qual se associa; c) grupo de leucogranodioritos e leucomonzogranitos enriquecidos em Ba e Sr com fracionamento de elementos terras raras pesados em relação aos leves e geralmente desprovidos de anomalia significativa de Eu. Essas rochas mostram notáveis similaridades geoquímicas com os granitos alto-CaO (TTGs transicionais) do Cráton Yilgarn e com os granitos calcico-alcalinos CA1. Propõe-se um modelo envolvendo mistura em diferentes proporções de magmas graníticos similares às amostras mais enriquecidas em Ba e Sr da Suíte Guarantã com magmas trondhjemíticos para explicar a gênese e a variação composicional das suítes de leucogranitos enriquecidos em Ba e Sr. Os líquidos graníticos que participaram da mistura foram derivados da cristalização de 35% de magma sanukitóide de composição granodiorítica (rocha dominante na Suíte Rio Maria) pelo fracionamento de plagioclásio (46,72%), hornblenda (39,05%), clinopiroxênio (10,36%), magnetita (3,12%), ilmenita (0,70%) e allanita (0,06%).

Para explicar a evolução tectônica do TGGRM, propõe-se um modelo envolvendo a subducção de uma placa oceânica sob um platô oceânico espesso. Neste contexto, o grupo de TTGs com baixa razão La/Yb teria sido derivado de magmas originados pela fusão de metabasaltos da base do platô, em condições relativamente mais baixas de pressão, ao passo que os grupos com razões La/Yb alta e moderada, seriam gerados a partir da fusão parcial de metabasaltos da crosta oceânica subductada, em condições de pressão mais elevada. Parte dos magmas TTG gerados a partir da fusão da placa oceânica subductada teria reagido com a cunha

do manto durante sua ascensão e foi totalmente consumida, levando ao metassomatismo do manto.

Por volta de 2,87 Ga, ou seja, 50 milhões de anos após a formação da crosta tonalítica-trondhjemítica de Rio Maria, manifestações termais, possivelmente relacionadas a processo de *slab-break-off* ou à ação de plumas mantélicas, induziram a fusão do manto metassomatizado e levaram à geração de magmas sanukitóides. A ascensão desses magmas aqueceu a crosta de Rio Maria e possivelmente induziu a fusão de metabasaltos localizados na base da crosta, originando o magma parental do Trondhjemito Água Fria. A fusão da crosta tonalitíca-trondhjemítica, em mais baixa profundidade, fora do campo de estabilidade da granada, teria gerado os magmas dos leucogranitos potássicos.

Palavras chaves: Cratón Amazônico, Terreno Granito-*Greenstone* de Rio Maria, Mesoarqueano, suítes TTG, suítes de leucogranitos.

ABSTRACT

TTG and granite suites are exposed in large domains of the Mesoarchean Rio Maria granite-greenstone terrane (RMGGT), southeastern Amazonian craton. Extensive field work in key areas of the RMGGT, integrated with petrographic, geochemical, and geochronological studies, the latter employing the Pb-Pb evaporation and U-Pb LA-ICP-MS on zircon techniques, indicates that the TTG magmatism record in the RMGGT can be divided into three episodes: (I) A first event at 2.96±0.2 Ga (the older rocks of the Arco Verde tonalite and the Mogno trondhjemite), (II) a second one at 2.93±0.1 Ga (Caracol tonalitic complex, Mariazinha tonalite, and the younger rocks of the Arco Verde tonalite), and (III) a restricted event at 2.86±0.1 Ga (Agua Fria trondhjemite). The new data demonstrate that the Mogno trondhjemite is significantly older than previously admitted, reveal the existence of a new TTG suite (Mariazinha tonalite) and indicate that the volume of TTG suites formed during the 2.87 event was limited. The Arco Verde tonalite yielded significant age variations (2.98 to 2.93 Ga) but domains with different ages could not be individualized so far. The tonalitic-trondhjemitic suites of the RMGGT derived from sources geochemically similar to the metabasalts of the Andorinhas supergroup, which were extracted from the mantle during the Mesoarchean (3.0 to 2.9 Ga) and had a short time of crustal residence.

Three groups of TTG granitoids were distinguished in Rio Maria: 1) high-La/Yb group, with high Sr/Y and Nb/Ta ratios, derived from magmas generated at relatively high pressures (≥1.5 GPa) from sources leaving garnet and amphibole as residual phases; 2) medium-La/Yb group which magmas formed at intermediate pressure conditions (~1.0-1.5 GPa), but still in the garnet stability field; and 3) low-La/Yb group, with low Sr/Y and Nb/Ta ratios, crystallized from magmas generated at lower pressures (≤1.0 GPa), from an amphibolitic source that left plagioclase as a residual phase. These three geochemical groups do not have a direct correspondence with the three episodes of TTGs generation and a same TTG unit can be composed of rocks of different groups.

The geochronological data indicate that the emplacement of the Archean granites of the RMGGT occurred during Mesoarchean (2.87 and 2.86 Ga) being coeval with the sanukitoid suite (~ 2.87 Ga) and post-dating the main timing of TTG suites formation (2.98 - 2.92 Ga). Three main types of Archean granites were distinguished in the RMGGT on the basis of petrographic and geochemical data: (1) Potassic leucogranites (Xinguara and Mata Surrão granites), that are

composed dominantly of biotite-monzogranites with high SiO_2, K_2O, and Rb contents and fractionated REE patterns with moderate to pronounced negative Eu anomalies. These granites are similar to the low-Ca granites of the Yilgarn craton and to the CA2 Archean granites. Their magmas resulted from the partial melting of sources similar to the older TTG suites of the RMGGT; (2) Amphibole-biotite monzogranites (Rancho de Deus granite) generated by fractional crystallization and differentiation of sanukitoid magmas; (3) leucogranodiorite-granite suites (Guarantã suite and Grotão granodiorite), which are Ba- and Sr-rich rocks with strongly fractionated REE patterns without significant Eu anomalies. These granites have affinity with the high-Ca granites of the Yilgarn craton and the CA1-type Archean granites. On the basis of modeling and geochemical data we suggest that the leucogranodiorite-granite suites were derived from mixing between a granite, similar to the Ba- and Sr-enriched samples of the Guarantã suite, and trondhjemitic liquids. The granite magmas participating in the mixture were originated by fractional cystallization of 35% of a sanukitoid magma of granodioritic composition. The fractionated mineral phases were: plagioclase (46.72%), hornblende (39.05%), clinopyroxene (10.36%), magnetite (3.12%), ilmenite (0.7%) and allanite (0.06%). The large compositional variations observed in the Guarantã suite can be apparently explained by mixing in different proportions between the granite and trondhjemitic liquids.

A model involving a subducting slab underneath a thick oceanic plateau was envisaged to explain the tectonic evolution of the RMGGT. In this context, the low-La/Yb group was formed from magmas originated by the melting of the base of a thickened basaltic oceanic crust at comparatively lower pressures (≤ 1.0 GPa), whereas the medium- and high-La/Yb groups were derived from the slab melting at increasing different pressures (1.0-1.5 and > 1.5 GPa, respectively). Part of these TTG magmas react during their ascent with the mantle wedge being totally consumed and leaving a metassomatized mantle. 50 m. y. later, at ca. 2870 Ma, thermal events, possibly related to the slab-break-off, causing asthenosphere mantle upwelling, or to the action of a mantle plume, may have induced the melting of the metassomatized mantle and the generation of sanukitoid magmas. These magmas may have heated the base of the Archean continental crust during their rising to the surface and could have lead to the local melting of the basaltic crust forming the Água Fria trondhjemite magma. This was accompanied by partial melting (at shallower crustal levels) of the Rio Maria tonalitic-thondhjemitic crust and generation of the potassic leucogranite.

Keywords: Amazonian craton, Rio Maria granite-greenstone terrane, Mesoarchean, TTG suites, granite suites.

Capítulo – 1

Introdução

1 – INTRODUÇÃO

1.1 – APRESENTAÇÃO

O Terreno Granito-*Greenstone* de Rio Maria (TGGRM), alvo da presente pesquisa, integra o domínio tectônico sul da Provincia Mineral de Carajás (Fig. 1), porção oriental do Cráton Amazônico. Este domínio corresponde a um núcleo arqueano bem preservado, composto por *greenstone belts* e granitóides diversos (associações TTG, associações sanukitóides e leucogranitoides de afinidade cálcico-alcalina), cobertos por metassedimentos também de idade arqueana e cortados por granitos anorogênicos paleoproterozóicos (Huhn et al. 1988, Souza et al. 1990, Araújo et al. 1994, Dall'Agnol et al. 1996, 1997, 2006), reproduzindo fortes analogias em termos litológicos ao verificado em outras regiões cratônicas com destaque para o Terreno Granito-*Greenstone* de Barberton, África do Sul (Condie & Hunter 1976, Lowe & Byerly 2007); da Província Slave, noroeste do Escudo Canadense (Davis et al. 1994); da Província Wyoming, centro-oeste do Estados Unidos (Frost et al., 2006); do Cráton Dharwar, no sul da Índia (Choukroune et al., 1997, Moyen et al., 2003), Província Karelia, Finlândia (Käpyaho et al., 2006) e dos cratons Pilbara e Yilgarn na Austrália (Cassidy et al., 1991, Champion & Sheraton, 1997, Champion & Smithies, 2001, 2003, Kranendonk et al., 2007).

Os granitóides arqueanos presentes no TGGRM têm sido sistematicamente estudados pelo Grupo de Pesquisa Petrologia de Granitóides (GPPG) do Instituto de Geociências da Universidade Federal do Pará (IG-UFPA), em particular os granitóides tonalítico-trondhjemíticos que compõem as típicas suítes TTG. Um conhecimento expressivo foi acumulado sobre o Tonalito Arco Verde (Althoff 1996, Althoff et al., 2000, Almeida et al., 2008, Costa 2009), Complexo Tonalítico Caracol (Leite 1995, 2001, Leite et al. 2004), Trondhjemito Água Fria (Leite 1995, 2001, Leite et al., 2004) e, de maneira menos aprofundada, Trondhjemítico Mogno (Pimentel & Machado 1994, Santos & Pena Filho 2000, Souza et al. 2001, Guimarães submetido a, este trabalho). Os leucogranitoides de afinidade cálcico-alcalina também são alvos de estudo do GPPG. Vários plutons representativos deste tipo de magmatismo, o qual é inteiramente distinto do magmatismo TTG e das associações sanikitóides, foram identificados no TGGRM. Dentre eles destacam-se os granitos Xinguara (Leite 1995, 2001), Mata Surrão (Duarte 1992) e Guarantã (Althoff 1996), bem como corpos leucograníticos nas áreas de Identidade (Souza 1994), Bannach e Xinguara.

Quando a presente pesquisa foi proposta, não havia nenhum trabalho de integração geológica consolidado que reunisse e discutisse de maneira integrada os dados gerados nas diferentes áreas do TGGRM estudadas. Além disso, embora se tenha avançado muito na caracterização geoquímica e petrogênese das principais associações granitóides arqueanas do TGGRM, havia muitas lacunas no conhecimento que precisavam ser preenchidas, em particular no caso das associações TTG e dos leucogranitóides arqueanos, os quais foram os alvos do presente trabalho. Finalmente, não havia um modelo de evolução geológica e geotectônica do TGGRM a luz dos modernos conceitos sobre a gênese de terrenos arqueanos (Smithies 2000, Smithies et al. 2003, Moyen et al. 2003, Martin et al. 2005, Lobach-Zuchenko et al. 2005, Condie 2005, Champion & Smithies, 2007, Moyen et al., 2007).

Portanto, o principal objetivo desta tese foi contribuir para esclarecer a petrogênese e o papel dos granitóides TTG e dos leucogranitóides arqueanos na evolução geológica e geotectônica mesoarqueana deste segmento do Cráton Amazônico. Para alcançar esses objetivos, os dados petrográficos, mineralógicos, geoquímicos, geocronológicos e isotópicos previamente existentes sobre tais unidades aflorantes nas distintas áreas do TGGRM estudadas foram integrados com estudos adicionais de petrografia, geoquímica e geocronologia em áreas chaves para o entendimento geológico do TGGRM.

O presente estudo foi executado paralelamente a outras pesquisas direcionadas para a geologia, petrografia e geoquímica de associações TTG e de leucogranitos ocorrentes no TGGRM, vinculadas às dissertações de mestrado de Fabriciana Vieira Guimarães e Samantha Barriga Dias, respectivamente, e ao trabalho de iniciação científica de Manoel A. C. da Costa, todos vinculados ao GPPG. Vale ressaltar que as associações sanukitóides, as quais incluem o Granodiorito Rio Maria e rochas associadas, que igualmente possuem uma grande importância na evolução do TGGRM, foram anteriormente estudadas (Medeiros 1987, Medeiros & Dall'Agnol 1988, Althoff 1996, Althoff et al., 2000, Oliveira et al., 2006) e um acervo de informações relacionadas aos processos de cristalização e diferenciação desses magmas sanukitoides, bem como estimativas dos parâmetros de cristalização (T, P, fO_2, XH_2O) prevalecentes durante a evolução dos mesmos foi recentemente introduzido na literatura através da tese de doutorado de Marcelo Augusto de Oliveira. A plena integração dessas pesquisas e o importante acervo de dados gerados pelo GPPG na região estudada ao longo dos últimos 25 anos foram fundamentais

para melhor entender a evolução geológica e tectônica mesoarqueano do Terreno Granito-*Greenstone* de Rio Maria.

A presente tese de doutorado, intitulada "Geologia, geoquímica, geocronologia e petrogenesis das suítes TTG e dos leucogranitos arqueanos do Terreno Granito-*Greenstone* de Rio Maria, sudeste do Cráton Amazônico" foi iniciada em 2005 e vinculada ao Programa de Pós-Graduação em Geologia e Geoquímica da Universidade Federal do Pará. A elaboração deste documento foi feita por agregação de 3 artigos científicos submetidos a periódicos internacionais, sendo apresentados na forma de capítulos (capítulos 2, 3 e 4) dentro de um texto integrador, o qual incorpora um capítulo introdutório (Capitulo 1), que inclui a apresentação da pesquisa, localização da área de estudo, contexto geológico e tectônico regional, as principais características do magmatismo TTG e granítico de idade arqueana, a apresentação dos problemas existentes no momento da proposição desta tese, os objetivos que foram traçados para solucioná-los. Em seguida, são descritas as atividades e procedimentos metodológicos que viabilizaram alcançar os objetivos propostos. O capitulo final (capitulo 5), sumariza de forma integrada as discussões e as conclusões abordadas nos três artigos científicos. Os artigos serão apresentados nos próximos capítulos, de acordo com a seguinte ordem:

Capítulo 2 – *Artigo 1* - **Zircon geochronology and geochemistry of the TTG suites of the Rio Maria Granite-Greenstone terrane: Implications for the growth of the Archean crust of Carajás Province, Brazil.** Submetido para publicação à revista *PRECAMBRIAN RESEARCH*. Este trabalho apresenta dados sobre a geologia, petrografia, geoquímica, geocronologia e geologia isotópica das suítes TTG aflorantes nas diferentes áreas do TGGRM. A discussão dos dados permitiu definir a assinatura geoquímica das suítes TTG, comparar com séries TTG presentes em outros crátons arqueanos, refinar a idade dos eventos magmáticos responsáveis pela gênese dessas associações, especular sobre o ambiente tectônico em que tais rochas foram originadas e discutir o papel do magmatismo TTG para a evolução crustal do TGGRM.

Capítulo 3 – *Artigo 2* - **Geochemistry and zircon geochronology of the Archean granite suites of the Rio Maria Granite-Greenstone terrane, Carajás Province, Brazil.** Submetido para publicação à revista *JOURNAL OF SOUTH AMERICAN EARTH SCIENCES*. O referido artigo exibe dados sobre a geologia, petrografia, geoquímica e geocronologia de diferentes

leucogranitóides aflorantes no TGGRM. Este trabalho foi fundamental para definir o comportamento geoquímico das diferentes suítes leucograníticas do TGGRM, estabelecer comparações com grupos de granitos arqueanos aflorantes em outros cratons, refinar o posicionamento estratigráfico das suítes leucograníticas e o ambiente tectônico em que tais associações foram originadas. O trabalho também mostra o papel dos diferentes grupos de leucogranítos na evolução geológica e geotectônica do TGGTM.

Capítulo 4 – *Artigo 3* - **Petrology of the leucogranodiorite-granite suites: implications for the Archean crustal evolution of the Rio Maria granite-greenstone terrane, Carajás province, Brazil.** Submetido para publicação à revista *LITHOS*. Com base em evidências geológicas e petrográficas, bem como na assinatura geoquímica da suíte de leucogranodioritos e leucomonzogranitos enriquecidos em Ba e Sr, as possíveis fontes e os processos petrogenéticos que deram origem aos magmas formadores desta suíte são discutidos em detalhe neste trabalho.

1.2 - LOCALIZAÇÃO DA ÁREA

A área selecionada para este estudo situa-se na porção sudeste do Estado do Pará, abrangendo partes dos municípios de Redenção, Pau D'Arco, Rio Maria, Bannach, Água Azul e Xinguara, sendo limitada pelos paralelos 7°00'e 8°00' S e pelos meridianos 50°00' e 49°30' W (Fig. 1). A área constitui um poligono, perfazendo aproximadamente 7.500 km². O acesso à área pode ser feito por via aérea até as cidades de Carajás, Marabá ou Redenção, seguindo-se por via terrestre pela rodovia PA-150. Por via terrestre, o acesso a partir de Belém é pela rodovia PA-150, passando por várias cidades da área, como Xingura, Rio Maria, Pau D'Arco e Redenção.

1.3 - CONTEXTO GEOLÓGICO REGIONAL

O Cráton Amazônico tem sido subdividido em várias províncias geocronológicas que apresentam idades diferentes, distintos padrões estruturais e evoluções geodinâmicas particulares (Tassinari & Macambira, 2004; Santos et al., 2006).

Tassinari & Macambira (2004) considera que a Província Amazônia Central (Fig. 2a) é segmento mais antigo do Cráton Amazônico, sendo dividida em dois blocos tectônicos principais, Carajás e Xingu-Iricoumé. Santos et al., (2006) considera o bloco Arqueano de Carajás como uma província independente (Fig. 2b), havendo um consenso que a região de Carajás constitui o

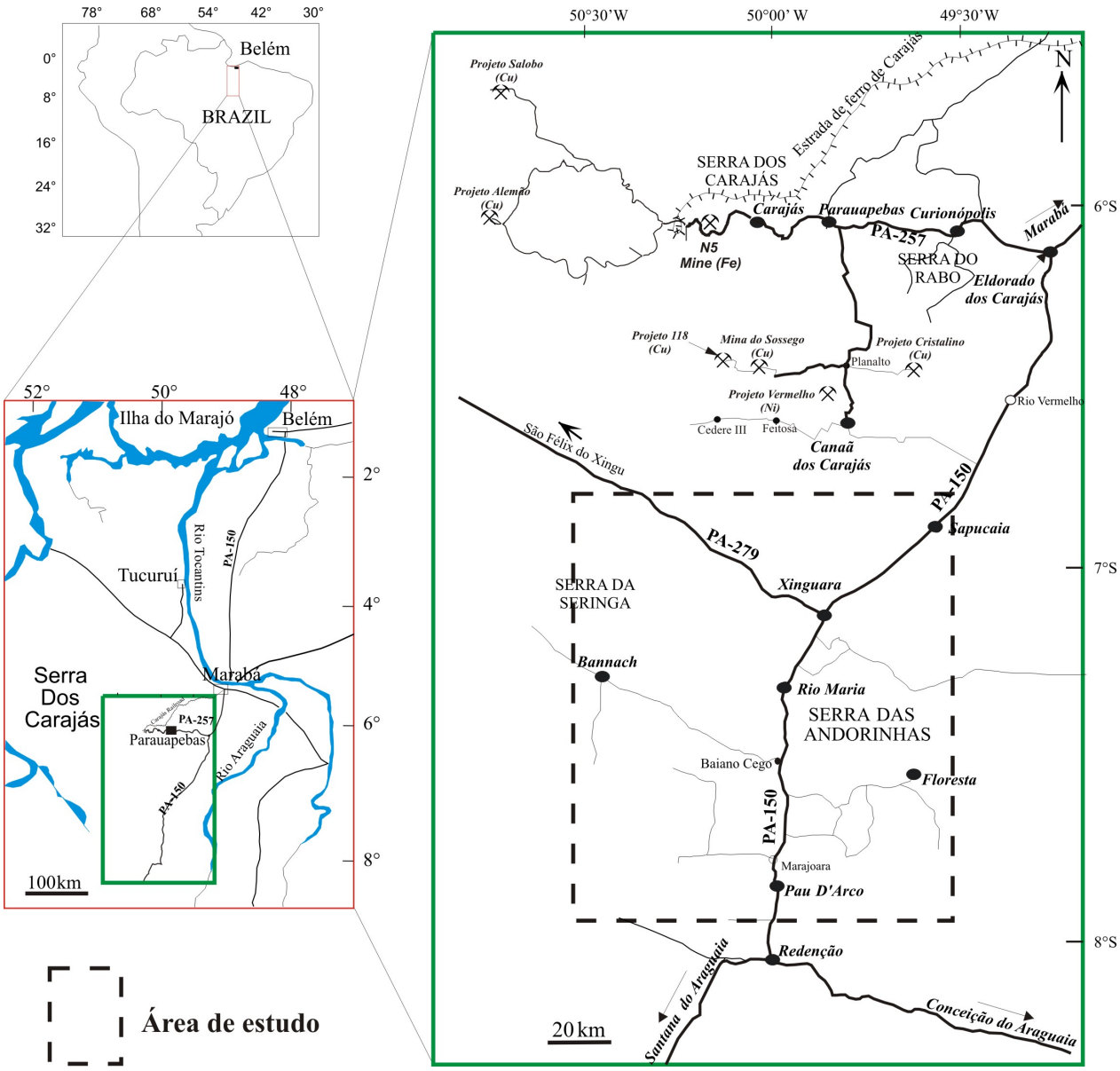

Figura 1 - Mapa de localização da Província Mineral de Carajás, indicando a área do Terreno Granito- *Greenstone* de Rio Maria

principal núcleo arqueano do Cráton Amazônico. Destaca-se, ainda, a presença de crosta arqueana na região do Amapá (Avelar 2002, Rosa-Costa et al., 2003, 2006, Rosa-Costa 2006; Fig. 2b), bem como evidências isotópicas de ocorrência de crosta arqueana no domínio vulcânico que se estende do Xingu à região próxima de Itaituba (Teixeira et al., 2002, Lamarão et al., 2005, Vasquez 2006).

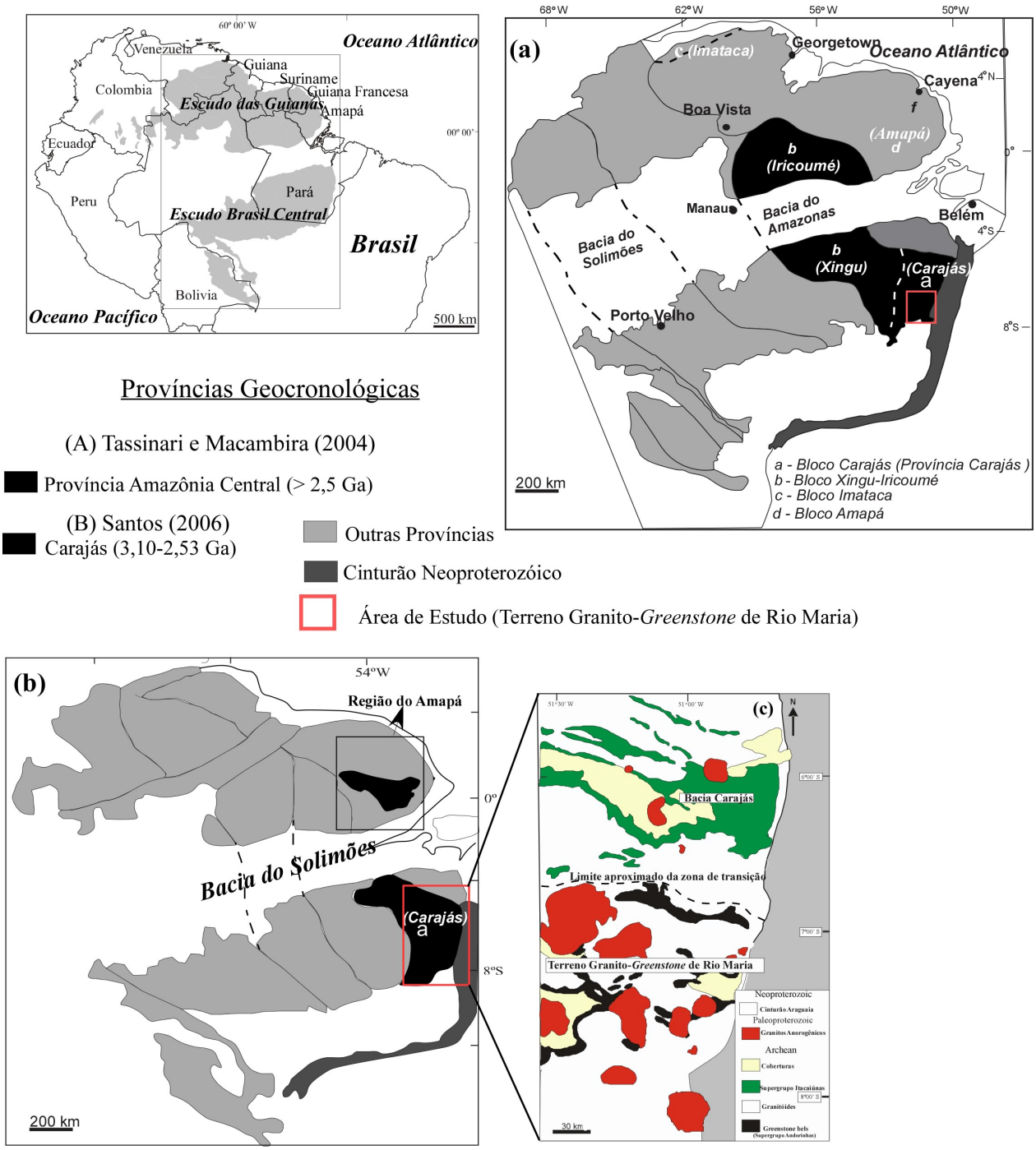

Figura 2 - Domínios Arqueanos do Cráton Amazônico, de acordo com os modelos de províncias geocronológicas de (a) Tassinari & Macambira (2004) e (b) Santos et. al. (2006); (c) Mapa geológico simplificado da Provincia Mineral de Carajás.

A Província Carajás (Fig. 2c) é limitada a oeste por um terreno dominado por granitóides proterozóicos e assembléias vulcânico-piroclásticas do Supergrupo Uatumã, com idades

próximas de 1,88 Ga (Teixeira et al., 2002) a leste, é bordejada pelo Cinturão Araguaia do Neoproterozóico, relacionado ao Ciclo Brasiliano (Pan-Africano), o qual não afetou significativamente o Cráton Amazônico; a norte e a sul, pela Província Maroni-Itacaiúnas e pelo domínio Santana do Araguaia (Vasquez et al., 2008), respectivamente, ambos formados durante o evento Trans-Amazônico (2,20 - 2,10 Ga). Baseado na idade e natureza das seqüências supracrustais, idade dos eventos magmáticos e deformacionais e na natureza das séries granitóides e no ambiente tectônico, a Província Carajás foi dividida em dois domínios tectônicos (Souza et al., 1996; Althoff et al., 2000; Dall'Agnol et al., 2000, 2006; Santos et al., 2006; Vasquez et al., 2008; Fig. 2c): O domínio de idade Mesoarqueana (3,0 – 2,86 G.a) denominado de Terreno Granito-*Greenstone* de Rio Maria (Machado et al., 1991; Macambira & Lafon, 1995; Macambira & Lancelot, 1996; Althoff et al., 2000; Souza et al., 2001; Leite et al., 2004; Dall'Agnol et al., 2006; Fig. 2c) e o domínio Neoarqueano de Carajás (2,76 – 2,54 Ga; Machado et al., 1991; Huhn et al., 1999; Barros et al., 2004; Sardinha et al., 2006; Fig. 2c). Dall'Agnol et al. (2006), considera que o dominio Carajás foi originado provavelmente em período similar ao do TGGRM, sendo, porém afetado a seguir pela formação de um profundo rift continental, desse modo tais autores optaram por designar o domínio de Carajás como Bacia de Carajás. Uma hipótese alternativa considera que o domínio de Carajás foi originado em um ambiente de subducção (Meirelles & Dardenne, 1991; Teixeira & Eggler, 1994; Lobato et al., 2006; Silva et al., 2006). Dall'Agnol et al. (2000, 2006) admitem a existência de um domínio de transição entre a Bacia de Carajás e o TGGRM. Esta região é interpretada por esses autores como um segmento do TGGRM que foi intensamente afetada pelos eventos magmáticos e tectônicos atuantes durante a fase compressiva da evolução tectônica da Bacia de Carajás. Atualmente, vários pesquisadores do GPPG se dedicam ao entendimento estratigráfico das unidades aflorantes no domínio de transição (por exemplo; Feio, 2009), isso contribuirá para nivelar o grau de conhecimento geológico em relação ao Terreno Granito-*Greenstone* de Rio Maria e a Bacia Carajás e para compreender como se deu a evolução geológica e tectônica da Província Carajás.

As associações TTG e as suítes de leucogranitóides arqueanos, alvo da presente pesquisa, estão situadas no Terreno Granito-*Greenstone* de Rio Maria (Fig. 2c, 3), o qual é formado por seqüências de *greenstone belts* do Supergrupo Andorinhas, com idades que variam de 2,97 a 2,90 Ga (Macambira 1992, Pimentel & Machado 1994, Souza 1994), sendo compostos

dominantemente por rochas metaultramáficas (komatiítos) e metamáficas (basaltos e gabros) com rochas intermediárias a félsicas ocorrendo de forma subordinada, além disso, intercalações de metagrauvacas, também são encontradas nestas seqüências (Docegeo, 1988; Huhn et al., 1988; Souza et al., 2001). Os *greenstone belts* são intrudidos por uma variedade de granitóides arqueanos originados entre 2,98 e 2,86 Ga (Tabela 1). Com base em aspectos petrográficos, geoquímicos e geocronológicos, Dall'Agnol et al., (2006) reconheceu quatro grupos de granitóides arqueanos no TGGRM: (1) Os granitóides mais antigos são representados por suítes de rochas TTG originadas entre 2,98 e 2,92 Ga (Tonalito Arco Verde, Complexo Tonalítico Caracol e Tonalito Mariazinha[1]; Althoff et al., 2000, Leite et al., 2004, Guimarães et al., submetido a, este trabalho); (2) granitóides sanukitóides com alto Mg, representados pelas diferentes ocorrências de rochas da Suíte Rio Maria, com idades em torno de 2,87 Ga (Medeiros 1987, Macambira & Lancelot 1996, Althoff 1996, Althoff et al., 2000, Leite et al., 2004, Oliveira et al., 2009, Oliveira et al., submetido). Essas rochas são intrusivas nos greenstone belts e nos granitóides TTG mais antigos e são seccionadas pelo Trondhjemito Água Fria; (3) granitóides das séries TTG jovens representados pelo Trondhjemito Mogno[2] e Trondhjemito Água Fria (2,86 Ga; Huhn et al., 1988, Pimentel & Machado 1994, Leite et al., 2004; este trabalho); (4) leucomonzogranitos e leucogranodioritos[3] com idade entre 2,87-2,86 Ga.

1.4 – GRANITÓIDES ARQUEANOS.

Os cratons arqueanos compõem menos que 10% dos continentes, porém importância conferida a esses terrenos deve-se, entre outros fatores, à existência de expressivos depósitos minerais. Esses terrenos são encontrados em várias partes do mundo, com destaque para a região de Barberton, leste do Cráton Kaapvaal, África do Sul (Condie & Hunter 1976); da Província Slave, noroeste do Escudo Canadense (Davis et al., 1994); do Cinturão Norseman-Wiluna, oeste da Austrália (Cassidy et al., 1991); Cráton Dharwar, no sul da Índia (Choukroune et al., 1995,

---

[1] Dados geocronológicos inéditos sobre esta unidade serão apresentados e discutidos no artigo do próximo capítulo (Capítulo 2) referente às suítes TTG do TGGRM.

[2] A idade e o posicionamento estratigráfico desta unidade foram redefinidos com base nas discussões do artigo referente às suítes TTG.

[3] Essas rochas são tema dos artigos referente a caracterização das suítes leucograníticas arqueanas do TGGRM (Capítulo 3) e da petrogênese da suíte de leucogranitos alto Ba e Sr (Capítulo 4).

Tabela 1 - Dados geocronológicos das unidades arqueanas do Terreno Granito-*Greenstone* de Rio Maria.

Unidade Estratigráfica	Rocha	Método	Material Analizado	Idade (Ma)
Leucogranitos Potássicos				
Granito Xinguara	Leucogranito	Pb-Pb	Zircão	2865±1 (5)
Granito Mata Surrão	Leucogranito	Pb-Pb	Rocha Total	2872±10 (12)
	Leucogranito	Pb-Pb	Zircão	2875±11 (3)
	Leucogranito	Pb-Pb	Zircão	2881±2 (3)
Grupo de leucogranodioritos-leucomonzogranitos				
Suíte Guarantã	Granodiorito	Pb-Pb	Zircão	2868±5 (11)
	Leucogranito	Pb-Pb	Zircão	2870±5 (10)
Série de TTG Jovem	Trondhjemito	U-Pb	Titanita	2871 ? (1)
Trondhjemito Mogno *	Trondhjemito	Pb-Pb	Zircão	2857±13 (9)
	Trondhjemito	Pb-Pb	Zircão	2900±21 (9)
Trondhjemito Água Fria	Trondhjemito	Pb-Pb		2864±21 (5)
Suíte sanukitóide Rio Maria	Granodiorito	U-Pb	Zircão	2874 + 9/-10 (2)
Granodiorito rio Maria e rochas associadas	Granodiorito	U-Pb	Zircão,Titanita	2872±5 (1)
	Quartzo-diorito	Pb-Pb	Zircão	2878±4 (8)
	Diorito	Pb-Pb	Zircão	2880±4 (3)
	Granodiorito	Pb-Pb	Zircão	2877±6 (3)
Tonalito Parazônia	Quartzo-diorito	Pb-Pb	Zircão	2876±2 (7)
	Tonalito	U-Pb	Titanita	2858 (1)
Série de TTG Antigo	Tonalito	Pb-Pb	Zircão	2948±5 (5)
Complexo Tonalítico Caracol	Tonalito	Pb-Pb	Zircão	2936±3 (5)
(Tonalito Mariazinha)**	Tonalito	Pb-Pb	Zircão	2924±2 (5)
Tonalito Arco Verde	Tonalito	Pb-Pb	Zircão	2964±4 (4)
	Tonalito	Pb-Pb	Zircão	2948±7 (3)
	Tonalito	Pb-Pb	Zircão	2981±8 (3)
	Tonalito	Pb-Pb	Zircão	2988±5 (3)
	Tonalito	Pb-Pb	Zircão	2957 + 25/-21 (2)
Greenstone Belts				
Supergrupo Andorinhas	Rocha metavulcânica félsica	U-Pb	Zircão	2904+29/-22 (2)
	Metagrauvaca	U-Pb	Zircão	2971±18 (2)
	Rocha metavulcânica félsica	U-Pb	Zircão	2972±5 (1)

Fonte dos Dados: (1) Pimentel & Machado (1994), (2) Macambira and Lancelot (1996), (3) Rolando & Macambira (2003), (4) Vasquez et al. (2008), (5) Leite et al. (2004), (7) Almeida (dados inéditos), (8) Dall'Agnol et al. (1999), (9) Macambira et al. (2000), (10) Althof et al., 2000, (11) Almeida et al., 2008, (12) Lafon et al. (1994).*A idade e o posicionamento estratigráfico desta unidade foram redefinidos com base nas discussões do artigo referente às suítes TTG, **Dados geocronológicos inéditos sobre esta unidade serão apresentados e discutidos no artigo do próximo capítulo (Capítulo 2) referente às suítes TTG do TGGRM.

1997, Moyen et al., 2003) e são comumente compostos por granitóides arqueanos e seqüências metavulcanosedimentares do tipo *greenstone-belts* (Windley, 1995). Dentre os principais grupos de granitóides arqueanos destacam-se as associações granitóides de composição tonalítica, trondhjemítica e granodiorítica (TTG), suítes sanukitóides e granitos e granodioritos *stricto sensu*.

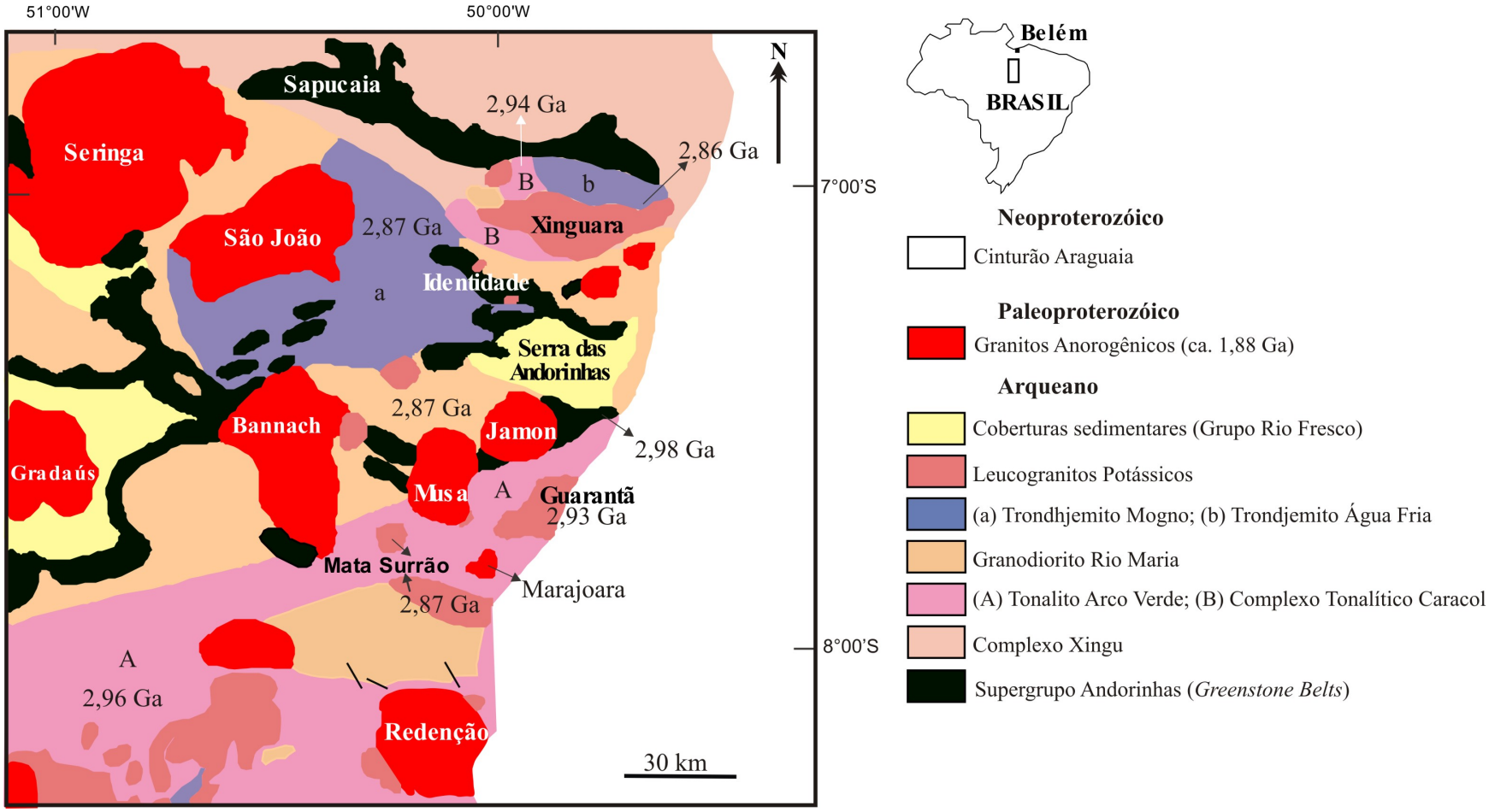

Figura 2 - Mapa Geológico simplificado do Terreno Granito-Greenstone de Rio Maria antes da proposição da presente pesquisa, reproduzido a partir de Oliveira, 2001(Fontes originais: Medeiros et al. 1987, Huhn et al. 1988, Docegeo 1988, Souza et al. 1990, Althoff et al. 1991, Duarte 1992, Souza 1994, Araújo et al. 1994, Vale & Neves 1994, Leite 1995, Althoff et al. 2000, Leite 2001, Oliveira, 2001).

1.4.1 - Suíte Tonalito-Trondjemito-Granodiorito (TTG)

As sequências Tonalito-Trondjemito-Granodiorito são consideradas como as principais suítes de granitóides arqueanos. Segundo Barker (1979), essas rochas são caracterizadas geoquimicamente pelo caráter félsico a intermediário (geralmente >65% SiO_2), alta razão Na_2O/K_2O (>1,5), baixo a moderado conteúdo de LILE e ausência de enriquecimento em K nos membros mais félsicos durante a diferenciação. Barker & Arth (1976) mostram que rochas sódicas podem ser subdivididas em subgrupos com alto ou baixo alumínio (o primeiro subgrupo se caracteriza por apresentar mais de 15% de Al_2O_3 em rochas com conteúdo de ~70% de SiO_2). O subgrupo de alta alumina é caracterizado pelo elevado conteúdo de Sr e Eu, forte fracionamento dos elementos terras raras (baixo conteúdo de elementos terras raras pesados), e altas razão Sr/Y. Essas características podem ser interpretadas como resultado da presença de granada e anfibólio e ausência de plagioclásio como fases residuais ou fracionadas durante a petrogênese dessas rochas. Já os TTGs com baixo alumínio são caracterizados por teores baixos de Sr e Eu, fracionamento de elementos terras rara pesados relativamente menos acentuado (conteúdos relativamente altos de elementos terras rara pesados), e baixa razão Sr/Y, sugerindo que durante os processos de formação dos magmas não houve participação efetiva de granada, sendo os mesmos amplamente controlados pela presença de plagioclásio como fase fracionada ou residual (Champion & Smithies 2003). Os TTGs alto alumínio são dominantes nos crátons arqueanos (Martin 1994) e são originados em condições de alta pressão (Champion & Smithies 2003).

Martin (1993) faz uma síntese dos principais modelos propostos para explicar a gênese dos TTGs, destacando os seguintes: (i) cristalização fracionada de um magma basáltico; (ii) fusão parcial direta do manto; (iii) fusão parcial de grauvacas maturas; (iv) fusão parcial de eclogito ou granulito básico; (vi) fusão parcial de anfibolito com granada. Este mesmo autor, baseado em dados geoquímicos e experimentais, propôs um modelo em três estágios para a gênese dos TTGs:

Estágio 1 - fusão parcial do manto gerando grande quantidade de magma toleítico;

Estágio 2 - esses toleitos, transformados em granada-anfibolitos, são parcialmente fundidos e originam o magma parental dos TTGs, deixando um resíduo de hornblenda + granada + clinopiroxênio + plagioclásio;

Estágio 3 - cristalização fracionada, principalmente de hornblenda + plagioclásio produzindo a suíte diferenciada TTG.

O modelo de fusão parcial de fontes máficas é sustentado pela ausência de termos máficos nos TTGs arqueanos. Além disso, a predominância dos TTGs alto alumínio (indicativo de alta pressão) e as altas temperaturas reinantes durante o arqueano conduzem diversos autores (Martin, 1986) a propor que a maioria das rochas TTG arqueanas foram originadas por fusão parcial de lascas da crosta oceânica em zonas de subducção, com uma participação efetiva da cunha do manto. Essa hipótese é sustentada pelos conteúdos de MgO, Cr, Ni e #Mg, mais altos do que aqueles esperados somente a partir de fusão parcial de material basáltico homogêneo. Martin & Moyen (2002) utilizam os teores de tais elementos para propor mudanças na composição das rochas TTG ao longo do Arqueano, sendo que o aumento do conteúdo desses elementos implicaria maior interação do magma félsico (magmas TTG oriundos da fusão de basaltos nas zonas de subducção) com o manto peridotítico. Segundo esses autores, há também um aumento do conteúdo de Sr nas rochas TTG durante o Arqueano. Tal aumento, está provavelmente relacionado com a menor participação do plagioclásio no resíduo, sendo reflexo do aumento da profundidade da fusão na fonte e das condições de pressão que favoreceram a desestabilização deste mineral. Portanto, segundo a hipótese adotada por Martin & Moyen (2002), no inicio do arqueano a fusão das fontes dos TTGs se dava a baixa profundidade em função do elevado gradiente geotérmico da terra, nessa condição o plagioclásio era estável e havia pouca interação entre o magma TTG e o manto peridotitico, refletindo nos baixos valores de MgO, Cr, Ni, #Mg e Sr dos TTGs do inicio do arqueano (>3,0 Ga). Já no final do arqueano (<3,0), onde o gradiente geotérmico era relativamente baixo, os magmas TTG seriam gerados a mais altas profundidades, proporcionando condição de pressão favorável para a desestabilização do plagioclásio na associação mineral das fontes dos magmas. Além disso, os líquidos gerados nessas condições, de maior pressão e profundidade, teriam interação mais intensa com o manto peridotitico, resultando em valores relativamente mais elevados de MgO, #Mg, Cr, Ni e Sr nos TTGs do final do arqueano. Smithies et al. (2003) afirmam que quanto maior for o ângulo da placa oceânica subductante maior será a interação entre o magma TTG (oriundo da fusão da mesma) com o manto peridotitico, e isso se refletirá nos valores de MgO, Cr, Ni, #Mg das rochas TTG.

Entretanto, o contraste composicional admitido por Martin & Moyen (2002) para os TTGs de diferentes períodos do Arqueano não é aceito sem discussão. Condie (2005) apresenta composições médias de TTGs do início e do final do Arqueano. Ambos correspondem à TTGs alto Al, com composições de modo geral similares, embora os TTGs do final do Arqueano mostrem teores um pouco mais elevados de MgO, #Mg, Ni e Sr, porém mais baixos de Cr, quando comparados aos TTGs do início do Arqueano. O modelo tectônico assumido por Condie (2005) também contrasta com o dos autores mencionados. Ele admite que os TTGs podem ter sua origem associada com plumas do manto que afetariam a base da litosfera, produzindo espessos platôs oceânicos que sofreriam fusão parcial em profundidade.

1.4.2 - Suítes Sanukitóides

Essas suítes ocorrem como intrusões nos segmentos de crosta constituídos pelas associações granitóides TTG. A idade dessas rochas são sempre mais novas do que 3,0 Ga, e geoquimicamente são caracterizadas pelos altos teores de Mg, Cr, Ni e também de LILE (Sr, Ba, P) e elementos terras raras leves. Os modelos discutidos para a gênese de magmas sanukitóides (Stern et al., 1989, Stern & Hanson 1991, Stevenson et al., 1999, Smithies & Champion 2000, Oliveira et al., 2009, Oliveira 2009) mostram que as origens dessas rochas contrastam com àquelas aceitas para formação de TTGs. A maioria dos modelos propostos para explicar a gênese dessas rochas considera a fusão de um manto peridotítico metassomatizado por fluídos ou por líquidos gerados a partir de uma zona de subducção (relacionados a fusão das fontes do TTGs), como processo mais provável para a formação dos sanukitóides arqueanos.

1.4.3 – Biotita-granitos e Biotita-granodioritos.

O magmatismo granítico *stricto sensu* possui uma importante distribuição areal em terrenos arqueanos. Condie (1993) estimou que os granitos arqueanos representam cerca de 20% do volume dos terrenos Arqueanos atualmente expostos. Desde o clássico trabalho de Sylvester (1994) intitulado "Archean granite plutons", os estudos sobre esse grupo de rochas foram intensificados. Essas rochas ocorrem como plútons de dimensões variáveis, comumente intrusivos em greenstone belts e granitóides dominados por tonalitos, trondhjemitos e granodioritos que formam as clássicas associações arqueanas TTG (Sylvester 1994, Leite 2001, Leite et al., 2004). A maioria desses plutons foi colocada durante o Neoarqueano entre 2,7 e 2,5

Ga (Goodwin, 1991). Segundo Ridley (1992) esse evento magmático granítico marca um importante estágio na evolução e estabilização da crosta arqueana, sendo sua gênese intimamente ligada à deformação e metamorfismo da litosfera, durante eventos tectônicos convergentes, transpressivos ou extensionais (Barton & Hanson 1989).

Os plutons graníticos arqueanos são compostos dominantemente por biotita-(raramente hornblenda) granodioritos, monzogranitos ou sienogranitos, mostrando moderada a alta razão K/Na (>0,5), enriquecimento de elementos terras rara leves em relação aos pesados com anomalia negativa de Európio variando desde forte até ausente (Davis et al., 1994; Sylvester, 1994; Champion & Sheraton, 1997; de Wit, 1998; Frost et al., 1998; Champion & Smithies, 1999; Leite et al., 1999; Althoff et al., 2000; Moyen et al., 2003). O avanço no conhecimento sobre os granitos arqueanos tem contribuído para identificar diferentes grupos de leucogranitos arqueanos - cálcico-alcalinos, fortemente peraluminosos e alcalinos (Sylvester, 1994). As diversidades geoquímicas sugerem distintos ambientes geodinâmicos para a gênese dessas rochas (Sylvester, 1994). Admite-se, em geral, que sejam derivadas de fusão parcial de granitóides similares às associações TTG arqueanas ou de rochas sedimentares, ou ainda através da cristalização fracionada de magmas do tipo TTG (Condie & Hunter 1976, Cassidy et al., 1991, Kröner 1991, Kröner & Layer 1992, Ridley 1992, Sylvester 1994, Davis et al., 1994).

Um grupo especial de granitóides arqueanos cuja composição é dominada por granitos e granodioritos, apresentando várias características geoquímicas similares aquelas das típicas suítes TTG, foi recentemente introduzido na literatura. Essas rochas são caracterizadas pelo forte fracionamento de elementos terras rara pesados e ausência de anomalia negativa de Európio, porém quando comparadas com os TTG *stricto sensu,* exibem alto conteúdo de LILE e forte enriquecimento em K_2O e Rb com a diferenciação magmática. Esses granitóides são comuns em muitos terrenos arqueanos e sua colocação se deu tanto conteporaneamente (Por exemplo, suítes granito-granodiorito da Provincia Wyoming; Frost et al., 2006) como posteriormente (Por exemplo, granitos potássicos do craton Dharwar; Jayananda et al., 2006; granitos do Craton Pilbara craton; Champion & Smithies, 2007) em relação aquelas das típicas suítes TTG. O termo "TTG transicional" foi proposto por Champion & Smithies (2003) para descrever este grupo de rochas, inicialmente identificadas nos cratons de Pilbara e de Yilgarn, Austrália.

1.5 – ASSOCIAÇÕES TONALÍTICA-TRONDHJEMÍTICA-GRANODIORITICA (TTG) DO TERRENO GRANITO-*GREENSTONE* DE RIO MARIA.

Os granitóides das séries tonalíticas-trondhjemíticas-granodioríticas apresentam vastas ocorrências no TGGRM (Fig. 3), e foram estudados com diferentes enfoques nas áreas de Xinguara (Leite 2001, Leite et al., 2004), Marajoara e Pau D'Arco (Althoff 1996, Althoff et al., 2000, Oliveira et al., 2006), e leste de Bannach (Guimarães 2007). Esses granitóides possuem normalmente dimensões batolíticas, porém ocorrem também na forma de *stocks* e plutons (Leite 2001, Guimarães 2007).

Dall'Agnol et al. (2006), a partir de relações estratigráficas e dados geocronológicos, sugerem pelo menos duas gerações distintas para os granitóides TTG do TGGRM (Tabela 1). A primeira geração englobaria os TTGs formados entre 2,98 e 2,92 Ga, correspondendo aos TTGs mais antigos da região, sendo representada pelo Tonalito Arco Verde, com idades em zircões variáveis entre 2988 ± 5 Ma e 2948 ± 7 Ma (Macambira 1992; Rolando & Macambira 2002, 2003, Vasquez et al., 2008; Tabela 1) e pelo Complexo Tonalítico Caracol, com idades de 2948 ± 5 Ma a 2924 ± 2 Ma (Leite et al., 2004; Tabela 1). Esses granitóides são, até o momento, os mais antigos datados na Província Mineral de Carajás. Idades similares foram obtidas para TTGs supostamente do Complexo Xingu (2972 ± 16 Ma, Avelar et al., 1999; Tabela 1). No TGGRM, essas associações são cortadas por granitóides ricos em MgO do tipo sanukitóide, TTGs jovens, leucogranitos potássicos e granitos paleoproterozóicos da Suíte Jamon.

O Trondhjemito Água Fria que possui idade de 2864 ± 21 Ma (Leite et al., 2004) juntamente com o Trondhjemito Mogno cuja idade é de 2871 ± ? Ma (em titanita, Pimentel & Machado 1994) ou 2857±13 Ma (Pb-Pb por evaporação em zircão, Macambira et al., 2000) representam segundo esses autores, a geração mais nova de TTGs registrada no TGGRM (TTGs jovens, Tabela 1). Relações de campo na região de Xinguara mostram que o Trondhjemito Água Fria é intrusivo em granitóides do tipo Rio Maria (sanukitóides) e contemporâneo aos leucogranitos potássicos do tipo Xinguara (Leite 2001, Leite et al., 2004). Além dessas unidades, o Tonalito Parazônia (Huhn et al., 1988) também foi anteriormente englobado nesta associação de TTG mais jovens, no entanto, estudos petrográficos e geoquímicos detalhados foram recentemente realizados sobre esta unidade e permitiram associar suas rochas à Suite sanukitóde Rio Maria (Guimarães, submetido b). Vale ressaltar que o artigo que será obordado no próximo capítulo, apresentará as principais características petrográficas, as assinaturas geoquímicas e as

idades das suítes TTG do TGGRM. Além disso, discutirá a redefinição e o significado da geração mais nova de TTGs, com base no reposicionamento estratigráfico do Trondhjemito Mogno. O trabalho também exibirá dados geocronológicos inéditos sobre o Tonalito Mariazinha, unidade recentemente mapeada e caracterizada petragraficamente e geoquimicamente nos domínios do Trondhjemito Mogno (Guimarães et al., submetido a).

1.6 – GRANITOS ARQUEANOS DO TERRENO GRANITO-*GREENSTONE* DE RIO MARIA.

Os leucogranitos potássicos são representados pelos granitos Xinguara (Leite 1995, Leite 2001, Leite et al., 2004), Mata Surrão (Duarte et al., 1991, Duarte 1992, Althoff et al., 2000) e por *stocks* e *apófises* graníticas encontrados em contato com o *Greenstone Belt* de Identidade (Souza 1994), a sudoeste do Granito Bannach, a sudeste da cidade de Bannach e sudoeste da Agrovila Mata Geral (Almeida et al., 2008). Vários outros corpos de composição granítica identificados no Terreno Granito-*Greenstone* de Rio Maria também foram correlacionados aos granitos mencionados (Araújo et al., 1994). O Granito Mata Surrão é intrusivo no Tonalito Arco Verde (Duarte 1992, Althoff et al., 2000) e é cortado na sua porção oeste pelo Granito Anorogênico Bannach (Almeida et al. 2006). Em sua área tipo, forneceu idade de 2872 ± 10 Ma (Pb-Pb em rocha total, Lafon et al. 1994, Macambira & Lafon 1995, Tabela 1). O Granito Xinguara é intrusivo no Complexo Tonalítico Caracol e no Granodiorito Rio Maria e contemporâneo do Trondhjemito Água Fria, tendo fornecido uma idade de 2865 ± 1 Ma (Leite et al. 2004, Tabela 1).

Trabalhos de mapeamento geológicos recentes no TGGRM, aliados à estudos petrográficos e geoquímicos (Almeida et al., 2008, Dias, 2009, este trabalho) permitiram identificar dois novos grupos de leucogranitos arqueanos no TGGRM. O primeiro grupo aflora dominantemente na área de Pau D'Arco, e é representado pelos plutons Guarantã, Azulona e Trairão, ambos incluídos na Suíte Guarantã (Dias, 2009, este trabalho). *Stocks* e apófises mapeados nas áreas de Xinguara e Bannach e o Granodiorito Grotão exposto a sudoeste de Xinguara, apresentam rochas com características petrográficas e geoquímicas similares àquelas da Suíte Guarantã. Esse grupo é constituído dominantemente por biotita-leucogranodioritos e biotita-leucomonzogranitos porfiríticos, porém termos equigranulares ocorrem de modo subordinado. O segundo grupo de leucogranitos é representado pelo Granito Rancho de Deus (Almeida et al., 2008, Dias, 2009, este trabalho) que aflora a sudoeste da cidade de Pau D'Arco,

como um pluton com forma elíptica, cujo eixo maior está orientado na direção E-W e mede aproximadamente 12 km. O Granito Rancho de Deus é composto por rochas monzograniticas porfiríticas e a principal diferença em relação aos outros grupos de leucogranitos, é a constante presença de anfibólio modal. As características petrográficas e geoquímicas do Granito Rancho de Deus se aproxima aquelas da suíte sanukitóide Rio Maria (Almeida et al., 2008, Dias, 2009, este trabalho).

Os dados petrográficos, geoquímicos e geocronológicos dos leucogranitos potássicos, do grupo de leucogranodioritos+monzogranitos e do Granito Rancho de Deus, serão apresentados e discutidos no capítulo 3, referente ao artigo sobre as suítes de granitos arqueanos do TGGRM. Com base na geologia e nas características petrográficas e geoquímica do grupo de leucogranodioritos+monzogranitos, será apresentada no capítulo 4 (artigo 3), uma discussão detalhada sobre as possíveis fontes e os processos petrogenéticos que deram origem a estas rochas.

1.7 - APRESENTAÇÃO DO PROBLEMA

As informações sobre as associações TTG e as suítes de leucogranitos arqueanos são oriundas de mais de 25 anos de pesquisas no Terreno Granito-*Greenstone* de Rio Maria, realizadas, em sua maioria, pelo Grupo de Pesquisa de Petrologia de Granitóides juntamente com pesquisadores do Laboratório de Geologia Isotópica do Centro de Geociências, ambos da Universidade Federal do Pará (Medeiros 1987, Souza et al. 1990, Macambira 1992, Duarte 1992, Souza 1994, Pimentel & Machado 1994, Althoff 1996, Dall'Agnol et al. 1996, Macambira & Lancelot 1996, Leite & Dall'Agnol 1997, Dall'Agnol et al. 1997, 2006, Althoff et al., 2000, Souza et al. 2001, Leite 2001, Leite et al 2004, Oliveira 2005, Oliveira et al. 2009). Esses trabalhos contribuíram para individualizar várias unidades, anteriormente vinculadas ao Complexo Xingu, gerando um expressivo acervo de dados de campo, petrográficos, geoquímicos e geocronológicos. Apesar do avanço do conhecimento científico sobre esta região, no momento da proposição desta tese, havia uma série de questões sem respostas sobre a evolução geológica do TGGRM, dentre as quais podemos destacar:

1) A maioria dos trabalhos efetuados no TGGRM buscou identificar e caracterizar as diferentes unidades, suas distribuições geográficas e seus posicionamentos estratigráficos. Foram

obtidos, assim, avanços importantes no conhecimento da evolução geológica e da história deformacional de segmentos isolados do Terreno Granito-*Greenstone* de Rio Maria. Não havendo, no entanto, nenhum trabalho de integração consolidado, englobando os dados gerados nos diferentes segmentos do TGGRM, que tenha levado à proposição de um modelo de evolução geológica de cunho regional, baseado em conceitos atuais sobre a gênese e evolução de terrenos arqueanos.

2) Estudos geológicos, petrográficos, geoquímicos e geocronológicos sobre o Trondhjemito Mogno eram muito limitados, ocasionando um flagrante desnível de conhecimento entre esta unidade e as demais pertencentes às séries TTG do TGGRM. Embora se tenha assumido nos mapas geológicos regionais que os TTG antigos ocorreriam a sul da cidade de Bannach (Tonalito Arco Verde) e os jovens a norte desta cidade (Santos & Pena Filho 2000; CPRM, 2004), a ausência de um maior detalhamento da geologia da área de ocorrência do Trondhjemito Mogno, causava dúvidas quanto ao posicionamento do limite entre os domínios das séries TTG antigas e jovens no TGGRM, além disso, havia questionamentos sobre a homogeneidade do Trondhjemito Mogno.

3) Embora, o *stock* TTG aflorante a leste de Bannach (Guimarães 2007), tenha tido suas rochas bem caracterizadas em termos petrográficos e geoquímicos, necessitava-se de dados geocronológicos a fim de testar a hipótese de sua associação temporal com os TTG jovens do TGGRM. Por fim, não se dispunha de mapeamento geológico, acompanhado de estudos petrográficos, geoquímicos e geocronológicos, na área de ocorrência do Tonalito Parazônia, de modo que esta unidade não se encontrava bem definida, nem tampouco o seu papel na evolução do TGGRM.

Portanto era necessário, o refinamento dos dados petrográficos, geoquímicos e principalmente geocronológicos para entender a real distribuição da geração mais nova de granitóides TTG e o seu significado na evolução geológica e tectônica do Terreno Granito-Greenstone de Rio Maria.

4) Dados geocronológicos forneceram para a geração mais antiga de TTGs do TGGRM idades variáveis num intervalo de 60 Ma (entre 2,98 e 2,93 Ga; Tabela 1). Como as idades em torno de 2,93 Ga, se tornavam cada vez mais comuns (cf. Tabela 1), surgiu a indagação se esses TTG eram relacionados efetivamente a um único evento ou se não haveria

duas ou mais gerações de TTGs anteriores à formação dos TTGs com idade de 2,87 Ga. Seria, portanto, necessário o refinamento de dados de campo, petrográficos e geoquímicos, integrados com novos dados geocronológicos, a fim de melhor caracterizar essas rochas e testar a hipótese de existência de diferentes gerações de TTGs com mais de 2,90 Ga no TGGRM.

Em vários crátons do mundo (Barberton, Moyen et al., 2007; Pilbara, Champion & Smithies, 2007; Karelia, Käpyaho et al., 2006), os granitóides TTG foram gerados a partir de eventos magmáticos intervalares durante o arqueano e, por vezes em diferentes ambientes geodinâmicos (por exemplo, os TTGs de Barberton, Moyen et al., 2007). Havia, portanto, a necessidade de se verificar se esse quadro era repreduzido no caso do Terreno Granito-*Greenstone* de Rio Maria.

5) Alguns autores (Smithies & Champion 2000, Martin & Moyen 2002) defendem a hipótese de que a origem de TTGs por fusão de crosta máfica hidratada espessada tectônicamente (processo de sagducção) ou por subducção de baixo ângulo só foi possível no início do Arqueano (> 3,5 Ga), quando a temperatura da terra era suficientemente alta. No meio (3,5 – 3,0 Ga) e final (< 3,0 Ga) do Arqueano, as fusão aconteceriam em mais altas profundidades, o que se refletiria em valores mais elevados de #Mg, Cr e Ni, resultados de diferentes graus de interação com o manto, e, ainda, maiores conteúdos de Sr em resposta à ausência do plagioclásio da fonte, devido à sua desestabilização a mais altas pressões. As características químicas contrastantes dos TTGs de diferentes períodos do Arqueano, sugeridas por Martin & Moyen (2002), demonstram que o aumento do conhecimento sobre as associações TTG do Terreno Granito-*Greenstone* de Rio Maria era imprescindível na construção de modelos geodinâmicos para esta porção do Cráton Amazônico, bem como no entendimento dos processos de formação das rochas sanukitóides e leucogranitos arqueanos. Além disso, o refinamento geoquímico dessas rochas pertimitiria estabelecer comparações com TTGs aflorantes de outros terrenos arqueanos.

6) O mapeamento geológico na área de Pau D'Arco (Almeida et al., 2008) permitiu a identificação de expressivas ocorrências de leucogranitos arqueanos com texturas e feições deformacionais bastante variadas em uma extensa área, além disso, possibilitou o reconhecimento do Granito Rancho de Deus, anteriormente tido como anorogênico. Naquele momento, os dados petrográficos e geoquímicos sugeriram que estas rochas apresentavam diferenças em relação aos

leucogranitos potássicos tipo Xinguara e Mata Surrão, e que o Granito Rancho de Deus não mostrava assinatura geoquímica compatível com aquelas dos granitos anorogênicos de Rio Maria (Almeida et al., 2008, Dias, 2009). Portanto, era necessário um estudo petrográfico, geoquímico e geocronológico minucioso sobre estas rochas, que permitiria comporações mais detalhados com os leucogranitos potássicos.

Desse modo, no momento da proposição deste trabalho, havia inúmeros questionamentos acerca da evolução do Terreno Granito-*Greenstone* de Rio Maria, dentre os que os quais podemos destacar:

1 A- Quantos eventos de geração de granitóides TTG houveram no TGGRM?

1 B – As rochas que afloram nos domínios do batólito trondhjemítico Mogno são homogêneas em termos petrográficos, geoquímicos e geocronológicos? Qual é a real representatividade da geração mais nova de granitóides TTG (~2,87 Ga)? Qual é o significado destas rochas na evolução geológica do TGGRM?

1 C – Há alguma evidência de mudança geoquímica substantiva nas associações TTG ao longo do tempo? Os TTGs antigos diferem geoquimicamente dos TTGs jovens? As assinaturas geoquímicas dos TTGs do TGGRM se assemelham a quais grupos de TTGs arqueanos?

1 D – Pode a assinatura geoquímica dos TTGs contribuir para esclarecer o seu ambiente tectônico de formação? Em se admitindo a hipótese de derivação a partir da fusão parcial de uma crosta oceânica subductada, qual seria a inclinação da placa subductante e quais seriam as implicações disso na evolução do TGGRM?

1 E – Qual é a idade real e as características geoquímicas e petrológicas do Tonalito Parazônia? Este corpo corresponde efetivamente a uma unidade distinta dos demais TTGs do TGGRM? Em caso positivo, qual seu significado na evolução do TGGRM?

2 A – Há mais de um grupo de leucogranitos cálcico-alcalinos arqueanos no TGGRM? Caso exista, eles foram gerados conteporaneamente? Eles podem ser diferenciados por suas idades e características estruturais, petrográficas e geoquímicas? Em que ambiente geodinâmico foram originados? Quais foram as fontes e os processos petrogenéticos que deram origem às suas rochas?

2 B – Como explicar a formação aproximadamente contemporânea de TTGs jovens, sanukitóides e leucogranitos? Qual a influência dos magmas TTG e sanukitóides na gênese dos leucogranitos?

3 A – Qual o ambiente tectônico em que se deu a evolução do TGGRM?

3 B – Como se deu a passagem entre o período de formação das associações com idades de 2,98 a 2,93 Ga e as associações mais jovens formadas em torno de 2,87 Ga? O regime tectônico foi o mesmo ao longo desse período de ca. 100 Ma ou mudou ao longo do tempo?

3 C – A evolução tectônica foi controlada essencialmente por processos de subducção ao longo de arcos magmáticos em que se deu a subducção de crosta oceânica, correspondente às associações basálticas formadoras dos *greenstone belts*, ou processos de sagducção também contribuíram para a evolução do TGGRM? Se houve a atuação de mais de um processo, como eles se distribuíram ao longo do tempo? Em outras palavras, a evolução tectônica foi dominada por tectônica horizontal ou tectônica vertical também foi importante?

3 D – Como o ambiente tectônico se refletiu na origem e petrogênese das associações magmáticas presentes no TGGRM?

3 E - Quais as fontes e processos responsáveis pela formação dessas associações magmáticas?

1.8 – OBJETIVOS

Os objetivos centrais desta tese é esclarecer os processos petrogenéticos responsáveis pela geração dos magmas formadores dos granitóides arqueanos do TGGRM, em particular dos granitóides da série TTG e dos leucogranitos calcico-alcalinos arqueanos, bem como entender o papel destes na evolução crustal deste segmento do Cráton Amazônico. Isso contribuíra para elaborar um quadro geológico integrado do TGGRM e propor um modelo de evolução geológica e tectônica baseado em conceitos atuais sobre a gênese e evolução de terrenos arqueanos.

Para tanto, os estudos realizados durante o desenvolvimento da tese visaram alcançar os seguintes objetivos específicos:

- Realizar estudos petrográficos, geoquímicos e geocronológicos na área do Trondhjemito Mogno, buscando definir com maior exatidão seus limites, idade e posicionamento estratigráfico (Este trabalho foi realizado em colaboração com a dissertação de mestrado de Fabriciana Vieira Guimarães);
- Aprofundar a caracterização petrográfica, geoquímica e geocronológica do Tonalito Arco Verde, bem como verificar o número e a idade dos ciclos de geração de granitóides TTG que por ventura compunha esta unidade (Este trabalho contou com a colaboração da pesquisa de iniciação científica de Manoel Augusto C. Costa);

- Reavaliar os dados geológicos, petrográficos e geoquímicos disponíveis sobre o Complexo Tonalítico Caracol e refinar a sua caracterização geoquímica;
- Estabelecer comparações entre as diferentes unidades TTG do TGGRM e destas com associações análogas de outros terrenos arqueanos;
- Aprofundar o estudo de leucogranitos calcico-alcalinos arqueanos na área de Pau D'Arco e no Granito Rancho de Deus, definir suas distribuições geográficas, idades e posicionamento estratigráfico (Este trabalho foi realizado em colaboração com a dissertação de mestrado de Samantha Barriga Dias);
- Efetuar comparações entre os leucogranitos calcico-alcalinos arqueanos do TGGRM, e destes com leucogranitos arqueanos aflorantes em outros cratons;
- Propor um modelo geodinâmico que explique a origem das diferentes gerações dos granitóides TTG e dos leucogranitos arqueanos do TGGRM, com base em conceitos atuais sobre os ambientes tectono-termais reinantes ao longo do arqueano.

1.9 - MATERIAIS E MÉTODOS

Para alcançar os objetivos propostos foram utilizados vários métodos e técnicas de investigação, relacionadas ao tema e compatíveis com os assuntos abordados.

1.9.1 – **Pesquisa Bibliográfica**

Existem inúmeros trabalhos com diferentes enfoques publicados sobre a região de Rio Maria, sendo que a quase totalidade destes foi consultada e seus dados compilados de acordo com a sua importância para o desenvolvimento do presente trabalho. Além disso, foram analisados artigos e livros sobre temas que abordam à geologia de terrenos arqueanos, com ênfase em evolução estrutural, petrologia, geoquímica, geocronologia e geoquímica isotópica.

1.9.2 – **Mapeamento Geológico**

Na região de Rio Maria, foram realizadas diversas pesquisas de iniciação científica, trabalho de conclusão de curso (TCC) de graduação, mestrado e doutorado, todos ligados ao Grupo de Pesquisa Petrologia de Rochas Granitóides (GPPG) da Universidade Federal do Pará (UFPA). Vários mapas geológicos foram gerados a partir desses trabalhos, porém em diferentes escalas. Esses mapas foram integrados e convertidos pelo autor, do formato analógico para digital

tendo sido configurados em uma base georeferenciada, sendo ajustados ao mosaico GeoCover 2000 (NASA) em valores geodésicos com datum WGS-84, dentro da filosofia de SIG geológico e banco de dados. Todos os arquivos gerados a partir dos mapeamentos geológicos, e das interpretações em imagens de radar e de levantamentos aerogeofísicos, foram digitalizados em ambiente SIG utilizando o programa *ESRI® ArcGis™ 9.1*.

As interpretações preliminares do acervo de dados, anteriormente obtidos pelos pesquisadores do GPPG, sobre a petrografia, geoquímica e geocronológica das unidades arqueanas, em particular das associações TTG e dos leucogranitos calcico-alcalinos, alvo da presente pesquisa, permitiram definir áreas chaves para o entendimento do quadro geológico regional destas unidades e verificar a importância de suas rochas na evolução geológica do Terreno Granito-*Greenstone* de Rio Maria.

Durante o desenvolvimento desta tese foram realizadas cinco etapas de campo nas seguintes áreas críticas:

1) *Área de Pau D'Arco* – foram realizadas duas etapas de mapeamento geológico na área de Pau D'Arco e dentre as principais contribuições para o avanço do conhecimento geológico nesta região podemos destacar: a) O prolongamento dos domínios do Tonalito Arco Verde para a porção sudoeste do Granito Bannach; b) A constatação de uma grande extensão areal de leucogranitos com texturas bastante variadas e diferentes daquelas apresentadas pelos leucogranitos potássicos do tipo Mata Surrão e Xinguara. *Stocks* leucograníticos também foram reconhecidos na porção sudoste da cidade de Pau D'Arco; b) O reconhecimento do *pluton* granítico Rancho de Deus como produto do magmatismo leucogranítico durante o Arqueano, uma vez que o mesmo era tido como anorogênico de idade paleoproterozóico (Santos & Pena Filho 2000), possivelmente afim daqueles da Suíte Jamon. A caracterização petrográfica e geoquímica dos leucogranitos arqueanos calcico-alcalinos na área de Pau D'Arco foi feita em colaboração com a pesquisa de mestrado de Samantha Barriga Dias. Vale ressaltar, que o trabalho de mapeamento geológico na área de Pau D'Arco foi um dos objetivos principais do Projeto Geobrasil (convênio entre UFPA/CPRM), que foi firmado em 2005 e consistiu da prestação de serviços de mapeamento geológico e levantamento de recursos minerais na Folha Marajoara (SB-22-Z-C V) por parte da UFPA (Almeida et al., 2008). O autor desta tese juntamente com outros pesquisadores pertencentes ao Grupo de Pesquisa Petrologia de Granitóides (GPPG) e ao Laboratório de Geologia Isotópica do Centro de Geociências/UFPA

foram responsáveis pela execução deste projeto, sob a coordenação do professor Roberto Dall'Agnol;

2) *Área de Bannach* - Na campanha de campo realizada na área de Bannach, um pluton com direção NNW constituído de granitóides tonalíticos-trondhjemíticos, afim das associações TTG que afloram em outras áreas do TGGRM, e um *stock* composto por rochas leucograníticas com texturas muito similares aquelas dos leucogranitos que ocorrem na área de Pau D'Arco, foram identificados na porção leste do município de Bannach. Os estudos petrográficos e geoquímicos dos granitóides TTG e das rochas leucograníticas foram realizados em colaboração com os trabalhos de iniciação científica de Fabriciana Vieira Guimarães e Samantha Barriga Dias, respectivamente;

3) *Área de ocorrência do Trondhjemito Mogno* – O mapeamento geológico nesta área, foi fundamental para definir com maior exatidão os limites do Trondhjemito Mogno e reconhecer novas unidades, como é o caso do Tonalito Mariazinha e o Granodiorito Grotão. Além disso, o mapeamento geológico das rochas do Tonalito Parazônia foi aprimorado. O resultado do mapeamento geológico, e a caracterização petrográfica e geoquímica das rochas da área de ocorrência do Trodhjemito Mogno, foi o objetivo da dissertação de mestrado de Fabriciana Vieira Guimarães e exibido na forma de dois artigos científicos submetidos à Revista Brasileira de Geociência, cujo os temas foram "Caracterização geológica, petrográfica e geoquímica do Trondhjemito Mogno e Tonalito Mariazinha, Terreno Granito-*Greenstone* de Rio Maria – Pará" e "Geologia, petrografia e geoquímica do Quartzo-Diorito Parazônia e Granodiorito Grotão, Terreno Granito-*Greenstone* de Rio Maria – Pará", com co-autoria de José de Arimatéia Costa de Almeida, entre outros.

4) *Etapa de campo para coleta de amostras para estudos geocronológicos* – Com base na integração e intepretação dos dados de campo, petrográficos, geoquímicos e geocronológico preexistentes e naqueles originados durante o desenvolvimento da tese, foi realizada uma viagem de campo voltada para coleta de amostras das diferentes associações TTG e de leucogranitos para estudos geocronológicos em áreas críticas para o entendimento do quadro geológico regional dessas unidades no TGGRM.

Os trabalhos de mapeamento geológico foram geralmente realizados nas escalas de 1:100.000 ou 1:50.000, e a sistemática desses trabalhos consistiu em levantamento de perfis e

coleta sistemática e criteriosa de amostras ao longo das estradas e caminhos existentes, além de eventuais caminhamentos, utilizando como apoio, imagens de radar, satélite e de levantamentos aereogeofísicos (magnetometria e radiometria) e imagens com superposição de dados aereogeofísicos e de sensores remotos. Os pontos de amostragem foram alocados através do aparelho GPS (Global Position System) e plotados em base georeferenciada.

1.9.3 – **Petrografia**

Os dados petrográficos sobre as associações TTG e de leucogranitos calcico-alcalinos arqueanos, anteriormente obtidos por pesquisadores do GPPG, foram revisados com o intuito de reavaliar a distribuição e uniformização das rochas em cada unidade. As descrições petrográficas e a análise textural em amostras oriundas de porções do TGGRM que foram mapeadas durante a execução deste trabalho, envolveram o reconhecimento das fases minerais, suas relações de contato, forma, presença de inclusões, estruturas de deformação, bem como suas relações de equilíbrio com as outras fases presentes, caracterização de paragêneses magmáticas e pós-magmáticas, e definição da ordem de cristalização magmática. Isso permitiu classificar e melhor caracterizar as diversas rochas estudadas, seguindo as recomendações da Comissão do IUGS (Streckeisen 1976, Le Maitre et al. 2002).

1.9.4 – **Geoquímica**

Os dados químicos foram reorganizados, integrados e alidos aos estudos geológicos e petrográficos, objetivando-se obter uma visão clara e integrada da relação dos dados petrográficos e geoquímicos das associações TTG e de leucogranitos calcico-alcalinos arqueanos, o que permitiu discriminar e classificar com maior segurança as diversas unidades do TGGRM, bem como compará-las com outros granitóides. Para tanto, foram seguidos os princípios gerais descritos em Ragland (1989) e Rollison (1993), inicialmente com a utilização de diagramas de variação do tipo Harker (1965), envolvendo os óxidos maiores plotados contra sílica (índice de diferenciação), bem como diagramas de elementos binários, contrapondo elementos ou razões de elementos incompatíveis, tais como K, Rb, Ba, Sr, U, Th, Nb, Y, Zr, K/Rb, Sr/Ba, Rb/Sr, Nb/Y, Rb/Zr. Diagramas de terras raras foram utilizados para comparar as assinaturas geoquímicas das diferentes unidades.

1.9.5 – **Geocronologia**

Além das diversas datações realizadas nas unidades do TGGRM, as quais colaboraram para esclarecer o posicionamento estratigráfico das mesmas, foram selecionadas para estudo geocronológico amostras representativas de granitóides TTG e de leucogranitos, de modo a definir a idade dessas amostras e enquadrá-las em suas respectivas unidades. Para isso foram realizadas análises geocronológicas utilizando os métodos Pb-Pb em zircão por evaporação (Pará-Iso) e U-Pb em zircão por meio de LAN-ICPMS (espectrômetros de massa com fonte de plasma e sistema de multicoletores e de ablação a laser) no laboratório da Universidade de Brasília. A descrição dos procedimentos analíticos para obtenção dos dados geocronológicos por Pb-Pb em zircão por evaporação e U-Pb em zircão por meio de LAN-ICPMS, são descritos em detalhe nos capítulos 2 e 3.

Capítulo – 2

Zircon geochronology and geochemistry of the TTG suites of the Rio Maria granite-greenstone terrane: Implications for the growth of the Archean crust of Carajás Province, Brazil.

José de Arimatéia Costa de Almeida
Roberto Dall'Agnol
Marcelo Augusto de Oliveira
Moacir José Buenano Macambira
Márcio Martins Pimentel
Osmo Tapani Rämö
Fabriciana Vieira Guimarães
Albano Antonio da Silva Leite

Submetido: Precambrian Research

Dear Mr. ALMEIDA,

Your submission entitled "Zircon geochronology and geochemistry of the TTG suites of the Rio Maria Granite-Greenstone terrane: Implications for the growth of the Archean crust of the Carajás Province, Brazil" has been received by Precambrian Research

Please note that submission of an article is understood to imply that the article is original and is not being considered for publication elsewhere. Submission also implies that all authors have approved the paper for release and are in agreement with its content.
You will be able to check on the progress of your paper by logging on to http://ees.elsevier.com/precam/ as Author.

Your manuscript will be given a reference number in due course.

Thank you for submitting your work to this journal.

Kind regards,

Precambrian Research

Zircon geochronology and geochemistry of the TTG suites of the Rio Maria Granite-Greenstone terrane: Implications for the growth of the Archean crust of the Carajás Province, Brazil.

José de Arimatéia Costa de Almeida[1,2] (ari@ufpa.br); Roberto Dall'Agnol[1,2] (robdal@ufpa.br); Marcelo Augusto de Oliveira[1,2] (mao@ufpa.br); Moacir José Buenano Macambira[2,4] (moamac@ufpa.br); Márcio Martins Pimentel (marcio@unb.br)[4]; Osmo Tapani Rämö (tapani.ramo@helsinki.fi)[5]; Fabriciana Vieira Guimarães[1,2] (fabricia@ufpa.br); Albano Antonio da Silva Leite (albano@ufpa.br)[1].

[1]Grupo de Pesquisa Petrologia de Granitóides, Instituto de Geociências (IG), Universidade Federal do Pará (UFPA), Caixa Postal 8608, CEP 66075-100, Belém, Pará, Brasil.
[2]Programa de Pós-Graduação em Geologia e Geoquímica – IG – UFPA.
[3]Laboratório de Estudos Geodinâmicos da Universidade de Brasília.
[4]Laboratório de Geologia Isotópica – IG – UFPA.
[5]Department of Geosciences and Geography, University of Helsinki.

ABSTRACT

TTG suites are the most voluminous granitoid rocks exposed in the Mesoarchean Rio Maria granite-greenstone terrane (RMGGT), southeastern Amazonian craton. Extensive field work in key areas of the RMGGT, integrated with petrographic, geochemical, and geochronological studies, the latter employing the Pb-Pb evaporation and U-Pb LA-ICP-MS on zircon techniques, indicates that the TTG magmatism in the RMGGT can be divided into three episodes: (I) The first at 2.96±0.2 Ga (the older rocks of the Arco Verde tonalite and the Mogno trondhjemite); (II) the second at 2.93±0.1 Ga (Caracol tonalitic complex, Mariazinha tonalite, and the younger rocks of the Arco Verde tonalite); and (III) the third at 2.86±0.1 Ga (Agua Fria trondhjemite). The new data demonstrate that the Mogno trondhjemite is significantly older than previously admitted, reveal the existence of a new TTG suite (Mariazinha tonalite) and indicate that the volume of TTG suites formed during the 2.86 event was relatively small. The Arco Verde tonalite yielded significant age variations (2.98 to 2.93 Ga) but domains with different ages could

not be individualized. The tonalitic-trondhjemitic suites of the RMGGT derived from sources geochemically similar to the metabasalts of the Andorinhas supergroup that were extracted from the mantle during the Mesoarchean (3.0 to 2.9 Ga) and with a short time of crustal residence.

Three groups of TTG granitoids were distinguished in Rio Maria: 1) high-La/Yb group, with high Sr/Y and Nb/Ta ratios, derived from magmas generated at relatively high pressures (>1.5 GPa) from sources leaving garnet and amphibole as residual phases; 2) medium-La/Yb group with magmas formed at intermediate pressure conditions (~1.0-1.5 GPa), but still in the garnet stability field; and 3) low-La/Yb group, with low Sr/Y and Nb/Ta ratios, crystallized from magmas generated at lower pressures (≤1.0 GPa), from an amphibolitic source that left plagioclase as a residual phase. These three geochemical groups do not have a direct correspondence with the three episodes of TTG generation and a same TTG unit can be composed of rocks of different groups.

A model involving a hot subduction zone underneath a thick oceanic plateau was envisaged to explain the tectonic evolution of the RMGGT. In this context, the low-La/Yb group was formed from magmas originated by the melting of the base of a thickened basaltic oceanic crust at comparatively lower pressures (ca. 1.0 GPa), whereas the medium- and high-La/Yb groups were derived from the slab melting at increasing different pressures (1.0-1.5 and > 1.5 GPa, respectively). Part of these TTG magmas react during their ascent with the mantle wedge being totally consumed and leaving a metassomatized mantle. 50 m. y. later, at ca. 2870 Ma, thermal events, possibly related to slab-break-off and asthenosphere mantle upwelling or to a mantle plume, may have induced melting of the metassomatized mantle and the generation of sanukitoid magmas. These magmas may have heated the base of the Archean continental crust and could have lead to the local melting of the basaltic crust, forming the Água Fria trondhjemite magma.

Keywords: Amazonian craton, Rio Maria granite-greenstone terrane, Mesoarchean, TTG suites, petrology.

1. Introduction

Tonalite-trondhjemite-granodiorite (TTG) associations constitute ~50 % of the surface rocks exposed in Archean cratons (Condie, 1993). The TTG associations are the oldest felsic components of cratons and generally correspond to the gneissic basement of preserved Archean continental crust or, occasionally, also form individual, syn- to post-tectonic plutons (Barker and Arth, 1976; Barker, 1979; Martin, 1987, 1994; Bickle et al., 1993; Kröner et al., 1996; Martin et al., 1997; Althoff et al., 2000; Souza et al., 2001; Champion and Smithies, 2007; Moyen et al., 2007). The TTG magmatism represents the transition from a dominantly mafic crust to a crust with a significant felsic component (Glikson, 1979). Crustal stabilization and cratonisation are believed to have developed in short, intense episodes of continental growth, involving magmatic accretion (e.g. Wells, 1981), tectonic thickening and, sometimes, high-grade metamorphism (e.g. De Wit, 1998). As a result, the TTG rocks form an essential element in the 'protocontinental' stage of crustal evolution (Barker, 1979).

TTG suites are the most voluminous granitoid rocks also in the Mesoarchean Rio Maria granite-greenstone terrane (RMGGT) in the southern part of the Carajás province, the largest Archean domain of the Amazonian craton (Althoff et al., 2000; Souza et al., 2001; Leite et al., 2004; Dall'Agnol et al., 2006; Vasquez et al., 2008). These rocks were not affected by superimposed younger events and generally preserve their textural igneous features (Althoff et al., 2000; Leite, 2001; Souza et al., 2001; Guimarães et al. a, submitted), therefore allowing a good opportunity for a detailed study of the original composition and comprehensive petrogenesis of TTG magmas. In spite of their location in the Amazonian craton, the studied rocks are relatively well exposed because they occur in dominantly deforested areas and fresh samples are available. In this paper we refine the characterization of the TTG suites of the RMGGT based on recent field work, petrography, new whole rock geochemical data and zircon geochronology. The results allow us to discuss the geochemical signature, timing of TTG magmatic events and the implications for crustal evolution of the RMGGT.

2. Geological setting

The Amazonian craton has been subdivided into several geochronological provinces that have distinct ages, structural patterns and geodynamic evolution (Tassinari and Macambira, 2004; Santos et al., 2006). According to the model of Tassinari and Macambira (2004), the Central Amazonian province (Fig. 1a) is the oldest province of the Amazonian Craton (>2.5 Ga) and is divided in two main tectonic blocks, Carajás and Xingu-Iricoumé. Santos et al. (2006) considered the Archean Carajás block as an independent tectonic province, however, there is consensus that the Carajás region is the most important Archean province of the Amazonian craton. Two distinct domains have been clearly distinguished in that province (Fig. 1b; Souza et al., 1996; Althoff et al., 2000; Dall'Agnol et al., 2000, 2006; Santos et al., 2006; Vasquez et al., 2008): The Mesoarchean Rio Maria granite-greenstone terrane (3.0 to 2.86 Ga; Machado et al., 1991; Macambira and Lafon, 1995; Macambira and Lancelot, 1996; Althoff et al., 2000; Souza et al., 2001; Leite et al., 2004; Dall'Agnol et al., 2006) and the Neoarchean Carajás domain (2.76 to 2.54 Ga; Machado et al., 1991; Huhn et al., 1999; Barros et al., 2004; Sardinha et al., 2006). The available data indicate that the basement of the Carajás domain was originated in a similar period as the RMGGT (Macambira and Lafon, 1995; Tassinari and Macambira, 2004; Dall'Agnol et al., 2006). However, the northern domain would differ from the RMGGT by the fact that it was affected by Neoarchean continental rifting (Gibbs et al., 1986; Macambira, 2003) that originated the Carajás basin, filled by large volume of mafic flows and banded iron formations, metamorphosed and intensely deformed during the subsequent closure of the basin. Dall'Agnol et al. (2000, 2006) admitted also the existence of a Transition domain (Fig. 1b) between the Carajás Basin and the RMGGT. The Transition domain, poorly known so far, is interpreted as a terrane originally similar to the RMGGT that was intensely affected by the Neoarchean magmatic and tectonic events recorded in the Carajás domain. As an alternative hypothesis, it was proposed that the Neoarchean Carajás domain corresponds to a magmatic arc related to subduction processes (Meirelles and Dardenne, 1991; Teixeira and Eggler, 1994; Lobato et al., 2006; Silva et al., 2006).

Although tonalitic-trondhjemitic associations have also been recognized in the Transition domain (Gomes et al., 2007; Feio, 2009), in this paper emphasis will be put on the typical Archean TTG suites that occur in the RMGGT (Figs. 1b, 2). The lithologies of the RMGGT

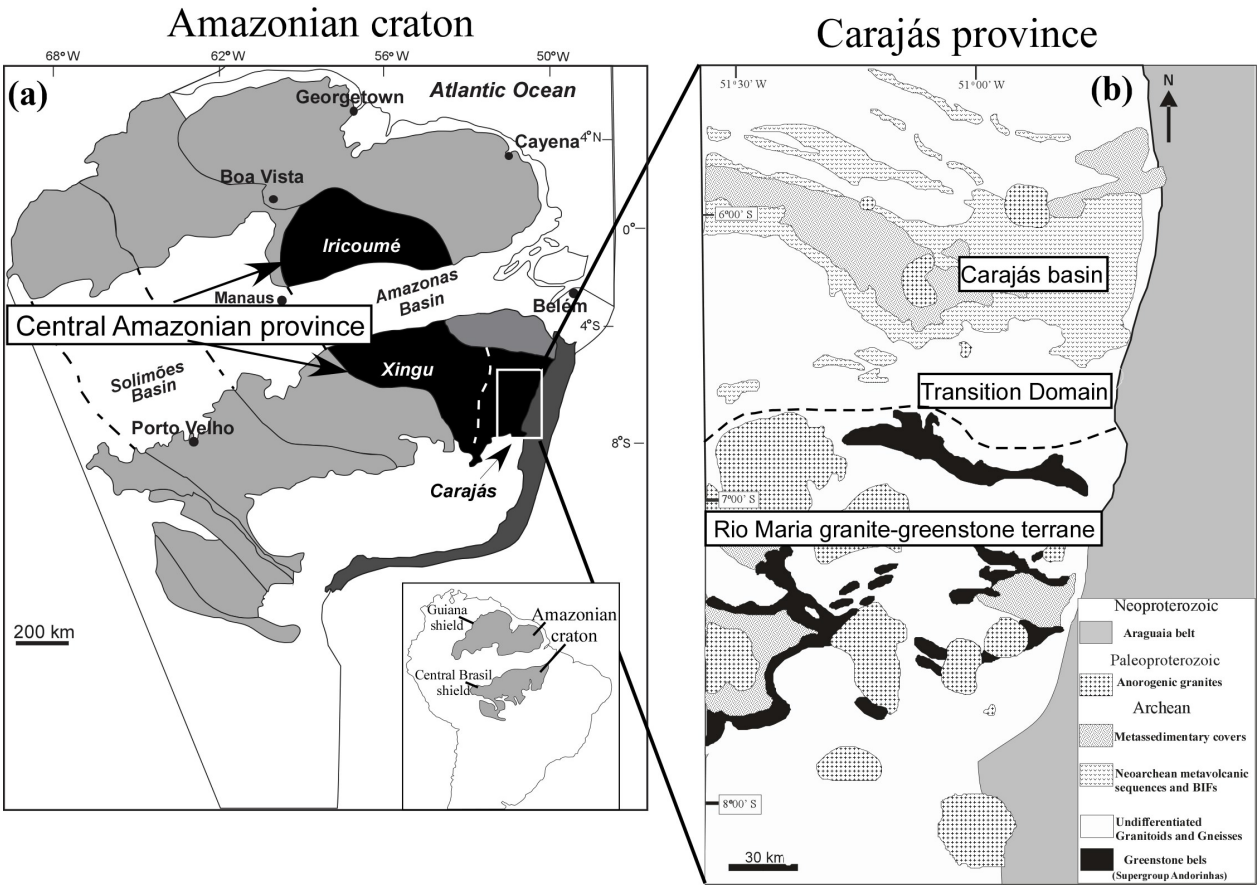

Figure 1 - a) Simplified sketch map of the Amazonian craton showing the geochronological provinces according to proposals of Tassinari and Macambira (2004) and b) Geological sketch map of the Carajás province showing the Mesoarchean Rio Maria granite-greenstone terrane, Neoarchean Carajás and Transition domains.

(Fig. 2) are similar in their broad aspects to those found in other Archean terranes of the world. That terrane is composed of greenstone belts consisting of meta-ultramafic (komatiites), dominant metamafic (basalts and gabbros) rocks and subordinate intermediate to felsic rocks, with intercalations of metagraywackes, all grouped into the Andorinhas supergroup (Docegeo, 1988; Huhn et al., 1988; Souza et al., 2001). These rocks are intruded by a variety of Archean granitoids (Dall'Agnol et al., 2006) originated between 2.98 and 2.86 Ga (Table 1). Four groups of granitoids have been distinguished (Dall'Agnol et al., 2006 and references therein): (1) An older TTG series (2.98– 2.93 Ga) represented by the Arco Verde tonalite (AVT) and the Caracol tonalite complex (CTC); (2) The Rio Maria sanukitoid suite (~2.87 Ga; Oliveira et al., 2009) composed dominantly by granodiorites, with associated mafic and intermediate rocks, forming

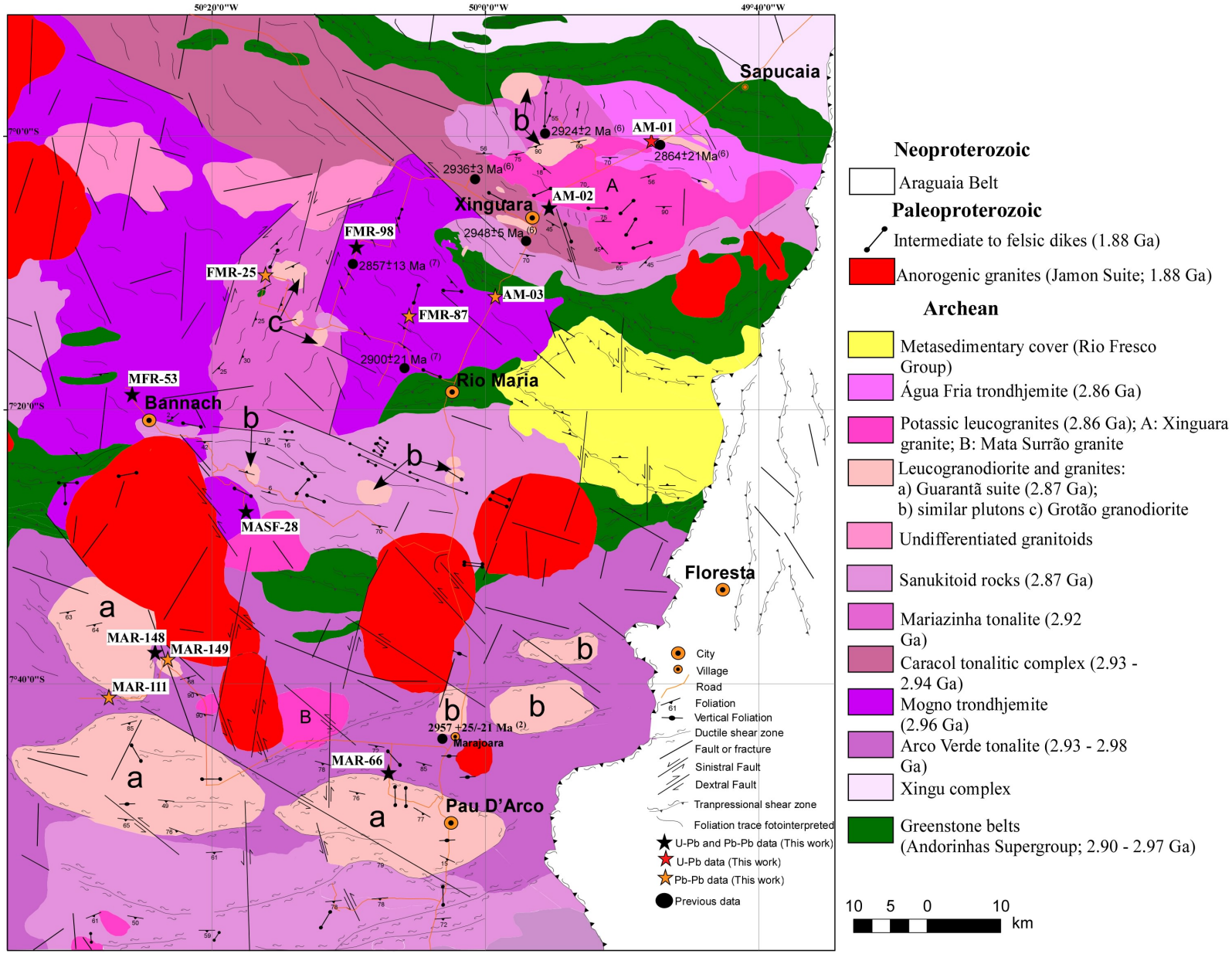
50°20'0"W
50°0'0"W
49°40'0"W
7°0'0"S
7°20'0"S
7°40'0"S
Sapucaia
Xinguara
Rio Maria
Bannach
Floresta
Pau D'Arco
Marajoara
AM-01
AM-02
AM-03
FMR-98
FMR-25
FMR-87
MFR-53
MASF-28
MAR-148
MAR-149
MAR-111
MAR-66
2924±2 Ma (6)
2864±21Ma(6)
2936±3 Ma(6)
2948±5 Ma (6)
2857±13 Ma (7)
2900±21 Ma (7)
2957 +25/-21 Ma (2)
A
B
C
a
b
City
Village
Road
Foliation
Vertical Foliation
Ductile shear zone
Fault or fracture
Sinistral Fault
Dextral Fault
Tranpressional shear zone
Foliation trace fotointerpreted
U-Pb and Pb-Pb data (This work)
U-Pb data (This work)
Pb-Pb data (This work)
Previous data
Neoproterozoic
Araguaia Belt
Paleoproterozoic
Intermediate to felsic dikes (1.88 Ga)
Anorogenic granites (Jamon Suite; 1.88 Ga)
Archean
Metasedimentary cover (Rio Fresco Group)
Água Fria trondhjemite (2.86 Ga)
Potassic leucogranites (2.86 Ga); A: Xinguara granite; B: Mata Surrão granite
Leucogranodiorite and granites:
a) Guarantã suite (2.87 Ga);
b) similar plutons c) Grotão granodiorite
Undifferentiated granitoids
Sanukitoid rocks (2.87 Ga)
Mariazinha tonalite (2.92 Ga)
Caracol tonalitic complex (2.93 - 2.94 Ga)
Mogno trondhjemite (2.96 Ga)
Arco Verde tonalite (2.93 - 2.98 Ga)
Xingu complex
Greenstone belts (Andorinhas Supergroup; 2.90 - 2.97 Ga)
10 5 0 10
km

Figure 2 - Geological map of the Rio Maria granite-greenstone terrane showing the location of the studied samples and a summary of geochronological data currently available. Superscript numbers are for references (see table 1 for references).

Table 1 -Geochronological overview of the previous available data for Archean units of the Rio Maria granite-greenstone terrane.

Stratigraphic Unit	Rock	Methods	Analized material	Age (Ma)
Potassic leucogranites				
Xinguara granite	Leucogranite	Pb-Pb	Zircon	2865±1 (5)
Mata Surrão granite	Leucogranite	Pb-Pb	Whole rock	2872±10 (12)
	Leucogranite	Pb-Pb	Zircon	2875±11 (3)
	Leucogranite	Pb-Pb	Zircon	2881±2 (3)
leucogranodiorite-granie group				
Guarantã suite	Granodiorite	Pb-Pb	Zircon	2868±5 (11)
	Leucogranite	Pb-Pb	Zircon	2870±5 (10)
Younger TTG series	Trondhjemite	U-Pb	Titanite	2871 ? (1)
Mogno trondhjemite	Trondhjemite	Pb-Pb	Zircon	2857±13 (9)
	Trondhjemite	Pb-Pb	Zircon	2900±21 (9)
Água Fria trondhjemite	Trondhjemite	Pb-Pb		2864±21 (5)
Rio Maria sanukitoid suite	Granodiorite	U-Pb	Zircon	2874 + 9/-10 (2)
Rio Maria Granodiorite and rocks related	Granodiorite	U-Pb	Zircon,Titanite	2872±5 (1)
	Quartz diorite	Pb-Pb	Zircon	2878±4 (8)
	Diorite	Pb-Pb	Zircon	2880±4 (3)
	Granodiorite	Pb-Pb	Zircon	2877±6 (3)
Parazônia Tonalite	Quartz diorite	Pb-Pb	Zircon	2876±2 (7)
	Tonalite	U-Pb	Titanite	2858 (1)
Older TTG series	Tonalite	Pb-Pb	Zircon	2948±5 (5)
Caracol Tonalitic Complex	Tonalite	Pb-Pb	Zircon	2936±3 (5)
(Mariazinha Tonalite)*	Tonalite	Pb-Pb	Zircon	2924±2 (5)
Arco Verde Tonalite	Tonalite	Pb-Pb	Zircon	2964±4 (4)
	Tonalite	Pb-Pb	Zircon	2948±7 (3)
	Tonalite	Pb-Pb	Zircon	2981±8 (3)
	Tonalite	Pb-Pb	Zircon	2988±5 (3)
	Tonalite	Pb-Pb	Zircon	2957 + 25/-21 (2)
Greenstone Belts				
Andorinhas Supergroup	Felsic Metavulcanic rock	U-Pb	Zircon	2904+29/-22 (2)
	Metagraywacke	U-Pb	Zircon	2971±18 (2)
	Felsic Metavulcanic rock	U-Pb	Zircon	2972±5 (1)

Data Source: (1) Pimentel & Machado (1994), (2) Macambira and Lancelot (1996), (3) Rolando & Macambira (2003), (4) Vasquez et al. (2008), (5) Leite et al. (2004), (7) Almeida (unpublished data), (8) Dall'Agnol et al. (1999), (9) Macambira et al. (2000), (10) Althof et al., 2000, (11) Almeida et al., 2008, (12) Lafon et al. (1994).*This rock is correlated with the Mariazinha tonalite in the present paper (see text).

enclaves or, locally, small bodies. These rocks are intrusive into the greenstone belts and the older TTG series and are intruded by the Água Fria trondhjemite (Leite et al., 2004); (3) An younger TTG series (~2.87-2.86 Ga) exposed only in the Rio Maria and Xinguara areas of the RMGGT, and represented by the Mogno trondhjemite, and the Água Fria trondhjemite (the age and stratigraphic position of the Mogno trondhjemite will be re-evaluated in the present paper on the basis of new and more accurate geochronological data); (4) Potassic leucogranites of calc-

alkaline affinity (~2.87-2.86 Ga) represented by the Xinguara (XG) and Mata Surrão (MSG) granite plutons and by small granitic stocks found all around the RMGGT (Fig. 2). The Mata Surrão granite is intrusive into the Arco Verde tonalite (Duarte 1992) and the Xinguara granite intruded the Caracol tonalitic complex and the Rio Maria granodiorite and is coeval with the Água Fria trondhjemite (Leite, 2001; Leite et al., 2004).

Recent geological mapping in the Pau D'Arco area, including petrographic and geochemical studies (Almeida et al., 2008; Dias, 2009) demonstrated the existence of an additional group of Archean granitoid rocks in the RMGGT. These granitoid rocks have granodioritic to monzogranitic composition, have low modal content of mafic minerals (generally < 5% in vol.) and were grouped in the Guarantã suite (Althoff et al., 2000; Dias, 2009; Almeida et al., in prep.). Small granitic stocks found in the Bannach and Xinguara areas and the Grotão granodiorite (Guimarães et al. b, submitted), exposed to the SW of Xinguara (Fig. 2), have petrographic and geochemical similarities with the Guarantã suite.

The mentioned Archean units of the RMGGT are locally covered by the sedimentary rocks of the Rio Fresco group (Fig. 2), probably also of Archean age (Macambira and Lafon, 1995), and were intruded by the Paleoproterozoic A-type granites of the Jamon suite and associated dikes (Dall'Agnol et al., 2005).

3. Geology of the TTG suites of the RMGGT.

The TTG suites of the RMGGT have been grouped so far in two main groups (Table 1): The older TTG suites were represented by the Arco Verde and Caracol tonalitic assemblages and the younger TTG suites by the Mogno and Água Fria trondhjemites. New data, summarized in Tables 3 and 4**,** Figures 4, 5, 6 and 7, modified substantially this picture (this paper; Guimarães et al. a, b, submitted). The age and stratigraphic position of the Mogno trondhjemite was radically changed and a new TTG suite, the Mariazinha tonalite, was recognized. Four distinct suites were formed during the interval between 2.98 and 2.92 b. y. (Tables 3 and 4; Figs. 2 and 14): 1) The Arco Verde tonalite (2.98 - 2.93 Ga; Macambira and Lafon, 1995; Rolando and Macambira, 2003; Almeida et al., 2008); 2) the Mogno trondhjemite (~2.96 Ga; this paper); 3) the Caracol tonalitic complex (2.95 to 2.93 Ga; Leite et al., 2004); and 4) the Mariazinha tonalite (~2.92 Ga;

this paper). The number of younger TTG suites was thus reduced substantially, embracing actually only the Água Fria trondhjemite.

The Arco Verde tonalite and the Mogno trondhjemite form large batholiths, whereas the Caracol tonalitic complex and the Mariazinha tonalite are exposed in smaller areas (Fig. 2). The rocks of all these units are weakly to strongly foliated and commonly show compositional banding. The intensity of deformation increases in the vicinity of shear zones where mylonitic textures develop. Away from the more intensely deformed zones, igneous textures are generally well preserved (Althoff et al., 2000).

In the southern sector of the RMGGT, the Arco Verde tonalite is the dominant unit (Fig. 2). It shows a E-W to WNW–ESE subvertical non penetrative foliation, includes quartz-dioritic microgranular enclaves and is cut by veins of leucogranites and pegmatites (Althoff et al., 2000; Almeida et al., 2008). During the magmatic stage vertical layering and, locally, syn-magmatic shear zones were formed, whereas in the subsolidus stage vertical schistosity, weak horizontal lineation, and conjugate vertical shear-zones were developed (Althoff et al., 2000). It was inferred that the Arco Verde tonalite suffered a strong regional shortening under conditions ranging from high-T (near solidus and subsolidus ductile deformation) to low-T (low grade brittle deformation). The structures developed mostly during cooling of the igneous batholith, under decreasing T gradient within a regional stress field (Althoff et al., 2000; Dall'Agnol et al., 2006). The Arco Verde tonalite is intruded by the Guarantã and Mata Surrão granites.

In most cases, the rocks of the Caracol tonalitic complex are strongly deformed, but in localized low-strain domains, they preserve magmatic structures (Leite, 2001). The compositional banding display NW-SE trend and is disturbed by folds or boudins. The tonalites show enclaves of the greenstone belts and are intruded by the Rio Maria granodiorite, Xinguara granite, and Água Fria trondhjemite.

The Mogno trondhjemite is exposed to the south of Xinguara and extends to the north of Bannach (Fig. 2). It is strongly deformed with NW-SE to E-W trending foliation (Guimarães et al. a, submitted; Viegas, 2009) and is intruded by the Mariazinha tonalite (Fig. 2). The Mogno trondhjemite includes mafic enclaves which probably represent metabasalts of the Andorinhas supergroup (Souza, 1994). Trondhjemitic stocks intruded by the Bannach Paleoproterozoic granite (Fig. 2) have been correlated with the Mogno trondhjemite (Guimarães, 2007) and this hypothesis was confirmed by the geochronological data obtained by us (Figs. 5g, h).

The Mariazinha tonalite shows conspicuous NE-SW to N-S foliation, commonly accentuated by a banded structure. Its structural trend contrasts with that of the Mogno trondhjemite. The Mariazinha tonalite contains mafic enclaves and is cross-cut by the Grotão granodiorite and by veins of leucogranites that are conformable or not with the foliation of the tonalite. This unit is also exposed to the north of the Xinguara pluton, where a tonalitic stock, previously embraced in the Caracol tonalitic complex, but showing similar structural trend and age than the Mariazinha tonalite was identified (Leite et al., 2004; this paper).

The youngest TTG generation is represented by the Água Fria trondhjemite (Fig. 2) that displays NW-SE to WNW-ESE composicional banding with subvertical dip and includes locally tonalitic enclaves that may represent xenoliths of older TTG. The Água Fria trondhjemite is cross-cut by granitic veins, but the composicional banding of the trondhjemite is deformed together with concordant leucogranitic veins from the Xinguara pluton, suggesting that both units are approximately coeval (Leite, 2001). This evidence was reinforced by the age of 2.86 Ga (Leite et al., 2004) obtained for the Água Fria trondhjemite, almost coincident with that of the Xinguara pluton (Table 1).

4. Petrography

The rocks which constitute the different TTG suites of the RMGGT are quite homogenous in texture and mineralogical composition. They have been classified as tonalites or trondhjemites according to their mafic mineral content (Fig. 3, Table 2; cf. Le Maitre, 2002), and, in most units, a transition between tonalites and trondhjemites is generally observed and granodiorites are extremely rare. The only exception is the Água Fria trondhjemite that is composed of trondhjemites grading to granodiorites (Fig. 3). The contents of mafic minerals vary normally between 15% and 5 vol. %. Nevertheless, some contrasts in modal composition exist: The Arco Verde and Mariazinha tonalites and the Caracol tonalitic complex are dominantly composed of tonalites, whereas in the Mogno unit trondhjemites are largely dominant over tonalites and in the Agua Fria unit tonalites are absent. These rocks are composed of calcic oligoclase, quartz, and biotite as the main minerals. Alkali feldspar is significant only in the rare granodioritic varieties. Hornblende is absent in all samples of the studied TTGs submitted to modal analyses (Table 2) and, in the rare samples where it occurs, it is accessory. Zircon, allanite, apatite, magnetite,

Table 2 - Modal composition (point counting) of representative samples of theTTG units of the RMGGT

Units	Arco Verde Tonalite								Trondhjemito Mogno													
Samples	F-15[1]	MAR-149[2]	F-58-1[1]	MP-19[3]	MAR-111[3]	MAR-148A [3]	MAR-66A[3]	MP-07[3]	AM-03[4]	MAS F- 19 [5	MASF-29[5]	FMR-101[4]	MASF- 21 [5]	MASF–28[5]	FMR-77[4]	MASF- 25[5]	FMR-98[4]	ADR-162	FMR-15A[4]	FMR-87[4]	MASF-20[5]	FMR-03[4]
Quartz	31.0	33.0	33.2	26.0	28.5	36.0	41.0	36.7	25.2	25.9	35.3	32.6	23.0	34.6	30.7	30.6	31.2	28.4	29.7	29.2	29.9	28.8
Plagioclase	49.5	50.4	52.6	62.5	60.1	55.0	51.0	49.2	61.2	61.4	46.4	58.1	67.0	51.5	61.6	55.3	58.2	63.6	59.5	63.8	61.2	63.9
Alcali-feldspar	1.3	n.d	2.4	n.d	0.5	n.d	n.d	7.6	0.5	1.6	8.8	0.1	1.0	5.6	0.1	6.0	2.3	1.1	3.9	0.0	2.8	2.1
Biotite	13.3	12.1	11.2	8.4	7.9	5.9	6.6	4.3	11.7	6.5	6.4	7.7	3.0	6.6	6.7	3.8	6.3	0.7	5.2	5.4	4.4	4.0
White mica	1.3	n.d	n.d	n.d	n.d	0.1	n.d	n.d	n.d	0.4	n.d	n.d	0.0	n.d	n.d	0.5	0.7	0.0	n.d	n.d	n.d	0.2
Chlorite	2.1	0.3	0.4	0.1	n.d	0.1	n.d	0.6	0.3	0.3	0.4	0.2	1.1	0.3	n.d	0.7	0.2	0.6	n.d	0.4	0.2	0.2
Opaques	0.0	0.0	0.2	0.3	0.3	n.d	0.6	0.1	0.0	0.3	0.2	0.1	0.2	n.d	0.3	0.9	0.0	0.1	0.2	n.d	0.1	n.d
Titanite	n.d	0.7	n.d	0.7	1.1	0.5	0.3	0.9	0.2	0.6	0.5	0.3	0.5	0.1	0.2	0.3	0.1	1.0	0.2	0.3	0.1	0.2
Epidotes	1.6	3.2	0.0	2.0	1.5	1.9	0.3	0.6	0.9	2.4	1.4	0.7	3.9	1.3	0.2	1.7	0.7	4.1	0.8	0.8	1.1	0.2
Accessory $_{(Ap+Zr)}$	n.d	0.3	n.d	n.d	n.d	0.5	0.1	n.d	n.d	0.5	0.5	0.1	0.3	n.d	0.1	0.2	0.3	0.4	0.4	n.d	0.2	0.3
Mafics	17.0	16.6	11.8	11.5	10.9	8.9	7.9	6.5	13.1	10.7	9.4	9.2	9.0	8.3	7.6	7.6	7.6	6.9	6.9	6.9	6.1	5.0
Felsics	83.1	83.4	88.2	88.5	89.1	91.1	92.1	93.5	86.9	89.3	90.6	90.8	91.0	91.7	92.4	92.4	92.4	93.1	93.1	93.1	93.9	95.0

Units	Caracol Tonalitic Complex					Mariazinha Tonalite										Água Fria Trodhjemite						
Samples	AL-163[6]	ALF-239[6]	AL-26A[6]	AL-54A[6]	AL-216[6]	FMR-25[4]	FMR-37A[4]	AL-59[6]	FMR-52[4]	FMR-46[4]	AL-210C[6]	AM-02A[3]	FMR-32[4]	FMR-62A[4]	FMR-29[4]	AL-80[6]	AL-16A[6]	AL-137[6]	ALF-248A[6]	AL-69A[6]	AM-01[3]	AL-13C[6]
Quartz	20.5	29.4	34.0	28.7	26.1	26.4	25.1	31.3	29.6	25.4	30.0	33.9	31.1	27.4	44.9	33.4	28.7	39.2	35.6	36.2	33.8	34.0
Plagioclase	64.9	58.1	54.6	59.8	64.0	55.5	57.5	50.4	55.7	59.0	59.0	57.2	60.0	66.1	48.8	57.7	62.9	52.4	50.0	50.1	51.9	56.8
Alcali-feldspar	n.d	n.d	n.d	n.d	n.d	2.2	2.5	4.9	1.8	4.0	n.d	0.7	1.0	0.3	4.8	0.5	0.3	1.1	7.4	7.9	8.0	3.9
Biotite	13.1	11.5	11.3	11.0	9.8	13.0	10.7	11.9	11.7	8.7	11.0	6.3	6.7	2.9	0.7	7.0	8.0	3.9	5.3	5.4	3.8	4.8
White mica	n.d	n.d	n.d	n.d	n.d	n.d	n.d	n.d	n.d	n.d	n.d	n.d	n.d	0.1	n.d	n.d	n.d	n.d	0.0	n.d	0.5	n.d
Chlorite	n.d	n.d	n.d	n.d	n.d	n.d	0.5	n.d	n.d	0.1	n.d	0.7	0.4	2.3	n.d	1.3	n.d	3.0	1.6	0.3	1.2	0.4
Opaques	n.d	n.d	n.d	n.d	n.d	0.6	1.2	n.d	0.3	0.2	n.d	0.2	n.d	n.d	n.d	n.d	n.d	n.d	n.d	n.d	0.2	n.d
Titanite	1.5	0.9	0.2	0.5	0.1	0.5	0.7	1.4	0.2	1.4	n.d	0.3	n.d	0.5	n.d	0.1	0.1	0.4	0.1	0.1	0.2	0.1
Epidotes	n.d	n.d	0.0	n.d	n.d	1.7	1.2	n.d	0.5	1.1	n.d	0.6	0.5	n.d	0.5	n.d	n.d	n.d	n.d	n.d	0.1	n.d
Accessory $_{(Ap+Zr)}$	n.d	n.d	0.0	0.0	n.d	0.1	0.6	n.d	0.2	0.1	n.d	0.1	0.3	0.3	0.2	n.d	n.d	n.d	n.d	n.d	0.1	n.d
Mafics	14.6	12.4	11.5	11.5	9.9	15.9	14.9	13.4	12.9	11.6	11.0	8.2	7.9	6.1	1.4	8.4	8.1	7.3	7.0	5.8	5.6	5.3
Felsics	85.4	87.6	88.5	88.5	90.1	84.1	85.1	86.6	87.1	88.4	89.0	91.8	92.1	93.9	98.6	91.6	91.9	92.7	93.0	94.2	94.2	94.7

Data source: [1] - Althoff (1996); [2] - Costa (2009); [3] - this work; [4] - Guimarães et al. (a, submitted); [5] - Guimarães 2007; [6] - Leite (2001). Ap= apatite; Zr=zircon. n.d=not determined

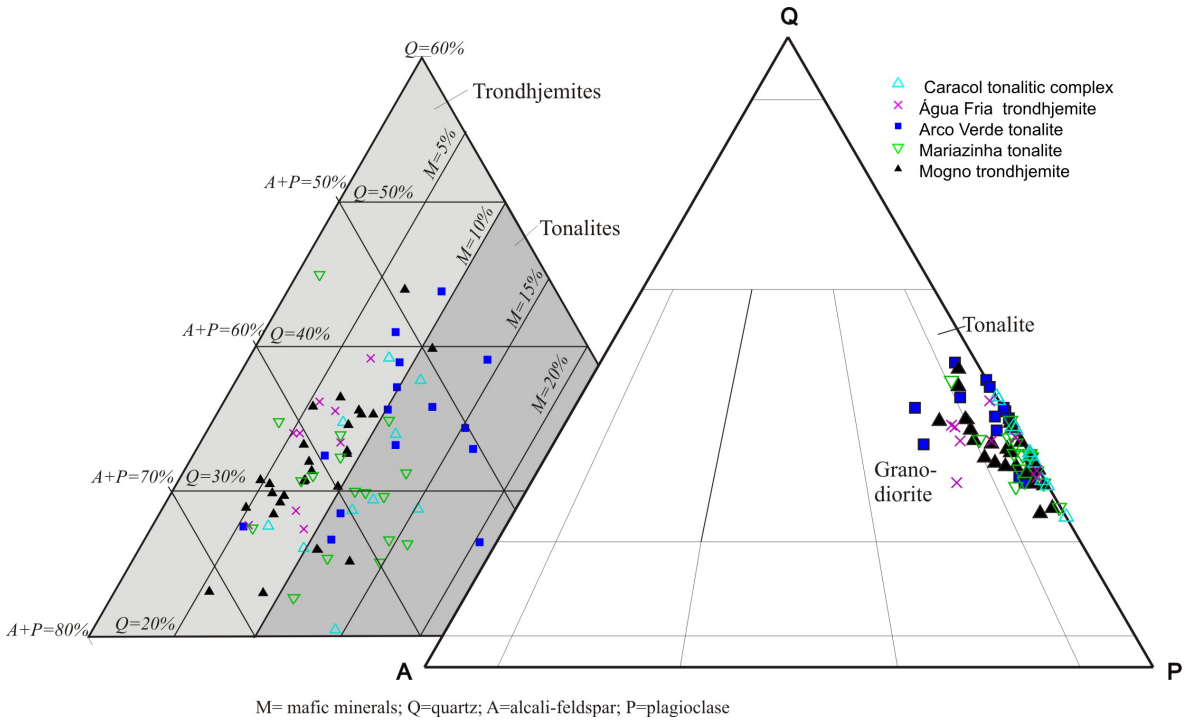

Figure 3 - QAP and Q-(A+P)-M for the TTG rocks of the Rio Maria granite-greenstone terrane (see table 2 for references).

epidote, and titanite are primary accessory phases and white mica, chlorite, epidote (replacing plagioclase), hematite, goethite, pyrite, and chalcopyrite are secondary minerals.

Gray, equigranular, medium- to coarse-grained or seriated rocks are dominant in most of the TTGs of the RMGGT. The igneous banding is indicated by the succession of levels relatively enriched in biotite and accessory minerals, alternating with light gray bands, with higher modal contents of plagioclase and quartz. Biotite and mafic accessory minerals are always found in close association and form small elongated aggregates disposed along the rock foliation.

In the TTGs, apatite, zircon, magnetite, and allanite are early crystallized phases. They are followed by plagioclase, which form euhedral to subhedral crystals usually saussuritized and zoned, a typical petrographic feature of the Mogno trondhjemite. The biotite began to crystallize after plagioclase and displays textural evidence of equilibrium with euhedral epidote. Two textural epidote types interpreted as magmatic are distinguished: Epidote with zoned allanite core and epidote associated with and partially enclosed by biotite. Similar textural features have been described in the Archean Mata Surrão and Xinguara potassic leucogranites (Duarte, 1992; Leite, 2001) and in Rio Maria sanukitoid suite (Oliveira et al., 2009) of the RMGGT. Quartz probably

initiated its crystallization synchronously or a little later than biotite + epidote, whereas titanite began to crystallize after these minerals. Alkali feldspar is a later phase forming small anhedral crystals. At the subsolidus stage, chlorite, epidote, and white mica were generated.

5. Geochronology

We present new geochronological data for the Arco Verde tonalite, Mogno trondhjemite, Caracol tonalitic complex, Mariazinha tonalite and Agua Fria trondhjemite. The new ages were obtained in representative samples of critical areas that were selected taking in account the previous available information and recent advances in the knowledge of the geology of the studied TTG units. The geochronological data were integrated resulting in a more comprehensive coverage of the RMGGT (Fig. 2). Besides the Pb-Pb zircon evaporation method, the LA-ICP-MS U-Pb zircon was used for the first time to assess the ages of the TTG suites of the area. For most samples, comparison of the results obtained by these two methods is now possible.

5.1. Sample selection and analytical procedures

Twelve samples of TTG granitoids of the RMGGT were selected (Fig. 2). The cover the four TTG units of the RMGGT: four of the Arco Verde tonalite (MAR-66, MAR-111, MAR-148, and MAR-149); five of the Mogno trondhjemite (MFR-53, FMR-98, MASF-28, AM-03, and FMR-87); two of the Mariazinha tonalite (AM-02A and FMR-25); and one (AM-01) of the Agua Fria trondhjemite. All theses samples were analyzed by single zircon Pb evaporation (Table 3), except for sample AM-01, and seven samples were analyzed also by LA-ICP-MS (Table 4).

Zircon crystals were concentrated from ca. 10 kg rock samples using conventional techniques, involving combination of magnetic and gravimetric separation with handpicking techniques. For *in situ* ICP-MS analyses, zircons from the nonmagnetic fractions were hand-picked and mounted on adhesive tape, imbedded in an epoxy-resin pellet and then polished to about half of their size. In order to investigate the internal structures of the zircon crystals prior to analysis, cathodoluminescence imaging was carried out using a Mono-CL detector attached to a scanning electron microscope (LEO 1430) at the Scanning Electron Microscopy Laboratory of the Geosciences Institute of Federal University of Pará (UFPA).

U–Pb isotopic analyses were performed at the geochronology laboratory of the University of Brasília (UnB) and followed the analytical procedures described by Buhn et al. (2009). Before LA-ICP-MS analyses, mounts were cleaned with dilute (ca. 2%) HNO3. The samples were mounted in an especially adapted laser cell and loaded into a New Wave UP213 Nd:YAG laser (λ - 213 nm), linked to a Thermo Finnigan Neptune multi-collector ICPMS. Helium was used as the carrier gas and mixed with argon before entering the ICP source. The laser was run at a frequency of 10 Hz and energy of 0.4 mJ/pulse and a focused laser beam of 20–40 μm in diameter was employed depending on the sample grain size.

Two international zircon standards were analyzed throughout the U–Pb analyses. GJ-1 (Jackson et al., 2004) was used as the primary standard in a standard-sample bracketing method, accounting for mass bias and drift correction. The resulting correction factor for each sample analysis considers the relative position of each analysis within the sequence of four samples bracketed by two standard and two blank analyses each (Albarède et al., 2004). UQZ was run at the start and the end of each analytical session, yielding an accuracy around 2% and a precision in the range of 1%. The errors of sample analyses were propagated by quadratic addition of the external uncertainty observed for the standards to the reproducibility and within-run precision of each unknown analysis. The instrumental set-up and further details of the analytical method applied are given by Buhn et al. (2009).

The masses of ^{204}Pb, ^{206}Pb and ^{207}Pb were measured with ion counters, and ^{238}U was analyzed on a Faraday cup. The signal of ^{202}Hg was monitored by an ion counter for the correction of the isobaric interference between ^{204}Hg and ^{204}Pb. The signals during ablation were taken in 40 cycles of 1s each. For data evaluation, only coherent intervals of signal response were considered. Data reduction was performed with an in-house Excel spreadsheet, which considers blank values, zircon standards composition and errors, and error propagation. The ^{204}Pb signal intensity was calculated and corrected using a natural ^{202}Hg/^{204}Hg ratio of 4.346. Common Pb correction was applied for zircons with ^{206}Pb/^{204}Pb lower than 1000, applying a common lead composition following the Stacey and Kramers (1975) model. Plotting of U–Pb data was performed by ISOPLOT v.3 (Ludwig, 2003) and errors for isotopic ratios are presented at the 1σ level.

Zircon dating by the single grain Pb evaporation method (Kober, 1986) was carried out at the Laboratório de Geologia Isotópica (Pará-Iso) of the UFPA, Brazil. Isotopic ratios were

measured in a FINNIGAN MAT 262 mass spectrometer and data were acquired in the dynamic mode using the ion-counting system of the instrument. Three evaporation steps of the Pb from zircon of a maximum of five minutes each were performed at 1450, 1500, and 1550° C. For every step of evaporation, a step age is calculated from the average of the $^{207}Pb/^{206}Pb$ ratios. The age of the sample is calculated from the results of the highest temperature step of all crystals. When different heating steps of the same grain gave similar ages, all of them were included in the age calculation. Crystals or steps showing lower ages probably reflect Pb loss after crystallization and are not included in sample age calculation. Weighted mean and errors on the ages were calculated following Gaudette et al. (1998). Common Pb corrections were made according to Stacey and Kramers (1975) and analyses with $^{206}Pb/^{204}Pb$ ratios lower than 2500 were rejected, thus minimizing the effects of common Pb correction. $^{207}Pb/^{206}Pb$ ratios were corrected for mass fractionation by a factor of 0.12±0.03 per a.m.u, given by repeated analysis of the NBS-982 standard. Analytical uncertainties are given at the 2σ level.

5.2. Zircon morphology and internal structure

Most zircon grains from the TTG rocks of the RMGGT are brownish elongated prismatic crystals (width/length ratios varying from 2:1 to 4:1), with length ranging from 150 to 400µm, euhedral to subhedral shape and, in some cases, rounded terminations. Under cathodoluminescence, these crystals show well developed oscillatory zoning (insert in figures 4b, d, 5h, 6c, and 7), which together with their high Th/U ratios (generally >0.1; U–Pb LA-ICP-MS analyses; cf. Table 4), indicates crystallization from a magma. In general, these crystals present low luminescence, but some grains also have U-enriched, bright zones (insert in Fig. 4b), preferentially located at the borders of the crystals and generally coincident with the rounded areas of the original euhedral crystals, probably reflecting processes of partial dissolution-reprecipitation of the original zircon grains. Inherited cores were not observed in the analyzed grains. Zircon grains from samples AM-03 (Mogno trondhjemite) and AM-01 (Água Fria trondhjemite) have distinct morphologies and internal structures. In sample AM-03 (Mogno trondhjemite), the dominant zircon population consists of clear, colorless to pink, transparent, unzoned crystals (Fig. 5f), which are rounded or shortly elongated (width/length ratios varying from 1:1 to 2:1 and lengths ranging from ca. 100 to 200 µm). Zircons from sample AM-01 (Água

Fria trondhjemite) are also subhedral to euhedral but differ from those of the other TTGs by their strongly metamict character and common occurrence of corroded border zones as well as of partially dissolved cores with a spongiform aspect (insert in Fig. 7). These features suggest a more complex evolution for the zircon of these rocks when compared with other TTGs of the RMGGT.

5.3. Results

Isotopic analyses are given in Table 3 for single grain Pb evaporation method and in Table 4 for LA-ICP-MS. The location of the dated samples is shown in Figure 2 and their modal and chemical compositions are given, in Table 2 and Table 5, respectively.

5.3.1. Arco Verde tonalite: samples MAR-66, MAR-148, MAR-149, and MAR-111

Single zircon Pb-evaporation analyses of seven zircon grains from MAR-66 gave a weighted mean age of 2928±2 Ma (MSWD=3.2; Fig. 4a). An older age of 2952±2 Ma was observed in one isolated crystal. Twenty one zircon grains from the same sample were investigated by U–Pb LA-ICP-MS. Five data-points are concordant (Table 4), defining a concordia age of 2936±13 Ma (MSDW=0.27; Table 4 and Fig. 4b). The 2952±2 Ma Pb-Pb age observed in one zircon crystal may indicate a slightly older inheritance.

Five grains from sample MAR-148 yielded a mean Pb-Pb age of 2926±2 Ma (MSWD=0.91) whereas two other grains which are morphologically distinct from the dominant population yielded the age of 2961±14 Ma (Fig. 4c) interpreted as inheritance. U-Pb LA-ICP-MS analyses of 10 zircon crystals (Fig. 4d) from the same sample defined an upper intercept age of 2935±5 Ma (MSWD=1.1).

Samples MAR-149 and MAR-111 were analyzed only by the single zircon Pb-evaporation method. Five zircon grains from MAR-149 yielded a mean age of 2937±3 Ma (MSWD=1.6; Fig. 4e), whereas three zircon grains from sample MAR-111 yielded a $^{207}Pb/^{206}Pb$ age of 2973±11 Ma (MSWD = 10; Fig. 4f) that we assume as the crystallization age of the sample.

Table 3 - Summary of zircon single-crystal evaporation Pb isotopic data from the TTG suites of the Rio Maria granite-greenstone terrane

Unit	Sample	Zircon	Evaporation Temperature (°C)	Number of Ratios	$^{204}Pb/^{206}Pb$	2s	$^{208}Pb/^{206}Pb$	2s	$^{207}Pb/^{206}Pb$	2s	Age step (Ma)	Age Crystal (Ma)	Mean age of sample (Ma)
ARCO VERDE TONALITE	MAR-66	1	1500	12	0.000018	0.000002	0.08239	0.00034	0.21311	0.00055	2930±4		
		1	1550	38	0.00002	0.000004	0.09096	0.00088	0.2133	0.00027	2931±2	2931±2	
		3	1500	22	0.000099	0.000004	0.09438	0.0005	0.21269	0.00028	2926±2	2926±2	
		5	1500	22	0.000033	0.000013	0.09758	0.00062	0.21258	0.00035	2926±3	2926±3	
		6	1500	4	0.000104	0.000022	0.12227	0.00186	0.21274	0.0006	2927±5	2927±5	
		7	1500	20	0.000014	0.000002	0.08982	0.00053	0.21276	0.00051	2927±4	2927±4	
		9	1550	8	0.000064	0.000006	0.07399	0.0022	0.21296	0.00142	2929±11	2929±11	
		17	1450	10	0.00017	0.000019	0.12821	0.00404	0.21345	0.00057	2932±4	2932±4	
		Mean age of crystals 1, 3, 5, 6, 7, 9 and 17	-	-	-	-	-	-	-	-	-	-	2928±2 (MSWD = 3.2)
		16	1500	32	0.000038	0.000008	0.12108	0.0004	0.21603	0.00026	2952±2	2952±2	
	MAR-148	9	1500	36	0.000027	0.000003	0.20502	0.00137	0.21242	0.00056	2924±4	2924±4	
		13	1500	38	0.000179	0.000007	0.13054	0.00371	0.21248	0.00037	2925±3	2925±3	
		15	1500	12	0.00015	0.000067	0.0722	0.00187	0.21271	0.00113	2926±9	2926±9	
		16	1500	34	0.000135	0.000009	0.05491	0.00156	0.21295	0.00046	2928±4	2928±4	
		25	1500	38	0.000151	0.000007	0.15399	0.00194	0.21278	0.00038	2927±3	2927±4	
		Mean age of crystals 9, 15, 16	-	-	-	-	-	-	-	-	-	-	2926 ± 2 (0.91)
		1	1450	38	0.000183	0.000005	0.09413	0.00043	0.2143	0.00074	2938±6		
		1	1500	22	0.000158	0.000048	0.10317	0.0016	0.21679	0.00044	2957±3		
		1	1550	40	0.000087	0.000015	0.11401	0.00334	0.2185	0.00035	2969±3		
		1	1600	38	0.000123	0.000005	0.09793	0.00147	0.21653	0.00091	2955±7	2961±19	
		10	1500	10	0.000074	0.000003	0.08395	0.00063	0.21728	0.003	2960±22	2961±22	
		Mean age of crystals 1, 10	-	-	-	-	-	-	-	-	-	-	2961±14 (MSWD=0.1)
	MAR-149	2	1550	30	0,000021	0,000005	0,13771	0,00106	0,21433	0,00034	2939±3	2939±3	
		3	1500	32	0,000011	0,000003	0,16108	0,00184	0,21396	0,00043	2936±3	2936±3	
		4	1500	36	0,000034	0,000008	0,09752	0,00064	0,21371	0,00035	2934±3	2934±3	
		7	1500	32	0,000171	0,000005	0,11473	0,00147	0,21369	0,00068	2934±5		
		7	1500	20	0,000069	0,000003	0,08803	0,00089	0,21419	0,00038	2938±3	2937±3	
		8	1500	20	0,000069	0,000003	0,08803	0,00089	0,21419	0,00038	2938±3	2938±3	
		Mean age of crystals 2, 3, 4, 7 and 8	-	-	-	-	-	-	-	-	-	-	2937±3 (MSWD=1.6)
	MAR-111	16	1500	28	0.000119	0.000009	0.1261	0.00137	0.21859	0.00029	2971±2	2971±2	
		17	1500	22	0.000042	0.000007	0.04245	0.00018	0.21864	0.00058	2971±4		
			1550	24	0.000039	0.000007	0.04667	0.00032	0.21908	0.00038	2974±3	2973±5	
		19	1500	38	0.000049	0.000006	0.1138	0.00464	0.21978	0.00038	2979±3	2979±3	
		Mean age of crystals 16, 17 and 19	-	-	-	-	-	-	-	-	-	-	2973±11 (MSWD=10.0)
MOGNO TRODHJEMITE	MFR-53	2	1500	8	0.000064	0.000008	0.06628	0.00042	0.21807	0.00129	2967±10		
			1550	36	0.000111	0.000011	0.08787	0.00071	0.21839	0.00053	2969±4		
												2969±4	
		3	1550	34	0.000073	0.000004	0.12586	0.0048	0.21733	0.00026	2961±2	2961±2	
		7	1500	38	0.00009	0.000009	0.03559	0.0008	0.21733	0.00033	2961±2	2961±2	
		Mean age of crystals 2, 3 and 7	-	-	-	-	-	-	-	-	-	-	2963±8 (MSWD=8.6)
	FMR-98	1	1500	24	0.000217	0.000056	0.08183	0.00152	0.21837	0.0005	2969±4	2969±4	
		5	1500	34	0.000181	0.000023	0.10633	0.00164	0.21824	0.00029	2968±2	2968±2	
		7	1500	12	0.000038	0.000006	0.05191	0.00202	0.2179	0.00075	2966±6	2966±6	
		-	-	-	-	-	-	-	-	-	-	-	2968±2 (MSWD=0.52)
		Mean age of crystals 1, 5 and 7											
	FMR-87	2	1500	8	0.000181	0.000002	0.09966	0.00085	0.21763	0.00071	2963±5	2963±5	
		4	1500	30	0.000114	0.000003	0.1208	0.00095	0.21732	0.00049	2961±4	2961±4	
		6	1500	24	0.0002	0.000015	0.12371	0.0008	0.21682	0.00047	2957±4	2957±4	
		7	1500	6	0.00016	0.000012	0.08721	0.00059	0.21655	0.0011	2955±8	2955±4	
		Mean age of crystals 2, 4, 6, 7	-	-	-	-	-	-	-	-	-	-	2959±5 (MSWD=1.8)
	AM-03	6	1500	24	0.000251	0.00002	0.24145	0.00394	0.21698	0.00049	2959±4	2959±4	
		12	1500	14	0.000177	0.000006	0.20331	0.00115	0.21704	0.00037	2959±3	2959±3	
		19	1450	12	0.00016	0.00004	0.2171	0.00141	0.21719	0.0008	2960±6	2960±6	
		Mean age of crystals 6, 12, 19	-	-	-	-	-	-	-	-	-	-	2959±2 (MSWD=0.048)
	MASF-28	2	1500	40	0.000057	0.000006	0.09005	0.00057	0.21811	0.00026	2967±2	2967±2	
		3	1450	4	0	0	0.08103	0.01408	0.21928	0.00168	2976±12		
			1500	4	0.000108	0.000034	0.09991	0.0012	0.21959	0.00067	2978±5	2978±9	
		Mean age of crystals 2 and 3	-	-	-	-	-	-	-	-	-	-	2968±30 (MSWD=5.7)
MARIAZINHA TONALITE	FMR-25	2	1500	36	0.000048	0.000008	0.15631	0.00158	0.21266	0.00027	2926±2	2926±2	
		8	1500	24	0.000034	0.000004	0.05782	0.00132	0.21268	0.00029	2926±2	2926±2	
		10	1500	28	0.000024	0.000001	0.06459	0.0006	0.21251	0.00029	2925±2		
			1550	24	0.000024	0.000005	0.05984	0.00028	0.2121	0.00027	2922±2	2923±5	
		14	1500	24	0.000023	0.000004	0.03753	0.00024	0.21243	0.00036	2925±3		
			1550	22	0.000019	0.000003	0.03524	0.00016	0.21218	0.00038	2923±3	2923±2	
		Mean age of crystals 2, 8, 10, 14	-	-	-	-	-	-	-	-	-	-	2925±3 (MSWD=2.6)
	AM-02A	5	1500	32	0.000174	0.000009	0.18055	0.00561	0.21157	0.00035	2918±3		
			1550	32	0.000164	0.000015	0.15889	0.0009	0.21137	0.00031	2916±2	2917±3	
		13	1500	34	0.00008	0.000003	0.07394	0.00036	0.21282	0.00024	2927±2		
			1550	32	0.000119	0.000007	0.07155	0.00054	0.21241	0.0003	2924±2	2926±3	
		14	1550	20	0.000325	0.000013	0.08722	0.00465	0.21142	0.00035	2917±3	2917±3	
		Mean age of crystals 5, 13, 14	-	-	-	-	-	-	-	-	-	-	2920±11 (MSWD=14.0)

Table 4 - Summary of LA-ICP-MS U–Th–Pb results for zircons from TTG suites of the Rio Maria granite-greenstone terrane.

				Isotopic ratios								Ages						
Units	Samples	Zircon n°/Spot	Th/U	$^{206}Pb/^{204}Pb$	$^{207}Pb/^{206}Pb$	1s(%)	$^{207}Pb/^{235}U$	1s(%)	$^{206}Pb/^{238}U$	1s(%)	ρ	$^{207}Pb/^{206}Pb$	1s(%)	$^{207}Pb/^{235}U$	1s(%)	$^{206}Pb/^{238}U$	1s(%)	Conc (%)
Arco Verde tonalite	MAR-66	8/1	0.290	49175	0.1677	2.0	4.3095	2.8	0.1864	2.0	0.7	2535	33.7	1695	23.0	1102	19.9	43.5
		14/1	0.134	96460	0.1683	0.8	5.1306	1.7	0.2211	1.5	0.9	2541	13.3	1841	14.1	1288	17.0	50.7
		2/1	0.237	86634	0.1868	0.7	7.3777	2.2	0.2864	2.1	1.0	2715	11.7	2158	19.8	1623	30.3	59.8
		3/1	0.135	73803	0.1935	0.9	7.5547	2.9	0.2832	2.7	1.0	2772	14.3	2180	25.4	1607	38.7	58.0
		18/1	0.229	157844	0.1850	0.8	7.7024	1.3	0.3019	1.0	0.7	2698	13.2	2197	11.6	1701	15.2	63.0
		12/1	0.276	4443	0.1877	0.6	8.3468	1.2	0.3226	1.0	0.7	2722	10.3	2269	10.4	1802	15.2	66.2
		20/1	0.286	44786	0.2035	4.4	11.9260	3.1	0.4250	3.0	0.9	2855	69.2	2599	29.0	2283	57.8	80.0
		1/1	0.054	2208	0.2189	0.7	12.8380	2.3	0.4254	2.2	1.0	2973	10.7	2668	21.8	2285	42.9	76.9
		7/1	0.285	72941	0.2072	3.0	14.3964	2.1	0.5040	2.0	1.0	2884	47.2	2776	20.2	2631	43.6	91.2
		5/1 *	0.171	56300	0.2141	1.8	16.6531	1.4	0.5640	1.2	0.9	2937	28.9	2915	12.9	2883	27.5	98.2
		10/1 *	0.165	62754	0.2136	0.7	17.0011	1.5	0.5773	1.3	0.9	2933	11.2	2935	14.3	2938	31.4	100.2
		21/1 *	0.150	14680	0.2135	0.8	17.0541	2.0	0.5792	1.8	0.9	2933	12.9	2938	19.1	2946	43.3	100.4
		17/1	0.149	65176	0.2167	2.7	17.2186	2.0	0.5762	1.9	0.9	2957	43.0	2947	18.8	2933	43.5	99.2
		11/1 *	0.118	73138	0.2150	0.6	17.2700	1.2	0.5825	1.0	0.8	2944	10.1	2950	11.4	2959	24.0	100.5
		5/2	0.165	43113	0.2146	0.7	17.2775	1.5	0.5838	1.4	0.9	2941	10.7	2950	14.5	2964	32.3	100.8
		6/2 *	0.264	83905	0.2146	0.7	17.3722	3.0	0.5871	2.9	0.9	2941	11.8	2956	28.0	2978	67.9	101.3
		16/1	0.132	29547	0.2162	0.9	18.1407	2.8	0.6085	2.6	0.9	2953	14.9	2997	26.1	3064	62.9	103.8
		14/2	0.135	79055	0.2152	0.6	18.5468	1.2	0.6250	1.0	0.8	2945	10.4	3019	11.7	3130	25.7	106.3
		4/1	0.214	104826	0.2183	0.8	18.6397	1.7	0.6194	1.6	0.8	2968	12.3	3023	16.7	3108	38.5	104.7
		13/1	0.271	121012	0.2155	0.7	18.7428	1.9	0.6307	1.8	0.9	2948	11.6	3029	18.3	3152	44.1	106.9
		6/1	0.200	78402	0.2161	0.6	18.7798	1.6	0.6302	1.5	0.9	2952	10.1	3031	15.2	3150	36.1	106.7
		9/1	0.163	59535	0.2153	0.8	18.8142	3.3	0.6338	3.2	0.9	2946	12.2	3032	31.3	3164	79.8	107.4
		15/1	0.142	176746	0.2144	0.6	18.8901	1.0	0.6389	0.8	0.7	2939	9.7	3036	9.4	3185	19.4	108.3
		19/1	0.093	59565	0.2150	0.7	18.9337	1.8	0.6386	1.6	0.9	2944	11.0	3038	17.0	3183	41.2	108.1
Arco Verde tonalite	MAR-148	3/1	0.176	7880	0.0971	4.6	1.3033	6.8	0.0974	5.0	0.7	1569	83.0	847	38.3	599	28.8	38.2
		18/1	0.194	8254	0.1238	1.2	2.5054	2.8	0.1468	2.6	0.9	2011	21.1	1274	20.3	883	21.1	43.9
		16/1	0.015	92623	0.1259	0.9	2.6838	1.9	0.1546	1.7	0.8	2042	15.3	1324	14.2	927	14.9	45.4
		11/1	0.023	59995	0.1440	0.7	3.1452	1.2	0.1584	1.0	0.8	2276	12.1	1444	9.3	948	8.7	41.6
		9/1	0.008	31300	0.1576	0.8	4.4568	1.5	0.2051	1.3	0.8	2430	14.2	1723	12.6	1203	14.0	49.5
		13/1	0.103	65604	0.1704	1.0	4.8296	1.6	0.2056	1.2	0.7	2562	16.3	1790	13.1	1205	13.5	47.0
		20/1 *	0.399	59203	0.2016	0.9	9.7003	2.5	0.3490	2.3	0.9	2839	14.4	2407	22.4	1930	38.1	68.0
		23/1	0.073	14763	0.1922	23.6	12.1682	16.9	0.4591	16.5	1.0	2761	342.9	2617	147.7	2435	325.6	88.2
		15/1 *	0.151	50294	0.2077	2.4	12.2895	1.8	0.4290	1.6	0.9	2888	38.0	2627	16.4	2301	30.7	79.7
		12/1 *	0.168	19257	0.2097	5.2	12.3718	3.8	0.4279	3.6	0.9	2903	82.2	2633	34.9	2296	69.2	79.1
		1/1	0.198	54899	0.2160	1.7	16.4998	1.3	0.5540	1.1	0.8	2951	27.8	2906	12.8	2842	25.3	96.3
		3/1 *	0.266	58207	0.2147	2.0	16.5118	1.5	0.5578	1.3	0.8	2941	31.4	2907	14.2	2858	29.3	97.2
		14/1	0.279	35956	0.2165	3.2	16.5264	2.4	0.5535	2.2	0.9	2955	51.4	2908	22.4	2840	51.0	96.1
		19/1	0.270	29742	0.2174	2.1	17.1850	1.6	0.5734	1.4	0.9	2961	33.7	2945	15.1	2922	33.0	98.7
		4/1 *	0.195	65274	0.2154	2.8	17.5219	2.1	0.5900	1.8	0.8	2946	43.8	2964	19.5	2990	43.8	101.5
		6/1	0.208	19502	0.2192	2.8	17.5242	2.1	0.5798	1.9	0.9	2975	44.7	2964	19.7	2948	45.2	99.1
		7/1 *	0.291	16019	0.2132	2.2	17.5593	1.7	0.5975	1.5	0.9	2930	35.2	2966	15.8	3020	35.1	103.1
		22/2 *	0.163	29905	0.2142	3.0	17.9073	2.2	0.6064	2.1	1.0	2937	47.8	2985	20.7	3056	50.3	104.0
		17/1 *	0.159	33733	0.2151	3.1	17.9140	2.2	0.6039	2.1	0.9	2945	48.8	2985	21.4	3046	50.8	103.4
		5/1	0.199	50808	0.2217	1.9	18.2856	1.5	0.5981	1.2	0.9	2993	30.5	3005	13.9	3022	30.1	101.0
		8/1 *	0.329	36859	0.2160	4.1	18.4096	2.9	0.6183	2.8	0.9	2951	63.9	3011	27.8	3103	68.7	105.2
		21/1.	0.129	240454	0.2174	1.4	18.7126	1.1	0.6243	0.9	0.8	2961	22.5	3027	10.3	3127	22.3	105.6
		10/1 *	0.202	29728	0.2156	2.3	19.0421	1.7	0.6406	1.5	0.9	2948	36.0	3044	16.0	3191	38.0	108.2
		22/1	0.092	4600	0.2229	2.6	22.4224	1.9	0.7295	1.8	0.9	3002	41.7	3202	18.7	3532	48.0	117.6
Mogno Trondhjemite	MFR-53	10/1	0.142	21910	0.2092	1.0	11.8596	2.0	0.4111	1.7	0.8	2899	16.7	2593	18.3	2220	31.4	76.6
		4/1	0.043	652	0.1883	4.0	12.5391	2.9	0.4831	2.7	0.9	2727	64.2	2646	27.2	2541	56.6	93.2
		11/1 *	0.179	34286	0.2080	4.2	12.9465	3.1	0.4515	2.8	0.8	2890	66.3	2676	28.9	2402	55.9	83.1
		2/1 *	0.160	1192	0.2089	3.2	14.2244	2.5	0.4939	2.0	0.8	2897	51.3	2765	23.5	2587	42.9	89.3
		1/1	0.136	617	0.2037	4.2	14.2926	3.1	0.5088	2.7	0.9	2856	66.2	2769	29.1	2651	59.9	92.8
		18/1	0.203	11163	0.2126	10.7	15.0121	7.7	0.5121	7.5	1.0	2926	163.7	2816	70.7	2666	161.2	91.1
		3/1	0.152	1122	0.2079	5.6	15.2501	4.1	0.5321	3.8	0.9	2889	88.1	2831	38.1	2750	85.5	95.2
		9/1	0.135	24455	0.2127	2.7	16.1686	2.0	0.5512	1.7	0.8	2926	42.6	2887	19.2	2830	39.6	96.7
		7/1 *	0.084	3763	0.2157	6.8	16.4191	4.9	0.5522	4.7	0.9	2949	105.2	2902	45.8	2834	106.3	96.1
		8/1 *	0.117	15216	0.2175	3.4	17.3626	2.5	0.5790	2.3	0.9	2962	54.1	2955	24.0	2945	53.9	99.4
		14/1 *	0.119	21121	0.2173	6.2	17.3839	4.5	0.5802	4.3	0.9	2961	96.2	2956	41.9	2950	100.3	99.6
		15/1 *	0.068	22128	0.2176	1.0	17.8733	2.4	0.5958	2.2	0.9	2963	15.9	2983	23.2	3013	53.5	101.7
		6/1	0.088	772	0.2156	1.0	17.9134	2.6	0.6026	2.4	0.9	2948	16.4	2985	24.8	3040	58.1	103.1
		21/1	0.098	75272	0.2135	1.0	18.1359	2.2	0.6161	2.0	0.8	2932	16.1	2997	21.3	3094	49.0	105.5
		13/1 *	0.109	19899	0.2189	1.0	18.2601	2.0	0.6051	1.8	0.9	2972	16.3	3004	19.4	3050	42.6	102.6
		5/1 *	0.092	368	0.2213	1.0	18.6862	2.5	0.6123	2.3	0.9	2990	16.0	3026	23.8	3079	55.9	103.0
		20/1	0.113	21287	0.2178	0.9	18.9932	2.0	0.6325	1.8	0.9	2964	15.2	3041	19.1	3160	43.7	106.6
		16/1 *	0.084	14594	0.2198	1.0	19.1641	2.6	0.6324	2.4	0.9	2979	16.1	3050	24.4	3159	58.5	106.0
		12/1 *	0.254	38969	0.2221	1.0	19.1652	1.6	0.6259	1.3	0.7	2996	15.6	3050	15.5	3133	31.9	104.6
		17/1	0.220	6586	0.2187	1.2	19.7630	9.4	0.6555	9.4	1.0	2971	19.0	3080	87.3	3250	234.6	109.4
		19/1	0.100	9120	0.2243	1.0	20.1828	9.5	0.6527	9.5	1.0	3012	15.8	3100	88.4	3239	237.2	107.5
Mogno Trondhjemite	FMR-98	13/1	0.056	50340	0.1832	0.5	5.7791	1.7	0.2288	1.6	1.0	2682	8.9	1943	14.9	1328	19.7	49.5
		27/1	0.042	9052	0.1802	0.8	6.2330	2.2	0.2508	2.0	0.9	2655	12.6	2009	18.8	1443	26.2	54.3
		1/1	0.047	228	0.2058	1.6	7.0599	3.2	0.2487	2.8	0.9	2873	25.1	2119	28.1	1432	35.9	49.8
		14/1	0.072	1786	0.1863	1.9	7.4757	3.1	0.2911	2.5	0.8	2710	31.3	2170	27.8	1647	36.2	60.8
		26/1	0.094	78046	0.1910	0.9	8.0382	3.0	0.3053	2.9	1.0	2751	14.7	2235	26.9	1717	43.3	62.4
		11/1	0.130	1360	0.2042	0.5	9.1271	2.0	0.3241	2.0	1.0	2860	8.4	2351	18.4	1810	30.8	63.3
		12/1	0.146	57267	0.2037	0.7	9.5759	3.3	0.3409	3.2	1.0	2856	11.8	2395	30.0	1891	52.7	66.2
		18/1 *	0.210	82604	0.2163	0.5	9.9023	3.3	0.3320	3.3	1.0	2954	8.8	2426	30.4	1848	52.9	62.6
		9/1	0.136	67107	0.2104	0.6	10.8929	2.5	0.3755	2.4	1.0	2909	9.1	2514	22.7	2055	42.2	70.7
		6/1	0.006	18589	0.2090	1.0	12.3296	1.9	0.4278	1.6	0.8	2898	16.7	2630	17.5	2296	30.2	79.2
		24/1	0.227	1420	0.2216	0.5	13.2606	1.2	0.4340	1.1	0.8	2993	8.4	2698	11.4	2324	21.2	77.6
		21/1	0.155	125998	0.2146	1.4	13.8467	1.0	0.4681	0.9	0.7	2940	21.9	2739	9.8	2475	18.2	84.2
		2/1	0.183	448	0.1873	3.5	12.6331	2.8	0.4892	2.1	0.7	2718	56.6	2653	25.8	2567	45.2	94.4
		5/1	0.138	8029	0.2129	3.8	15.3744	2.8	0.5238	2.6	0.9	2927	60.0	2839	26.2	2715	56.7	92.8
		10/1 *	0.061	33113	0.2180	3.5	16.1112	2.6	0.5360	2.5	0.9	2966	56.0	2883	24.1	2767	55.1	93.3
		3/1	0.134	360	0.2094	1.6	16.1491	3.7	0.5593	3.3	0.8	2901	25.4	2886	34.7	2864	76.7	98.7
		16/1 *	0.220	10146	0.2175	1.5	16.0752	1.1	0.5360	1.0	0.9	2962	24.2	2881	10.9	2767	22.3	93.4
		19/1 *	0.223	156694	0.2192	2.3	16.3551	1.7	0.5412	1.6	1.0	2975	36.3	2898	15.7	2789	35.5	93.8
		28/1 *	0.035	3436	0.2170	0.7	17.3145	1.6	0.5786	1.4	0.8	2959	12.0	2952	15.0	2943	32.7	99.5
		25/1	0.116	42808	0.2145	0.5	17.8620	1.3	0.6038	1.2	0.9	2940	8.5	2982	12.7	3045	29.5	103.6
		17/1 *	0.104	128042	0.2177	0.7	18.0064	4.0	0.5998	3.9	1.0	2964	11.7	2990	37.6	3029	94.0	102.2
		7/1	0.269	153599	0.2206	0.7	18.2232	1.4	0.5992	1.2	0.7	2985	11.4	3002	13.3	3027	28.8	101.4
		22/1 *	0.205	119095	0.2178	0.5	18.3586	1.6	0.6114	1.5	1.0	2964	8.0	3009	15.3	3075	37.1	103.7
		15/1	0.170	24573	0.2202	0.6	18.4600	1.1	0.6079	0.9	0.8	2982	9.6	3014	10.4	3062	22.1	102.7
		23/1 *	0.191	202174	0.2190	0.5	19.0889	1.0	0.6321	0.9	0.9	2974	7.8	3046	9.7	3158	22.2	106.2
		4/1 *	0.097	14067	0.2173	1.1	19.5374	3.8	0.6521	3.6	1.0	2961	17.3	3069	36.0	3236	91.8	109.3
		8/1	0.228	109011	0.2203	0.5	19.6579	1.5	0.6472	1.4	0.9	2983	8.7	3075	14.0	3217	34.3	107.9
		20/1	0.022	278972	0.2223	0.5	21.8843	1.6	0.7141	1.5	1.0	2997	8.5	3179	15.4	3474	40.3	115.9

Table 4 – Continued

				Isotopic ratios								Ages						
Units	Samples	Zircon n°/Spot	Th/U	$^{206}Pb/^{204}Pb$	$^{207}Pb/^{206}Pb$	1s(%)	$^{207}Pb/^{235}U$	1s(%)	$^{206}Pb/^{238}U$	1s(%)	ρ	$^{207}Pb/^{206}Pb$	1s(%)	$^{207}Pb/^{235}U$	1s(%)	$^{206}Pb/^{238}U$	1s(%)	Conc (%)
Mogno Trondhjemite	MASF-28	10/1	0.004	6541	0.0757	2.7	0.8774	3.0	0.0841	1.3	0.3	1086	53.7	640	14.2	521	6.5	47.9
		18/1	0.002	493	0.1101	3.6	0.8869	4.7	0.0584	3.0	0.5	1800	64.9	645	22.4	366	10.8	20.3
		6/1	0.001	21617	0.0757	2.9	0.9818	3.6	0.0941	2.0	0.4	1087	57.7	695	17.8	580	11.3	53.3
		16/1	0.167	1233	0.1248	2.4	1.0976	3.0	0.0638	1.9	0.6	2027	41.8	752	16.0	398	7.2	19.7
		13/2	0.001	8717	0.0879	2.6	1.1723	3.7	0.0967	2.6	0.5	1381	48.9	788	19.9	595	14.8	43.1
		8/1 *	0.001	4958	0.1339	3.3	1.7073	4.8	0.0925	3.6	0.7	2149	56.2	1011	30.6	570	19.4	26.5
		1/3 *	0.002	2123	0.1428	2.5	2.0535	3.1	0.1043	1.8	0.6	2262	41.9	1133	20.8	639	11.2	28.3
		9/2 *	0.113	2374	0.1530	4.3	2.3662	6.9	0.1121	5.3	0.7	2380	71.5	1232	47.8	685	34.6	28.8
		17/1	0.005	20207	0.1640	2.4	4.3108	3.6	0.1907	2.6	0.7	2497	40.1	1695	29.0	1125	27.1	45.1
		2/1 *	0.124	2652	0.1832	2.3	5.1193	3.7	0.2027	2.9	0.8	2682	37.8	1839	31.1	1190	31.6	44.4
		3/1 *	0.017	3875	0.1823	4.3	5.1782	7.5	0.2060	6.2	0.7	2674	69.4	1849	62.0	1208	67.6	45.2
		15/1 *	0.158	6958	0.2196	7.9	13.9538	5.9	0.4610	5.2	0.7	2977	121.4	2747	54.3	2444	105.5	82.1
		5/1 *	0.198	2507	0.2178	9.4	14.5648	7.0	0.4849	6.3	0.9	2965	144.6	2787	64.8	2549	131.0	86.0
		11/1 *	0.218	3395	0.2165	6.6	15.4673	4.9	0.5180	4.3	0.9	2955	102.0	2844	45.8	2691	94.7	91.1
		14/2	0.003	13663	0.2109	3.5	15.9740	2.9	0.5493	1.9	0.6	2913	55.6	2875	27.8	2822	43.2	96.9
		17/2 *	0.005	20862	0.2145	3.5	16.5673	2.9	0.5602	1.9	0.6	2940	55.4	2910	27.8	2868	43.7	97.5
		4/1	0.158	2879	0.2262	9.5	16.7283	7.0	0.5364	6.3	0.9	3025	144.3	2919	65.3	2768	140.9	91.5
		14/1	0.004	13439	0.2124	3.0	17.4224	2.6	0.5949	1.4	0.5	2924	47.4	2958	25.0	3009	33.3	102.9
		1/1	0.002	21786	0.2117	3.1	17.5963	2.8	0.6029	1.4	0.4	2918	50.1	2968	26.5	3042	34.9	104.2
		7/2	0.058	5078	0.2277	22.3	19.2999	16.1	0.6147	15.4	0.9	3036	318.1	3057	144.5	3089	367.4	101.7
		12/1	0.426	1219	0.2224	10.2	20.2298	7.4	0.6598	7.0	1.0	2998	155.4	3102	69.2	3266	177.9	108.9
		9/1	0.711	400	0.2257	4.4	108.1404	47.3	3.4745	47.1	1.0	3022	69.5	4765	390.5	9659	2010.2	319.6
Caracol Tonalitic Complex	AM-02A	1/1	0.225	26627	0.2167	3.9	19.2180	2.8	0.6433	2.7	1.0	2956	61.8	3053	26.7	3202	68.6	108.3
		2/1	0.077	89009	0.2109	3.5	16.0564	2.5	0.5522	2.4	1.0	2912	54.9	2880	23.4	2834	55.0	97.3
		3/1	0.251	48562	0.2151	3.4	24.2401	2.5	0.8173	2.3	0.9	2944	53.9	3278	24.1	3851	66.5	130.8
		3/1	0.117	46297	0.2097	4.4	15.7211	3.1	0.5437	3.0	0.9	2903	69.2	2860	29.5	2799	68.8	96.4
		4/1	0.348	124395	0.2165	0.6	16.7602	2.2	0.5613	2.1	0.9	2955	9.4	2921	20.6	2872	48.4	97.2
		5/1	0.186	49732	0.2089	0.6	14.7246	2.3	0.5111	2.2	0.9	2897	9.8	2798	21.7	2661	48.3	91.9
		5/1	0.229	14677	0.2130	1.3	18.2335	7.5	0.6210	7.4	1.0	2928	21.1	3002	69.8	3114	179.8	106.3
		6/1	0.340	21396	0.2176	0.8	17.3776	3.7	0.5793	3.6	0.9	2963	13.0	2956	34.5	2946	83.7	99.4
		7/1	0.298	38454	0.2122	0.7	16.2695	1.8	0.5562	1.6	0.9	2922	11.2	2893	16.8	2851	37.5	97.6
		7/2 *	0.168	38206	0.2112	0.7	17.0102	1.7	0.5840	1.6	0.9	2915	11.0	2935	16.5	2965	37.7	101.7
		7/3	0.252	16411	0.2114	1.0	17.7522	4.4	0.6091	4.3	0.9	2916	16.5	2976	41.2	3066	103.0	105.1
		8/1 *	0.310	42124	0.2102	0.7	16.5999	2.4	0.5727	2.2	1.0	2907	12.0	2912	22.3	2919	52.3	100.4
		9/2	0.352	24913	0.2052	0.8	17.8695	1.7	0.6315	1.5	0.9	2868	13.1	2983	16.2	3155	37.2	110.0
		9/1	0.276	77957	0.2093	0.8	22.0048	1.6	0.7625	1.4	0.9	2900	12.4	3184	15.8	3653	40.2	126.0
		10/1	0.238	30583	0.2087	0.9	18.7977	3.4	0.6533	3.2	0.9	2895	14.2	3031	31.8	3241	81.8	111.9
		11/1	0.217	39714	0.1157	0.7	4.0812	1.7	0.2557	1.6	0.9	1892	11.9	1651	14.1	1468	21.1	77.6
		12/1	0.398	86810	0.1113	0.6	3.1940	4.5	0.2081	4.4	1.0	1821	11.7	1456	34.2	1219	49.2	66.9
		12/2	0.231	24955	0.1169	0.8	3.8678	2.2	0.2400	2.1	0.9	1909	13.5	1607	17.6	1387	25.8	72.6
		13/1	0.295	12650	0.0825	1.0	1.6145	5.4	0.1420	5.3	1.0	1257	20.0	976	33.6	856	42.7	68.1
		13/2 *	0.241	3447	0.2108	0.7	16.8459	1.4	0.5796	1.2	0.8	2912	11.8	2926	13.4	2947	28.4	101.2
		14/1	0.517	81304	0.2164	1.1	17.1633	3.1	0.5753	2.9	0.9	2954	18.1	2944	29.0	2930	66.9	99.2
		15/1 *	0.225	18456	0.2109	1.0	16.8372	3.3	0.5789	3.1	0.9	2913	16.6	2926	30.8	2944	72.9	101.1
		16/1 *	0.322	33928	0.2093	0.7	16.6931	1.4	0.5785	1.2	0.8	2900	12.0	2917	13.3	2943	27.8	101.5
		17/1	0.123	336642	0.2141	0.7	17.2726	1.2	0.5851	1.0	0.7	2937	11.5	2950	11.5	2970	22.9	101.1
		18/1	0.437	27164	0.2167	0.7	17.9930	2.3	0.6022	2.2	1.0	2956	11.7	2989	22.0	3039	52.9	102.8
		4/2	0.188	69107	0.2192	1.0	20.8622	4.3	0.6903	4.2	0.9	2975	16.7	3132	41.0	3384	109.5	113.8
		1/2	0.160	11492	0.2155	0.8	9.8413	4.8	0.3312	4.7	1.0	2947	13.1	2420	43.4	1844	75.6	62.6
Água Fria Trondhjemite	AM-01	1/1	0.050	51	0.1460	0.9	3.0189	1.5	0.1500	1.2	0.8	2299	15.3	1412	11.5	901	10.3	39.2
		2/2 *	0.286	119304	0.2028	2.1	15.7751	1.5	0.5642	1.4	0.9	2849	33.1	2863	14.6	2884	31.7	101.2
		3/1 *	0.258	7462	0.1478	2.9	3.7015	4.1	0.1816	2.9	0.7	2321	49.0	1572	32.2	1076	28.5	46.3
		3/2	0.249	1121	0.1143	0.9	1.8795	1.9	0.1193	1.7	0.9	1868	15.6	1074	12.7	727	11.8	38.9
		4/1	0.095	4258	0.1261	1.7	2.1415	2.0	0.1232	1.0	0.4	2044	30.1	1162	13.7	749	7.0	36.6
		4/2	0.050	587	0.1279	0.9	2.5450	1.6	0.1443	1.3	0.8	2070	16.1	1285	11.3	869	10.2	42.0
		5/1	0.052	113168	0.1902	3.2	11.8717	2.4	0.4528	2.2	0.9	2744	51.8	2594	21.8	2408	43.6	87.8
		6/1 *	0.040	147	0.1593	0.8	5.0395	1.4	0.2294	1.1	0.8	2449	12.6	1826	11.6	1331	13.8	54.4
		7/1	0.244	10187	0.1520	2.2	5.8493	3.6	0.2790	2.9	0.8	2369	37.4	1954	31.1	1586	40.4	67.0
		7/2	0.267	6303	0.1595	4.8	4.3547	17.1	0.1980	16.4	1.0	2450	78.5	1704	131.9	1165	172.1	47.5
		8/1	0.025	1593	0.1645	4.4	11.5963	3.2	0.5111	3.0	1.0	2503	71.6	2572	29.1	2661	65.4	106.3
		9/1 *	0.703	133011	0.2061	1.8	16.9394	1.4	0.5961	1.2	0.8	2875	29.3	2931	13.2	3014	28.5	104.8
		10/1 *	0.046	6492	0.1828	0.9	7.9729	1.8	0.3164	1.6	0.9	2678	14.1	2228	16.3	1772	24.8	66.2
		11/1 *	0.080	672	0.1242	2.5	2.5553	6.9	0.1492	6.5	0.9	2018	43.0	1288	49.2	897	53.8	44.4
		12/1 *	0.389	5108	0.1520	1.5	4.2555	4.2	0.2031	3.9	0.9	2368	25.2	1685	33.7	1192	42.1	50.3
		1/3	0.456	5516	0.1756	10.6	11.2004	7.6	0.4626	7.3	1.0	2612	166.0	2540	68.7	2451	147.4	93.9
		7/3	0.140	2069	0.1421	1.0	5.1635	1.8	0.2635	1.5	0.8	2253	17.2	1847	15.1	1508	19.8	66.9
		14/1	0.442	12964	0.1937	6.9	19.2675	5.0	0.7213	4.7	0.8	2774	108.3	3055	47.5	3501	124.7	126.2
		15/1	0.035	315213	0.0972	1.3	1.3840	1.8	0.1033	1.2	0.7	1571	24.2	882	10.5	634	7.4	40.3
		16/1	0.007	9165	0.1115	1.2	1.8163	1.8	0.1182	1.4	0.8	1824	20.8	1051	11.8	720	9.5	39.5
		17/1	0.015	53425	0.1137	1.5	2.0454	2.1	0.1305	1.5	0.7	1859	27.0	1131	14.3	791	10.9	42.5
		18/1	0.033	2102	0.1056	1.0	1.9208	2.4	0.1319	2.2	0.8	1725	18.5	1088	15.8	799	16.2	46.3
		19/1	0.022	6049	0.0405	23.4	0.4553	26.2	0.0815	11.7	0.4	-318	513.0	381	79.9	505	56.7	-158.8
		20/1	0.015	31510	0.1080	2.0	2.4817	2.4	0.1666	1.4	0.6	1767	35.5	1267	17.5	993	13.2	56.2
		21/1	0.178	32832	0.2129	1.9	17.8775	1.5	0.6091	1.0	0.6	2928	29.7	2983	14.8	3066	24.9	104.7
		22/1	0.025	3663	0.1637	7.9	8.5444	5.6	0.3787	5.5	1.0	2494	126.9	2291	49.8	2070	97.0	83.0
		23/1	0.086	926	0.0944	1.8	1.1888	3.1	0.0913	2.5	0.8	1516	33.4	795	16.9	563	13.6	37.2

Conc (%) denotes degree of concordance. For each studied rock, analyses labelled * were included in the age calculation, whereas others were omitted.

Three of the new ages obtained for the Arco Verde tonalite are ca. 2935 Ma, whereas the forth dated sample is significantly older (2973±11 Ma; MAR-111). This latter age and those of the inherited zircon grains in samples MAR-66 and MAR-148 approach most of the ages available in the literature for this TTG unit (~2980 to 2960 Ma; cf. Table 1). The data, therefore, indicate the possibility of the existence of two different TTG suites in the southern domain of the RMGGT. However, it is not possible so far to distinguish these two units using geological, petrographic, and geochemical data. For this reason, all the studied rocks are considered to belong to the Arco Verde tonalite suite. A similar picture is described in other Archean cratons

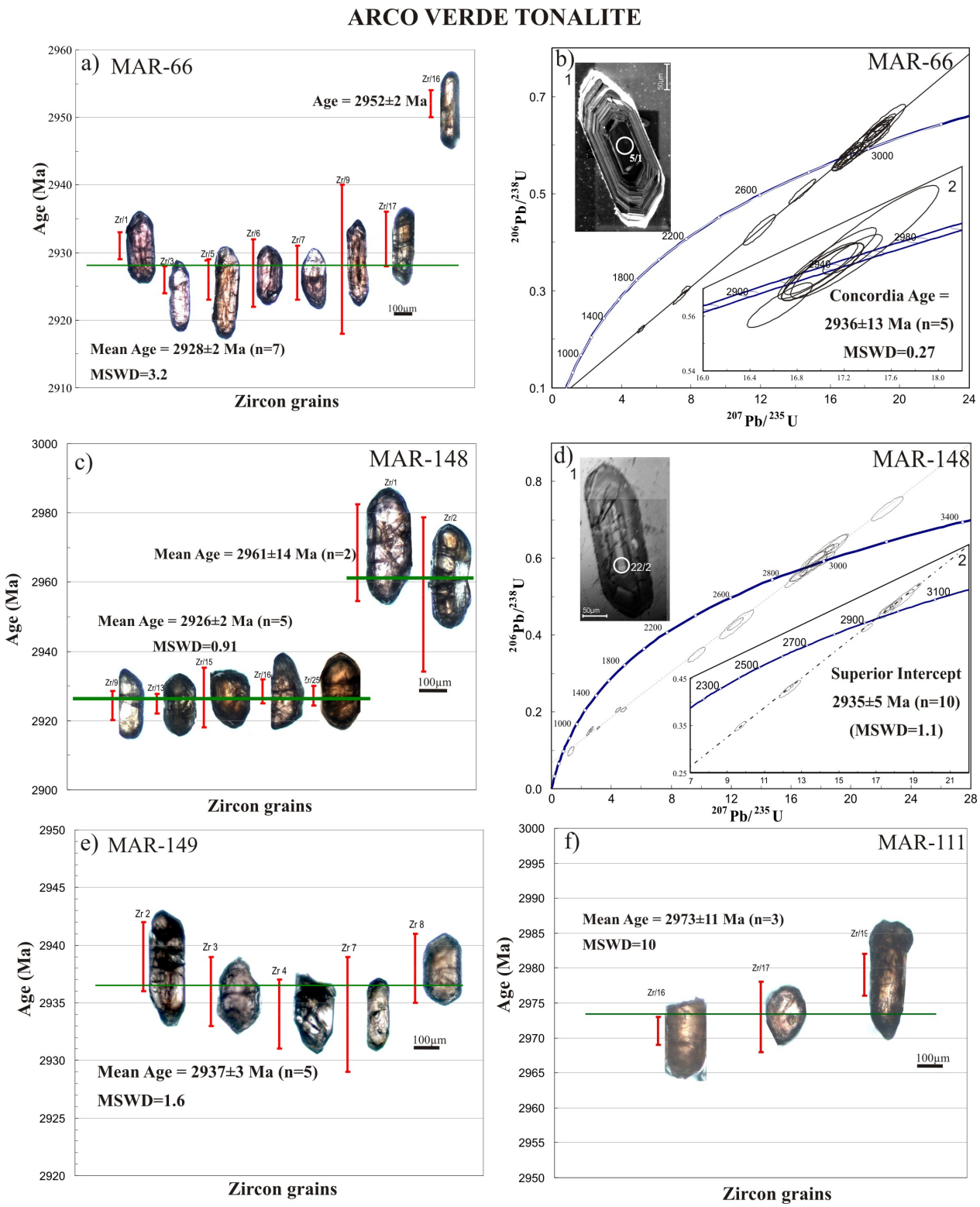

Figure 4 - Diagrams for the dated samples from the Arco Verde Tonalite: a) Pb-evaporation diagram for the sample MAR-66; b) Concordia diagram of U–Pb zircon analytical results for sample MAR-66; c) Pb-evaporation diagram for the sample MAR-148. Note that the zircon 1 and

10 are distinctive from 9, 15 and 16; d) Concordia diagram showing discordia line for zircons from sample MAR-148; e) Pb-evaporation diagram for the sample MAR-149; f) Pb-evaporation diagrams for the sample MAR-111. The Inserts 4b1 and 4d1 show representative cathodoluminescence image of zircon grains with well-developed oscillatory zoning, a typical magmatic feature. The Inserts 4b2 and 4d2 show the analyses that were included in the age calculation. In the figures 4a, 4c and 4e, the vertical red bar represents the error for each zircon grain and horizontal thick green bar corresponds to the mean age for the sample.

where TTG units show age variations in an interval of ~50 m. y. (Barberton, Moyen et al., 2007; Pilbara, Champion and Smithies, 2007; Karelia, Käpyaho et al., 2006).

5.3.2 - Mogno trondhjemite: samples MFR-53, FMR-98, FMR-87, and AM-03

Three zircon grains from sample MFR-53 yielded a mean Pb-Pb age of 2962±8 Ma (Fig. 5a). Additional analyses were made on 21 zircon crystals from the same sample by the U–Pb LA-ICP-MS method and ten analyses defined an upper intercept age at 2965±7 Ma (MSWD=0.85; Fig. 5b), which coincides with the Pb-Pb age and is interpreted as the crystallization age of the rock.

Three zircon crystals from sample FMR-98 yielded a mean Pb-Pb evaporation age of 2968±2 Ma (MSWD=0.52; Fig. 5c). U–Pb analyses by LA-ICP-MS and 9 spots give an upper intercept at 2968 ± 3 Ma (MSWD=1.7; Fig. 5d) identical to the Pb-Pb age, interpreted as the crystallization age of sample FMR-98.

The FMR-87 and AM-03 samples were analyzed only by the single zircon Pb-evaporation method. Four zircon grains from sample FMR-87 yielded a mean age of 2959±5 Ma (MSWD=1.8; Fig. 5e) and three crystals from sample AM-03 yielded a mean age of 2959±2 Ma (MSWD=0.048; Fig. 5f). These ages were interpreted as the crystallization ages of the FMR-87 and AM-03 samples.

A representative sample (MASF-28) of the thondhjemitic stock located to the east of the Paleoproterozoic Bannach pluton (Fig. 2) was selected for zircon dating by the U–Pb LA-ICP-MS and single zircon Pb-evaporation methods. Pb-evaporation analyses were performed on eight zircon crystals from sample MASF-28. Two grains yielded individual ages of 2967±2 Ma and

MOGNO TRONDHJEMITE

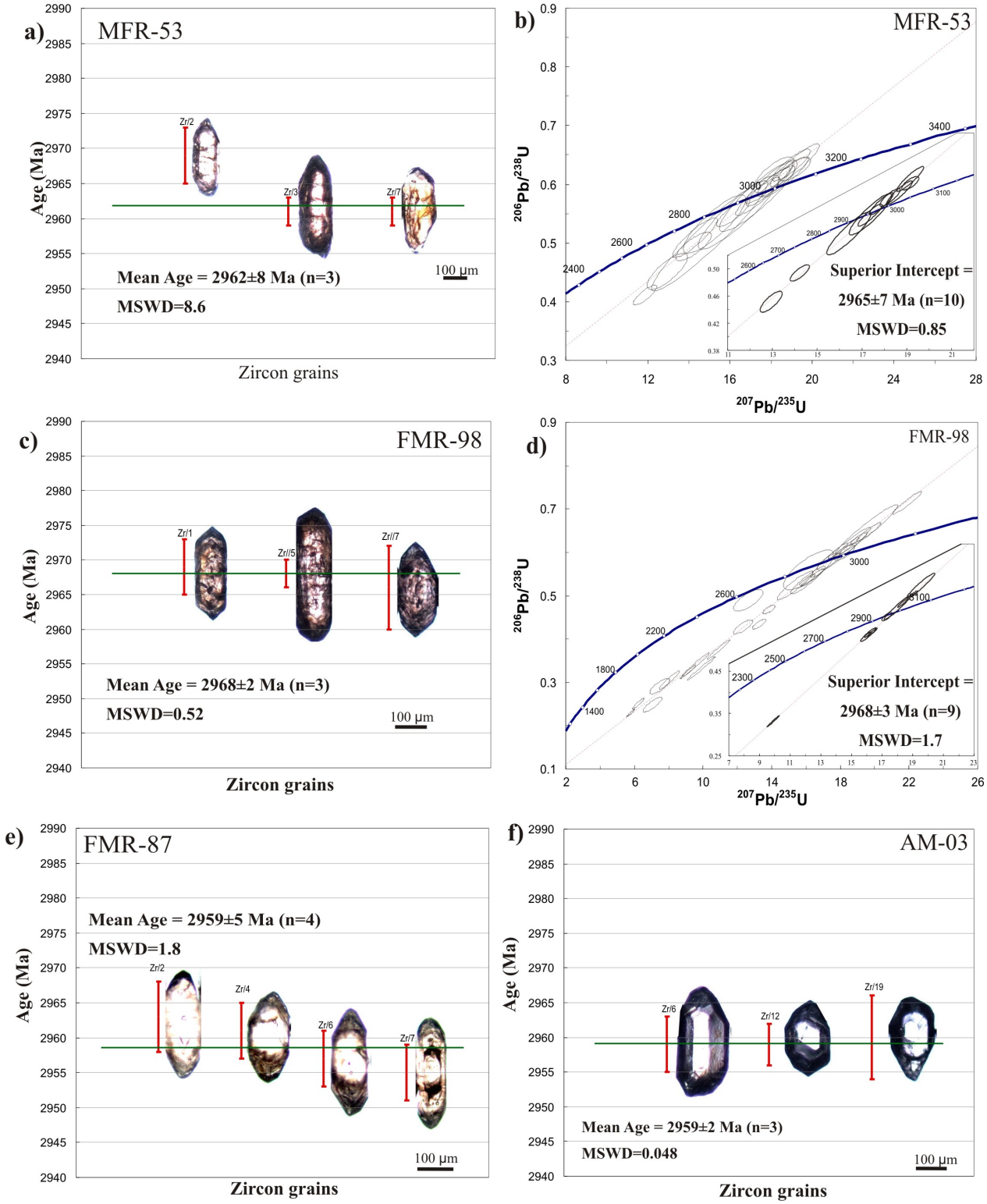

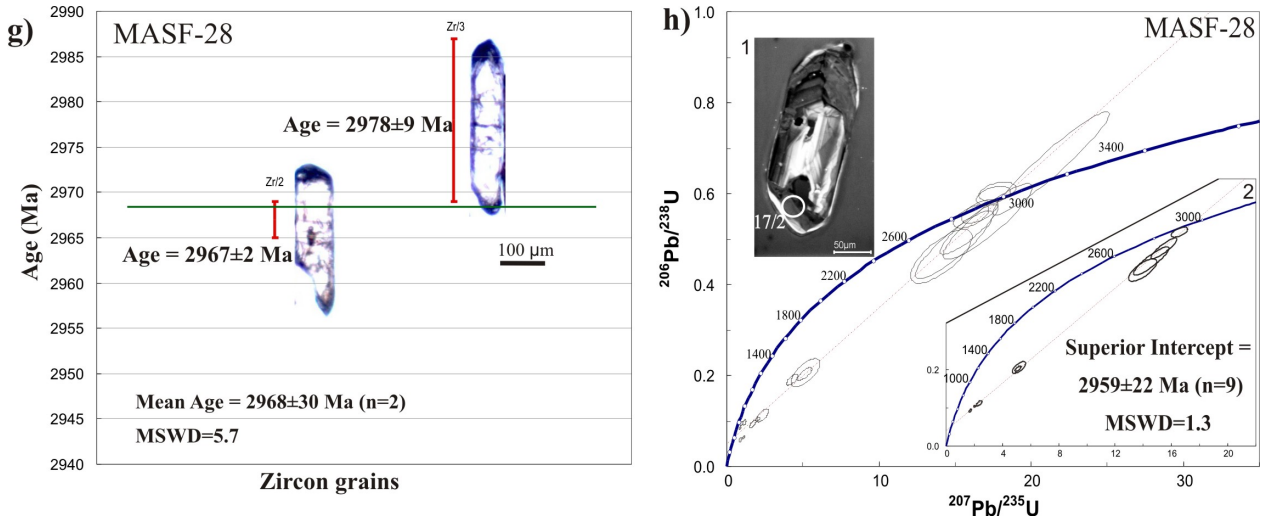

Figure 5 - Diagrams for the dated samples from Mogno trondhjemite: a) Single zircon Pb-evaporation age diagram for the sample MFR-53; b) U–Pb concordia diagram for zircons from sample MFR-53; c) Pb-evaporation diagram for the sample FMR-98; d) Concordia diagram showing discordia line for zircons from sample FMR-98; e) Pb-evaporation diagram for the sample FMR-87; f) Pb-evaporation diagram for the sample AM-03. Note that the zircons are transparent crystals and rounded to slightly elongated; g) Pb-evaporation diagrams for the sample MASF-28; h) Concordia diagram of U–Pb zircon analytical results for the sample MASF-28 (Salobro Trondhjemite). The Insert 5h1 shows representative cathodoluminescence image of zircon grains with well-developed oscillatory zoning, a typical magmatic feature. The Inserts in figure 5b, 5d and 5h2 show the analyses that were included in the age calculation. In the figures 5a, 5c, 5e, 5f and 5g, the vertical red bar represents the error for each zircon grain and horizontal thick green bar corresponds to the mean age for the sample.

2978±9 Ma (Fig. 5g) defining a mean age of 2968±30. Twenty-two spot analyses on 18 zircon grains of the sample MASF-28 were also performed by the U–Pb LA-ICP-MS. Nine of the 22 spots define an upper intercept age of 2959±22 Ma (MSWD=1.3; Fig. 5h), which is interpreted as the crystallization age of the stock.

The five samples from the Mogno trondhjemite yielded ages around 2965 Ma which is interpreted as the crystallization age of the Mogno trondhjemite. It differs remarkably from the ages available in the literature which are ~100 m.y. younger (Pimentel and Machado, 1994; Macambira et al., 2000; cf. Table 1).

5.3.3 –Mariazinha Tonalite: samples FMR-25 and AM-02A

Four zircon grains from sample FMR-25 yielded a mean age of 2925±3 Ma (MSWD=2.6; Fig. 6a), interpreted as the best estimate for the crystallization age.

Sample AM-02A was collected in a large quarry, near the town of Xinguara, in the vicinities of the southern contact between the Xinguara pluton and the Caracol tonalitic complex (Fig. 2), where TTG rocks are well exposed. This sample was initially considered as related to the Caracol complex and was selected for geochronological study. Three zircon crystals gave a weighted Pb-Pb average age of 2920±11 Ma (MSWD=14; Fig. 6b). Eighteen zircon crystals were analyzed by U–Pb LA-ICP-MS. Five spot analyses yielded a concordia age of 2918±13 Ma (Fig. 6c). This age coincides within error with the Pb-evaporation age and is interpreted as the crystallization age of sample AM-02A.

Leite et al. (2004) reported the Pb-evaporation age of 2924 ± 2 Ma for a tonalite representative of a TTG pluton located to the northwest of Xinguara (Fig. 2; Table 2). This pluton was included by Leite et al. (2004) in the Caracol tonalitic complex. However, the TTG rocks forming that pluton display a NS to NE-SW foliation, discordant with the dominant NW-SE to EW foliation trend of the Caracol tonalitic complex. The structural trend and the age of that pluton are coincident with those of the Mariazinha tonalite and, for this reason, it is interpreted here as associated with that TTG unit. The same is true for the banded TTG rocks (sample AM-02A) exposed in the quarry near Xinguara, which gave an age similar to that of the Mariazinha tonalite.

The geochronological data demonstrate that the Mariazinha Tonalite is younger than the Mogno Trondhjemite and significantly older than the Parazônia quartz diorite (2876 ± 2 Ma; Table 1; J. A. C. Almeida, unpublished data; Guimarães et al. b, submitted). The Mariazinha tonalite is also older than the Grotão granodiorite (Fig. 2), which includes angular enclaves of the former (Guimarães et al. b, submitted), and show a yet poorly defined but apparently younger age (J. A. C. Almeida, unpublished data).

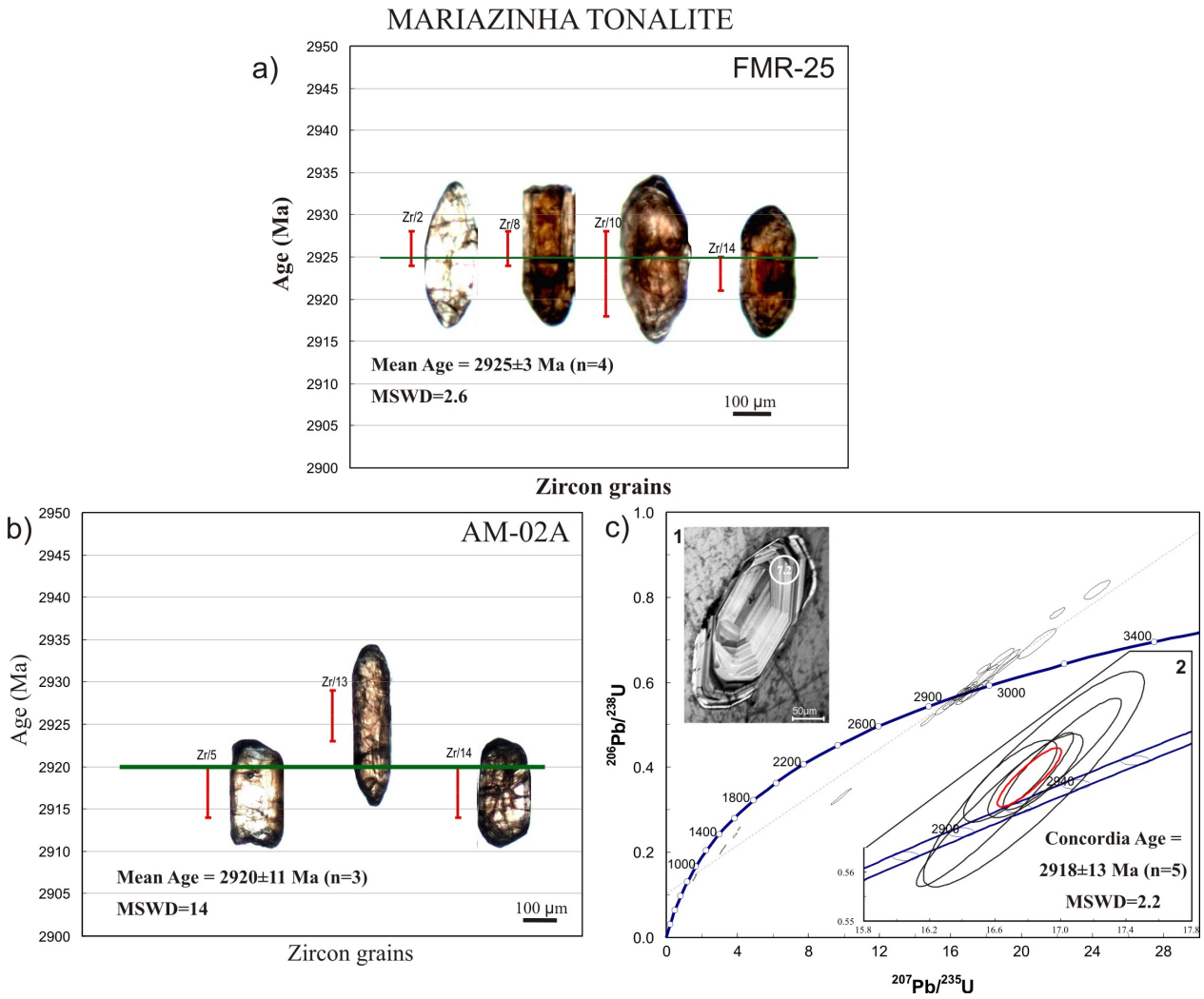

Figure 6 - Diagrams for the dated samples from Mariazinha tonalite. a) Single zircon Pb-evaporation age diagram for the sample FMR-25; b) Single zircon Pb-evaporation age diagram for the sample AM-02A; c) Concordia diagram of U–Pb zircon analytical results for sample AM-02A. The Insert 6c1 show representative cathodoluminescence images of zircon grains from sample AM-02A. Note the concentrically oscillatory zoning, typical of crystallization from magma.The inserts 6c2 show the analyses that were included in the age calculation. In the figures 6a and 6b, the vertical red bar represents the error for each zircon grain and horizontal thick green bar corresponds to the mean age for the sample.

5.3.4 – Caracol Tonalitic Complex

Sample AM-02A, associated with the Caracol tonalitic complex, was selected for the present study. It has been originally. However, as discussed above, the age obtained for that sample suggested its correlation with the Mariazinha tonalite. As a consequence, the only age available for the Caracol tonalitic complex are the Pb-evaporation ages in zircon previously published (Table 1; Leite et al., 2004). Those ages were obtained in samples located to the south and west of Xinguara and are, respectively, of 2948 ± 5 Ma and 2936 ± 3 Ma. These ages suggest that the Caracol tonalitic complex is significantly younger than the Mogno trondhjemite and a little older than the Mariazinha tonalite from which it differs also in the dominant structural trend (Fig. 2; Guimarães et al. a, submitted). For these reasons, we consider the Caracol tonalitic complex as a distinct TTG unit.

5.3.5 - Agua Fria Trondhjemite: sample AM-01

Sample AM-01 was analyzed by the U–Pb LA-ICP-MS method. Twenty-seven analyses performed on 23 zircons resulted on strongly discordant analytical points. This aspect, associated with the corroded and irregular shape of zircon cores of this sample (Fig. 7), indicates that zircon grains of this sample were affected by strong Pb loss. However, seven spots define a discordant line with an upper intercept age of 2854 ± 17 Ma (MSWD = 0.86; Fig. 7). This age is similar to that obtained by the Pb-evaporation method (Table 1; Leite et al. 2004) and is interpreted as the crystallization age of the Agua Fria Trondhjemite.

The age of ~2860 Ma assumed for the Água Fria trondhjemite is around 100 to 60 m. y. younger than those obtained for the other TTG units of the RMGGT. It demonstrates that the younger TTGs are almost coeval with the sanukitoid series (Rio Maria granodiorite and similar rocks) and the potassic leucogranites (Xinguara and Mata Surrão plutons). However, it is also clear now that the relevance of this younger event of TTG formation for the evolution of the Rio Maria Granite-Greenstone Terrane was more limited than previously supposed (Dall'Agnol et al., 2006; Vasquez et al., 2008). The area of occurrence of younger TTG units is relatively small and restricted to the Água Fria trondhjemite, exposed solely to the northeastern of Xinguara (Fig. 2).

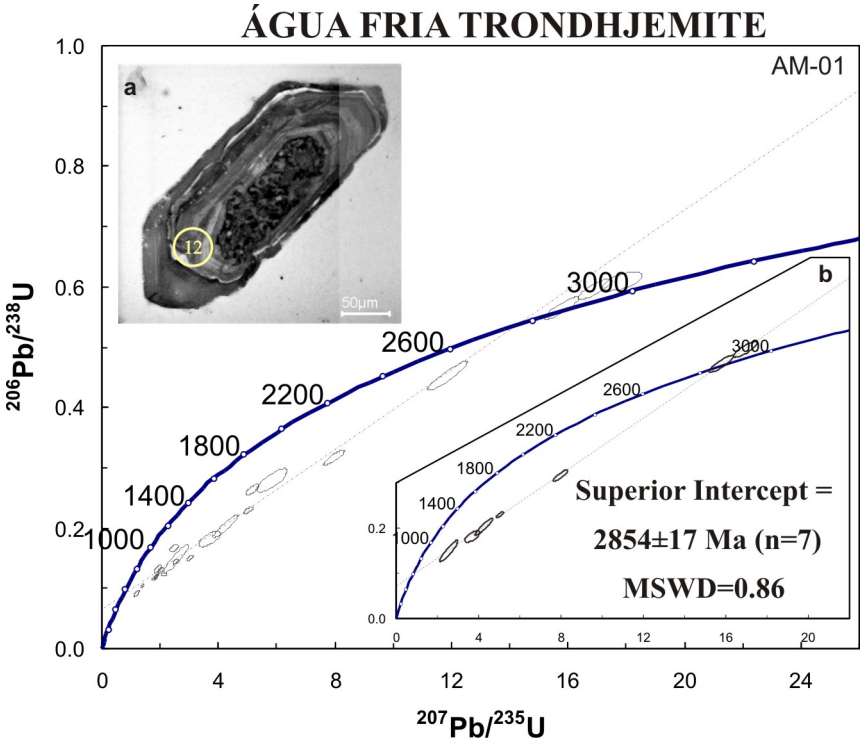

Figure 7 - Concordia diagram of U–Pb zircon analytical results for sample AM-01 from Água Fria trondhjemite. Note that the zircon grains are strongly discordant plotting below of the concordia curve. The insert 7a shows that the zircon crystals are strongly metamict with dissolved and corroded cores yield a spongiform aspect. The insert 7b shows the analyses that were included in the age calculation.

6. Geochemistry

6.1. Major elements

The representative chemical compositions of the TTG of the RMGGT are given in Table 5 and analytical procedures in Appendix A. The SiO_2 contents range between 64 and 73.5 wt. % and most oxides are negatively correlated with SiO_2 (Fig. 8). The exceptions are K_2O and Na_2O which do not define clear trends in Harker diagrams. These correlations are generally shown by the samples of individual suites, as well as by the whole analyzed samples. A large majority of the TTG of the RMGGT belong to the high-Al group (Barker and Arth, 1976), with subordinate low-Al TTG occurring in the Arco Verde tonalite, the Caracol tonalitic complex and the Água Fria trondhjemite. However, variations in Al contents in the different studied suites are

perceptible. Higher Al contents are shown by the Mariazinha tonalite and Mogno trondhjemite, and comparatively lower Al contents are observed in the Arco Verde tonalite, Caracol tonalitic complex and Água Fria trondhjemite (Fig. 8b). The studied TTG have geochemical affinities with rocks of the sub-alkaline, calc-alkaline series (Fig. 9a), and most of the analyzed samples plot in the medium-K series domain, with the Mariazinha tonalite showing lower K_2O contents compared to the other TTG suites and plotting preferentially in the low-K series field (Fig. 8g). For rocks of similar silica contents, Na_2O is generally lower in the Arco Verde tonalite and Caracol tonalitic complex compared with the Mogno and Agua Fria trondhjemites and Mariazinha tonalite (Fig. 8f). Using the geochemical classification of Barker (1979), the studied rocks are essentially tonalites and trondhjemites, with rare granodiorite components (Fig. 9b). They are ferromagnesian element-poor (Fe_2O_3+MgO+MnO+TiO_2 mostly ≤5%, except for the tonalites with lower silica contents), displays A/CNK values between about 0.9 and 1.1 (Fig. 9c), have low K_2O/Na_2O ratios (generally <0.5) and moderate to low #Mg (0.45-0.27). The sodic character of the TTG granitoids of the RMGGT is demonstrated in the K–Na–Ca plot (Fig. 9d; Barker and Arth, 1976; Martin, 1994), as they fall near the sodium-rich extremity of the trondhjemitic differentiation line and inside the field defined for typical Archean TTG rocks (Martin, 1994). All the geochemical characteristics observed in the studied rocks are typical of TTG rocks (Martin, 1994).

6.2. Trace elements and geochemical signatures

Considering only high precision ICP-MS data and rejecting anomalous values, the RMGGT TTG rocks display low concentrations of compatible transition elements [Ni (1-24 ppm), Cr (2-29 ppm) and V (11-75 ppm)], relatively low HFSE [Nb (2-17 ppm), Ta (0.1-2.9 ppm), Zr (95-254 ppm), Y (2-34 ppm), Hf (3-8 ppm)], and variable LILE contents, with low Rb (24-137 ppm) and moderately high Sr (218-771 ppm) and Ba (156-965 ppm) (Fig. 10; Table 5).

The whole analyzed samples of the TTG suites of the RMGGT show scattered distribution of LILE and HFSE contents in Harker variation diagrams (Fig. 10). However, some relevant geochemical contrasts between rocks of the different suites can be observed: Ba contents are remarkably lower in the Mariazinha tonalite compared to the Mogno trondhjemite, and quite

Table 5 - Representative chemical compositions of the different TTG units of the Rio Maria granite-greenstone terrane.

Unit	Arco Verde tonalite										Mogno trondhjemite									
Ages ranges	2.93-2.98 Ga										2.96 Ga									
Sample	F-57 / 92-36 [1]	AM-04[2]	MAR-148A[2]	MAR-149[2]	MAR-111[2]	MAR-117[2]	F-62 / 92-26[3]	MAR-66A[2]	MP-19[2]	ADR-245[2]	AM-03[2]	MFR-53[2]	FMR-98[2]	FMR-87[4]	FMR-101[4]	FMR-89[4]	MASF-28[5]	FMR-77[4]	FMR-01[4]	FMR-15A[4]
Group	Low La/Yb	Low La/Yb	Low La/Yb	Low La/Yb	Low La/Yb	Low La/Yb	Middle La/Yb	High La/Yb	High La/Yb	Middle La/Yb	Middle La/Yb	High La/Yb	High La/Yb	High La/Yb	High La/Yb	Middle La/Yb	High La/Yb	High La/Yb	Middle La/Yb	High La/Yb
SiO_2 (%wt)	64.20	66.22	66.55	66.59	67.46	68.96	69.43	69.73	70.81	71.28	68.27	68.66	68.99	70.01	70.28	71.35	71.45	71.69	72.08	73.43
TiO_2	0.38	0.47	0.56	0.43	0.32	0.38	0.32	0.31	0.24	0.33	0.35	0.34	0.42	0.29	0.29	0.23	0.25	0.24	0.22	0.23
Al_2O_3	17.17	15.11	15.26	16.13	17.12	15.53	15.38	15.58	15.03	14.96	15.14	15.57	14.82	16.19	16.10	15.48	15.61	15.33	14.94	14.25
$Fe_2O_{3(t)}$	4.37	4.95	4.88	4.13	2.75	3.71	3.54	3.16	2.63	2.80	3.13	3.12	3.61	2.08	2.33	1.84	1.93	1.94	2.06	2.01
MnO	0.08	0.07	0.06	0.06	0.04	0.05	0.04	0.03	0.03	0.04	0.05	0.04	0.05	0.03	0.03	0.02	0.03	0.03	0.03	0.02
MgO	1.63	1.50	1.26	1.09	0.82	0.97	0.79	0.72	0.66	0.65	1.23	0.89	1.15	0.66	0.76	0.57	0.59	0.58	0.55	0.52
CaO	4.94	3.90	4.30	3.88	3.47	3.69	3.20	3.38	3.13	3.14	2.92	3.25	2.23	3.09	3.26	2.96	2.72	2.79	2.49	2.37
Na_2O	4.72	3.60	3.74	4.39	5.52	4.22	4.80	4.70	4.45	3.89	4.52	4.73	5.40	5.44	5.09	5.03	4.84	4.88	4.52	4.52
K_2O	1.38	2.26	1.82	1.72	1.19	1.34	1.38	1.18	1.53	2.00	1.92	1.30	1.58	1.24	1.23	1.31	2.16	1.58	2.16	1.90
P_2O_5	0.22	0.13	0.16	0.16	0.10	0.14	0.15	0.10	0.08	0.09	0.10	0.11	0.16	0.10	0.09	0.08	0.09	0.09	0.06	0.07
LOI	0.78	1.50	1.30	1.20	1.00	0.80	0.74	0.80	1.10	0.60	2.10	1.70	1.30	0.70	0.40	1.00	0.20	0.70	0.70	0.50
Total	99.87	99.71	99.89	99.78	99.79	99.79	99.77	99.69	99.69	99.78	99.73	99.71	99.71	99.83	99.86	99.87	99.87	99.85	99.81	99.82
Ba (ppm)	156	683	608	337	241	344	234	765	707	618	641	586	531	534	487	568	890	472	666	793
Sr	317	302	273	281	512	218	255	361	460	290	434	507	355	668	554	520	556	506	499	533
Rb	87	137	96	105	63	61	76	35	70	67	53	32	58	25	28	41	55	24	47	40
Zr	173	167	211	254	163	144	239	174	132	152	174	154	150	140	141	104	114	129	109	126
Y	27	60	34	29	10	11	9	4	2	7	10	4	5	3	3	9	4	4	6	3
Hf	4	5	6	7	4	4	6	5	3	5	4	4	4	4	3	3	3	4	3	3
Nb	11	17	11	16	5	9	14	6	4	8	4	3	6	3	2	3	4	2	4	2
Ta	1	2	2	3	1	3	1	0	1	2	1	0	1	0	0	0	0	0	1	0
V	45	75	54	40	33	28	11	26	30	32	49	30	34	24	28	21	22	23	17	14
Ni	5	15	13	10	6	8	1	8	8	3	19	9	13	4	5	4	8	3	3	3
Cr	6	27	n.d	n.d	20	n.d	2	16	n.d.	n.d	26	23	21	n.d	n.d	n.d	n.d	n.d	n.d	n.d
Cu	33	46	14	60	107	41	0	36	36	17	37	51	45	4	9	4	7	4	10	11
U	1	4	3	3	1	1	2	0	1	1	2	0	1	0	0	1	0	1	1	0
Th	8	10	15	16	1	1	16	16	<0.2	11	3	4	10	3	3	4	3	5	3	6
Pb	10	7	5	5	2	1	11	4	3	4	2	4	3	3	2	2	2	2	3	2
Zn	80	65	62	71	52	62	75	53	34	43	36	38	66	41	43	14	41	33	41	44
Co	9	127	36	49	121	46	3	116	172	38	134	141	118	21	23	23	15	23	9	22
Cs	2	5	2	3	11	1	2	1	3	2	1	1	2	1	3	1	4	0	1	1
Ga	26	20	22	24	22	20	23	17	18	16	19	18	14	18	18	16	19	19	18	19
Mo	0	1	1	0	1	0	0	1	1	0	1	1	1	0	0	0	1	0	0	0
Sc	n.d	9	7	11	4	7	n.d	3	2	4	5	4	5	3	2	3	3	3	3	3
W	0	743	219	313	681	337	Tr	724	1074	268	660	890	709	146	121	129	87	155	44	139
La	20.96	34.20	55.60	60.10	10.60	7.00	61.99	76.70	15.80	40.40	21.60	28.10	39.10	23.60	34.10	48.00	17.00	23.40	24.60	33.70
Ce	40.14	52.10	95.70	106.60	21.70	13.50	109.10	135.40	24.50	71.20	35.20	51.70	70.80	40.60	40.60	30.50	31.90	43.90	39.00	61.50
Pr	4.05	7.61	10.25	10.83	2.54	1.41	10.45	14.08	2.32	6.84	5.04	5.62	7.72	4.61	5.90	8.81	3.28	4.83	5.25	6.59
Nd	15.07	29.50	32.70	34.70	9.90	4.90	34.56	45.50	7.70	20.50	18.40	19.80	26.80	16.20	19.10	32.60	12.00	17.00	17.90	22.60
Sm	3.26	5.86	5.90	6.10	2.05	1.40	5.06	5.29	0.90	3.00	2.98	2.79	3.51	1.89	2.25	4.37	1.40	2.21	2.58	2.45
Eu	0.80	1.10	1.19	1.06	0.68	0.51	0.87	1.07	0.69	0.75	0.93	0.59	0.68	0.58	0.71	1.55	0.52	0.51	0.61	0.54
Gd	3.51	6.49	4.36	4.48	1.97	1.26	3.83	2.73	0.61	1.60	2.28	1.72	2.23	1.32	1.57	3.41	1.03	1.42	2.10	1.70
Tb	0.67	1.24	0.85	0.85	0.34	0.37	0.44	0.28	0.07	0.34	0.34	0.20	0.26	0.13	0.14	0.44	0.15	0.16	0.26	0.13
Dy	4.23	7.45	4.37	4.70	1.90	1.61	2.01	1.01	0.29	1.21	1.68	0.90	1.07	0.58	0.69	2.27	0.73	0.59	1.45	0.54
Ho	1.01	1.64	0.84	0.96	0.38	0.35	0.34	0.14	0.05	0.19	0.33	0.14	0.16	0.10	0.10	0.36	0.10	0.13	0.23	0.10
Er	2.40	4.85	2.61	2.60	1.14	1.15	0.78	0.31	0.14	0.67	0.85	0.33	0.42	0.24	0.27	0.89	0.33	0.38	0.59	0.17
Tm	0.35	0.80	0.36	0.45	0.18	0.18	0.10	0.04	0.02	0.10	0.13	0.04	0.06	0.04	0.03	0.15	<.05	0.06	0.08	0.04
Yb	2.37	4.88	2.55	2.43	1.10	0.88	0.72	0.25	0.14	0.67	0.76	0.31	0.36	0.27	0.14	0.86	0.26	0.30	0.59	0.24
Lu	0.31	0.69	0.37	0.40	0.16	0.14	0.12	0.04	0.02	0.11	0.11	0.05	0.05	0.03	0.04	0.13	0.04	0.05	0.08	0.03
A/CNK	0.94	0.98	0.96	1.00	1.03	1.03	1.01	1.03	1.02	1.05	1.02	1.03	1.01	1.02	1.03	1.03	1.02	1.04	1.04	1.03
K_2O/Na_2O	0.29	0.63	0.49	0.39	0.22	0.32	0.29	0.25	0.34	0.51	0.42	0.27	0.29	0.23	0.24	0.26	0.45	0.32	0.48	0.42
Fe2O3+MgO+ $MnO+TiO_2$	6.46	6.99	6.76	5.71	3.93	5.11	4.69	4.22	3.56	3.82	4.76	4.39	5.23	3.06	3.41	2.66	2.80	2.79	2.86	2.78
#Mg	0.42	0.38	0.34	0.34	0.37	0.34	0.31	0.31	0.33	0.31	0.44	0.36	0.39	0.39	0.39	0.38	0.38	0.37	0.35	0.34
Sr/Y	11.96	5.01	8.16	9.81	52.21	19.81	27.90	97.51	287.63	44.65	44.76	137.03	69.67	230.28	205.26	60.49	146.21	117.70	78.02	204.88
Nb/Ta	8.01	7.86	5.10	6.36	7.50	3.10	20.29	18.67	6.33	3.67	6.33	9.67	11.00	13.50	23.00	12.50	10.00	16.00	7.40	24.00
Zr/Hf	38.96	35.57	35.71	37.85	41.90	35.17	40.99	38.69	39.85	28.11	41.33	38.53	39.45	35.95	41.47	35.79	38.13	33.87	34.00	42.07
La/Yb	8.84	7.01	21.80	24.73	9.64	7.95	86.10	306.80	112.86	60.30	# 28.42	90.65	108.61	87.41	243.57	55.81	65.38	78.00	41.69	140.42
$(La/Yb)_N$	6.34	5.03	15.64	17.74	6.91	5.71	61.76	220.07	80.95	43.25	20.39	65.02	77.91	62.70	174.71	40.04	46.90	55.95	29.91	100.72
Eu/Eu*	0.72	0.54	0.69	0.59	1.02	1.15	0.58	0.77	2.7*	0.94	1.05	0.76	0.69	1.07	1.10	1.18	1.27	0.82	0.78	0.77
$(La/Sm)_N$	4.15	3.77	6.08	6.36	3.34	3.23	7.91	9.36	11.33	8.69	4.68	6.50	7.19	8.06	9.78	7.09	7.84	6.84	6.16	8.88
$(Gd/Yb)_N$	1.23	1.10	1.41	1.53	1.48	1.18	4.40	9.03	3.60	1.98	2.48	4.59	5.12	4.04	9.28	3.28	3.28	3.92	2.94	5.86

Unit	Caracol tonalitic complex					Mariazinha tonalite										Água Fria trondhjemite				
Ages ranges	2.94 Ga					2.92 Ga										2.86 Ga				
Sample	AL-163[6]	AL-03A[6]	AL-216[6]	ALF-237A[6]	AL-54A[6]	FMR-46[4]	FMR-27[4]	AL-210[6]	FMR-25[4]	AL-59[6]	ALF-253A[6]	FMR-37A[4]	FMR-52[4]	FMR-32[4]	AM-02A[2]	AL-16A[6]	AL-122[6]	AM-02B[2]	ALF-248A[6]	AM-01[2]
Type	Low La/Yb	Middle La/Yb	High La/Yb	Middle La/Yb	Middle La/Yb	High La/Yb	High La/Yb	Middle La/Yb	High La/Yb	High La/Yb	Middle La/Yb	High La/Yb	High La/Yb	High La/Yb	High La/Yb	High La/Yb	Middle La/Yb	High La/Yb	High La/Yb	Middle La/Yb
SiO_2 (%wt)	64.45	70.35	70.60	71.30	71.50	65.91	68.06	68.30	68.58	68.90	69.20	69.22	70.11	70.83	71.99	69.46	69.60	69.92	71.30	71.63
TiO_2	0.41	0.28	0.30	0.20	0.34	0.63	0.35	0.30	0.31	0.34	0.23	0.32	0.26	0.31	0.19	0.28	0.27	0.23	0.21	0.20
Al_2O_3	16.54	15.11	15.80	15.00	14.90	15.93	16.74	16.80	16.63	15.00	16.40	16.26	16.04	15.16	15.21	15.42	16.80	15.95	15.30	14.93
$Fe_2O_{3(t)}$	4.67	2.86	2.60	2.20	3.20	4.10	2.94	2.80	2.75	3.70	2.20	2.85	2.58	2.80	1.89	2.69	2.90	1.96	1.80	2.25
MnO	0.04	0.05	0.02	0.01	0.02	0.04	0.05	0.04	0.04	0.03	0.03	0.03	0.04	0.03	0.02	0.02	0.03	0.02	0.02	0.02
MgO	1.44	0.86	0.54	0.42	0.67	1.39	1.01	0.90	0.91	0.78	0.54	0.87	0.77	0.71	0.49	0.83	0.60	0.64	0.44	0.45
CaO	4.28	3.10	3.00	2.70	3.40	3.90	3.22	3.70	3.49	3.90	3.30	3.78	3.36	3.07	3.02	3.12	3.50	2.36	2.30	2.53
Na_2O	4.80	5.04	4.70	4.40	4.40	4.51	5.64	4.70	5.18	4.30	5.10	4.88	5.07	4.84	5.20	5.17	4.90	5.07	4.70	5.08
K_2O	1.81	1.13	1.40	1.50	0.97	2.27	1.24	1.30	1.52	1.20	1.10	1.11	1.20	1.39	0.94	1.35	1.10	2.60	2.10	1.98
P_2O_5	0.24	0.19	0.08	0.04	0.13	0.19	0.11	0.10	0.12	0.37	0.08	0.10	0.08	0.10	0.05	0.18	0.09	0.08	0.06	0.06
LOI	0.85	0.46	0.56	0.67	0.51	0.90	0.50	0.52	0.30	0.37	0.45	0.40	0.30	0.60	0.70	0.57	0.63	0.80	0.35	0.60
Total	99.53	99.43	99.60	98.44	100.04	99.77	99.86	99.46	99.83	98.89	98.63	99.82	99.81	99.84	99.70	99.09	100.42	99.63	98.58	99.73
Ba (ppm)	448	236	800	481	387	918	173	272	388	1199	749	418	626	429	444	193	230	1485	563	468
Sr	366	345	658	338	358	592	521	426	771	548	526	517	434	504	506	342	464	606	398	313
Rb	106	141	42	41	90	67	56	34	51	46	31	38	37	43	58	72	40	124	52	69
Zr	156	142	172	138	182	136	137	150	146	240	177	149	109	196	131	108	194	118	124	110
Y	21	12	6	11	10	9	4	13	3	9	11	4	2	4	3	5	12	4	3	4
Hf	n.d	n.d	n.d	n.d	n.d	3	4	n.d	4	n.d	n.d	4	3	5	4	n.d	n.d	3	n.d	3
Nb	10*	13*	<5*	<5*	<5*	7	3	<5*	3	<5*	<5*	2	3	2	3	10*	5*	5	6*	5*
Ta	n.d	n.d	n.d	n.d	n.d	1	0	n.d	0	n.d	n.d	0	0	0	0	n.d	n.d	1	n.d	1
V	-	-	25	21	25	57	29	40	24	53	15	27	22	27	23	-	24	24	23	29
Ni	n.d	n.d	n.d	n.d	n.d	7	8	n.d	7	n.d	n.d	6	6	6	8	n.d	n.d	9	n.d	7
Cr	n.d	n.d	n.d	n.d	n.d	n.d	n.d	n.d	n.d	n.d	n.d	n.d	n.d	n.d	21	n.d	n.d	29	n.d	27
Cu	n.d	n.d	n.d	n.d	n.d	17	18	n.d	9	n.d	n.d	21	6	8	68	n.d	n.d	38	n.d	47
U	n.d	n.d	n.d	n.d	n.d	2	1	n.d	1	n.d	n.d	0	0	1	2	n.d	n.d	2	n.d	1
Th	<5	<5	<5	<5	<5	6	8	<5	7	<5	<5	1	2	9	6	11	<5	8	<5	9
Pb	n.d	n.d	n.d	n.d	n.d	4	4	n.d	2	n.d	n.d	1	1	4	4	n.d	n.d	5	n.d	3
Zn	n.d	n.d	n.d	n.d	n.d	69	82	n.d	56	n.d	n.d	57	52	70	30	n.d	n.d	41	n.d	36
Co	n.d	n.d	n.d	n.d	n.d	15	18	n.d	12	n.d	n.d	14	14	28	138	n.d	n.d	137	n.d	146
Cs	n.d	n.d	n.d	n.d	n.d	2	2	n.d	1	n.d	n.d	1	1	1	2	n.d	n.d	3	n.d	1
Ga	14	16	28	29	25	20	21	25	21	38	26	18	20	19	18	21	31	20	30	20
Mo	n.d	n.d	n.d	n.d	n.d	0	0	n.d	0	n.d	n.d	0	0	1	1	n.d	n.d	1	n.d	1
Sc	n.d	n.d	n.d	n.d	n.d	4	4	n.d	4	n.d	n.d	3	3	3	2	n.d	n.d	2	n.d	3
W	n.d	n.d	n.d	n.d	n.d	45	62	n.d	46	n.d	n.d	74	73	173	814	n.d	n.d	772	n.d	861
La	12.56	18.77	16.61	14.96	18.46	32.60	46.10	9.96	33.40	70.50	6.91	15.10	9.70	44.90	23.10	19.37	14.01	20.90	7.93	14.50
Ce	30.43	34.04	31.81	30.51	38.95	60.00	85.80	17.31	61.00	106.70	13.80	27.90	18.50	78.10	39.80	34.43	22.15	36.70	14.80	24.30
Pr	n.d	n.d	n.d	n.d	n.d	7.45	9.22	n.d	6.57	n.d	n.d	3.04	1.92	7.83	4.16	n.d	n.d	4.07	n.d	2.60
Nd	16.12	10.97	9.03	11.38	12.11	30.50	32.30	5.40	24.10	36.01	5.12	11.50	5.90	28.60	13.40	14.59	7.51	13.80	5.04	8.90
Sm	4.07	2.03	1.33	2.50	2.16	4.43	3.70	1.21	2.83	6.61	1.20	1.54	1.05	3.40	1.57	2.31	1.43	1.80	1.13	1.38
Eu	0.77	0.32	0.41	0.65	0.61	1.11	0.77	0.34	0.64	1.31	0.39	0.57	0.51	0.81	0.49	0.47	0.48	0.56	0.32	0.56
Gd	3.48	1.39	0.97	1.89	1.60	3.63	2.43	0.89	1.87	3.32	1.08	1.42	0.86	2.28	0.92	1.49	0.95	1.17	0.83	1.21
Tb	n.d	n.d	n.d	n.d	n.d	0.40	0.22	n.d	0.15	n.d	n.d	0.15	0.10	0.20	0.11	n.d	n.d	0.14	n.d	0.16
Dy	3.35	0.92	0.41	1.53	0.92	1.41	1.14	0.46	0.72	1.15	0.67	0.69	0.48	0.85	0.54	0.74	0.54	0.70	0.38	0.76
Ho	0.66	0.18	0.06	0.23	0.15	0.25	0.15	0.08	0.11	0.18	0.10	0.11	0.07	0.12	0.09	0.12	0.09	0.12	0.07	0.14
Er	1.70	0.49	0.12	0.62	0.29	0.54	0.42	0.17	0.33	0.39	0.21	0.26	0.16	0.45	0.23	0.22	0.20	0.32	0.17	0.37
Tm	n.d	n.d	n.d	n.d	n.d	0.07	0.04	n.d	0.06	n.d	n.d	0.05	0.03	0.05	0.04	n.d	n.d	0.05	n.d	0.05
Yb	1.08	0.38	0.12	0.40	0.27	0.40	0.34	0.15	0.24	0.23	0.21	0.24	0.22	0.32	0.26	0.15	0.18	0.38	0.22	0.36
Lu	0.14	0.07	0.03	0.08	0.07	0.04	0.04	0.05	0.04	0.04	0.07	0.03	0.02	0.05	0.04	0.03	0.05	0.05	0.04	0.05
A/CNK	0.94	1.00	1.07	1.09	1.03	0.94	1.02	1.06	1.01	0.97	1.05	1.01	1.02	1.01	1.01	0.99	1.08	1.03	1.08	0.99
K_2O/Na_2O	0.38	0.22	0.30	0.34	0.22	0.50	0.22	0.28	0.29	0.28	0.22	0.23	0.24	0.29	0.18	0.26	0.22	0.51	0.45	0.39
Fe2O3+MgO+ $MnO+TiO_2$	6.56	4.05	3.46			6.16	4.35	4.04	4.01	4.85	3.00	4.07	3.65	3.85	2.59	3.82	3.80	2.85		2.92
#Mg	0.38	0.37	0.29	0.27	0.29	0.40	0.40	0.39	0.40	0.29	0.33	0.38	0.37	0.33	0.34	0.38	0.29	0.39	0.33	0.28
Sr/Y	17.43	28.75	109.67	30.73	35.80	68.84	121.26	32.77	233.64	60.89	47.82	136.13	255.29	144.11	187.48	68.40	38.67	147.76	132.67	72.72
Nb/Ta						9.29	30.00		16.00			9.50	9.33	12.00	6.75			6.00		8.33
Zr/Hf						39.88	33.41		41.69			40.35	35.16	41.77	36.44			40.66		35.58
La/Yb	11.64	49.39	144.43	37.31	67.37	81.50	135.59	65.07	139.17	305.19	33.24	62.92	44.09	140.31	88.85	# 129.13	77.83	55.00	36.05	40.28
$(La/Yb)_N$	8.35	35.43	103.60	26.76	48.33	58.46	97.26	46.67	99.82	218.92	23.84	45.13	31.63	100.65	63.73	92.63	55.83	39.45	25.86	28.89
Eu/Eu*	0.61	0.56	1.07	0.87	0.96	0.82	0.74	0.95	0.80	0.76	1.03	1.16	1.6*	0.84	1.15	0.72	1.19	1.11	0.97	1.30
$(La/Sm)_N$	1.99	5.97	8.08	3.87	5.51	4.75	8.04	5.30	7.62	6.88	3.72	6.33	5.96	8.53	9.50	5.42	6.34	7.50	4.53	6.78
$(Gd/Yb)_N$	2.67	3.03	6.96	3.90	4.83	7.51	5.91	4.83	6.45	11.90	4.28	4.89	3.23	5.89	2.93	8.20	4.36	2.55	3.12	2.78

Data Source: (1) Althoff (1996); (2) This work; (3) Althoff et al., 2000; (4) Guimarães et al. a, submitted; (5) Guimarães 2007; (6) Leite (2001). (6) Samples where the trace elements were analyzed by X-ray fluorescence; (1,2,3, 4 and 5) Samples where the trace elements were analyzed by ICP-MS.
Fe2O3 t=total iron recalculated as Fe2O3.LOI=loss on ignition.A/CNK: Molecular ratio (Al/Ca+Na+K).Mg# molecular ratio Mg/(Mg + Fe). LaN, YbN, SmN, GdN, EuN:Normalized REE value (Evesen et al 1978).Eu/Eu*=europium anomaly calculated as [Eu/(Eu*)]=[(EuN)/((SmN+GdN)/2)].nd: not determinated. * anamalous value

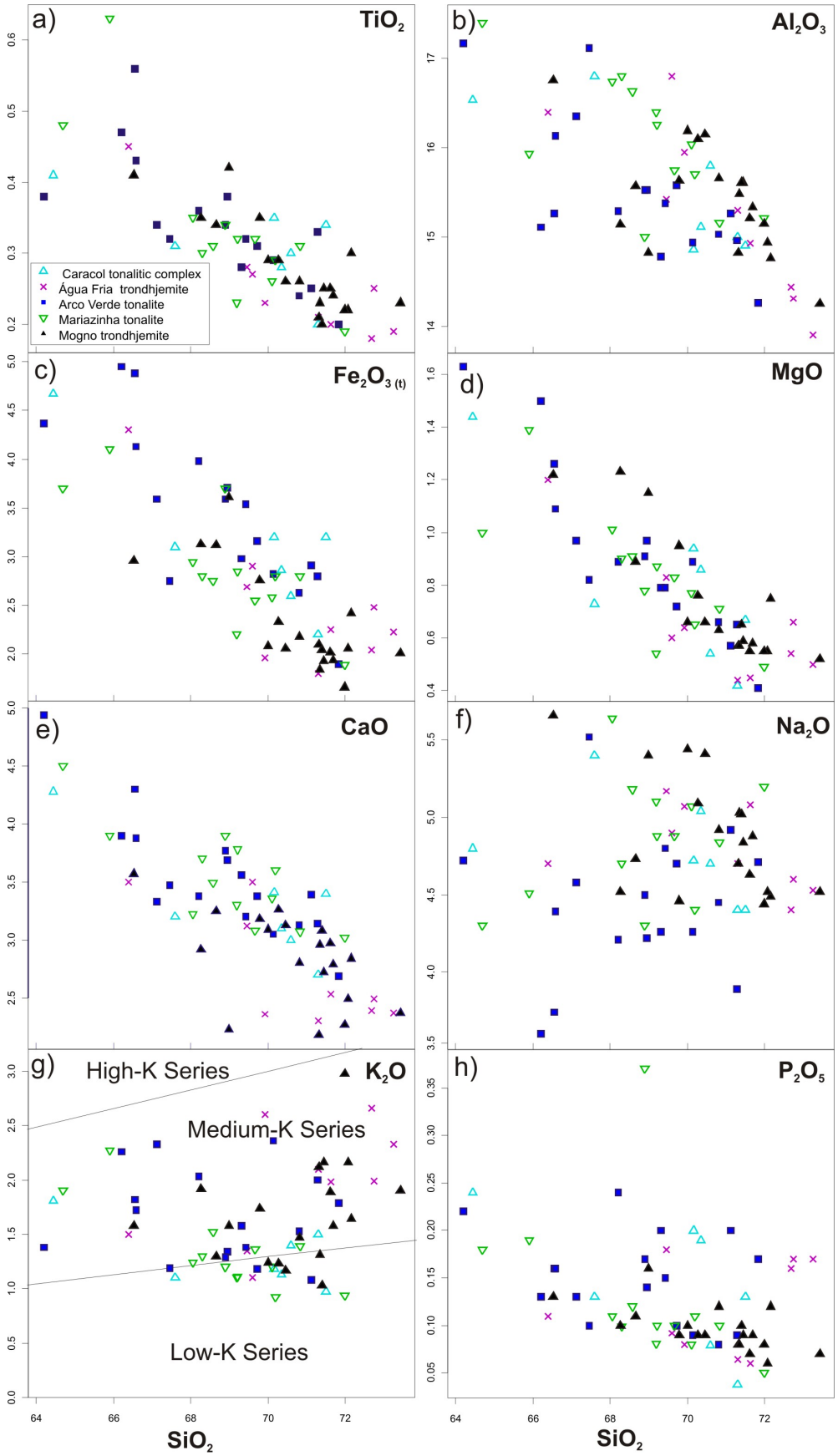
a)
TiO_2
Caracol tonalitic complex
Água Fria trondhjemite
Arco Verde tonalite
Mariazinha tonalite
Mogno trondhjemite
b)
Al_2O_3
c)
$Fe_2O_{3\,(t)}$
d)
MgO
e)
CaO
f)
Na_2O
g)
High-K Series
K_2O
Medium-K Series
Low-K Series
h)
P_2O_5
SiO_2
SiO_2

Figure 8 - (a-h) Major element Harker diagrams (in %wt) for the TTG suites of the Rio Maria granite-greenstone terrane. Field in g according to Peccerillo and Taylor (1976). (see table 5 for data sources).

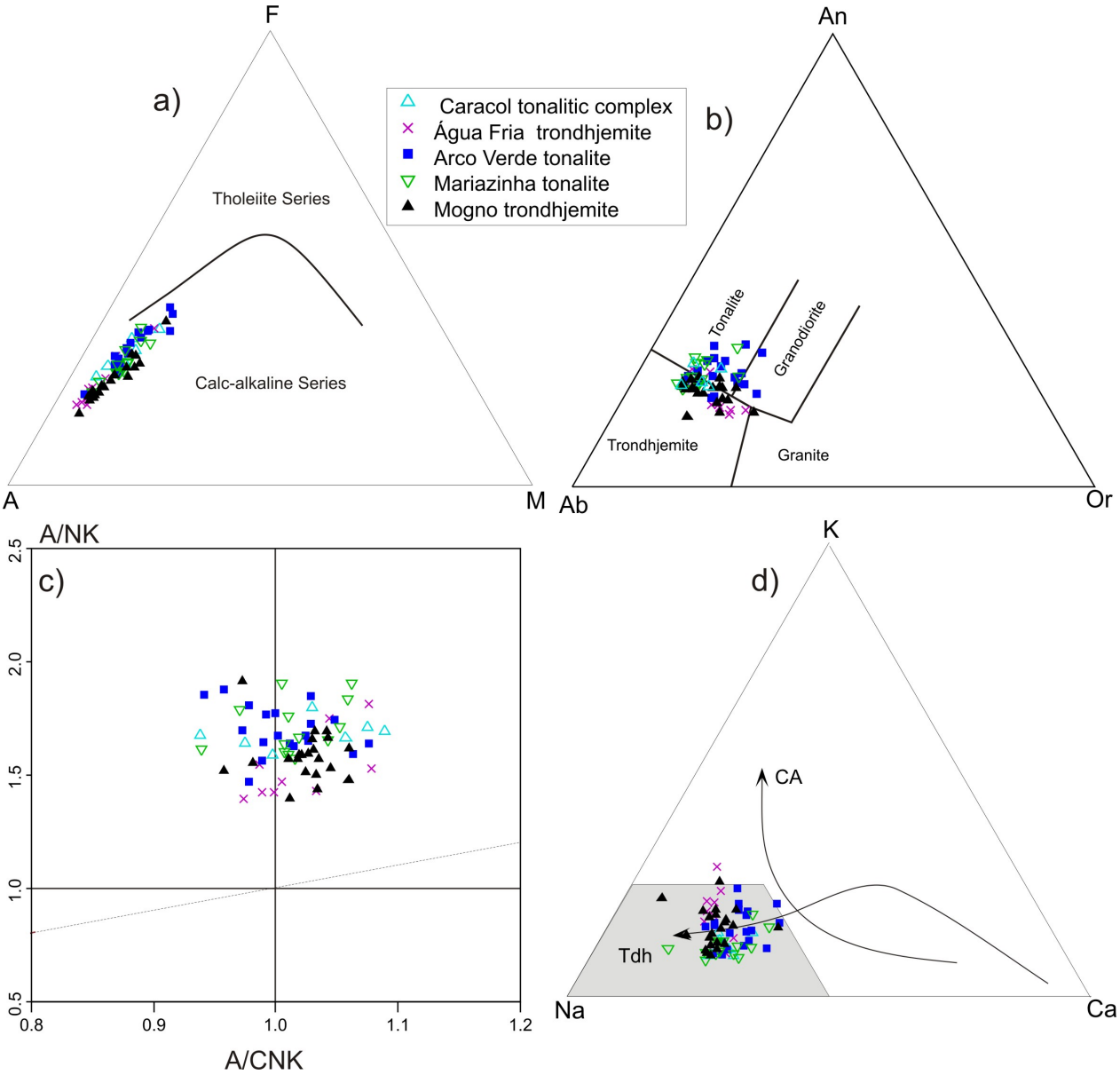

Figure 9 - Diagrams showing the distribution of samples of the TTG granitoids of the Rio Maria granite-greenstone terrane (see table 5 for references). (a) FMA (Fe-Mg-alkali) diagram (Irvine and Baragar, 1971); (b) Normative feldspar triangle (O'Connor, 1965) with fields from Barker (1979); c) Rio Maria TTG rocks plot in the transition between the metaluminous and peraluminous fields of the [Al_2O_3/ (CaO + Na_2O + K_2O)]mol vs. [Al_2O_3/(K_2O + Na_2O)]mol diagram (Shand, 1950); (d) K–Na–Ca plot. Trends for calc-alkaline (CA) and trondhjemite (Tdh) series as defined by Barker and Arth (1976). Grey field of Archaean TTG (Martin, 1994).

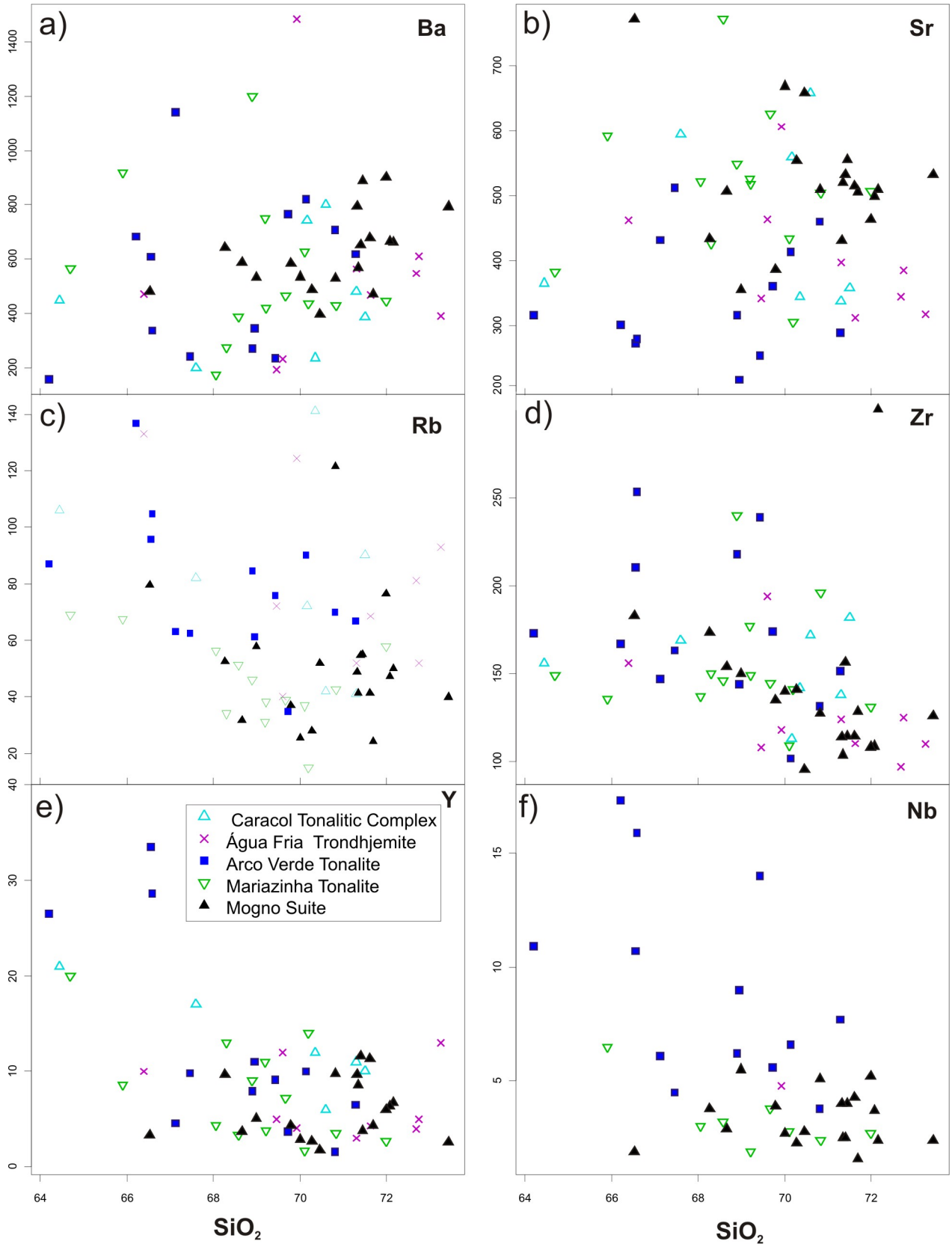
a)
Ba
b)
Sr
c)
Rb
d)
Zr
e)
Y
f)
Nb
Caracol Tonalitic Complex
Água Fria Trondhjemite
Arco Verde Tonalite
Mariazinha Tonalite
Mogno Suite
SiO2
SiO2

Figure 10 - Harker plots for selected trace elements (in ppm) for the Rio Maria TTGs. For Nb, only high precision ICP-MS analyses were considered.

variable in the other TTG units (Fig. 10a). Sr contents are significantly distinct in the different suites. They tend to increase from the Arco Verde tonalite (lowest Sr contents of the studied TTGs), to the Mariazinha tonalite and Mogno trondhjemite, passing by the Agua Fria trondhjemite and Caracol tonalitic complex (Fig. 10b). It is also worth noting that, despite the higher silica content of its rocks, the Mogno trondhjemite shows similar Sr contents than the Mariazinha tonalite, indicating the relative Sr-rich signature of the former. The Arco Verde tonalite, Caracol tonalitic complex and Agua Fria trondhjemite are enriched in Rb compared to the Mariazinha tonalite and Mogno trondhjemite (Fig. 10c). There is also a clear distinction in niobium contents that are higher in the Arco Verde tonalite compared to the Mariazinha tonalite and Mogno trondhjemite (Fig. 10f).

The REE patterns of the RMGGT TTGs show enrichment in LREE and are variably depleted in HREE, allowing the discrimination of three distinct groups (Fig. 11; Table 6): *High La/Yb ratio TTGs* – This group is characterized by high $(La/Yb)_N$ ratios [mostly 40-131 (mean = 78)], absence of significant Eu negative anomaly [generally 0.8 <Eu/Eu*< 1.1 (mean=0.9)]. This group embraces the majority of the analyzed samples and is the dominant group for the Mariazinha tonalite and Mogno trondhjemite. However, it contains also samples of the Arco Verde tonalite, Agua Fria trondhjemite and Caracol tonalitic complex (Fig. 11a); *Medium La/Yb ratio TTGs* – The second group displays less fractionated REE patterns [20 <$(La/Yb)_N$< 49; mean = 33] and is also devoid of significant negative Eu anomalies [0.7<Eu/Eu*<1.0 (mean=0.9)]. This group is composed of samples of all TTG units, but it is the major group for the Caracol tonalitic complex (Fig. 11b); *Low La/Yb ratio TTGs* - This group is characterized by flat HREE patterns [5 <$(La/Yb)_N$< 18 (mean =9.4)] and moderate to pronounced negative Eu anomalies [generally, 0.5<Eu/Eu*<0.7 (mean=0.6)]. This group is formed essentially by the Arco Verde tonalite, including also an isolate sample of the Caracol tonalitic complex (Fig. 11c). In La/Yb vs Sr/Y and La/Yb vs Yb plots (Martin 1986, 1995), the three groups are perfectly distinguished (Figs. 12a, b). A concave shape of the HREE patterns is commonly observed in the Caracol tonalitic complex, Mariazinha tonalite, and in the samples of the high La/Yb group of the Arco Verde

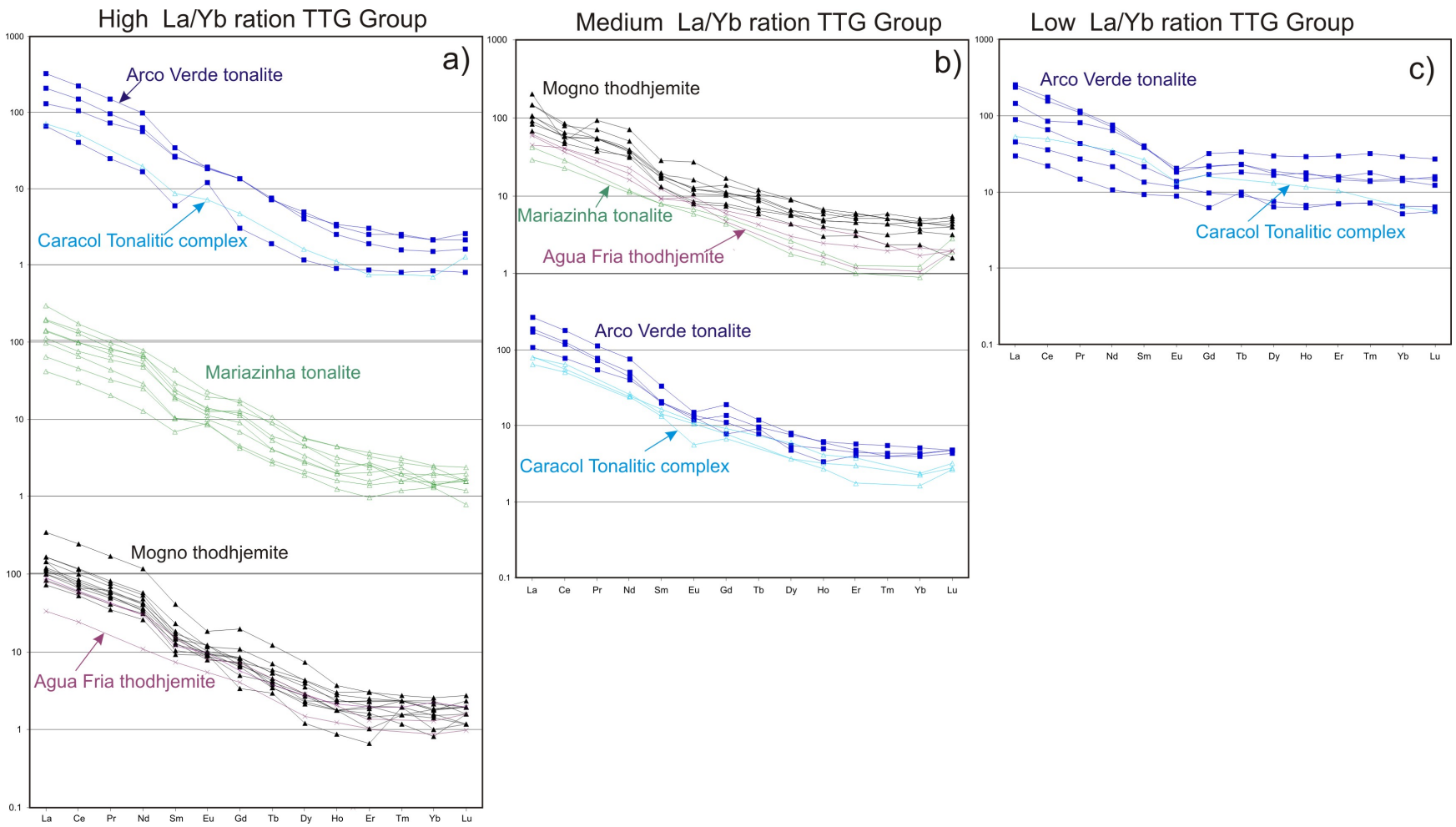

Figure 11 - Chondrite normalised (Evensen et al., 1978) REE patterns for TTG suites of the Rio Maria granite-greenstone terrane.

Table 6 - Geochemical characteristics for the TTG groups discussed in this paper

Types	SiO_2 (%Wt)	Al_2O_3	$(La/Yb)_N$ ratio	Nb/Ta ratio	Sr/Y ratio	Eu/Eu*	#Mg	Cr	Ni	A/CNK
High-La/Yb Group	65-73 (70)	14-17 (16)	40-131 (78)	6-30 (14)	61-366 (113)	0.8-1.1 (0.9)	0.2-0.4 (0.3)	10-29 (20.3)	0.7-24 (7.2)	0.86-1.08 (1.01)
Medium-La/Yb Group	66-73 (70)	14-16 (15)	20-49(33)	4-17 (9)	28-86 (47)	0.7-1.0 (0.9)	0.3-0.5 (0.3)	1.5-26 (14)	0.6-19 (7)	0.97-1.18 (1.03)
Low-La/Yb Group	64-72 (68)	14-17 (15)	5-18 (9.4)	3-8 (6)	5-52 (10.5)	0.5-0.7 (0.6)	0.3-0.5 (0.3)	6.5-27 (17)	5-15 (10)	0.93-1.06 (0.99)

(15) - Average

tonalite, suggesting that hornblende was probably an important fractionating phase during the evolution of these rocks.

The *Low La/Yb* group tends to have higher Y and low Sr contents compared to the other groups (Figs. 10b, 12c). As a consequence, their rocks have the lowest Sr/Y ratios (5-52), and these ratios increase to the *Medium-La/Yb* group (28-86), attaining the highest values in the *High-La/Yb* group (61-366; Fig. 12b; Table 5). Moreover, there is a positive correlation between Sr/Y and La/Yb ratios (Fig. 12b).

The Nb/Ta ratios are variable and normally lower than the primitive mantle. They tend to decrease from the *High-La/Yb* group [6-30 (mean=14)] to the *Medium-La/Yb* group [(4-17 (mean=9)], the lowest values being found in the *Low-La/Yb* group [3-8 (mean=6)]. There is a reasonably strong positive correlation between Nb/Ta and Sr/Y (Fig. 12d) and between Nb/Ta and La/Yb (Fig. 12e).

The different TTG groups do not show remarkable contrasts in their #Mg (0.45-0.27) values, as well as in their Cr (2-29 ppm) and Ni (1-24 ppm) contents, which are relatively low in all studied TTG units. The mentioned values of #Mg, Cr, and Ni differ notably from the maximum values found in Mesoarchean to Neoarchean TTGs (Martin and Moyen, 2002).

Reflecting essentially the observed variations in Al_2O_3 contents, the rocks of the *High-La/Yb* and *Medium-La/Yb* groups are somewhat more peraluminous than those of the *Low La/Yb* group.

6.3. Nd isotopes

Whole-rock Nd isotope data for the TTG of the RMGGT have been obtained by Rämö et al. (2002) and Rolando and Macambira (2003) and are compiled in Table 7. The corresponding εNd (t) vs age diagram is shown in Figure 13. According to the new geochronological data obtained, the age of 2871 (U-Pb on titanite; Table 1) previously assumed for the Mogno

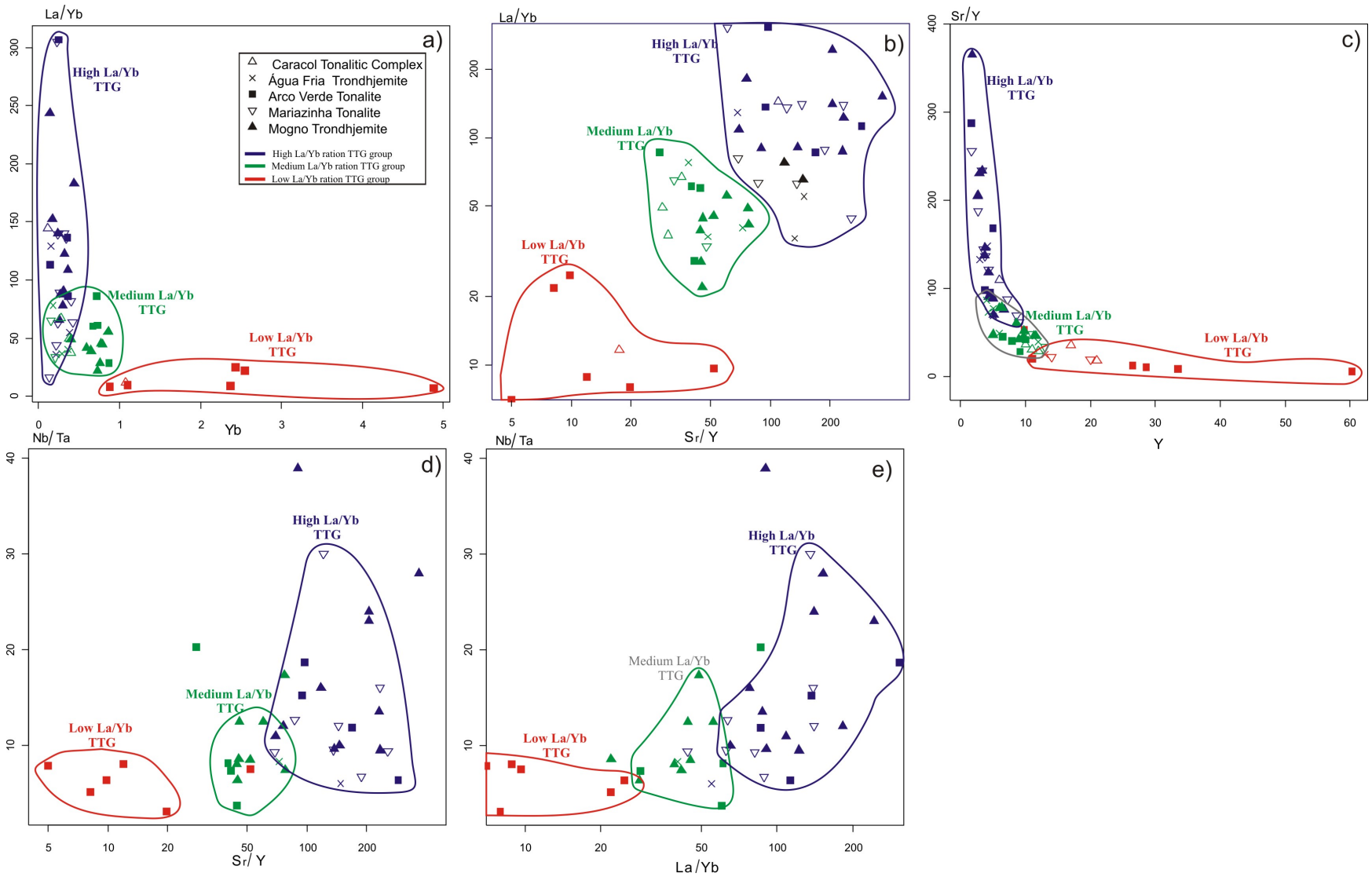

Figure 12 - a) La/Yb vs Yb; b) La/Yb vs Sr/Y; c) Sr/Y vs Y; d) Nb/Ta vs Sr/Y; e) Nb/Ta vs La/Yb diagrams used to discriminate the different groups of TTG granitoids of the Rio Maria granite-greenstone terrane.

trondhjemite (Rämö et al., 2002) is not relevant. Thus, the εNd values were recalculated at 2968 Ma, the new U-Pb zircon age (cf. Table 4; Fig. 5). The Arco Verde tonalite and Caracol tonalitic complex show lower values of $^{147}Sm/^{144}Nd$ compared to the Mariazinha tonalite and Agua Fria trondhjemite. εNd values vary from +1.4 to +2.6 (Table 7) and are similar in the different TTG units. The T_{DM} ages (DePaolo, 1981) show restrict variation and tend to be a little older in the Arco Verde tonalite, Mogno trondhjemite, and Caracol tonalitic complex (2911 to 3020 Ma), compared to the Mariazinha tonalite (2919 Ma) and Agua Fria trondhjemite (2857 to 2914 Ma).

Table 7 - Sm-Nd isotopic data for the TTG granitoids of the Rio Maria granite-greenstone terrane.

Sample	Unit	Age	Methods	Rock type	Group	Sm (ppm)	Nd(ppm)	$^{147}Sm/^{144}Nd$	$^{143}Nd/^{144}Nd$	εNd	T_{DM}(Ma)
Água Fria trondhjemite											
AL-13C [(a)]		2864±21 Ma [(1)]	Pb-Pb on zircon	Biotite trondhjemite	High-La/Yb	1.61	8.07	0.1203	0.411267 9	1.4	2914
AL-16A [(a)]		2864±21 Ma [(1)]	Pb-Pb on zircon	Biotite trondhjemite	High-La/Yb	1.96	11.24	0.1053	0.511017 10	2.0	2857
AL-122 [(a)]		2864±21 Ma [(1)]	Pb-Pb on zircon	Biotite trondhjemite	High-La/Yb	2.14	12.5	0.1036	0.510964 11	1.6	2885
Mariazinha tonalite											
AL-210 [(a)]		2924 ±2 Ma [(1)]	Pb-Pb on zircon	Biotite tonalite	High-La/Yb	2.4	13.13	0.1104	0.5110750 8	1.9	2919
Caracol tonalitic complex											
AL-216 [(a)]		2948±5 Ma [(1)]	Pb-Pb on zircon	Biotite tonalite	High-La/Yb	1.44	10.75	0.08069	0.510485 11	2.1	2936
Mogno trondhjemite											
CR-91A [(a)]		2963±8 Ma [(2,5)]	U-Pb on zircon	Biotite trondhjemite	High-La/Yb	2.42	18	0.07992	0.51048	2.5	2949
Z-343 [(a)]		2963±8 Ma [(2,5)]	U-Pb on zircon	Biotite trondhjemite	Medium-La/Yb	3	16.87	0.1075	0.510994	2.0	2976
Arco Verde tonalite											
MP-07 [(b)]		2948±7 [(3)]	Pb-Pb on zircon	Biotite tonalite	Medium-La/Yb	n.d.	n.d.	0.06553	0.510136	1.6	3020
PPA-18 [(b)]		2981±8 [(3)]	Pb-Pb on zircon	Biotite tonalite	X	n.d.	n.d.	0.098	0.510783	1.7	3010
MJ-08 [(a)]		2957 + 25/-21 [(4)]	U-Pb on zircon	Biotite tonalite	X	2.55	18.6	0.08272	0.510516	2.0	2946
92-26 [(a)]		2957 + 25/-21 [(4,5)]	U-Pb on zircon	Biotite tonalite	Medium-La/Yb	5.57	39.16	0.08594	0.51067	2.6	2911

Key to isotopic data reference: (a) - Rämö et al. (2002); (b)Rolando & Macambira (2003); Key to age reference: (1) - Leite (2001); (2) This work; (3) Rolando & Macambira (2003); (4) Macambira (1992);(5) age assumed; n.d: not determinated; X: Chemical analyse unavailable

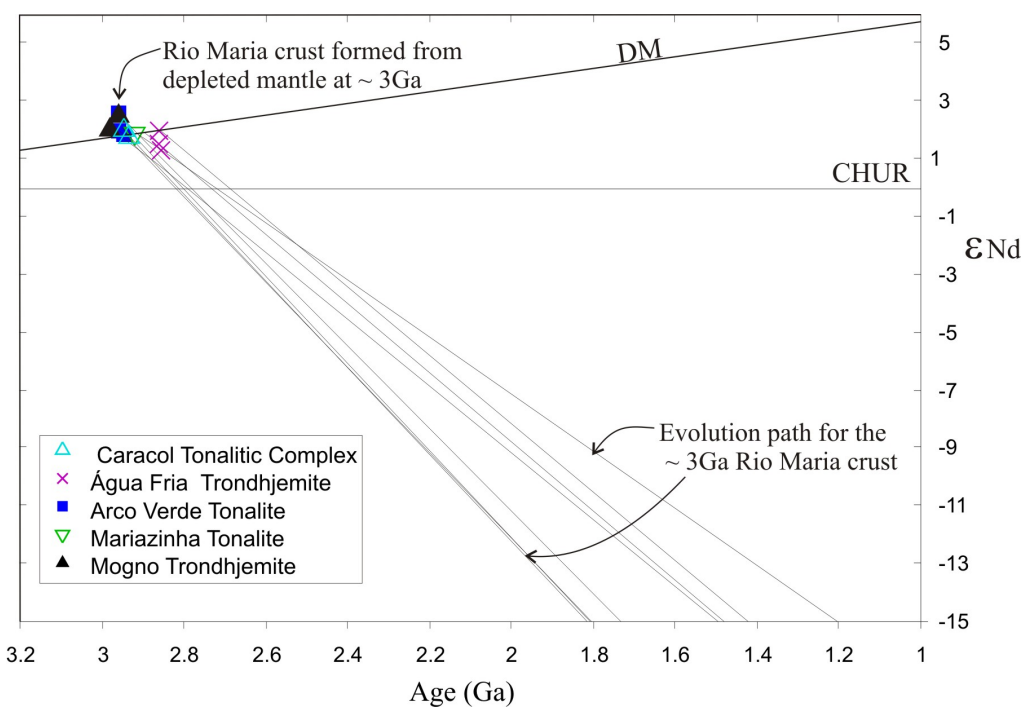

Figure 13 - εNd vs age diagram showing inicial isotopic composition of TTG granitoids of the Rio Maria granite-greenstone terrane (Rämö et al., 2002, modified; including two addtional analyses from Rolando and Macambira, 2003). CHUR undifferentiated earth (De Paolo and Wasserburg 1976), DM is depleted mantle (De Paolo, 1981). Descendent lines represent evolution of each individual sample.

7. Discussion

7.1. Timing of TTG magmatism in the Rio Maria granite-greenstone terrane

The geochronological data (Tables 3, 4) together with previously reported data, define a sequential evolution for the TTG rocks in the Rio Maria granite-greenstone terrane (Fig. 14). The earliest TTG magmatism is recorded by the 2.98-2.93 Ga Arco Verde tonalite (Macambira and Lancelot, 1996; Rolando and Macambira, 2002, 2003; this study) and the 2.96 Ga Mogno trondhjemite (this study). The Caracol tonalitic complex (Leite et al., 2004) shows ages around 2.94 Ga. A subsequent tonalitic-trondhjemitic intrusive event took place at ~2.92 Ga and is represented by the Mariazinha tonalite. The youngest period of TTG generation happened ~ 60 m.y later at ca. 2.86 Ga and is represented by the Agua Fria trondhjemite of limited areal distribution in the RMGGT.

It is now demonstrated that the major activity of TTG magmatism in the RMGGT was concentrated between 2.98 and 2.92 Ga (Fig. 14). The older age defined for the Mogno trondhjemite (Figs. 5, 14; Tables 3, 4) indicated that the younger TTG event (~2.86 Ga) was less relevant for the evolution of the RMGGT than previously assumed. The Arco Verde tonalite is the TTG unit with the largest geochronologic data set and it shows significant age variations in between 2.98 and 2.93 Ga. The data obtained in the present work are mostly concentrated around 2.93 Ga and are generally superposed within errors with those of the Caracol tonalitic complex and Mariazinha tonalite (Fig. 14). Some of the new dated samples with lower ages carry inherited zircons with ages of ~2.95 to 2.97 Ga (Figs. 4a, c). The available data on the Arco Verde tonalite suggest that this TTG unit is not uniform and includes TTGs with significant age variation. These TTGs could not be individualized in the present scale of mapping. A similar picture is also described in other Archean cratons (Barberton, Moyen et al., 2007; Pilbara, Champion and

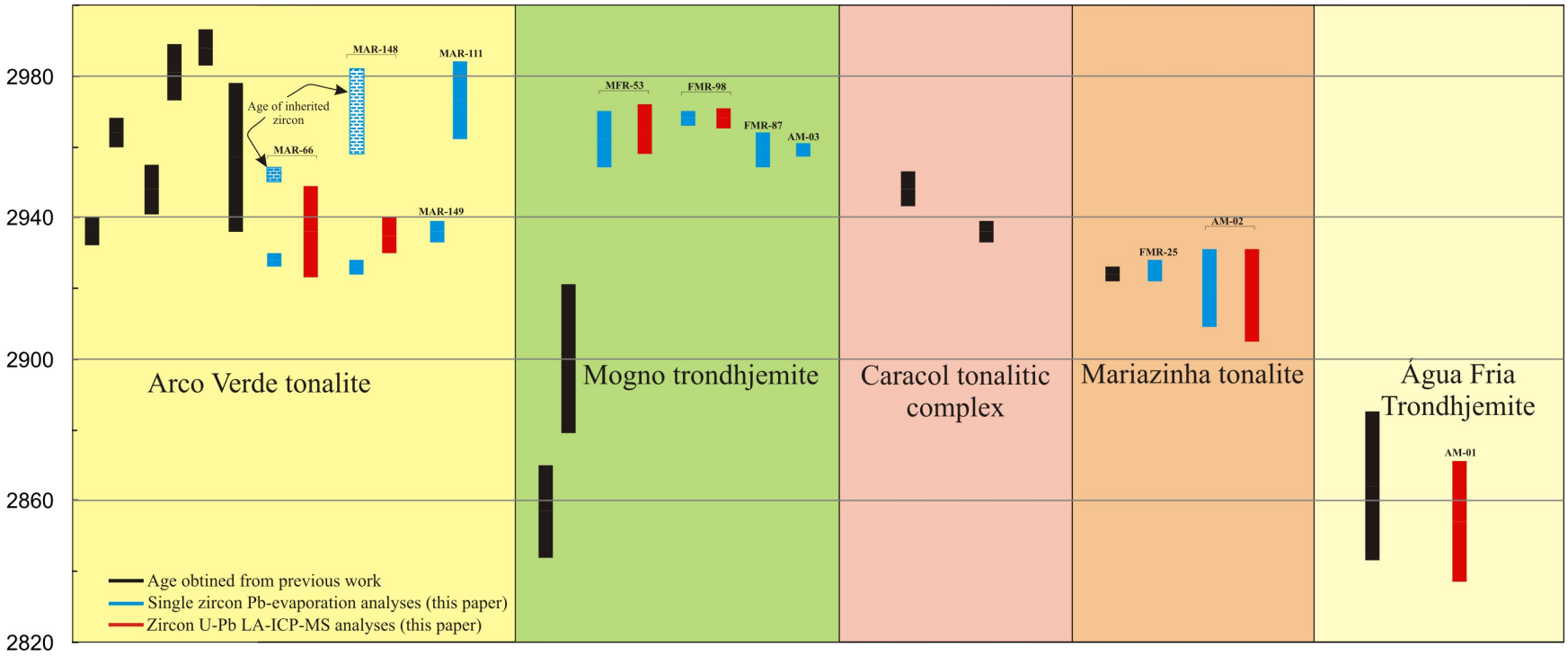

Figure 14 - Summary of geochronological data presented in this study obtained by Pb-Pb on zircon evaporation (blue bars) and LA-ICP-MS on zircon methods (red bars) together with previously reported data (black bars) for the timing of TTG magmatism in the Rio Maria granite-greenstone terrane (references in the text).

Smithies, 2007; Karelia, Käpyaho et al., 2006). Three major events of TTG formation can be identified in the RMGGT (Fig. 14): A first event at 2.96±0.2 Ga (Mogno trondhjemite and the older rocks of the Arco Verde tonalite), a second one at 2.93±0.1 Ga (Caracol tonalitic complex, Mariazinha tonalite, and the younger rocks of the Arco Verde tonalite), and finally a restricted event at 2.86±0.1 Ga (Agua Fria trondhjemite).

The little variation in age (2.0±0.6; Table 7), almost constant positive values of εNd, and T_{DM} ages close to the crystallization ages imply that the tonalitic-trondhjemitic crust of the RMGGT derived from sources extracted from the mantle during the Mesoarchean (3.0 to 2.9 Ga) and with short time of crustal residence. The admitted source for the TTG magmas of the RMGGT are the metabasalts of the Andorinhas supergroup or rocks with similar geochemical compositions (greenstone belts; Althoff et al., 2000; Souza et al., 2001; Leite, 2001). Considering the areal distribution of the TTG older than 2.92 Ga, we can estimate that at least ca 60% of the present Archean crust of the RMGGT was formed at that time.

7.2. Geochemical characteristics as petrogenetic indicators of the RMGGT TTG magmas

The distinction between high- and low-Al_2O_3 TTGs has been done by Barker and Arth (1976) and Barker (1979) that emphasized the determinant role of, respectively, garnet + hornblende vs. plagioclase as residual phases. Barker (1979) defined high-Al_2O_3 TTGs as those series presenting more than 15% wt. % of Al_2O_3 at 70 wt. % of SiO_2. This TTG group presents generally low Rb and moderate to high Sr contents, is moderately enriched in light REEs, but depleted in heavy REE and shows either no negative europium anomalies or a small one that may be positive or negative. The low-Al type has $A1_2O_3$ < 15% at 70% wt.% of SiO_2, low abundances of Sr and Rb and commonly shows moderately enriched light REE and flat heavy REE patterns, with negative europium anomalies. Following strictly the definition of Barker (1979), almost all analyzed TTGs of the RMGGT can be classified as the high-Al_2O_3 type. However, there are significant contrasts in Al_2O_3 contents in the studied TTGs (Fig. 8b), with the Mogno trondhjemite and Mariazinha tonalite showing higher Al_2O_3, the Caracol tonalitic complex and the Água Fria trondhjemite intermediate values and the Arco Verde tonalite the lowest Al_2O_3 contents. A similar picture is shown by Na_2O (Fig. 8f), whereas the K_2O displays a reverse behavior (Fig. 8g).

It is demonstrated in the literature that some traces elements (REE, Sr, Y, Nb, and Ta) are extremely sensitive to the pressure of melting and are partitioned in markedly different ways in eclogitic (garnet-clinopyroxene-rutile) or amphibolitic (amphibole-plagioclase-ilmenite) assemblages (Martin, 1994; Foley et al., 2002; Klemme et al., 2002; Rapp et al., 2003; Xiong et al., 2005; Moyen and Stevens, 2006; Moyen, 2009). It is also known that the nature and modal proportion of minerals phases is modified with pressure (plagioclase is in disequilibrium and garnet becomes stable and more abundant at higher pressure). As a consequence, the abundance of residuals phases showing high partition coefficients for REE, Sr, Y, Nb, and Ta, controls the geochemical characteristics and imply pressure conditions of TTG magmas genesis.

The strongly fractionated REE patterns, with low HREE and Y, and the high Sr and Eu contents and Sr/Y ratios exhibited by high- and medium-(La/Yb) groups of the RMGGT (Figs. 11, 12a, b, c) could reflect either melting in the presence of garnet and amphibole (both have high Kd for HREE and Y) or magma evolution controlled by fractionation of hornblende and garnet. In contrast, the less fractionated REE patterns, with higher HREE and Y, and the lower Sr and Eu contents and Sr/Y ratios displayed by the low-(La/Yb) group (Figs. 11, 12a, b, c) indicate the presence of plagioclase among the fractionated phases (Kd>1 for Sr and Eu in plagioclase), either by the presence of residual plagioclase during partial melting or via its fractionation during magma differentiation. Previous studies have shown that TTG liquids in equilibrium with garnet were produced at pressures of 1 GPa and above (Sen and Dunn, 1994; Wolf and Wyllie, 1994; Rapp and Watson, 1995; Winther, 1996; Moyen and Stevens, 2006) and that pressure is the determinant parameter for garnet or plagioclase equilibrium in mafic assemblages. Moyen and Stevens (2006) emphasized that low pressure melts in equilibrium with plagioclase but not garnet show low Sr but high Y and Yb contents, whereas in high pressure melts in equilibrium with garnet, the reverse is observed because Sr should be released due to plagioclase breakdown while Y and Yb are locked in the garnet. They have also shown that tonalite liquids are obtained at ca. 1000°C, below 15 kbar, but require higher temperatures as pressure goes up (to ca. 1200°C at 30 kbar), whereas trondhjemite liquids are generated at temperatures below 1000°C.

Experimental studies show that partial melting of an amphibolitic source composed of relatively low Mg# amphiboles (Mg# less than about 70) yield low Nb/Ta liquids (Foley et al., 2002). However, Rapp et al. (2003) argued that Archaean TTG displays a very wide range in Nb/Ta ratios and partial melting of hydrous basalt in the eclogite facies initially with

subchondritic Nb/Ta also produces granitoid liquids with low Nb/Ta. Therefore, the meanings of the Nb/Ta ratios remain contentious and they can indicate either distinctive pressure condition or different source for the TTG magmas.

Similar to most Archean TTG, the Rio Maria TTGs display low and variable Nb/Ta ratios that increase from the low-(La/Yb) to the high-(La/Yb) group (Fig. 12e). The Nb/Ta ratios display positive correlation with (La/Yb) and Sr/Y ratios (Figs. 12d, e). This behavior can be explained by pressure variations, with the presence of residual rutile (in the case of an eclogitic source), or by changes in the magma sources, with the occurrence of an amphibolitic source with low Mg# amphiboles.

The overall geochemical characteristics of the RMGGT TTGs give strong indication that the high-(La/Yb) group, represented dominantly by the Mogno trondhjemite and Mariazinha tonalite, derived from magmas generated at relatively high pressures (estimated at ca. 1.5 GPa) from sources able to leave garnet and possibly amphibole as residual phases. In contrast, the magmas forming the low-(La/Yb) group, dominated by the Arco Verde tonalite, were generated at lower pressures (ca. 1.0 GPa), from an amphibolitic source containing plagioclase as a residual phase. The medium-(La/Yb) group, which embraces the Caracol tonalitic complex and the Água Fria trondhjemite, was formed at intermediate pressure conditions, but still in the garnet stability field, allowing its presence as a relevant residual phase.

These conclusions are reinforced by geochemical modelling (Leite, 2001), which indicates that the dominant TTGs from Caracol tonalitic complex [medium- and subordinate high-(La/Yb) groups; Fig. 11] were probably originated from the partial melting of garnet amphibolites derived from tholeiites similar in composition to Archean metabasalts (Martin, 1987) or from the metabasalts of the Identidade greenstone belt (Souza et al., 2001). The calculate residue comprised garnet, clinopyroxene, plagioclase, hornblende, orthopyroxene, and ilmenite, and the degree of partial fusion required would be, respectively, 25-30% and 10-15%. On the other hand, the low-(La/Yb) TTGs from the same unit were possibly formed from a liquid derived from a garnet-free and plagioclase-enriched similar source with a degree of partial fusion around 10%.

7.3. Comparison with other TTG series.

In the East Pilbara Terrane of the Pilbara craton, Champion and Smithies (2007) identified both high- and low- Al_2O_3 series in TTG granitoids that range in age from ca. 3.50 to 3.42 Ga and ca. 3.32 to 3.24 Ga. The two series are not temporally distinct, in the sense that both age groups contain low- and high-Al TTGs. On the other hand, in the Barberton granite-greenstone terrane (Moyen et al., 2007), all TTG suites are included in the high-Al series and divided in two sub-series, one composed manly of leucocratic trondhjemites with high Sr and Na_2O contents and low values of Y, referred as high-Sr sub-series, and another formed of tonalites to trondhjemites and granodiorites showing lower values of Sr and Na_2O and more elevated Y contents, called low-Sr sub-series. In contrast with the TTG suites of Pilbara, in Barberton there is a correlation between geochemical signature and age of TTG granitoids (Moyen et al., 2007). The older plutons (ca. 3.45 Ga) belong to high-Sr sub-series, whereas the younger (3.23–3.21 Ga) plutons are predominantly of the low-Sr sub-series type. In the Karelian and Kola cratons of the Fennoscandian shield, two different groups of TTGs could also been distinguished, on the basis of Sr content (Halla, 2005; Käpyhao et al., 2006, Halla et al., 2009), a low silica, high-Sr group and a relatively low-Sr group with variable silica content.

In the case of the TTGs suites of the TGGRM, almost all analyzed samples belong to the high-Al group, but there are significant contrasts in Al_2O_3 and Sr between different TTG units (Figs. 8b, 10b). In contrast to Barberton and similar to Pilbara TTGs, there is no discernible correlation between geochemical series and either the TTGs units of the RMGGT or the ages of those units. Some units, as the Arco Verde tonalite and Caracol tonalitic complex, contain rocks of both groups spatially and apparently also temporally associated. The studied TTGs are plotted in a Sr vs. SiO_2 diagram (Fig. 15), originally proposed by Moyen et al. (2007) to compare the TTGs from Barberton with those of Pilbara. Data on the TTGs from the Karelian and Kola cratons are also shown for comparison. The field of the high-Al, high-Sr TTG group of Pilbara is largely superposed with those of the low-Sr subseries of Barberton, and of both TTG groups of Karelian and Kola cratons. The low-Al, low-Sr TTG group of Pilbara and the high-Sr sub-series of Barberton define two independent and distinct fields. Most of the RMGGT TTGs are concentrated in the field of high-Al, high-Sr of Pilbara and in the low-Sr sub-series of Barberton (Fig. 15). However, a large number of samples of the Arco Verde tonalite plot in the the low-Al,

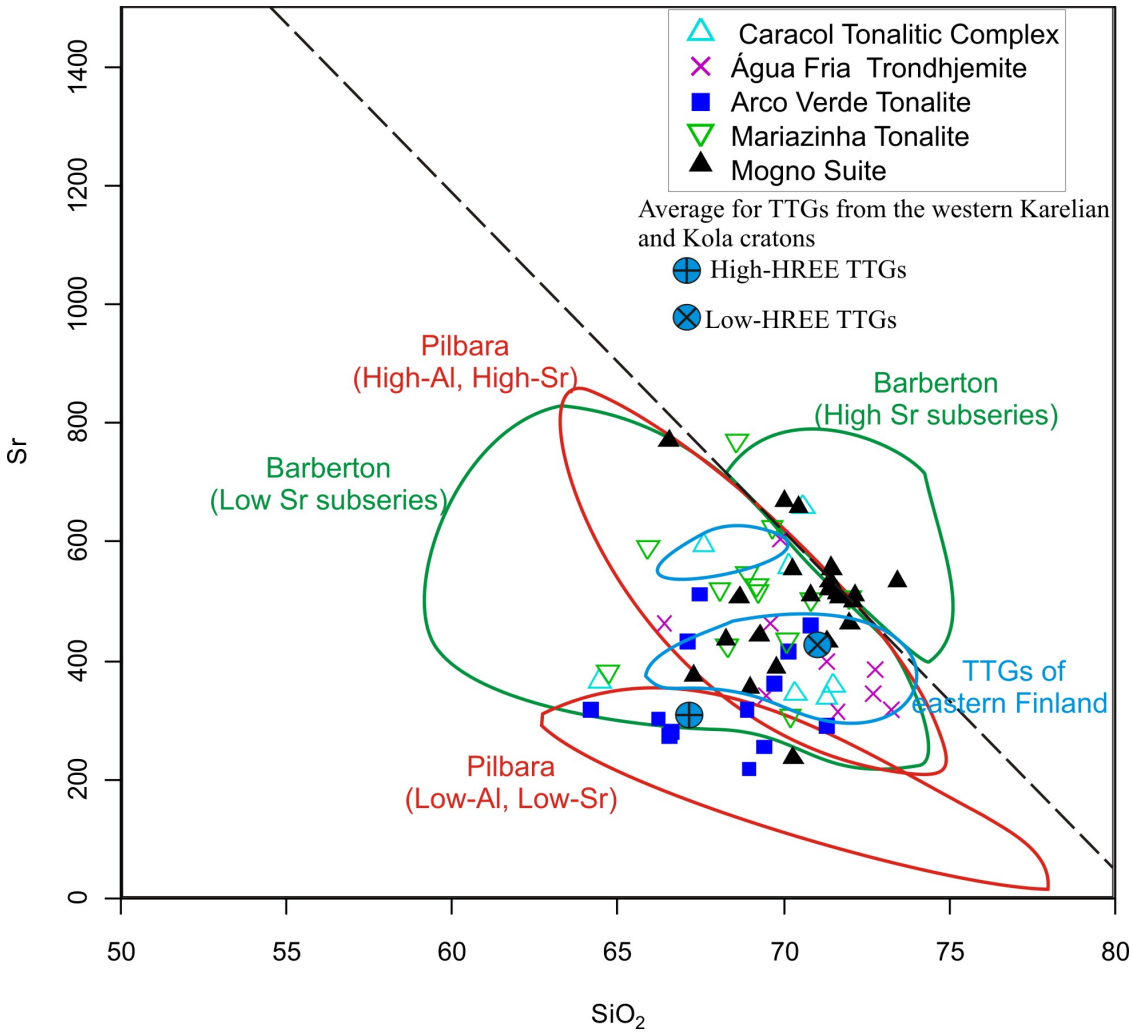

Figure 15 - SiO_2 vs Sr diagram showing the distribution of samples of the TTG suites of the Rio Maria granite-greenstone terrane and the fields for TTG series of Pilbara craton (Champion and Smithies, 2007), Barberton granite-greenstone terrane (Moyen et al., 2007) and eastern Finland (Martin, 1987). The average composition of TTGs from the western Karelian and Kola cratons (Halla et al., 2009) is also shown for comparison.

low-Sr field of Pilbara and the Mogno trondhjemite samples tend to plot along the border between the low-Sr and high-Sr sub-series of Barberton.

Following the extensive discussions presented by Moyen et al. (2007) and Halla et al. (2009), the three distinct TTG geochemical groups distinguished in this paper in the RMGGT [low-, medium- and high-(La/Yb)] can be most probably correlated to depth or pressure of their magma genesis. In the RMGGT, the high- to medium-(La/Yb) dominant TTGs are similar in Sr

and SiO_2 contents to the high-Al, high-Sr group of Pilbara, to the low-Sr sub-series of Barberton and to both Sr groups of Karelian and Kola cratons (Fig. 15). These rocks include samples of all TTG units and were probably formed in the stability field of garnet at pressures of 10 to 15 kbar. In order to explain their geochemical characteristics, the low-Al, low-Sr, low-(La/Yb) TTGs, dominant in the Arco Verde tonalite, should be formed at comparatively lower pressures (≤ 10 kbar) in the stability field of plagioclase. Finally, the high-(La/Yb) TTGs of the Mogno trondhjemite that fall between the low-Sr and high-Sr fields of Barberton TTGs (Fig. 15) should be derived from magmas formed in the garnet stability field at relatively higher pressure (≥15 kbar) and probably at somewhat lower temperature (< 1000°C; cf. Moyen et al., 2007). The Mariazinha tonalite magma is also formed at relatively higher pressures compared to the dominant TTGs of RMGGT, but it should result from a larger degree of partial melting compared to the Mogno trondhjemite magma to explain its lower silica contents. This implies a higher melting temperature for the Mariazinha tonalite magma, estimated at ≥1100°C.

The positive correlation between Nb/Ta and Sr/Y and La/Yb ratios observed in the RMGGT TTGs (Figs. 12d, e) is indicative that the Nb/Ta ratio is also sensitive to pressure and thus indicative of the depth of magma generation of the studied TTG suites.

FIGURE 15

7.4. Possible mantle wedge influence in TTG composition

Many authors argue that TTG magmas generated in subduction zones show high #Mg, Ni, and Cr due to assimilation of mantle peridotite during their ascent (Martin, 1999; Rapp et al., 1999; Martin et al., 2005). According to Smithies and Champion (2000), some TTG from the Abitibi subprovince (Superior Province) and Pilbara craton (e.g., Shaw Granitoid Complex) show geochemical evidence of mantle interaction. The same is true for adakites, modern equivalents of Archean TTG restricted to subduction zones (Martin and Moyen, 2002).

Martin and Moyen (2002) emphasized the variable influence of the mantle wedge in the composition of TTGs along geological time and claimed that Early Archean TTG were relatively impoverished in #Mg, Ni, Cr, and Sr compared to Late Archean TTGs. They explained these compositional contrasts between TTGs along time by slab melting at different depths. Higher geothermal gradients in Early Archean induced slab melting at lower pressures in the plagioclase

stability field and explained the reduced influence of the mantle wedge in TTG composition and the relatively lower Sr contents of older TTGs. However, Smithies (2000) and Condie (2005) argued that these geochemical features are not uniform in different Archean cratons and could also be explained by an origin of TTG magmas by partial melting of the root zones of thick oceanic plateaus.

The TTGs of the RMGGT are younger than 3.0 Ga and have ages concentrated in between 2.98 and 2.86 Ga (Fig. 14). Their compositions in terms of #Mg, Cr, Ni, and Sr are not compatible with those estimated for < 3.0 Ga TTGs and generally approach those registered in >3.0 Ga TTGs (Martin et al., 2005). Some subtle differences are observed in the RMGGT, with the Mogno trondhjemite and Mariazinha tonalite showing higher Sr contents (Fig. 15) and the former also presenting a little higher #Mg and Ni values compared to the other TTG units (Table 5). These particular features reinforce the hypothesis of origin of the Mogno trondhjemite magma at higher pressures. For the remainder TTG units of the RMGGT and, to some degree also for the Mogno trondhjemite, there is little geochemical evidence of significant interaction between their magmas and the mantle wedge. This could be explained by an origin of their magmas from slab melting at shallow depths (Martin and Moyen, 2002), for a relatively low temperature of the mantle wedge, making geochemical changes between TTG magmas and the peridotitic mantle little effective, or for generation of TTG magmas from the melting of thickened basalt plateaus, precluding interaction between TTG magmas and the mantle (Smithies, 2000; Condie, 2005). The first explanation is little plausible because geochemical contrasts between the TTG units of the RMGGT indicate significant variations in depth of magma generation with increasing influence of garnet in the melting residue from the low-(La/Yb) to the high-(La/Yb) groups.

7.5. Petrogenesis of the RMGGT TTGs and geodynamic implications

There is a general agreement that TTG magmas were generated by partial melting of hydrous metabasaltic rocks transformed into garnet bearing amphibolite or eclogite, under a variety of fluid conditions. These conclusions are supported by geochemical modelling (Martin, 1994; Martin and Moyen, 2002; Moyen et al., 2003) and experimental petrology (Rapp, 1994; Sen and Dunn, 1994; Zamora, 2000; Moyen and Stevens, 2006), as well as by the study of their modern analogues such as adakites (Defant and Drummond, 1990; Martin, 1999).

The geodynamic context of TTG sources is subject to controversy and dependent on whether or not plate tectonics operated during the Archaean (De Wit, 2001). Some authors contend that TTG are generated by melting of basalt at the base of a thickened oceanic crust (Smithies, 2000; Condie, 2005). Others believe that TTG are produced by partial melting of a subducted, basaltic oceanic crust (Condie, 1989; Martin, 1994; Rollinson, 1997; Martin and Moyen, 2002, Moyen et al., 2003). Low-angle, and flat- subduction of oceanic crust has also been proposed as a model for Archaean crustal growth. In this model the Archean oceanic crust may have been thickened, either underplated through magmatic processes (Rudnick, 1995; Albarède, 1998) or underthrust during flat subduction (De Wit, 1998; Smithies, 2000) and locally precluding the mantle wedge. More recently, Moyen et al. (2007) admitted that there is no conclusive evidence in favor of either hypothesis. An alternative hypothesis considers that deep melting in the lower part of thick basaltic oceanic crust could produce low-HREE TTGs, whereas melting of subducting slab and possible interactions with the mantle wedge in shallow depths should be capable of generating high-HREE TTGs (Halla et al., 2009).

Althoff et al. (2000) admitted that strong external forces associated with plate convergence were operative between 2.96 and 2.90 Ga in the Rio Maria terrane. Leite et al. (2001) suggested that the evolution of the Xinguara area of that terrane involved two different stages: During the first stage (2.96 to 2.92 Ga), the evolution would not been related to subduction and should be similar to that of Pilbara (Champion and Smithies, 2007) and Dharwar (Chockroune et al., 1997) cratons. The second stage, at ca. 2.87 Ga was subduction-related and would be responsible for the generation of sanukitoid series and younger TTG units. Souza et al. (2001) proposed an intra-oceanic island arc setting for the metavolcanics rocks and associated plutonic rocks of the RMGGT.

A model to explain the tectonic setting of the RMGGT should consider that most TTG units were formed in a limited time interval (2.98 to 2.92 Ga) and show significant geochemical variations pointing to generation of their magmas at different depths. It could be admitted that those TTGs were derived from magmas formed from slab melting at different depths. This could explain the geochemical contrasts between TTGs. However, in this case one would expect a stronger interaction between TTG magmas and the mantle wedge and there is little geochemical evidence for that. On the other hand, if the TTG magmas were generated from melting at the base of a dominantly basaltic thickened crust, (high geothermal gradient) the minimum melting

temperature should reach 700–800°C (Condie, 2005), which would be realistic. Nevertheless, it is doubtful that a depth corresponding to the stability domain of garnet, necessary to explain the generation of high-(La/Yb) TTGs, could be attained. In this context, a mixed model, similar to that proposed by Halla et al. (2009), can be envisaged, with the difference that in the case of the RMGGT, the low-(La/Yb) group (similar to the high-HREE of Halla et al., 2009) would be formed by the melting of the base of a thickened basaltic oceanic crust at comparatively lower pressures (ca. 1.0 GPa), whereas the medium- and high-(La/Yb) groups were derived from the slab melting at increasing different pressures (1.0-1.5 and > 1.5 GPa, respectively). Some of these TTG magmas react enroute with the mantle wedge and are totally consumed,leaving a metassomatized mantle.

This model requires that the Rio Maria crust at around 3.0 Ga was thick enough to generate the low-(La/Yb) TTGs at the pressures required. 50 m. y. later, at ca. 2870 Ma, thermal events possibly related to the slab-break-off and asthenosphere mantle upwelling (Halla et al., 2009) or to the action of a mantle plume, may have induced the melting of metassomatized mantle transformed by assimilation of TTG melts and the generation of sanukitoid magmas (Oliveira et al. b, submitted). These magmas may have heated the base of the Archean continental crust and could have lead to the local melting of the basaltic crust forming the Água Fria trondhjemite magma. The lower εNd values shown by the samples of the Água Fria trondhjemite compared with those of the remainder TTG suites (Fig. 13; Table 7) are indicative of small but significant crustal residence time for the protoliths of the Agua Fria trondhjemite and are consistent with the proposed model.

8. Conclusions

The TTG record in the RMGGT comprise three magmatic events at at 2.96±0.2 Ga (the older rocks of the Arco Verde tonalite and the Mogno trondhjemite), 2.93±0.1 Ga (Caracol tonalitic complex, Mariazinha tonalite, and the younger rocks of the Arco Verde tonalite), and at 2.86±0.1 Ga (Agua Fria trondhjemite). The new data demonstrate that the Mogno trondhjemite is significantly older than previously admitted, reveal the existence of a new TTG suite (Mariazinha tonalite) and indicate that the volume of TTG suites formed during the ~2.87 Ga event was limited. The Arco Verde tonalite yielded significant age variations (2.98 to 2.93 Ga) but domains

with different ages are not known. The tonalitic-trondhjemitic crust of the RMGGT derived from sources geochemically similar to metabasalts of the Andorinhas supergroup extracted from the mantle during the Mesoarchean (3.0 to 2.9 Ga) and with short time of crustal residence.

Three groups of TTG granitoids were distinguished in Rio Maria: 1) high-La/Yb group, with high Sr/Y and Nb/Ta ratios, derived from magmas generated at relatively high pressures (>1.5 GPa) from sources leaving garnet and amphibole as residual phases, 2) medium-La/Yb group which magmas formed at intermediate pressure conditions (~1.0-1.5 GPa), but still in the garnet stability field, and 3) low-La/Yb group, with low Sr/Y and Nb/Ta ratios, crystallized from magmas generated at lower pressures (~1.0 GPa), from an amphibolitic source that left plagioclase as a residual phase. These three geochemical groups do not have a straight correspondence with the three episodes of TTG generation and a same TTG unit can be composed of rocks of different groups. However, rocks of the high-La/Yb group are related dominantly to the Mogno trondhjemite and Mariazinha tonalite; those of the medium-La/Yb group are common in the Mogno trondhjemite and Arco verde tonalite but dominate in the Agua Fria trondhjemite and Caracol tonalitic complex; finally, the low La/Yb group is composed essentially of rocks of the Arco Verde tonalite with an unique associated sample of the Caracol tonalitic complex (Fig. 11).

A model involving a hot subduction zone underneath a thick oceanic plateau was envisaged to explain the tectonic evolution of the RMGGT. In this context, the low-La/Yb group was formed from magmas originated by the melting of the base of a thickened basaltic oceanic crust at comparatively lower pressures (ca. 1.0 GPa), whereas the medium- and high-La/Yb groups were derived from the slab melting at increasing different pressures (1.0-1.5 and > 1.5 GPa, respectively). Part of these TTG magmas react during their ascent with the mantle wedge being totally consumed and leaving a metassomatized mantle. 50 m. y. later, at ca. 2870 Ma, thermal events, possibly related to the slab-break-off and asthenosphere mantle upwelling or mantle plume, may have induced the melting of the metassomatized mantle and the generation of sanukitoid magmas. These magmas may have heated the base of the Archean continental crust and could have lead to the local melting of the basaltic crust forming the Água Fria trondhjemite magma.

Acknowledgements

A. T. R.Ferreira, A. L. Paiva Junior, G. R. L. Feio, M. A. C. Costa and S. B. Dias are acknowledged for support in geological mapping, petrographical, geochemical, and geochronological work. The authors thank to the M. A. Galarza Toro for their skilful laboratory assistance for obtainment of the single zircon Pb-evaporation analyses. C. N. Lamarão is also thanked for his assistance in the cathodoluminescence imaging. Authors also thank to E. L. Dantas, B. Lima and S. Junges for his assistance on LA-ICP-MS analyses. The authors express special thanks to J. Halla, E. Heilimo, M. I. Kurhila, and A. Heinonen for support during field trip in Karelia craton and for numerous discussions on Archean geology. The Brazilian Geological Survey, CPRM, is acknowledged for permission to include in this paper data generated in the GEOBRASIL Project (mapping of Marajoara sheet). This research received financial support from CNPq (R. Dall'Agnol – Grants 0550739/2001-7, 476075/2003-3, 307469/2003-4, 484524/2007-0; PRONEX – Proc. 66.2103/1998-0, M. A. Oliveira – doctor scholarship; J. A. C. Almeida – doctor scholarship), CAPES (F. V. Guimarães, master scollarship), and Federal University of Pará (UFPA). This paper is a contribution to the Brazilian Institute of Amazonia Geosciences (INCT program – CNPq/MCT/FAPESPA – Proc. 573733/2008-2).

Appendix A. Analytical procedures for whole rock chemical analyses

The 65 whole rock chemical analyses used in this work comprise both previously published data (8 analyses from Althoff, 1996; 19 analyses from Leite, 2001; 7 analyses from Guimarães, 2007; 17 analyses from Guimarães et al. a, submitted) and 14 additional analyses (this work). All new analyses and those obtained by Guimarães (2007) and Guimarães et al. (a, submitted) were performed by ICP-ES for major elements and ICP-MS for trace-elements, including the rare-earth elements, at the Acme Analytical Laboratories Ltd. in Canada. The chemical analyses obtained by Althoff (1996) were done at the Centre de Recherches Petrographiques et Geochimiques (CRPG-CNRS, France); the major and minor elements and Sc were analyzed using ICP-Emission and all other trace elements, including the rare-earth elements were analyzed by ICP-MS. Chemical diagrams were mostly generated using the GCDkit software (Janousek et al., 2003).

References

Albarède, F., 1998. The growth of continental crust. Tectonophysics 196, 1–14.

Albarède, F., Telouk, P., Blichert-Toft, J., Boyet, M., Agranier, A., Nelson, B., 2004. Precise and accurate isotopic measurements using multiple collector ICP-MS. Geochim. Cosmochim. Acta 68, 2725–2744.

Almeida, J.A.C., Oliveira, M.A., Dall'agnol, R., Althoff, F.J., Borges, R.M.K., 2008. Relatório de mapeamento geológico na escala 1:100.000 da Folha Marajoara (SB-22-ZC V). Programa Geobrasil, CPRM – Serviço Geológico do Brasil. 147p. (In portuguese).

Althoff, F.J., 1996. Étude pétrologique et structurale des granitoïdes de Marajoara (Pará, Brésil): leur rôle dans l'évolution archéenne du craton Amazonien (2.7– 3.2 Ga). Ph.D thesis. Université Henri Poincaré, Nancy I, France, 296p. (in French).

Althoff, F.J., Barbey, P., Boullier, A.M., 2000. 2.8–3.0 Ga plutonism and deformation in the SE Amazonian craton: the Archean granitoids of Marajoara (Carajás Mineral province, Brazil). Precambrian Res. 104, 187–206.

Barker, F., Arth, J.G., 1976. Generation of trondhjemite-tonalite liquids and Archean bimodal trondhjemite-basalt suites. Geology 4, 596–600.

Barker, F., 1979. Trondhjemite: a definition, environment and hypotheses of origin. In: Barker, F. (Ed.), Trondhjemites, Dacites and Related Rocks. Elsevier, Amsterdam, pp. l–12.

Barros, C.E.M., Macambira, M.J.B., Barbey, P., Scheller, T., 2004. Dados isotópicos Pb-Pb em zircão (evaporação) e Sm-Nd do Complexo Granítico Estrela, Província Mineral de Carajás, Brasil: Implicações petrológicas e tectônicas. Rev. Bras. Geociências 34, 531-538.

Bickle, M.J., Bettenay, L.F., Chapman, H.J., Groves, D.I., McNaughton, N.J., Campbell, I.H., de Laeter, J.R., 1993. Origin of the 3500–3300 Ma calc-alkaline rocks in the Pilbara Archaean: isotopic and geochemical constraints from the Shaw Batholith. Precambrian Res. 60, 117–149.

Buhn, B., Pimentel, M.M., Matteini, M., Dantas, E.L., 2009. High spatial resolution analysis of Pb and U isotopes for geochronology by laser ablation multi-collector inductively coupled plasma mass spectrometry (LA-MC-ICP-MS). Anais Acad. Brasil. Ciências 81 (1), 1–16.

Champion, D.C., Smithies, R.H., 2007. In: Van Kranendonk, M.J., Smithies, R.H., Bennett, V.C. (Eds.), Geochemistry of Paleoarchean Granites of the East Pilbara Terrane, Pilbara Craton,

Western Australia: Implications for Early Archean Crustal Growth. Earth's Oldest Rocks, Developments in Precambrian Geology, vol. 15. Elsevier, Amsterdam, pp. 369–410.

Choukroune, P., Ludden, J.N., Chardon, D., Calvert, A.J., Bouhallier, H., 1997. Archean crustal growth and tectonics processes: a comparison of the Superior Province, Canada and the Dharwar Craton, India. In: Burg, J.P., Ford, M. (Eds.*),* Orogeny Through Time, vol. 121. Geol. Soc. Spec. Publ., London, pp. 63-98.

Condie, K.C., 1989. Geochemical changes in basalts and andesites across the Archean-Proterozoic boundary: Identification and significance. Lithos 23, 1–18.

Condie, K.C. 1993. Chemical composition and evolution of the upper continental crust: Contrasting results from surface samples and shales. Chem. Geol., 104, 1-37.

Condie, K.C. 2005. TTGs and adakites: are they both slab melts? Lithos 80, 33-44.

Dall'Agnol, R.; Rämö, O.T.; Magalhães, M.S.; Macambira, M.J.B. 1999. Petrology of the Anorogenic, Oxidised Jamon and Musa granites, Amazonian craton: implications for the genesis of Proterozoic A-type granites. Lithos, 46, 431-462.

Dall'Agnol, R., Lafon, J.M., Fraga, L.M., Scandolara, J., Barros, C.E.M. 2000. The Precambrian Evolution of the Amazonian Craton: one of the last Unknown Precambrian Terranes in the World. In: International Geological Congress, 31. Rio de Janeiro. Abstracts. Rio de Janeiro: CPRM. K.4 (CD ROM).

Dall'Agnol, R., Teixeira, N.P., Rämö, O.T., Moura, C.A.V., Macambira, M.J.B., Oliveira, D.C., 2005. Petrogenesis of the Paleoproterozoic, rapakivi, A-type granties of the Archean Carajás Metallogenic Province, Brazil. Lithos 80, 01-129.

Dall'Agnol, R., Oliveira, M.A., Almeida, J.A.C., Althoff, F.J., Leite, A.A.S., Oliveira, D.C. & Barros, C.E.M. 2006. Archean and Paleoproterozoic granitoids of the Carajás metallogenetic province, eastern Amazonian craton. In: Dall'Agnol, R., Rosa-Costa, L.T., Klein, E.L. (eds.). Symposium on Magmatism, Crustal Evolution, and Metallogenesis of the Amazonian Craton. Abstracts Volume and Field Trips Guide. Belém, PRONEX-UFPA/SBGNO, 99-150.

De Paolo, D.J., 1981. Neodymium isotope in the Colorado Front Range and crust–mantle evolution in the Proterozoic. Nature 291, 193– 196.

De Wit, M.J., 1998. On Archean granites, greenstones, craton and tectonics: does the evidence demand a verdict. Precambrian Res. 91, 181–226.

De Wit, M., 2001. Archaean Tectonics: Wading Through a Mine-Field of Controversies. Australian Geological Survey Organisation, Record 2001/37, 4th International Archaean Symposium. Perth, WA, p. 8.

Dias, S. B., 2009. Caracterização geológica, petrográfica e geoquímica de granitos Arqueanos da Folha Marajoara, terreno granito-greenstone de Rio Maria, sudeste do Pará. Federal University of Para. 129p. M.Sc. Thesis. Graduated Program on Geology and Geochemistry, Institute of Geosciences (in Portuguese).

DOCEGEO. 1988. Revisão litoestratigráfica da Província Mineral de Carajás. In: Congresso Brasileiro de Geologia, 35. Belém. Anais do Congresso Brasileiro de Geologia. SBG. p. 11-54.

Drummond, M.S., Defant, M.J., 1990. A model for trondhjemite–tonalite–dacite genesis and crustal growth via slab melting: Archaean to modern comparisons. J. Geophys. Res. 95, 21503–21521.

Duarte, K. D., 1992. Geologia e geoquímica do granito Mata Surrão (SW de Rio Maria – Pa): um exemplo de granito "stricto sensu" Arqueano. Federal University of Para. 217p. M.Sc. Thesis. Graduated Program on Geology and Geochemistry, Institute of Geosciences (in Portuguese).

Evensen, N.M., Hamilton, P.T., O'nions, R.K. 1978. Rare earth abondances in chondritic meteorites. Geochim. Cosmochim. Acta, 39: 55.64.

Feio, G.R.L. 2009. Magmatismo granitóide arqueano da região de Canaã dos Carajás: implicações para a evolução crustal da Província Carajás. Federal University of Para. 97p. Qualifying examination. Graduated Program on Geology and Geochemistry, Institute of Geosciences (in Portuguese).

Foley, S.F., Tiepolo, M., Vannucci, R., 2002. Growth of early continental crust controlled by melting of amphibolite in subduction zones. Nature 417, 837– 840.

Gaudette, H.E., Lafon, J.M., Macambira, M.J.B., Moura, C.A.V., Scheller, T., 1998. Comparison of single filament Pb evaporation/ionization zircon ages with conventional U-/Pb results: examples from the Precambrian of Brazil. J. South Am. Earth Sci. 11, 351-/363.

Gibbs, A.K., Wirth, K.R., Hirata, W.K., Olszewski Jr., W.J., 1986. Age and composition of the Grão Pará Group volcanics, Serra dos Carajás. Rev.Bras. Geociências 16, 201–211.

Glikson, A.Y., 1979. Early Precambrian tonalite-trondhjemite sialic nuclei. Earth Sci. Rev. 15, 1–73.

Gomes A.C.B., Dall'Agnol R. 2007. Nova associação tonalítica-trondhjemítica Neoarqueana na região de Canaã dos Carajás: TTGs com altos conteúdos de Ti, Zr e Y. Rev. Bras. Geociências, 37(1), 182-193.

Guimarães, F.V., 2007. Mapeamento Geológico e Petrografia de granitóide Tonalítico-Trondhjemítico da Região a Leste de Bannach, Terreno Granito-*Greenstone* de Rio Maria - PA. Federal University of Para. 46p. Trabalho de Conclusão de Curso. Institute of Geosciences (in Portuguese).

Guimarães, F.V.G., Dall'Agnol, R., Almeida, J.A.C., Oliveira, M.A., submitted a. Caracterização geológica, petrográfica e geoquímica do trondhjemito Mogno e tonalito Mariazinha, terreno granito-greenstone de Rio Maria - Pará. Rev. Bras. Geociências.

Guimarães, F.V.G., Dall'Agnol, R., Oliveira, M.A., Almeida, J.A.C., submitted b. Geologia, petrografia e geoquímica do quartzo-diorito Parazônia e granodiorito Grotão, terreno granito-greenstone de Rio Maria – Pará. Rev. Bras. Geociências.

Halla, J., 2005. Late Archean high-Mg granitoids (sanukitoids) in the Southern Karelian craton, Eastern Finland. Lithos 79, 161–178.

Halla, J., van Hunen, J., Heilimo, E., Hölttä P., 2009. Geochemical and numerical constraints on Neoarchean plate tectonics. Precambrain Res.179, 155–162.

Huhn, S. R. B., Santos, A. B. S., Amaral, A. F., Ledsham, E. J., Gouveia, J. L., Martins, L. B. P., Montalvão, R. M. G. & Costa,V. G. 1988. O terreno granito-greenstone da região de Rio Maria - Sul do Pará. In: Congresso Brasileiro de Geologia, 35., Belém. Anais do congresso Brasileiro de Geologia. Belém, SBG. v. 3, p. 1438-1453.

Huhn, S.R.B., Macambira, M.J.B., Dall'Agnol, R., 1999. Geologia e Geocronologia Pb/Pb do Granito Alcalino Arqueano Planalto, Região da Serra do Rabo, Carajás-PA. In: Simp. Geol. Amaz., 6. Manaus. Boletim de resumos expandidos. Manaus, SBG/NO. p. 463-466.

Irvine, T.N. & Baragar, W.R.A. 1971. A guide to the chemical classification of the common volcanic rocks. Can. J. Earth Sci. 8, 523-547.

Jackson, S.E., Pearson, N.J., Griffin,W.L., Belousova, E.A., 2004. The application of laser ablation-inductively coupled plasma-mass spectrometry to in situ U–Pb zircon geochronology. Chem. Geol. 211, 47–69.

Janousek, V., Farrow, C.M., Erban, V., 2003. GCDkit: new PC software for interpretation of whole-rock geochemical data from igneous rocks. Godschmidt Conf. Abstr., A186.

Käpyaho, A. Mänttäri, I., Huhma, H., 2006. Growth of Archaean crust in the Kuhmo district, Eastern Finland: U−Pb and Sm−Nd isotope constraints on plutonic rocks. Precambrian Res.146, 95–119.

Klemme, S., Blundy, J. D. & Wood, B. J., 2002. Experimental constraints on major and trace element partitioning during partial melting of eclogite. Geochim. Cosmochim. Acta 66, 3109–3123.

Kober, B., 1986. Whole-grain evaporation for 207Pb/206Pb-age-investigations on single zircons using a double-filament thermal ion source. Contrib. Mineral. Petrol. 93, 482–490.

Kröner, A., Hegner, E., Wendt, J.I., Byerly, G.R., 1996. The oldest part of the Barberton granitoid-greenstone terrain, South Africa: evidence for crust formation between 3.5 and 3.7 Ga. Precambrian Res.78, 105–124.

Lafon, J.M., Rodrigues, E., Duarte, K.D. 1994. Le granite Mata Surrão: un magmatisme monzogranitique contemporain des associations tonalitiques-trondhjemitiques-granodioritiques archéennes de la région de Rio Maria (Amazonie Orientale, Brésil). Comptes Rendues de la Academie de Sciences de Paris, t. 318, serie II, p. 642- 649.

Leite, A.A.S., 2001. Geoquímica, petrogênese e evolução estrutural dos granitóides arqueanos da região de Xinguara, SE do Cráton Amazônico. Federal University of Para. 330p. PhD Thesis. Graduated Program on Geology and Geochemistry, Institute of Geosciences (in Portuguese).

Leite, A. A. S., Dall'Agnol, R., Macambira, M. J. B., Althoff, F. J., 2004. Geologia e geocronologia dos granitóides arqueanos da região de Xinguara (PA) e suas implicações na evolução do terreno granito-greenstone de Rio Maria. Rev. Bras. Geociências. 34, 447-458.

Le Maitre, R.W. 2002. A classification of igneous rocks and glossary of terms. 2nd Edition, London, 193 p.

Lobato, L.M., Rosière, C.A., Silva, R.C.F., Zucchetti, M., Baars, F.J., Sedane, J.C.S., Javier Rios, F., Pimentel, M., Mendes, G.E., Monteiro, A.M., 2006. A mineralização hidrotermal de ferro da Província Mineral de Carajás – controle estrutural e contexto na evolução metalogenética da província. 72p. Caracterização de Depósitos Minerais em Distritos Mineiros da Amazônia. Capítulo II, DNPM, CT-Mineral / FINEP, ADIMB. (CD-ROM.)

Ludwig, K.R., 2003, User's Manual for Isoplot/Ex v. 3.00. A Geochronological Toolkit for Microsoft Excel. BGC Special Publication 4, Berkeley, 71 pp.

Macambira, M.J.B., Lafon, J.M., 1995. Geocronologia da Província Mineral de Carajás; Síntese dos dados e novos desafios. Boletim do Museu Paraense Emílio Goeldi, série Ciências da Terra, Belém, 7, 263-287.

Macambira, M.J.B., Lancelot, J., 1996. Time constraints for the formation of the Archean Rio Maria crust, southeastern Amazonian Craton, Brazil. Intern. Geology Rev., 38 (12), 1134-1142.

Macambira, M.J.B., Costa, J.B.S., Althoff, F.J., Lafon, J.-M., Melo, J.C.V., Santos, A., 2000. New geochronological data for the Rio Maria TTG terrane; implications for the time constraints of the Carajás Province, Brazil. In: 31st Intern. Geol. Congr., Rio de Janeiro (CD-ROM).

Macambira J.B. 2003. O ambiente deposicional da Formação Carajás e uma proposta de modelo evolutivo para a Bacia Grão Pará. State University of Campinas. 217p. Ph.D. thesis. Institute of Geosciences (in Portuguese).

Machado, N., Lindenmayer, Z.G., Krogh, T.E., Lindenmayer, D. 1991. U-Pb geochronology of Archean magmatism and basement reactivation in the Carajás area, Amazon shield, Brazil. Precambrian Res., 49: 329-354.

Martin, H., 1987. Petrogenesis of Archaean trondhjemites, tonalites and granodiorites from eastern Finland: major and trace element geochemistry. J. Petrol. 28, 921–953.

Martin, H. 1994. The Archean grey gneisses and the gneisses of continental crust. In: Condie, K. C. (ed.) Developments in precambrian geology 11. Archeancrustal evolution, Amsterdam, Elsevier. p. 205-259.

Martin, H.; Peucat, J.J.; Sabaté, J.C.; Cunha, J.C. 1997. Crustal evolution in the early Archaean of South America: example of the Sete Voltas Massif, Bahia State, Brazil. Precambrian Res. 82, 35-62.

Martin, H., 1999. The adakitic magmas: modern analogues of Archaean granitoids. Lithos 46 (3), 411– 429.

Martin, H., Moyen, J.-F., 2002. Secular changes in TTG composition as markers of the progressive cooling of the Earth. Geology 30 (4), 319– 322.

Martin, H., Smithies, R.H., Rapp, R., Moyen, J.-F., Champion, D., 2005. An overview of adakite, tonalite-trondhjemite-granodiorite (TTG) and sanukitoid: relationships and some implications for crustal evolution. Lithos 79, 1–24.

Meirelles, M.R., Dardenne, M.A., 1991. Vulcanismo basáltico de afinidade shoshonítica em ambiente de arco Arqueano, Grupo Grão-Pará, Serra dos Carajás, Estado do Pará. In: Congresso Brasileiro Geologia, 33, Rio de Janeiro, 1991. Anais. Rio de Janeiro, SBG, v. 5: 2164-2174.

Moyen, J.F., Martin, H., Jayananda, M., Auvray, B., 2003. Late Archaean granites: a typology based on the Dharwar Craton (India). Precambrian Res. 127, 103– 123.

Moyen, J.-F., Stevens, G., Kisters, A.F.M., Belcher, R.W., 2007. TTG plutons of the Barberton granitoid-greenstone terrain, South Africa. In: Van Kranendonk, M.J., Smithies, R.H., Bennet, V. (Eds.), Earth's Oldest rocks. Developments in Precambrian geology. Elsevier, pp. 606–668.

Moyen, J.-F., Stevens, G., 2006. Experimental constraints on TTG petrogenesis: implications for Archean geodynamics. In: Benn, K., Mareschal, J.-C., Condie, K.C. (Eds.), Archean geodynamics and environments. monographs. AGU, pp. 149–178.

Moyen, J.-F., 2009. High Sr/Y and La/Y ratios: The meaning of the "adakitic signature". Lithos. 112, 556–574.

O'Connor J.T. 1965. A classification for quartz-rich igneous rocks based on feldspar rations. US Geological Survey Profissional Papers, 525B: 79-84.

Oliveira, M.A., Dall'Agnol, R., Althoff, F.J., Leite, A.A.S. 2009. Mesoarchean sanukitoid rocks of the Rio Maria Granite-Greenstone Terrane, Amazonian craton, Brazil. J. South Am. Earth Sci.. 27, 146-160.

Oliveira, M.A., Dall'Agnol, R., Almeida J.A.C. submitted. Petrology of the Mesoarchean Rio Maria Suite: Implications for the genesis of Sanukitoid Rocks. Lithos.

Peccerillo, A., Taylor, S.R., 1976. Geochemistry of Eocene calc-alkaline volcanic rocks from the Kastamonu area, Northern Turkey. Contribution to Mineralogy and Petrology 58, 63–81.

Pimentel, M.M., Machado, N., 1994. Geocronologia U-Pb dos terrenos granito-greenstone de Rio Maria, Pará. In: Congr. Bras. Geol., 38., São Paulo, 1994, Boletim de Resumos Expandidos, Camboriú, SBG, 1: 390-391.

Rämö, O.T., Dall'Agnol, R., Macambira, M.J.B., Leite, A.A.S., Oliveira, D.C., 2002. 1.88 Ga oxidized A-type granites of the Rio Maria region, eastern Amazonian craton, Brazil: Positively anorogenic! J. Geology 110, 603-610.

Rapp, R.P., 1994. Partial melting of metabasalts at 2–7 GPa: experimental results and implications for lower crustal and subduction zone processes. Miner. Mag. 58A, 760–761.

Rapp, R.P., Watson, E.B., 1995. Dehydration melting of metabasalt at 8–32 kbar implications for continental growth and crust–mantle recycling. J. Petrol. 36, 891– 931.

Rapp, R.P., Shimizu, N., Norman, M.D., Applegate, G.S., 1999. Reaction between slab-derived melts and peridotite in the mantle wedge: experimental constraints at 3.8 GPa. Chem. Geol. 160, 335– 356.

Rapp, R.P., Shimizu, N., Norman, M.D., 2003. Growth of early continental crust by partial melting of eclogite. Nature 425, 605– 609.

Rolando, A.P., Macambira, M.J.B. 2002. Geocronologia dos granitóides arqueanos da região da Serra do Inajá, novas evidências sobre a formação da crosta continental no sudeste do Cráton Amazônico, SSE Pará. In: Congresso Brasileiro de Geologia, 41**.** Anais do Congresso Brasileiro de Geologia. João Pessoa. SBG. p. 525.

Rolando, A.P., Macambira, M.J.B. 2003. Archean crust formation in Inajá range area, SSE of Amazonian Craton, Brazil, basead on zircon ages and Nd isotopes. *In*: South American Symposium on Isotope Geology, 4, Salvador. Expanded Abstracts. Salvador. (CD-ROM).

Rollinson, H., 1997. Eclogite xenoliths in west African kimberlites as residues from Archaean granitoid crust formation. Nature 389, 173–176.

Rudnick, R.L., 1995. Making continental crust. Nature 378, 571– 577.

Santos, J.S.O., Hartmann, L.A., Faria, M.S., Riker, S.R., Souza, M.M., Almeida, M.E., Mcnaughton, N.J. 2006. A compartimentação do Cráton Amazonas em províncias: avanços ocorridos no período 2000-2006. In: Simpósio de geologia da Amazônia, 9, Belém. Resumos Expandidos, Belém, SBG. (CD-ROM).

Sardinha A.S., Barros C.E.M., Krymsky R. 2006. Geology, geochemistry, and U–Pb geochronology of the Archean (2.74 Ga) Serra do Rabo granite stocks,Carajás Metallogenetic Province, northern Brazil. J. South Am. Earth Sci. 20, 327–339.

Sen, C., Dunn, T., 1994. Experimental modal metasomatism of a spinel lherzolite and the production of amphibole-bearing peridotite. Contrib. Miner. Petrol. 119, 422–432.

Shand, S. J. 1950. Eruptive rocks their genesis, composition, classification e their relation to ore deposit. 4ed., London, 488p.

Silva, M.G., Teixeira, J.B.G, Pimentel, M.M., Vasconcelos, P.M., Arielo, A., Rocha, W.J.S.F. 2006. Geologia e mineralização de Fe-Cu-Au do alvo GT46 (Igarapé Cinzento), Carajás. 60p. Caracterização de Depósitos Minerais em Distritos Mineiros da Amazônia. Capítulo III. DNPM, CT-Mineral / FINEP, ADIMB (CD-ROM).

Smithies, R.H., 2000. The Archean tonalite–tondhjemite–granodiorite (TTG) series is not an analogue of cenozoic adakite. Earth Plan. Sci. Letters 182, 115– 125.

Smithies, R.H., Champion, D.C., 2000. The Archaean high-Mg diorite suite: links to tonalite–trondhjemite–granodiorite magmatism and implications for early Archaean crustal growth. J. Petrol. 41 (12), 1653– 1671.

Souza, S. Z., Dall'Agnol, R., Althoff, F. J., Leite, A. A. S., Barros, C. E. M. 1996. Carajás mineral province: geological, geochronological and tectonic constrasts on the Archean evolution of the Rio Maria Granite- Greenstone Terrain and the Carajás block. In: Simp. Arch. Terr. South Amer. Plataform, Brasîlia, 1996, Extended abstracts, Brasília, SBG. p 31-32.

Souza, Z.S., Potrel, H., Lafon, J.M., Althoff, F.J., Pimentel, M.M., Dall'agnol, R., Oliveira, C.G. 2001. Nd, Pb and Sr isotopes of the Identidade Belt, an Archaean greenstone belt of the Rio Maria region (Carajas Province, Brazil): Implications for the Archaean geodynamic evolution of the Amazonian Craton. Precambrian Res.109, 293–315.

Souza, Z. S., 1994. Geologia e petrogênese do Greenstone Belt Identidade: implicações sobre a evolução geodinâmica do Terreno Granito- "Greenstone" de Rio Maria, SE do Pará. Federal University of Para. 2. v. Ph.D. thesis. Graduated Program on Geology and Geochemistry, Institute of Geosciences (in Portuguese).

Stacey, J.S., Kramers, J.D., 1975. Approximation of terrestrial lead isotope evolution by a two-stage model. Earth Planet. Sci. Lett. 26, 207–221.

Tassinari, C.C.G., Macambira, M. 2004. A evolução tectônica do Craton Amazonico. In: Mantesso – Neto, V.; Bartorelli, A.; Carneiro, C.D.R.; Brito Neves, B.B. (Eds.), Geologia do Continente Sul Americano: Evolução da obra de Fernando Flávio Marques Almeida. São Paulo, p. 471-486.

Teixeira, J. B. G., Eggler, D. H. 1994. Petrology, geochemistry, and tectonic setting of Archean basaltic and dioritic rocks from the N4 iron deposit, Serra dos Carajás, Pará, Brazil. Acta Geology Leopoldensia 17 (40), 71-114.

Vasquez L.V., Rosa-Costa L.R., Silva C.G., Ricci P.F., Barbosa J.O., Klein E.L., Lopes E.S., Macambira E.B., Chaves C.L., Carvalho J.M., Oliveira J.G., Anjos G.C., Silva H.R. 2008. Geologia e Recursos Minerais do Estado do Pará: Sistema de Informações Geográficas – SIG : texto explicativo dos mapas Geológico e Tectônico e de Recursos Minerais do Estado do Pará. Organizadores, Vasquez M.L., Rosa-Costa L.T. Escala 1:1.000.000. Belém: CPRM.

Viegas, L.G.F., 2009. Partição da deformação na transição entre o Terreno Granito-Greenstone de Rio Maria e o Cinturão Itacaiúnas, Carajás (PA). Federal University of Para. 156p. M.Sc. thesis. Graduated Program on Geology and Geochemistry, Institute of Geosciences (in Portuguese).

Wells, P.R.A., 1981. Accretion of continental crust: thermal and geochemical consequences. Phil. Trans. R. Soc. Lond. A301, 347–357.

Wolf, M.B., Wyllie, P.J., 1994. Dehydration-melting of amphibolite at 10 kbar: the effects of temperature and time. Contrib. Mineral. Petrol. 115, 369– 383.

Winther, K.T., 1996. An experimentally based model for the origin of tonalitic and trondhjemitic melts. Chem. Geol. 127, 43–59.

Xiong, X.L., Adam, J., Green, T.H., 2005. Rutile stability and rutile/melt HFSE partitioning during partial melting of hydrous basalt: implications for TTG genesis. Chem. Geol. 218, 339–359.

Zamora, D., 2000. Fusion de la croûte océanique subductée: approche expérimentale et géochimique. Ph.D. thesis. Université Blaise-Pascal, Clermont-Ferrand.

Capítulo – 3

Geochemistry and zircon geochronology of the Archean granite suites of the Rio Maria granite-greenstone terrane, Carajás province, Brazil.

José de Arimatéia Costa de Almeida

Roberto Dall'Agnol

Albano Antonio da Silva Leite

Submetido: Journal of South American Earth Sciences

Dear Ari,

We have received your article "Geochemistry and zircon geochronology of the Archean granite suites of the Rio Maria Granite-Greenstone terrane, Carajás Province, Brazil." for consideration for publication in Journal of South American Earth Sciences.

Your manuscript will be given a reference number once an editor has been assigned. To track the status of your paper, please do the following:

1. Go to this URL: http://ees.elsevier.com/sames/

2. Enter these login details:

Your username is: ari

Your password is: almeida6248

3. Click [Author Login]

This takes you to the Author Main Menu.

4. Click [Submissions Being Processed]

Thank you for submitting your work to this journal.

Kind regards,

Elsevier Editorial System

Journal of South American Earth Sciences

****

Please note that the editorial process varies considerably from journal to journal. To view a sample editorial process, please click here:

http://ees.elsevier.com/eeshelp/sample_editorial_process.pdf

For any technical queries about using EES, please contact Elsevier Author Support at authorsupport@elsevier.com

Global telephone support is available 24/7:

For The Americas: +1 888 834 7287 (toll-free for US & Canadian customers)

For Asia & Pacific: +81 3 5561 5032

For Europe & rest of the world: +353 61 709190

Geochemistry and zircon geochronology of the Archean granite suites of the Rio Maria Granite-Greenstone terrane, Carajás Province, Brazil.

José de Arimatéia Costa de Almeida[1,2] (ari@ufpa.br); Roberto Dall'Agnol[1,2] (robdal@ufpa.br); Albano Antonio da Silva Leite (albano@ufpa.br)[1]

[1]Grupo de Pesquisa Petrologia de Granitóides, Instituto de Geociências (IG), Universidade Federal do Pará (UFPA), Caixa Postal 8608, CEP 66075-900, Belém, Pará, Brasil;
[2]Programa de Pós-Graduação em Geologia e Geoquímica – IG – UFPA.

ABSTRACT

The Archean granites exposed in the Mesorchean Rio Maria granite-greenstone terrane (RMGGT), southeastern Amazonian craton can be divided into three groups on the basis of petrographic and geochemical data. (1) Potassic leucogranites (Xinguara and Mata Surrão granites), composed dominantly of biotite monzogranites that have high SiO_2, K_2O, and Rb contents and show fractionated REE patterns with moderate to pronounced negative Eu anomalies. These granites share many features with the low-Ca granite group of the Yilgarn craton and CA2-type of Archean calc-alkaline granites. These granites result from the partial melting of rocks similar to the older TTG of the RMGGT. (2) Leucogranodiorite-granite group (Guarantã suite, Grotão granodiorite, and similar rocks), which is composed of Ba- and Sr-rich rocks which display fractionated REE patterns without significant Eu anomalies and show geochemical affinity with the high-Ca granite group or Transitional TTG of the Yilgarn craton and the CA1-type of Archean calc-alkaline granites. These rocks appear to have been originated by complex processes involving varied crustal sources or, alternatively, mixed crustal and mantle sources. (3) Amphibole-biotite monzogranites (Rancho de Deus granite) associated with sanukitoid suites. These granites were probably generated by fractional crystallization and differentiation of sanukitoid magmas enriched in Ba and Sr.

The emplacement of the granites of the RMGGT occurred during the Mesoarchean (2.87 to 2 .86 Ga). They are approximately coeval with the sanukitoid suites (~2.87 Ga) and post-dated the main timing of TTG suites formation (2.98-2.92 Ga). The crust of Rio Maria was probably still quite warm at the time when the granite magmas were produced. In these conditions, the underplating in the lower crust of large volumes of sanukitoid magmas may have also contributed

with heat inducing the partial melting of crustal protoliths and opening the possibility of complex interactions between different kinds of magmas.

Keywords: Amazonian craton, Rio Maria granite-greenstone terrane, Mesoarchean, Archean granites, calc-alkaline.

1. Introduction

Although TTGs are the dominant granitoids in Archaean terranes, granodiorite-granite associations are also a widespread and voluminous constituent of Archean cratons. Condie (1993) estimated that granites represent around 20% of the presently exposed Archean terranes. Most of these rocks form individual, syn- to post-tectonic plutons, usually intrusive in greenstone belts and TTG granitoids (Sylvester, 1994). They were emplaced generally during the Neoarchean in between 2.7 and 2.5 Ga (Goodwin, 1991). The presence of large volumes of granites in Archean terranes is commonly interpreted as an evidence of the stabilization of the oldest cratons (Nisbet, 1987; Kröner, 1991; Davis et al., 1994). It points also to the existence of rigid plates in the Late Archean and to the operation of conventional plate tectonics at that time (Hawkesworth and Kemp, 2006). An origin of Archean granites through partial melting of igneous or sedimentary sources in the middle or lower crust was admitted (Sylvester, 1994).

Archaean granitic plutons are composed dominantly of biotite- (and rarely hornblende-) bearing granodiorites to monzo- to syenogranites, with moderate to high K/Na ratios (>0.5), enrichment of the light REE over the heavy REE and Eu anomalies variable from absent to pronounced (Davis et al., 1994; Sylvester, 1994; Champion and Sheraton, 1997; de Wit, 1998; Frost et al., 1998; Champion and Smithies, 1999; Leite et al., 1999; Althoff et al., 2000; Moyen et al., 2003).

Several plutons and stocks representative of this kind of magmatism have been identified in the Archean Rio Maria granite-greenstone terrane (RMGGT) in the southeastern domain of the Amazonian craton. The aim of this paper is to present a synthesis on the available data on the Archean granite suites of the RMGGT, discuss their geochemical signature and refine the timing of this magmatism employing new chemical and geochronological data. It is hoped that such

studies will contribute to a better understanding of the origin of these rocks and help to decipher the processes involved in the generation and evolution of the Rio Maria crust.

2. Geological setting

The Rio Maria Granite-Greenstone terrane is located in the southern part of the Carajás Province (Docegeo, 1988; Dall'Agnol et al., 2006; Vasquez et al., 2008), the largest Archean domain of the Amazonian craton identified so far (Fig. 1a). The Carajás Province has been included into the Central Amazonian Province (Tassinari and Macambira, 2004) or considered an independent tectonic province (Santos et al., 2000). Its is limited to the west by a terrane dominated by Proterozoic granitoids and volcanic-pyroclastic assemblages (Uatumã Supergroup); to the east, by the Neoproterozoic Araguaia belt, whose evolution is associated with the Brasiliano (Pan-African) cycle that did not significantly affect the Amazonian craton; and to the north and south, respectively, by the Maroni-Itacaiúnas province and Santana do Araguaia domain (Vasquez et al., 2008), both formed during the 2.2–2.1 Ga Trans-Amazonian event. The Carajás province is divided in two major tectonic domains (Souza et al., 1996; Dall'Agnol et al., 2000, 2006; Santos et al., 2006; Vasquez et al., 2008), the Mesoarchean (3.0– 2.86 Ga) Rio Maria granite-greenstone terrane and the dominantly Neoarchean Carajás domain, mostly composed of 2.76–2.55 Ga metavolcanic rocks, banded iron formations, and granitoids (Machado et al., 1991; Macambira and Lafon, 1995; Barros et al., 2001; Dall'Agnol et al., 2006). The cratonization of both domains occurred at the end of the Archean and they were later affected by the intrusion of Paleoproterozoic A-type granites (Dall'Agnol et al., 2005).

The studied Archean granites are exposed in the Rio Maria granite-greenstone terrane (Fig 1b), which is composed of greenstone belts and a variety of Archean granitoids (Dall'Agnol et al., 2006). The former gave ages of 2.97 to 2.9 (Fig. 2) and consist of meta-ultramafic (komatiites), metamafic (basalts and gabbros) rocks and subordinate intermediate to felsic rocks, with intercalations of metagraywackes, all grouped into the Andorinhas supergroup (Souza et al., 2001). The granitic rocks were originated between 2.98 and 2.86 Ga (Fig. 2) and the oldest granitoids are represented by typical Archean TTG suites originated between 2.98-2.92 Ga (Arco Verde, Caracol, and Mariazinha tonalites and Mogno trondhjemite; Docegeo, 1988; Althoff et al., 2000; Souza et al., 2001; Leite et al., 2004; Dall'Agnol et al., 2006; Guimarães et al. a, submitted;

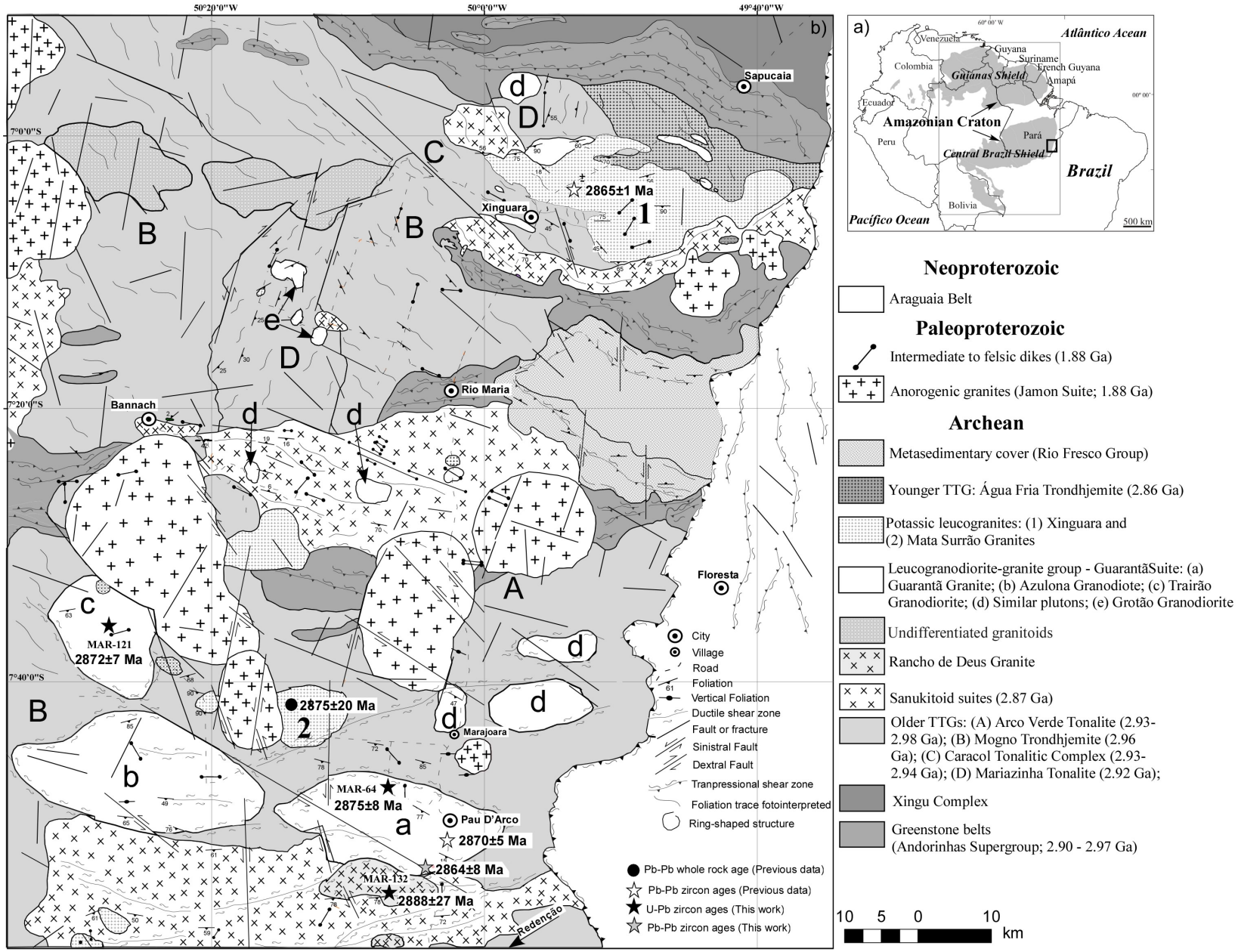
b)
50°20'0"W
50°0'0"W
49°40'0"W
7°0'0"S
7°20'0"S
7°40'0"S
Sapucaia
Xinguara
Rio Maria
Bannach
Floresta
Marajoara
Pau D'Arco
Redenção
2865±1 Ma
2875±20 Ma
2872±7 Ma
MAR-121
MAR-64
2875±8 Ma
2870±5 Ma
2864±8 Ma
MAR-132
2888±27 Ma
City
Village
Road
Foliation
Vertical Foliation
Ductile shear zone
Fault or fracture
Sinistral Fault
Dextral Fault
Tranpressional shear zone
Foliation trace fotointerpreted
Ring-shaped structure
Pb-Pb whole rock age (Previous data)
Pb-Pb zircon ages (Previous data)
U-Pb zircon ages (This work)
Pb-Pb zircon ages (This work)
a)
Atlântico Acean
Venezuela
Guyana
Suriname
French Guyana
Amapá
Colombia
Guianas Shield
Ecuador
Amazonian Craton
Pará
Peru
Central Brazil Shield
Brazil
Bolivia
Pacífico Ocean
500 km
Neoproterozoic
Araguaia Belt
Paleoproterozoic
Intermediate to felsic dikes (1.88 Ga)
Anorogenic granites (Jamon Suite; 1.88 Ga)
Archean
Metasedimentary cover (Rio Fresco Group)
Younger TTG: Água Fria Trondhjemite (2.86 Ga)
Potassic leucogranites: (1) Xinguara and (2) Mata Surrão Granites
Leucogranodiorite-granite group - GuarantãSuite: (a) Guarantã Granite; (b) Azulona Granodiote; (c) Trairão Granodiorite; (d) Similar plutons; (e) Grotão Granodiorite
Undifferentiated granitoids
Rancho de Deus Granite
Sanukitoid suites (2.87 Ga)
Older TTGs: (A) Arco Verde Tonalite (2.93-2.98 Ga); (B) Mogno Trondhjemite (2.96 Ga); (C) Caracol Tonalitic Complex (2.93-2.94 Ga); (D) Mariazinha Tonalite (2.92 Ga);
Xingu Complex
Greenstone belts (Andorinhas Supergroup; 2.90 - 2.97 Ga)
10 5 0 10
km

Figure 1 - (a) Location of the studied area in Amazonian Craton. (b) Geological map of the Rio Maria granite-greenstone terrane showing the location of the dated samples.

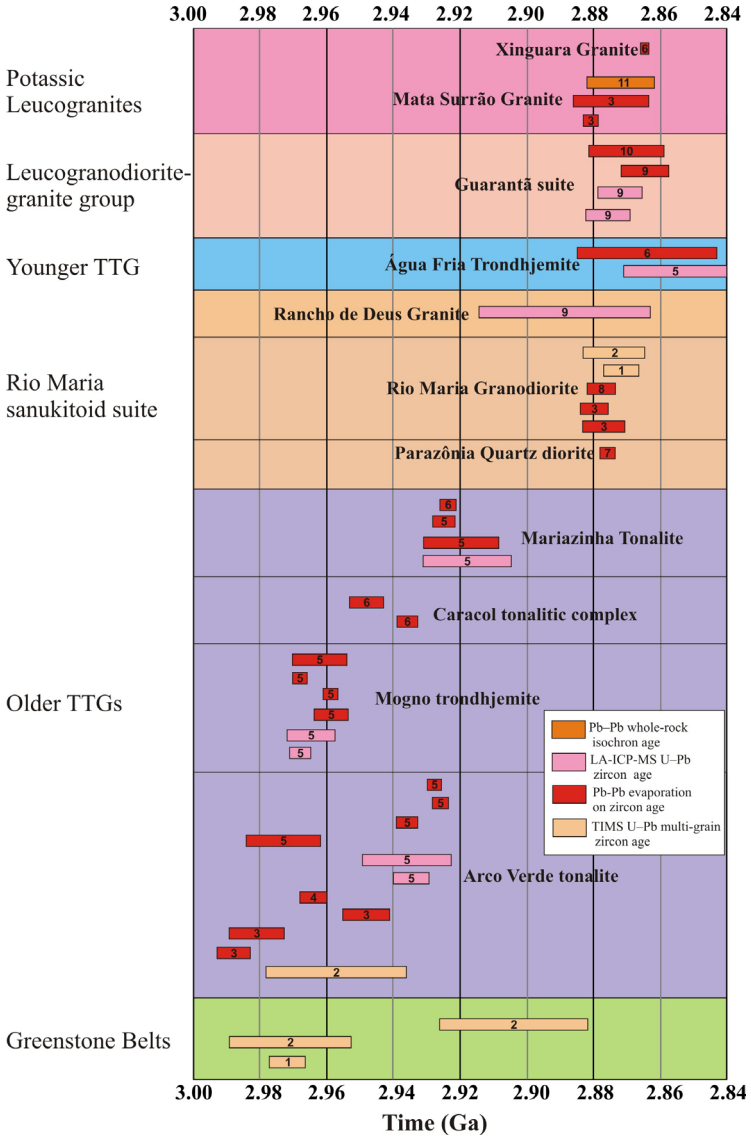

Figure 2 - Geochonological overview of the previous available data for Archean units of the Rio Maria granite-greenstone terrane and new geochronological data for the Guarantã suite and Rancho de Deus granite obtined in this work. Data Source: (1) Pimentel & Machado (1994), (2) Macambira (1992), (3) Rolando & Macambira (2003), (4) Vasquez et al., (2008), (5) Almeida et al., (submitted), (6) Leite et al., (2004), (7) Almeida (unpublished data), (8) Dall'Agnol et al., (1999), (9)This work, (10) Althoff et al., (2000), (11) Lafon et al., (1994).

Almeida et al., submitted). The contact relationships between these rocks and the greenstone sequences are not exposed, but enclaves of greenstone belts in these granitoids have been found. The oldest TTG suites were intruded by: (1) The Rio Maria sanukitoid suite (~2.87 Ga; Oliveira et al., 2009), composed dominantly of granodiorites, with associated mafic and intermediate rocks, forming enclaves in the granodiorites or, locally, small bodies. These rocks are intrusive in the greenstone belts and in the older TTG series and are intruded by the Água Fria Trondhjemite (Leite et al., 2004); (2) A small occurrence of younger TTG granitoids exposed in the Xinguara area, represented by the Água Fria Trondhjemite. It was dated at ca. 2.86 Ga and is intrusive in the Caracol tonalitic complex and coeval with the Xinguara potassic leucogranite (Leite et al., 2004); and (3) ~2.87-2.86 Ga Archean leucomonzogranites and leucogranodiorites (the age and stratigraphic position of these granitoids will be discussed in the present paper on the basis of new and more accurate geochronological data). The last shearing deformational event identified in this terrane occurred at around 2.86 Ga (Althoff et al., 2000; Souza et al., 2001; Leite et al., 2004) and, after it, the RMGGT remained stable until the emplacement of the 1.88 Ga A-type granites and associated dikes.

3. Geology of the Archean granite suites of the RMGGT

Three main types of Archaean granites were distinguished in the RMGGT (Fig. 1b) on the basis of petrographic and geochemical data: a) Potassic leucogranites (Xinguara and Mata Surrão granites); b) leucogranodiorite-granite group (Guarantã suite, Grotão granodiorite, and similar granites); and c) Granites associated with sanukitoid suites (Rancho de Deus granite).

3.1. Potassic leucogranites

In the RMGGT, the Archean potassic leucogranites are represented by the Xinguara (Leite et al., 2004) and Mata Surrão (Duarte et al., 1992) plutons and by small granitic stocks dispersed in the whole terrane (Fig. 1b). These granites are disposed as E-W to WNW-ESE elongated bodies, which are generally concordant with the dominant structures in the Archean units. The Xinguara and Mata Surrão plutons occupy relatively high-relief areas and display positive

radiometric anomalies, being easily delimited from the older country rocks. The rocks of the Mata Surrão granite are weakly deformed and yielded an age of 2875 ± 20 Ma (whole rock Pb-Pb isochron; Lafon et al., 1994). The pluton is intrusive in the Arco Verde tonalite and is crosscut by the Bannach anorogenic granite (Fig. 1b; Duarte, 1992). Plutons of monzogranitic composition located in the Inajá area (southern domain of the RMGGT, not represented in Fig. 1b) were dated at around 2.87 Ga (single zircon evaporation Pb-Pb age; Rolando and Macambira 2003) and correlated to the Mata Surrão granite. The Xinguara granite crosscuts the Caracol tonalitic complex and the Rio Maria sanukitoid suite and contains xenoliths of the mentioned rocks and also of metamafic rocks interpreted as related to the greenstone belts. Field relationships, structural evidence and geochronological data indicate that the Xinguara granite is coeval with the Água Fria trondhjemite (Leite, 2001, Leite et al., 2004). The Xinguara granite was dated at 2865 ± 1 Ma (Pb-Pb evaporation on zircon; Leite et al., 2004).

In the Xinguara pluton, the E-W to WNW-ESSE foliation is marked by flow structures, magmatic banding, and schistosity, which are more conspicuous in the border of the pluton. The foliation dips at high angles or is vertical near the contacts with the country rocks but it can be almost horizontal (10 to 20°) locally near the center of the pluton (Leite, 2001). Discrete shear bands affect locally the foliation. Partial recrystallization of quartz and feldspars generating core and mantle textures is a common feature in the Xinguara granite. These structural features were interpreted as evidence that the Xinguara granite was deformed initially in the submagmatic stage and prolonged its deformation during the high-temperature subsolidus stage (Leite, 2001, following Hutton, 1988; Paterson et al. 1989, 1998; Althoff et al., 2000). The recrystallization of plagioclase and K-feldspar should have occurred at temperatures above 500°C (Voll, 1976; Tullis, 1983; Tullis and Yund, 1985; Gapais, 1989).

3.2. Leucogranodiorite-granite group (LGdG)

Recent geological mapping in the Pau D'Arco area, including petrographic and geochemical studies (Almeida et al., 2008; Dias, 2009) demonstrated the existence of three plutons (Guarantã granite, Azulona and Trairão granodiorites) compositionally different from the Xinguara and Mata Surrão granites (Fig 1b). These plutons were included in a granitic suite denominated Guarantã suite (Dias, 2009). Small granitic stocks found in the Bannach and

Xinguara areas and the Grotão granodiorite (Guimarães et al. b, submitted), exposed to the SW of Xinguara (Fig. 1b), are similar to the rocks of the Guarantã suite and were embraced in the same Archean granitoid group. The rocks of the Guarantã suite crosscut the Arco Verde tonalite (oldest TTG group; Fig. 1b). They are strongly deformed and large shear zones, most of them located along the contacts between the Guarantã suite and the country rocks, have been identified. The plutons are elongated along the dominant regional trend and their rocks display a widespread and well-developed WNW–ESE trending subvertical foliation associated to a subhorizontal stretching lineation (Althoff et al., 2000; Dias, 2009). Except for the Trairão granodiorite, these plutons are exposed in low-relief areas. They give all moderate to low radiometric responses. The Grotão granodiorite was recently mapped (Guimarães et al. b, submitted). It occurs as small stocks formed by quite homogeneous equigranular fine-grained rocks that cross-cuts the Mariazinha tonalite (Fig. 1b). Similar rocks were previously described in the type area of the Rio Maria granodiorite and also to the north of Xinguara (Fig. 1b; respectively, Medeiros, 1987, and Leite, 2001).

3.3. Granites associated with sanukitoid suites (Rancho de Deus granite)

The Rancho de Deus pluton is in contact with the Rio Maria sanukitoid suite and the Guarantã Granite, but contact relationships between these units were not observed in the field. The Rancho de Deus pluton has an ellipsoid shape and is elongated along E-W, concordantly with the dominant regional trend in the Archean units. Its rocks are strongly deformed and display a E-W trending foliation. In the northern border of the Rancho de Deus pluton, a large shear zone delimitates its contact with the Guarantã granite pluton. A strong positive radiometric anomaly is observed in the area of occurrence of this pluton, which contrasts with the behaviour of the TTGs and Guarantã suite.

4. Petrography

The potassium leucogranites exhibit a remarkable homogeneity, being composed essentially of equigranular medium-grained monzogranite with scarce associated granodiorites and syenogranites (Fig. 3; Table 1). They show a rose or gray color and massive aspect in hand

samples. However, in thin sections, the strong recrystallization of quartz and feldspars is noteworthy.

The rocks of the LGdG are strongly deformed and consist dominantly of foliated coarse-grained porphyritic pink granites sometimes with a well-developed mineral lineation (Guarantã Suite and granodiorites of Xinguara area) or of equigranular fine-grained weakly foliated rocks (Grotão granodiorite). In contrast to the potassium granites, the LGdG show equal proportions of leucogranodiorites and leucomonzogranites (Fig. 3; Table 1).

The granites associated with sanukitoid series are composed dominantly of porphyritic gray or pink monzogranites that differs from the granites of the other Archean groups by the presence of amphibole as an important mafic phase (Fig. 3; Table 1).

All studied plutons are composed of hololeucocratic granites (mafics minerals <10%; Le Maitre, 2002), being composed of alkali feldspar, quartz, and plagioclase as essential minerals, biotite as main mafic mineral (hornblende was only observed in Rancho de Deus Granite), titanite, allanite, epidote, apatite, zircon, and magnetite as primary accessory minerals, chlorite, white mica, and carbonate as secondary phases. A typical feature of all Archean granite suites of the RMGGT is the presence of magmatic epidote. This kind of epidote is generally automorph, if envolving zoned allanite cores or associated with and partially enclosed in biotite, or xenomorphic and corroded if in contact with felsic minerals. Chemical data on the magmatic epidote indicate values of pistacite component of 25 to 33% mol (Guarantã suite; J.A.C. Almeida, unpublished data), or 27 to 30% mol (Xinguara pluton; Leite, 2001). These values are consistent with the hypothesis of magmatic origin for the epidote (Tulloch, 1979; Sial et al., 1999). The occurrence of magmatic epidote has been also noticed in the TTG suites (Leite, 2001; Almeida et al., submitted; Guimarães et al. a, submitted) and in the Rio Maria sanukitoid suite (Oliveira et al., 2009) of the RMGGT, as well as in the Arsikere granite of the Dharwar craton (Rogers, 1988; Jayananda et al., 2006).

Table 1 - Modal compositions (point counting) of representative samples of the Archean granite suites of the Rio Maria granite-greenstone terrane

Mineral	Leucogranodiorite-granite group																	
	Guarantã Suite															Grotão Granodiorite		
Samples	MAF-33 [1]	AL-86 [2]	MAR-123 [1]	MAR-38A [3]	MAR-121 [1]	MAR-114 [1]	MAF-58 [3]	MAR-50A [3]	MAR-164A [1]	MAR-93A [1]	MAR-101A [3]	MAR-97A [1]	MAR-64A [1]	MASF- 1 [4]	MASF- 7 [4]	FMR-49 [5]	FMR-69A [5]	FMR-45 [5]
Quartz	26.8	21.7	26.1	26.9	27.8	23.6	27.0	24.0	33.3	34.5	26.7	35.3	27.8	30.3	19.4	26.9	32.2	27.1
Plagioclase	58.3	59.3	44.4	38.0	46.1	43.9	46.8	48.4	35.1	47.7	46.9	46.8	47.6	36.0	53.4	48.4	52.6	48.0
Alkali-feldspar	9.6	11.7	18.5	27.3	19.3	24.4	16.3	19.8	24.1	12.0	21.0	11.1	16.6	29.6	22.4	15.9	11.8	17.3
Amphibole	0.0	0.0	0.0	0.0	0.0	0.0	0.0	0.0	0.0	0.0	0.0	0.0	0.0	0.0	0.0	0.0	0.0	0.0
Biotite	0.2	5.5	4.7	Tr	4.0	3.2	Tr	Tr	0.9	2.7	2.7	5.6	4.2	1.6	2.7	6.5	0.2	5.8
Epidote	2.9	0.0	4.8	4.5	1.9	3.3	5.1	2.6	2.5	0.5	2.1	0.3	1.4	2.0	2.1	0.9	0.0	0.8
Opaques	0.2	0.1	0.2	0.1	Tr	Tr	Tr	0.2	0.5	0.2	0.2	0.2	0.5	0.1	Tr	0.2	0.1	0.0
Titanite	0.4	Tr	0.4	Tr	0.3	0.6	0.3	Tr	0.4	0.7	0.1	0.2	0.2	Tr	Tr	0.5	0.1	0.5
Muscovite	0.0	1.5	0.1	1.0	0.1	0.4	2.7	1.8	1.9	0.2	0.0	0.1	0.5	0.0	0.0	0.4	0.2	0.2
Chlorite	0.7	Tr	0.2	2.2	0.2	0.1	1.4	2.9	0.5	0.5	Tr	Tr	0.5	0.4	Tr	0.1	2.8	Tr
Accessory (Ap+ Zr)	1.0	0.2	0.6	0.1	0.3	0.6	0.3	0.2	0.9	1.0	0.3	0.4	0.7	Tr	Tr	0.2	0.1	0.3
Félsic	94.6	92.7	89.0	92.1	93.2	91.8	90.2	92.3	92.5	94.2	94.5	93.2	92.0	95.9	95.2	91.2	96.5	92.4
Máfic	5.4	5.8	10.9	6.9	6.7	7.8	7.1	5.9	5.7	5.6	5.5	6.7	7.5	4.1	4.8	8.4	3.3	7.4

Mineral	Potassic leucogranites													Granites associeted with sanukitoid suites				
	Xinguara Granite								Mata Surrão Granite					Rancho de Deus Granite				
Samples	AL-2D [2]	AL-95 [2]	ALF-266 [2]	Al-152 [2]	AL-89 [2]	AL-65A [2]	AL-24 [2]	AL-56B [2]	KY-31B [6]	KY-89A [6]	KY-89E [6]	KZ-7C [6]	KY-104 [6]	MAR-144 [1]	MAR-132 [1]	MAR-129 [1]	MAR-126 [1]	MAF-22 [1]
Quartz	35.2	36.2	43.0	28.4	38.9	34.5	33.9	50.4	31.9	27.3	31.1	28.9	26.2	29.0	24.9	25.9	32.9	36.3
Plagioclase	17.1	29.7	19.3	37.2	29.8	24.6	33.1	27.7	33.2	34.6	37.9	33.5	38.0	34.0	45.3	40.1	37.5	19.5
Alkali-feldspar	41.2	31.9	34.4	32.6	27.4	38.5	31.6	18.8	23.2	33.8	23.2	31.3	32.2	30.9	19.0	29.0	25.0	41.3
Amphibole	0.0	0.0	0.0	0.0	0.0	0.0	0.0	0.0	0.0	0.0	0.0	0.0	0.0	1.1	1.4	Tr	0.1	0.6
Biotite	3.0	0.3	1.9	0.0	2.3	0.9	0.0	1.2	7.8	3.4	5.4	3.6	1.1	2.6	4.2	2.1	0.8	1.0
Epidote	0.8	1.0	0.2	0.8	0.4	0.4	0.2	1.1	3.3	0.8	2.2	2.1	2.3	1.8	2.9	1.3	0.8	0.0
Opaques	1.1	0.3	0.1	0.2	0.2	0.3	0.5	0.2	0.0	0.0	0.0	0.3	0.1	0.0	0.1	0.5	0.4	0.2
Titanite	Tr	Tr	Tr	Tr	Tr	Tr	Tr	Tr	Tr	Tr	Tr	Tr	Tr	0.2	0.9	0.1	0.1	Tr
Muscovite	1.4	0.1	1.0	0.0	0.1	0.4	0.2	0.6	0.4	0.0	0.1	0.0	0.1	0.0	0.1	0.3	1.2	0.0
Chlorite	0.2	0.5	Tr	0.8	0.9	0.3	0.5	Tr	Tr	Tr	Tr	0.2	0.1	0.1	0.2	Tr	0.7	0.9
Accessory (Ap+ Zr)	Tr	Tr	0.1	Tr	Tr	0.1	Tr	Tr	0.3	Tr	Tr	Tr	Tr	0.3	1.1	0.6	0.5	0.2
Félsic	93.5	97.8	96.7	98.2	96.1	97.6	98.6	96.9	88.3	95.8	92.3	93.8	96.3	93.9	89.2	95.1	95.4	97.1
Máfic	5.1	2.1	2.3	1.8	3.8	2.0	1.2	2.5	11.4	4.2	7.6	6.2	3.6	6.1	10.7	4.6	3.4	2.9

Data Source: [1] Almeida et al., (2008); [2] Leite (2001); [3] Dias (2009); [4] Dias (2007); [5] Guimarães (2009); [6] Duarte (1992)
Ap: Apatite
Zr: Zircon

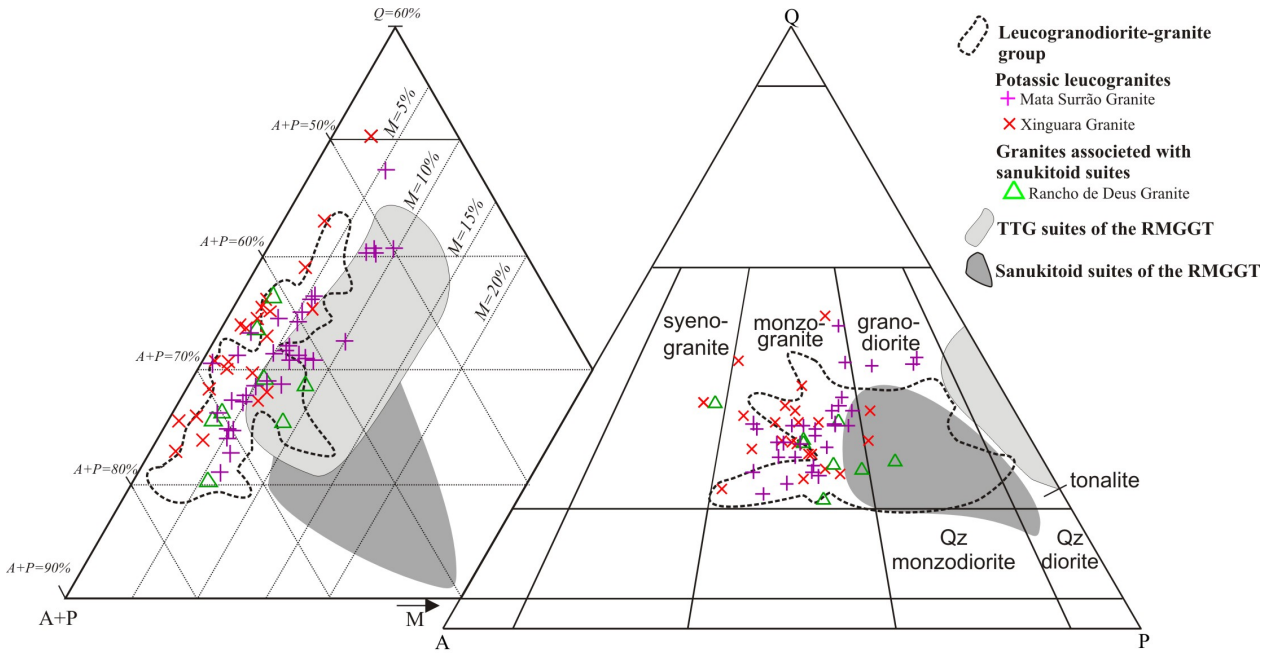

M= mafic minerals; Q=quartz; A=alcali-feldspar; P=plagioclase

Figure 3 - QAP and Q-(A+P)-M for the Archean granite suites of the Rio Maria granite-greenstone terrane (see table 1 for source data).

5. Geochronology

5.1. Potassic leucogranites

The available geochronological data on this group of granite is limited. The Mata Surrão granite was dated by Pb-Pb whole rock isochron and an age of 2872±10 Ma was obtained (Lafon et al., 1994). A granite exposed to the south of Redenção gave an age of 2875±11 Ma with inherited zircon yielding ages between 2.98 to 2.90 Ga and was correlated with the Mata Surrão granite (Rolando and Macambira, 2003). However, compared to the Archean high-K granites, that granite (MP-17 sample, Table 4) shows high Y and Nb, and low $(La/Yb)_N$ ratio, suggesting geochemical affinity with A-type granites.

The Xinguara granite was dated at 2865 ± 1 Ma (Pb-Pb evaporation on zircon; Leite et al., 2004; Fig. 2). Field relationships and structural features suggest that the Xinguara granite is coeval with the Agua Fria trondhjemite (Leite et al., 2004) and this was reinforced by the ages obtained for the latter unit (~2860 Ma; Leite et al., 2004; Almeida et. al., submitted; Fig. 2).

5.2. Leucogranodiorite-granite group

5.2.1. Available geochronological data

A leucogranite sample located immediately to the south of Pau D'Arco town, on the southeastern area of the Guarantã granite pluton, was dated and yielded an age of 2870±5 Ma (Fig. 1b; Althoff et al., 2000). This granite was initially correlated with the Mata Surrão granite, but geological and geochemical evidence suggest that it has more affinities with the Guarantã granite (sample F77-92-29; Table 4). For this reason, it is associated with that pluton in the present paper. Another granite sample located to the south of Redenção was also dated and gave an age of 2881±2 Ma, being correlated with the Rio Maria granodiorite (Rolando and Macambira, 2003). However, the mentioned granite (sample PPA-20, Table 4) has clear geochemical affinities with the Guarantã suite and is correlated with it in this paper.

5.2.2 - New geochronological data for the Guarantã Suite.

In this paper we present new geochronological data for the Guarantã granite and Trairão granodiorite obtained by Pb-Pb on zircon evaporation and LA-ICP-MS on zircon methods. The localization of the studied samples can be viewed in Fig. 1b and the summary of isotopic results is presented in Table 2 and 3. The analytical procedures are described in the Appendix A.

5.2.1.1 – Guarantã granite: samples MAR-64 and MAF-33

The dated samples of the Guarantã pluton contain colorless to brownish elongate prismatic zircon crystals (width/length ratios varying from 2:1 to 4:1) with well-formed faces. Single zircon Pb-evaporation analyses were performed on 23 grains from sample MAF-33 (southeastern portion of the pluton), but only three crystals were found to be suitable for age interpretation. These grains yielded a mean age of 2864±8 (MSWD= 4.3; Table 2 and Fig. 4a). On a concordia plot (Fig. 4b), U-Pb analyses of 21 zircons (LA-ICP-MS) from sample MAR-64 (north portion of the pluton; Fig. 1b) define a discordia line (MSWD= 0.7) with upper intercepts at 2875±8 Ma, which is estimated as the crystallization age of that sample. These ages are similar

Table 2 - Summary of zircon single-crystal evaporation Pb isotopic data from the Guarantã granite of the Guarantã suite.

Sample	Zircon	Evaporation Temperature (°C)	Number of Ratios	$^{204}Pb/^{206}Pb$	2σ	$^{208}Pb/^{206}Pb$	2σ	$^{207}Pb/^{206}Pb$	2σ	$^{207}Pb/^{206}Pb^{*}$	2σ	Age steep (Ma)	Age Crystal (Ma)	Mean age of sample (Ma)
	14	1500	36/36	0.000137	0.000005	0.16893	0.00215	0.20679	0.00025	0.20518	0.00026	2868±2		
MAF-33		1550	30/38	0.000367	0.000028	0.21771	0.00083	0.21005	0.00053	0.20588	0.00037	2874±3	2871±9	
	16	1550	30/30	0.000135	0.000004	0.03367	0.00028	0.20604	0.00026	0.20451	0.00027	2863±2	2863±3	
	21	1500	28/34	0.000360	0.000004	0.16982	0.00354	0.21010	0.00093	0.20561	0.00084	2872±7	2872±8	
	Mean age of crystals 14, 16 and 21													2864±8 (MSWD= 4.3)

$^{207}Pb/^{206}Pb^{*}$ - ratios corrected for commom Pb.

Table 3 - Summary of LA-ICP-MS U–Th–Pb results for zircons of the Guarantã granite, Trairão granodiorite and Rancho de Deus granite.

				Isotopic ratios								Ages						
Units	Samples	Zircon - Spot	Th/U	$^{206}Pb/^{204}Pb$	$^{207}Pb/^{206}Pb$	1s(%)	$^{207}Pb/^{235}U$	1s(%)	$^{206}Pb/^{238}U$	1s(%)	ρ	$^{207}Pb/^{206}Pb$	1s(%)	$^{207}Pb/^{235}U$	1s(%)	$^{206}Pb/^{238}U$	1s(%)	Conc (%)
GUARANTÃ GRANITE	MAR-64	3 - 1	0.070	274	0.2309	2.75	6.5395	5.2952	0.2054	4.53	0.81	3058	43.2	2051	45.6	1204	49.6	39.4
		2 - 1 *	0.060	544	0.1917	1.55	6.8280	3.1371	0.2584	2.73	0.80	2756	25.3	2089	27.4	1482	36.0	53.7
		13 - 1	0.056	4512	0.1938	0.89	8.3979	1.5338	0.3143	1.25	0.81	2774	14.5	2275	13.8	1762	19.2	63.5
		11 - 1 *	0.066	1257	0.1975	1.08	8.8534	4.4731	0.3251	4.34	0.93	2806	17.5	2323	40.0	1815	68.3	64.7
		14 - 1	0.064	5144	0.2050	1.78	9.5434	5.3367	0.3376	5.03	0.91	2867	28.6	2392	47.9	1875	81.3	65.4
		7 - 1	0.067	10662	0.1920	4.14	11.2463	3.0568	0.4249	2.79	0.84	2759	66.4	2544	28.1	2283	53.5	82.7
		8 - 1	0.145	32966	0.1969	2.05	11.9077	1.5996	0.4386	1.28	0.78	2801	33.1	2597	14.9	2344	25.1	83.7
		9 - 1 *	0.169	69939	0.2039	5.66	13.3102	4.0548	0.4734	3.94	0.98	2858	89.2	2702	37.6	2499	81.2	87.4
		6 - 1	0.056	17371	0.2075	2.82	13.5653	2.1195	0.4742	1.86	0.88	2886	45.1	2720	19.8	2502	38.6	86.7
		1 - 1 *	0.077	1449	0.2025	3.86	13.9409	2.8902	0.4992	2.54	0.84	2847	61.5	2746	27.0	2610	54.7	91.7
		21 - 1 *	0.007	31661	0.2027	3.40	14.8048	2.5574	0.5297	2.24	0.72	2848	54.4	2803	24.0	2740	49.9	96.2
		12 - 1	0.073	24205	0.2075	2.26	14.8093	1.7472	0.5176	1.44	0.82	2886	36.3	2803	16.5	2689	31.6	93.2
		20 - 1	0.065	67300	0.2000	2.75	15.0631	2.1960	0.5461	1.66	0.74	2827	44.2	2819	20.7	2809	37.7	99.4
		16 - 1	0.046	38500	0.2000	1.42	15.7431	1.9625	0.5709	1.35	0.67	2826	23.0	2861	18.6	2911	31.6	103.0
		18 - 1 *	0.131	40937	0.2050	1.88	15.8260	3.0991	0.5599	2.47	0.59	2866	30.2	2866	29.2	2866	56.8	100.0
		19 - 1	0.074	50466	0.2083	2.70	16.2525	2.1140	0.5659	1.68	0.78	2892	43.2	2892	20.0	2891	39.1	100.0
		10 - 1	0.283	7117	0.2163	4.49	16.1656	3.2661	0.5421	3.08	0.95	2953	70.7	2887	30.8	2792	69.5	94.6
		4 - 1 *	0.079	51001	0.2071	0.96	17.0023	2.1560	0.5955	1.93	0.90	2883	15.5	2935	20.5	3012	46.3	104.5
		15 - 1	0.048	32068	0.1971	1.29	17.0130	1.8558	0.6259	1.33	0.70	2803	20.9	2936	17.6	3133	33.0	111.8
		5 - 1 *	0.064	21364	0.2085	0.90	18.8011	2.1128	0.6541	1.91	0.91	2894	14.6	3032	20.2	3244	48.5	112.1

Table 3 – Continued

				Isotopic ratios									Ages						
Units	Samples	Zircon - Spot	Th/U	$^{206}Pb/^{204}Pb$	$^{207}Pb/^{206}Pb$	1s(%)	$^{207}Pb/^{235}U$	1s(%)	$^{206}Pb/^{238}U$	1s(%)	ρ	$^{207}Pb/^{206}Pb$	1s(%)	$^{207}Pb/^{235}U$	1s(%)	$^{206}Pb/^{238}U$	1s(%)	Conc (%)
TRAIRÃO GRANODIORITE	MAR-121	14 - 1	0.050	36472	0.1353	1.14	2.9128	2.4209	0.1562	2.13	0.87	2168	19.8	1385	18.1	935	18.5	43.2
		8 - 2	0.123	21213	0.1463	1.02	2.9746	1.6260	0.1475	1.27	0.77	2303	17.4	1401	12.3	887	10.5	38.5
		1 - 1	0.184	40040	0.1759	0.61	5.7933	1.2276	0.2388	1.06	0.86	2615	10.2	1945	10.6	1381	13.2	52.8
		7 - 2 *	0.187	31419	0.1751	0.62	5.9822	1.0876	0.2478	0.90	0.82	2607	10.2	1973	9.4	1427	11.5	54.7
		11 - 1 *	0.157	134017	0.1834	0.63	7.3246	1.3877	0.2897	1.23	0.89	2684	10.5	2152	12.3	1640	17.8	61.1
		18 - 1	0.130	242	0.2217	1.39	8.6390	2.3335	0.2827	1.87	0.79	2993	22.2	2301	21.0	1605	26.5	53.6
		12 - 2	0.097	117698	0.1840	1.18	9.2641	3.4848	0.3652	3.28	0.94	2689	19.4	2364	31.4	2007	56.3	74.6
		13 - 1	0.219	183321	0.1902	1.01	9.6013	2.2566	0.3661	2.02	0.89	2744	16.4	2397	20.5	2011	34.8	73.3
		19 - 1 *	0.135	31063	0.1941	1.60	10.1355	3.4746	0.3788	3.08	0.78	2777	26.0	2447	31.6	2071	54.4	74.6
		2 - 1	0.149	30	0.2211	0.61	12.7933	1.2848	0.4196	1.13	0.88	2989	9.8	2665	12.0	2259	21.5	75.6
		10 - 1 *	0.118	46122	0.2020	1.94	13.5398	1.4525	0.4862	1.29	0.89	2842	31.3	2718	13.6	2554	27.2	89.9
		4 - 2	0.088	848	0.1827	5.51	12.5311	3.9652	0.4975	3.77	0.94	2677	88.4	2645	36.6	2603	81.5	97.2
		8 - 1	0.173	22024	0.2181	1.16	14.1516	0.9459	0.4706	0.66	0.61	2967	18.5	2760	8.9	2486	13.7	83.8
		16 - 1 *	0.162	97567	0.2040	2.66	14.4275	2.0769	0.5129	1.67	0.79	2858	42.7	2778	19.5	2669	36.3	93.4
		7 - 1	0.242	24539	0.2230	0.70	14.5420	2.0315	0.4730	1.91	0.95	3002	11.2	2786	19.1	2497	39.3	83.1
		17 - 1	0.143	54153	0.2098	2.88	15.4478	2.2103	0.5341	1.85	0.83	2904	45.9	2843	20.9	2759	41.3	95.0
		4 - 1 *	0.224	110057	0.2062	3.43	16.3345	2.4572	0.5746	2.39	0.98	2876	54.6	2897	23.2	2927	55.9	101.8
		11 - 2	0.108	76607	0.2049	1.74	16.6365	1.3137	0.5888	1.14	0.87	2866	28.1	2914	12.5	2985	27.3	104.1
		15 - 1 *	0.124	46520	0.2069	4.06	17.5388	3.0270	0.6147	2.71	0.75	2882	64.5	2965	28.7	3089	66.2	107.2
		6 - 1	0.181	22846	0.2233	0.72	18.2877	1.5627	0.5940	1.39	0.90	3005	11.5	3005	14.9	3006	33.3	100.0
		9 - 1	0.225	57541	0.2232	0.82	18.6557	2.0064	0.6061	1.83	0.82	3004	13.0	3024	19.2	3054	44.4	101.7
		5 - 1	0.209	16754	0.2229	2.25	18.9225	1.7022	0.6158	1.48	0.87	3001	35.8	3038	16.3	3093	36.2	103.1
		12 - 1	0.357	75133	0.2206	11.23	21.9180	7.9616	0.7205	7.92	0.99	2985	170.1	3180	74.5	3498	210.3	117.2
		20 - 1	0.102	259177	0.2306	13.63	25.1192	14.8822	0.7900	5.98	0.22	3056	202.7	3313	135.8	3753	167.9	122.8
RANCHO DE DEUS GRANITE	MAR-132	7 - 2	0.158	198	0.1207	2.15	1.8010	2.7692	0.1083	1.74	0.61	1966	37.9	1046	17.9	663	11.0	33.7
		1 - 1 *	0.277	8258	0.1971	3.61	12.3812	2.7090	0.4555	2.37	0.88	2803	57.8	2634	25.1	2420	47.9	86.3
		1 - 2	0.237	529	0.2060	1.26	11.5482	1.9262	0.4066	1.46	0.75	2874	20.4	2568	17.8	2199	27.1	76.5
		2 - 1 *	0.242	6058	0.2010	3.93	12.8820	3.1676	0.4648	2.32	0.66	2835	62.7	2671	29.4	2461	47.4	86.8
		2 - 2 *	0.252	4380	0.1428	1.24	3.8761	1.8800	0.1968	1.41	0.74	2262	21.2	1609	15.1	1158	15.0	51.2
		3 - 1 *	0.384	9993	0.1967	2.17	11.3391	1.7324	0.4181	1.30	0.74	2799	35.0	2551	16.0	2252	24.7	80.5
		4 - 1 *	0.150	591	0.1715	1.43	6.5693	1.9291	0.2778	1.30	0.65	2572	23.7	2055	16.9	1580	18.1	61.4
		5 - 1 *	0.017	27098	0.1158	1.69	2.3901	3.1459	0.1497	2.66	0.76	1893	30.0	1240	22.3	899	22.2	47.5
		6 - 1 *	0.271	1640	0.1708	1.05	6.5771	2.3153	0.2793	2.07	0.89	2566	17.4	2056	20.2	1588	29.0	61.9
		6 - 2	0.300	112	0.2014	1.01	6.0559	2.3206	0.2181	2.09	0.90	2838	16.4	1984	20.0	1272	24.1	44.8
		8 - 1 *	0.276	858	0.1966	6.03	13.5287	4.5217	0.4990	3.93	0.86	2799	95.4	2717	41.9	2609	85.0	93.2
		9 - 1 *	0.279	257133	0.2058	1.50	14.2649	1.2584	0.5026	0.81	0.56	2873	24.1	2767	11.9	2625	17.4	91.4
		10 - 1 *	0.261	12986	0.2118	1.23	16.8988	5.1901	0.5787	5.04	0.97	2919	19.8	2929	48.6	2943	118.1	100.8
		10 - 2	0.305	271	0.2264	3.35	9.3283	4.0589	0.2989	2.29	0.52	3027	52.7	2371	36.6	1686	33.9	55.7
		11 - 1	0.014	25530	0.2194	1.00	17.7630	1.8577	0.5872	1.57	0.84	2976	16.0	2977	17.7	2978	37.2	100.1
		11 - 2	0.201	365	0.1231	3.19	3.4280	4.7480	0.2020	3.52	0.74	2001	55.6	1511	36.7	1186	38.0	59.3
		12 - 1	0.325	825	0.1931	3.08	12.1492	2.4211	0.4564	1.87	0.80	2768	49.6	2616	22.5	2424	38.3	87.5
		13 - 1	0.158	599	0.1856	2.71	3.4322	5.7845	0.1341	5.11	0.85	2704	44.0	1512	44.5	811	38.8	30.0
		8 - 2 *	0.265	833	0.1905	2.95	10.5508	2.2728	0.4018	1.85	0.84	2746	47.7	2484	20.9	2177	34.7	79.3
		4 - 2	0.143	10622	0.1381	1.65	3.1826	2.6517	0.1672	2.08	0.78	2203	28.3	1453	20.3	997	19.2	45.2
		12 - 2	0.201	4787	0.1907	1.49	9.0235	3.0466	0.3432	2.66	0.87	2748	24.2	2340	27.5	1902	43.6	69.2
		7 - 1	0.159	180	0.1203	2.74	1.8026	3.8384	0.1087	2.69	0.70	1960	48.1	1046	24.8	665	17.0	33.9

Conc (%) denotes degree of concordance. For each studied rock, analyses labelled * were included in the age calculation, whereas others were omitted.

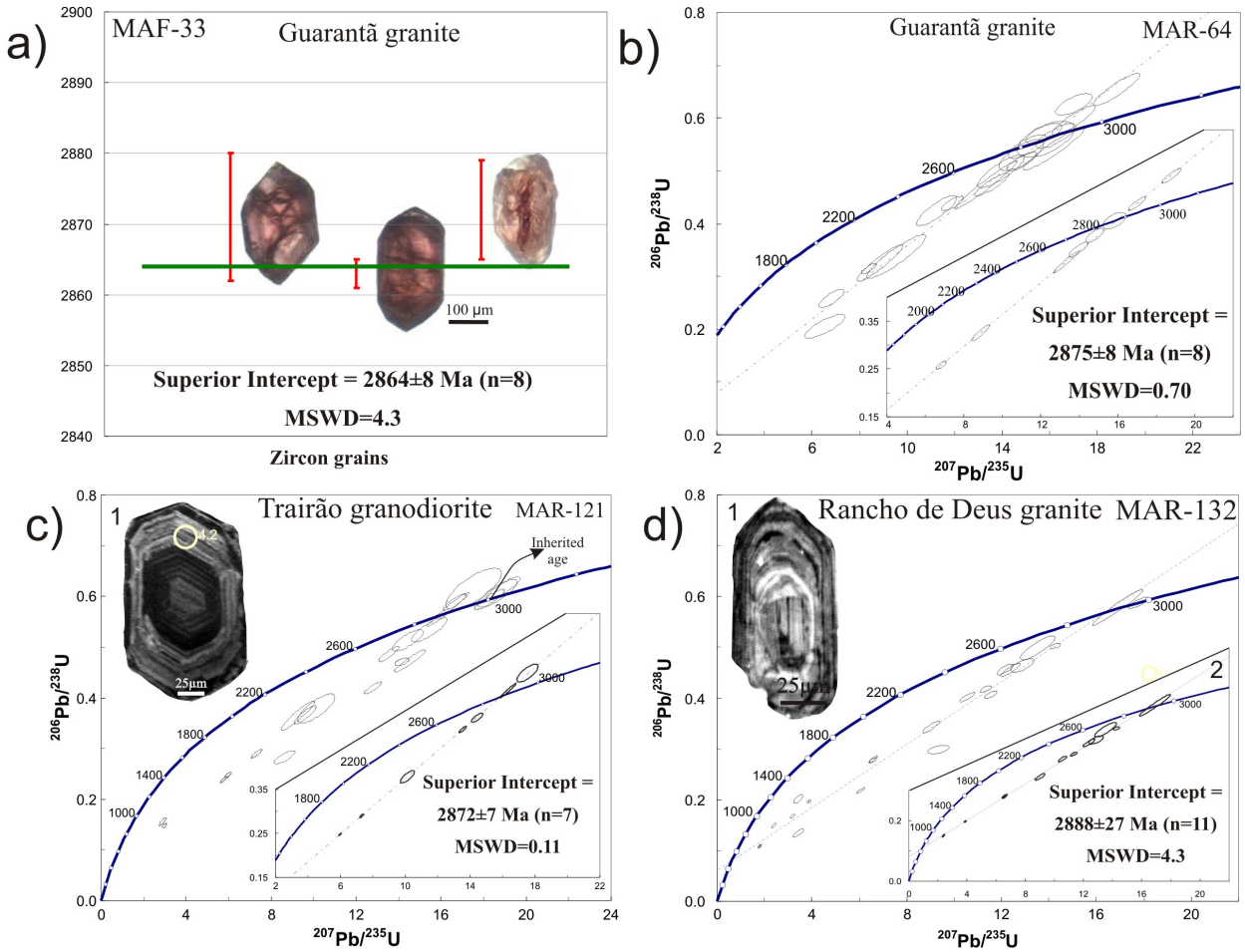

Figure 4 - Diagrams for the samples dated from the Guarantã suite. a) Single zircon Pb-evaporation age diagram for the sample MAF-33 (Guarantã pluton). The vertical red bar represents the error for each zircon grain and horizontal thick green bar corresponds to the mean age for the sample; b) U–Pb concordia diagram for zircons from sample MAR-64 (Guarantã pluton); c) U-Pb Concordia diagram for zircons showing discordia line for zircons from sample MAR-121 (Trairão granodiorite); d) U-Pb Concordia diagram for zircons analytical results for sample MAR-132 (Rancho de Deus granite). The Inserts 4c1 and 4d1 show representative cathodoluminescence images of zircon grains with well-developed oscillatory zoning, a typical magmatic feature. The Inserts in figure 4b, 4c2 and 4d2 show the analyses that were included in the age calculation.

to that of 2870 ±5 Ma obtained by the Pb-Pb evaporation method in zircon in a granite exposed immediately to the south of Pau D'Arco town (Fig. 1b; Althoff et al., 2000), correlated in the present paper with the Guarantã granite.

5.2.1.2 – Trairão Granodiorite: sample MAR-121

The zircon crystals from sample MAR-121 are euhedral and prismatic in shape, with 70–150 μm in length and length/width ratios of about 2 to 4. Cathodoluminescence images show well-developed oscillatory zoning (insert in Fig. 4c), which, together with the high Th/U ratios obtained on U–Pb LA-ICP-MS analyses (usually >0.1; Table 3), indicate a magmatic origin for the zircon. A total of 24 analyses were made on 20 zircon grains from sample MAR-121 (Trairão Granodiorite), and 7 of the 24 spots define a discordia chord with the upper intercepts at 2872±7 Ma (MSWD=0.1; Fig. 4c). The mentioned age is quite similar to the ages obtained for the Guarantã Granite and is interpreted as the crystallization age of that sample.

A granitic stock composed of rocks geochemically similar to those of the Guarantã suite, located along the road to Floresta town (Fig. 1b), yielded a Pb-evaporation age on zircon of 2930±19 Ma (Althoff et al. 2000, Table 1), suggesting that it could be older than the Guarantã suite. However, this age can reflect the presence of inherited zircons in the analyzed sample and more detailed geochronological studies are necessary to define if that granitic pluton is really older than the Guarantã suite or if it can be embraced in that suite.

5.3. Granites associated with sanukitoid suites (Rancho de Deus pluton)

The sample MAR-132 is localized in the south portion of the Rancho de Deus pluton (Fig. 1b) and was dated only by the U–Pb LA-ICP-MS on zircon method. The dominant zircon population of the dated sample is comprised of brownish elongated prismatic crystals, with length ranging from 100 to 200μm and euhedral to subhedral shape. Under cathodoluminescence, these crystals show well-developed oscillatory zoning (insert in Fig. 4d), which, together with their high Th/U ratios (generally >0.2; cf. Table 3), indicates crystallization from a magma. Almost all of the twenty-two spot analyses performed on 13 zircons from this sample plot below the concordia curve. However, eleven spots define a discordant line with an upper intercept at 2888 ±

27 Ma (MSWD = 4.3; Fig. 4d). This age is poorly constrained but it is superposed within errors with the ages obtained in the different occurrences of sanukitoid rocks of the Rio Maria terrane (ca. 2.87 Ga; cf. Rio Maria granodiorite and Parazônia quartz diorite, Fig. 2; Oliveira et al., 2009) and is interpreted as the probable crystallization age of the Rancho de Deus granite.

6. Geochemistry

Representative analyses of the three types of Archean granites distinguished in the RMGGT are given in Table 4 and the analytical procedures are presented in the Appendix A. The geochemistry of the Guarantã suite and of the Rancho de Deus granite and that of the Grotão granodiorite were firstly discussed by Dias (2009) and Guimarães et al. (b, submitted), respectively.

6.1. Potassic leucogranites

Overall, potassic leucogranites show a narrow range of chemical composition (Table 4), with SiO_2 varying from 71 to 77%. TiO_2, Al_2O_3, Fe_2O_{3t}, CaO, MgO, and P_2O_5 are all negatively correlated with SiO_2, generally forming poorly defined trends (Fig. 5). A remarkable characteristic of these rocks is their high–K_2O (generally > 4.5 wt.%), associated with low MgO (normally <0.3 wt.%; #Mg usually also <0.3), moderate to high Al_2O_3 (>13 wt.%; the Mata Surrão samples tend to present higher Al_2O_3 contents compared to the Xinguara ones), and moderate CaO (mean = 1.2 wt.%), and Na_2O (mean = 3.5 wt.%) contents. The K_2O/Na_2O ratios are usually between 1 and 2 (Fig. 5h) and the FeO/FeO+MgO ratios are normally higher than 0.8 and increase with SiO_2 (Fig. 5i). These granites vary from metaluminous to peraluminous (Fig. 6a) and fall in the high-K field of calc-alkaline series (Fig. 5g; fields of Peccerillo and Taylor, 1976). In the K–Na–Ca triangular diagram (Barker and Arth, 1976; Martin, 1994) these granites follow the calc-alkaline trend showing enrichment in potassium (Fig. 6b). They plot in the granite field in the Ab-An-Or normative diagram (Fig. 6c), as well as in the P-Q (Debon & Le Fort, 1988) and R1-R2 diagrams (De la Roche et al. 1980) (Figs. 6d, e, respectively). The Mata Surrão and Xinguara granites overlap in SiO_2 range and are quite similar in their geochemical characteristics. However, the rocks of the Mata Surrão granite are a little enriched in Al_2O_3, #Mg,

Table 4 - Representative chemical compositions of the different Archean granite suites of the Rio Maria granite-greenstone terrane.

	Leucogranodiorite-granite group																		
Element	**Guarantã Suite**																**Grotão Granodiorite**		
Sample	MAR-146 (1)	MAF-33 (1)	AL-86 (2)	MAR-123 (1)	MAR-38A (3)	MAR-121 (1)	MAR-114 (1)	MAF-58 (3)	MAR-50A (3)	MAR-164A (1)	MAR-93A (1)	MAR-101A (3)	MAR-97A (1)	MAR-64A (1)	MASF- 1 (4)	MASF- 7 (4)	FMR-49 (5)	FMR-59 (5)	FMR-105 (5)
SiO_2	68.20	68.86	69.44	70.08	70.12	70.32	70.89	71.13	71.36	71.71	71.92	72.07	72.27	72.39	72.73	73.14	67.57	67.89	71.02
TiO_2	0.40	0.45	0.21	0.27	0.18	0.21	0.25	0.22	0.20	0.17	0.21	0.15	0.17	0.19	0.17	0.09	0.56	0.50	0.25
Al_2O_3	15.30	15.14	15.42	15.40	15.56	15.66	14.60	15.08	15.39	15.22	15.52	15.00	14.99	14.93	14.59	14.68	15.64	15.85	15.64
$Fe_2O_{3(t)}$	2.97	3.21	2.25	1.95	1.25	1.71	2.10	1.66	1.66	1.26	1.40	1.14	1.40	1.50	1.35	0.90	3.20	2.82	1.88
MnO	0.03	0.04	0.02	0.03	0.02	0.02	0.03	0.02	0.03	0.02	0.02	0.02	0.02	0.02	0.02	0.01	0.03	0.03	0.02
MgO	1.38	1.03	0.70	0.77	0.39	0.59	0.82	0.58	0.54	0.35	0.36	0.29	0.42	0.45	0.37	0.17	1.15	1.06	0.59
CaO	3.00	2.81	1.80	2.31	1.74	2.09	2.03	2.04	1.97	1.90	2.32	1.39	1.97	2.05	1.54	1.18	3.27	3.04	2.57
Na_2O	4.91	4.44	4.97	4.87	4.48	4.98	4.56	4.72	5.17	5.02	5.00	4.55	4.86	4.92	4.27	4.64	4.72	4.43	4.82
K_2O	2.41	2.68	3.74	2.91	4.86	3.31	3.44	3.05	2.51	3.24	2.73	4.51	2.98	2.64	3.72	4.29	2.54	3.18	2.54
P_2O_5	0.16	0.16	0.19	0.10	0.08	0.08	0.10	0.07	0.08	0.06	0.05	0.06	0.06	0.07	0.07	0.05	0.18	0.15	0.09
LOI	1.00	1.10	0.83	1.00	1.00	0.70	1.00	1.20	0.90	0.80	0.40	0.60	0.70	0.70	0.90	0.70	0.90	0.80	0.40
Total	99.76	99.92	99.57	99.69	99.68	99.67	99.82	99.77	99.81	99.75	99.93	99.78	99.84	99.86	99.73	99.85	99.76	99.75	99.82
Ba	1203	1173	1211	1170	2230	1436	1218	1578	964	1020	918	1363	1247	1066	1067	1297	1088	1020	851
Sr	919	554	861	737	767	725	673	739	643	534	484	571	696	650	459	396	599	417	539
Rb	74	78	126	84	173	78	128	60	59	81	62	170	64	70	94	140	78	117	57
Zr	137	132	168	112	98	92	104	122	91	82	82	101	90	96	84	75	146	139	118
Y	9	13	9	12	11	3	41	7	8	6	12	7	5	6	3	5	4	8	6
Hf	4	4	n.d	4	3	3	4	3	3	3	3	3	3	3	3	3	4	4	3
Nb	6	6	11	6	6	4	6	5	4	6	4	5	4	7	3	3	5	8	3
Ta	2	2	n.d	2	1	2	2	n.d	n.d	2	2	n.d	2	2	1	1	1	1	1
Ni	19	8	n.d	11	5	8	12	6	7	5	3	3	7	8	3	1	7	9	4
Cu	18	54	n.d	13	4	10	68	2	4	6	10	3	54	27	10	4			
Th	5	5	n.d	5	3	5	8	3	3	3	4	8	2	5	13	12	7	12	4
Zn	52	47	n.d	40	29	28	43	36	41	31	38	31	36	46	18	16			
Ga	20	20	17	19	19	19	20	18	21	20	16	20	21	21	19	19	20	21	19
La	31.60	56.80	49.58	32.10	15.90	13.00	27.50	18.10	15.70	14.00	28.00	18.10	15.70	18.00	21.60	13.10	27.40	31.90	16.50
Ce	63.80	80.70	106.90	47.60	34.30	29.50	44.20	34.20	29.80	26.10	46.40	46.80	28.70	32.90	36.40	29.60	58.70	62.80	26.30
Pr	7.18	10.07	n.d	6.84	4.78	2.51	5.73	4.13	3.71	2.88	5.26	4.04	3.16	3.54	4.14	2.77	6.70	6.97	3.58
Nd	27.40	36.00	36.58	23.90	18.30	8.10	20.00	16.30	12.70	9.70	16.90	15.80	10.00	12.30	13.20	9.30	24.70	27.00	14.90
Sm	4.50	4.90	5.04	4.30	3.75	1.30	4.00	2.70	2.44	2.00	2.80	2.33	1.90	1.90	1.80	1.50	3.83	3.74	2.32
Eu	1.04	1.22	0.72	1.11	0.83	0.38	1.07	0.62	0.67	0.40	0.72	0.61	0.50	0.53	0.44	0.45	0.96	0.83	0.63
Gd	2.58	2.98	2.63	2.90	2.69	0.71	3.56	1.79	1.85	1.17	1.83	1.61	1.06	1.29	0.99	0.88	2.70	2.91	1.86
Tb	0.38	0.44	n.d	0.39	0.38	0.12	0.60	0.26	0.27	0.17	0.30	0.22	0.25	0.25	0.12	0.18	0.29	0.37	0.22
Dy	1.78	2.07	1.24	1.82	2.08	0.51	3.87	1.28	1.34	0.78	1.83	1.16	0.92	0.95	0.57	0.88	1.32	1.83	1.18
Ho	0.26	0.38	0.22	0.29	0.37	0.13	0.88	0.23	0.25	0.18	0.35	0.21	0.16	0.16	0.10	0.16	0.16	0.30	0.18
Er	0.81	0.92	0.40	0.89	1.11	0.36	3.17	0.60	0.69	0.52	1.14	0.59	0.52	0.60	0.27	0.50	0.37	0.72	0.50
Tm	0.14	0.15	n.d	0.14	0.19	0.08	0.47	0.09	0.11	0.08	0.18	0.09	0.06	0.08	0.05	0.09	0.05	0.10	0.07
Yb	0.74	0.88	0.25	0.69	1.14	0.43	2.53	0.52	0.57	0.63	1.00	0.58	0.26	0.63	0.29	0.48	0.32	0.60	0.38
Lu	0.10	0.13	0.04	0.11	0.15	0.06	0.47	0.07	0.08	0.07	0.14	0.09	0.07	0.08	0.06	0.08	0.03	0.08	0.07
A/CNK	0.95	0.99	1.00	1.00	0.99	1.01	0.98	1.02	1.04	1.00	1.01	1.01	1.01	1.02	1.05	1.02	0.95	0.97	1.02
K_2O/Na_2O	0.49	0.60	0.75	0.60	1.08	0.66	0.75	0.65	0.49	0.65	0.55	0.99	0.61	0.54	0.87	0.92	0.54	0.72	0.53
#Mg	0.48	0.39	0.38	0.44	0.38	0.41	0.44	0.41	0.39	0.36	0.34	0.34	0.37	0.37	0.35	0.27	0.42	0.43	0.38
Rb/Sr	0.54	0.59	0.75	0.74	1.76	0.85	1.23	0.49	0.65	0.99	0.76	1.69	0.71	0.74	1.12	1.87	0.54	0.84	0.49
$(La/Yb)_N$	30.63	46.30	142.25	33.37	10.00	21.69	7.80	24.97	19.76	15.94	20.08	22.38	43.31	20.49	53.43	19.58	61.42	38.14	31.15
Eu/Eu*	0.85	0.90	0.54	0.91	0.76	1.10	0.85	0.81	0.93	0.74	0.91	0.91	0.98	0.98	0.91	1.10	0.87	0.74	0.90

Table 4 – Continued

	Potassic leucogranites																Granites associeted with sanukitoid suites					
Element	Xinguara Granite								Mata Surrão Granite								Rancho de Deus Granite					
Sample	AL-2D (2)	AL-95(2)	ALF-266(2)	Al-152(2)	AL-89(2)	AL-65A(2)	AL-24(2)	AL-56B(2)	KY-31B(1)	KY-24B(1)	KY-89A(1)	KY-100C(1)	KY-89E(1)	KZ-7C(1)	KY-104(1)	KY-75(1)	MAR-144(1)	MAR-132(1)	MAR-129(1)	MAR-126(1)	MAF-24(1)	MAF-22(1)
SiO_2	72.53	72.54	72.90	73.49	73.69	73.99	74.80	75.39	72.24	72.39	72.71	73.12	73.25	73.37	73.42	73.60	67.74	69.82	71.93	72.36	73.09	73.42
TiO_2	0.14	0.12	0.10	0.21	0.12	0.15	0.11	0.08	0.18	0.14	0.19	0.09	0.13	0.10	0.11	0.11	0.29	0.25	0.20	0.20	0.28	0.28
Al_2O_3	13.68	13.87	14.50	13.69	13.50	12.84	12.79	12.87	14.41	14.57	14.46	14.55	14.23	14.00	14.34	14.22	15.59	14.62	14.45	14.28	14.18	13.86
$Fe_2O_{3(t)}$	1.88	1.88	1.40	2.27	1.40	1.84	1.42	1.32	1.74	1.53	1.61	1.19	1.21	1.37	1.23	1.27	2.87	2.55	1.85	1.66	1.92	1.90
MnO	0.01	0.01	0.03	0.02	0.02	0.02	0.01	0.01	0.03	0.04	0.04	0.02	0.03	0.03	0.02	0.02	0.04	0.04	0.03	0.02	0.04	0.04
MgO	0.25	0.25	0.23	0.60	0.33	0.22	0.12	0.10	0.37	0.35	0.34	0.21	0.25	0.26	0.23	0.25	1.13	0.95	0.65	0.52	0.30	0.29
CaO	1.15	1.23	1.30	2.23	1.35	0.93	0.93	0.99	1.35	1.41	1.39	1.27	1.18	1.29	1.47	1.45	2.47	2.02	1.57	1.15	0.92	1.20
Na_2O	3.29	3.17	3.70	4.20	3.77	2.93	3.60	3.56	3.66	3.97	4.10	3.80	3.81	3.56	3.77	3.90	4.18	4.37	4.11	4.05	3.99	3.97
K_2O	6.29	6.57	4.60	3.00	4.86	6.41	5.24	5.01	5.14	4.63	4.22	5.15	5.16	5.00	4.65	4.47	4.14	4.07	4.44	4.65	4.89	4.64
P_2O_5	0.16	0.16	0.05	0.17	0.16	0.16	0.14	0.14	0.07	0.04	0.07	0.02	0.07	0.04	0.03	0.03	0.13	0.12	0.08	0.07	0.05	0.05
LOI	0.51	0.60	0.46	0.40	0.42	0.31	0.40	0.32	0.60	0.70	0.70	0.40	0.50	0.80	0.60	0.50	1.10	0.90	0.50	0.93	0.40	0.40
Total	99.89	100.40	99.27	100.28	99.62	99.80	99.56	99.79	99.79	99.77	99.83	99.82	99.82	99.82	99.87	99.82	99.68	99.71	99.81	99.89	100.06	100.05
Ba	871	950	1024	589	851	806	920	484	738	477	516	552	603	630	507	503	1554	1392	976	722	1214	1182
Sr	300	231	363	326	243	192	289	174	176	229	106	179	112	216	173	164	576	528	374	281	139	146
Rb	198	175	190	109	181	211	152	181	244	183	261	182	266	190	206	221	132	167	186	176	112	121
Zr	256	198	363	140	206	216	184	106	165	101	182	94	119	120	94	111	163	128	116	95	210	239
Y	11	4	16	4	3	11	6	7	8	43	12	30	14	8	11	7	13	9	6	14	15	17
Hf	n.d	n.d	n.d	n.d	n.d	n.d	n.d	n.d	5	4	6	3	4	4	3	4	5	4	4	4	6	7
Nb	5	4	5	8	8	9	8	4	6	8	8	4	7	4	5	6	6	8	7	5	9	11
Ta	n.d	n.d	n.d	n.d	n.d	n.d	n.d	n.d	n.d	1	1	1	1	n.d	1	n.d	2	2	3	2	3	3
Ni	n.d	n.d	n.d	n.d	n.d	n.d	n.d	n.d	4	3	3	2	3	3	3	3	12	13	8	6	2	2
Cu	n.d	n.d	n.d	n.d	n.d	n.d	n.d	n.d	3	9	2	2	2	2	2	2	19	16	8	32	6	4
Th	94	90	10	78	78	77	78	43	37	71	43	32	38	48	35	59	10	19	17	15	17	22
Zn	n.d	n.d	n.d	n.d	n.d	n.d	n.d	n.d	36	30	42	24	28	25	23	27	34	38	26	23	19	19
Ga	11	10	22	14	13	10	10	12	18	17	20	16	18	16	16	17	19	19	17	18	15	17
La	68.42	19.98	10.07	36.99	47.47	66.00	51.36	36.16	48.60	61.30	51.60	68.70	59.10	34.70	24.00	35.90	42.40	42.60	35.80	53.50	58.90	57.30
Ce	106.90	39.45	18.66	89.23	97.23	125.10	110.40	59.12	85.40	115.40	95.70	95.80	108.80	72.60	43.10	64.70	75.00	73.80	58.20	65.70	111.30	107.50
Pr									8.29	14.42	8.79	12.04	11.10	7.87	5.09	6.57	7.69	7.29	5.59	7.81	11.54	11.00
Nd	41.14	11.88	5.51	30.07	43.20	39.05	45.75	25.00	26.70	54.00	27.60	42.90	36.60	28.80	17.40	22.30	28.10	23.10	14.50	22.90	39.00	38.00
Sm	6.64	1.88	1.02	6.32	5.80	6.56	6.81	4.83	4.21	12.10	4.26	7.58	6.39	4.97	3.23	3.65	4.60	3.70	2.10	3.20	5.50	5.40
Eu	0.59	0.25	0.22	0.60	0.44	0.62	0.49	0.45	0.53	1.33	0.46	1.03	0.44	0.51	0.49	0.47	0.87	0.75	0.50	0.73	0.85	1.01
Gd	3.23	0.97	0.69	2.47	1.77	3.94	3.22	1.99	2.81	10.48	2.77	6.47	4.35	2.95	2.23	2.26	3.19	1.83	1.14	2.66	3.22	3.41
Tb									0.40	1.85	0.44	0.95	0.65	0.41	0.39	0.33	0.49	0.31	0.14	0.37	0.52	0.57
Dy	1.43	0.39	0.30	1.29	0.76	1.68	1.25	1.65	1.75	9.57	1.89	4.62	2.75	1.74	1.86	1.60	1.92	1.35	0.91	1.67	3.01	3.13
Ho	0.24	0.05	0.05	0.25	0.15	0.25	0.19	0.34	0.28	1.71	0.37	0.87	0.49	0.28	0.37	0.25	0.42	0.30	0.15	0.29	0.52	0.57
Er	0.57	0.14	0.11	0.64	0.45	0.65	0.38	1.02	0.63	4.38	1.00	2.25	1.25	0.70	0.98	0.66	1.11	0.73	0.49	0.91	1.36	1.62
Tm									0.11	0.66	0.15	0.33	0.20	0.12	0.16	0.10	0.17	0.16	0.10	0.14	0.17	0.25
Yb	0.42	0.15	0.11	0.55	0.43	0.39	0.24	1.09	0.59	3.89	0.91	1.70	1.14	0.70	0.91	0.60	0.89	0.72	0.59	0.65	1.14	1.45
Lu	0.10	0.05	0.04	0.11	0.08	0.08	0.04	0.14	0.10	0.49	0.15	0.24	0.17	0.11	0.15	0.09	0.19	0.15	0.11	0.15	0.19	0.22
A/CNK	0.96	0.95	1.08	0.96	0.97	0.95	0.96	0.98	1.03	1.03	1.04	1.03	1.02	1.03	1.03	1.02	0.98	0.96	1.00	1.04	1.05	1.01
K_2O/Na_2O	1.91	2.07	1.24	0.71	1.29	2.19	1.46	1.41	1.40	1.17	1.03	1.36	1.35	1.40	1.23	1.15	0.99	0.93	1.08	1.15	1.23	1.17
#Mg	0.21	0.21	0.25	0.34	0.32	0.19	0.14	0.13	0.30	0.31	0.30	0.26	0.29	0.27	0.27	0.28	0.44	0.43	0.41	0.38	0.24	0.23
Rb/Sr	0.77	0.88	0.52	0.78	0.88	0.98	0.83	1.71	1.48	1.81	1.43	1.94	2.24	1.59	2.20	1.99	0.81	1.31	1.60	1.85	0.53	0.51
$(La/Yb)_N$	117.41	98.84	68.79	48.24	79.19	120.16	153.50	23.80	59.09	11.30	40.67	28.99	37.19	35.56	18.92	42.92	34.17	42.44	43.52	59.04	37.06	28.35
Eu/Eu*	0.35	0.51	0.76	0.39	0.33	0.34	0.28	0.38	0.44	0.35	0.38	0.44	0.24	0.38	0.53	0.46	0.66	0.78	0.89	0.74	0.57	0.67

Data Source: (1) This work; (2) Leite (2001); (3) Dias (2009); (4) Dias (2007); (5) Guimarães (2009). Fe2O3 t=total iron recalculated as Fe2O3.LOI=loss on ignition.A/CNK: Molecular ratio (Al/Ca+Na+K).
Mg# molecular ratio Mg/(Mg + Fe). LaN, YbN, SmN, GdN, EuN:Normalized REE value (Evesen et al 1978).Eu/Eu*=europium anomaly calculated as [Eu/(Eu*)]=[(EuN)/((SmN+GdN)/2)].
nd: not determinated.

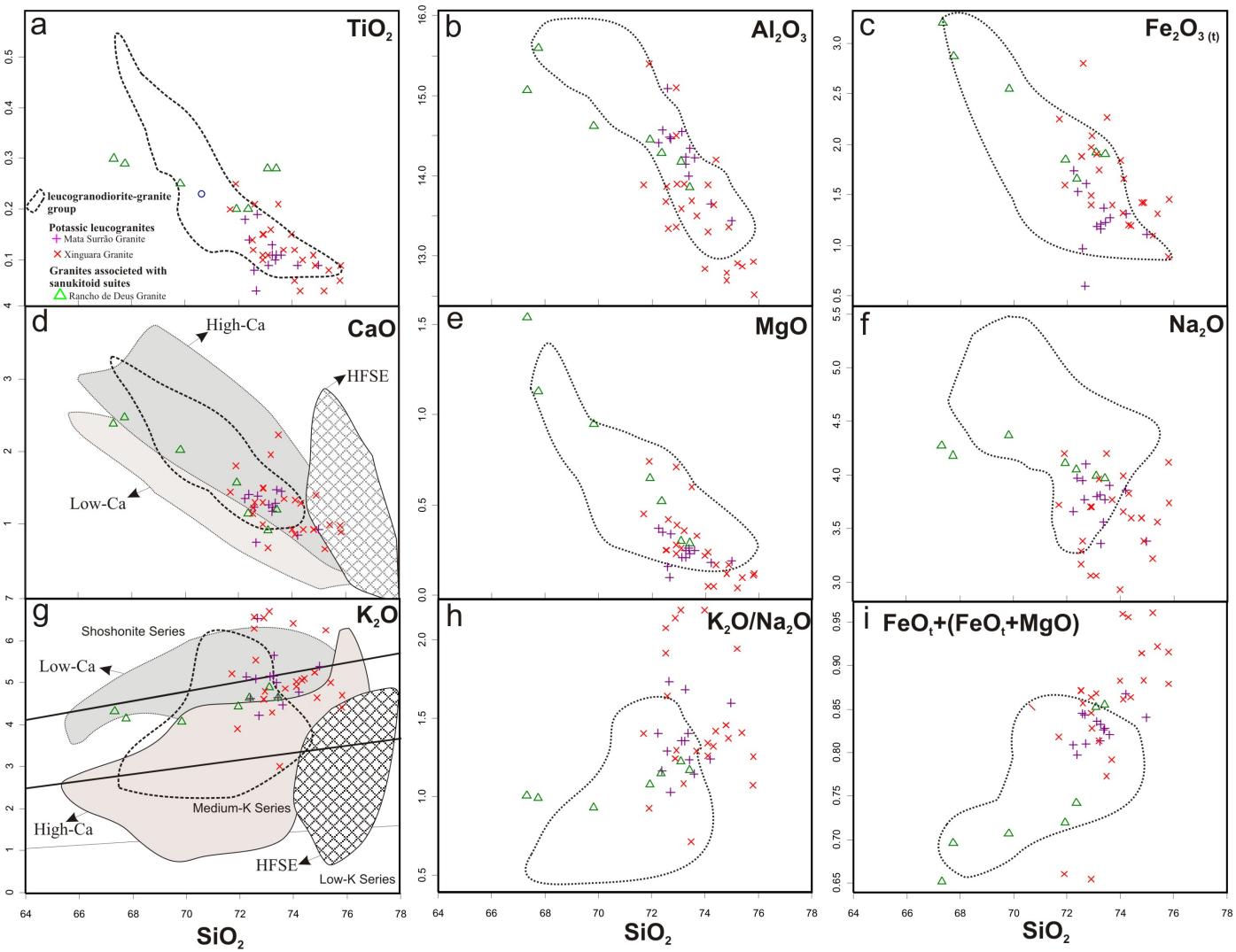

Figure 5 - Harker diagrams for the Archean granite suites of the Rio Maria granite-greenstone terrane. The fields for High-Ca, Low-Ca and High-HFSE granites of Yilgarn craton (Champion and Sheraton, 1997) are plotted in d and g for comparison. The fields in g are according to Peccerillo and Taylor (1976).

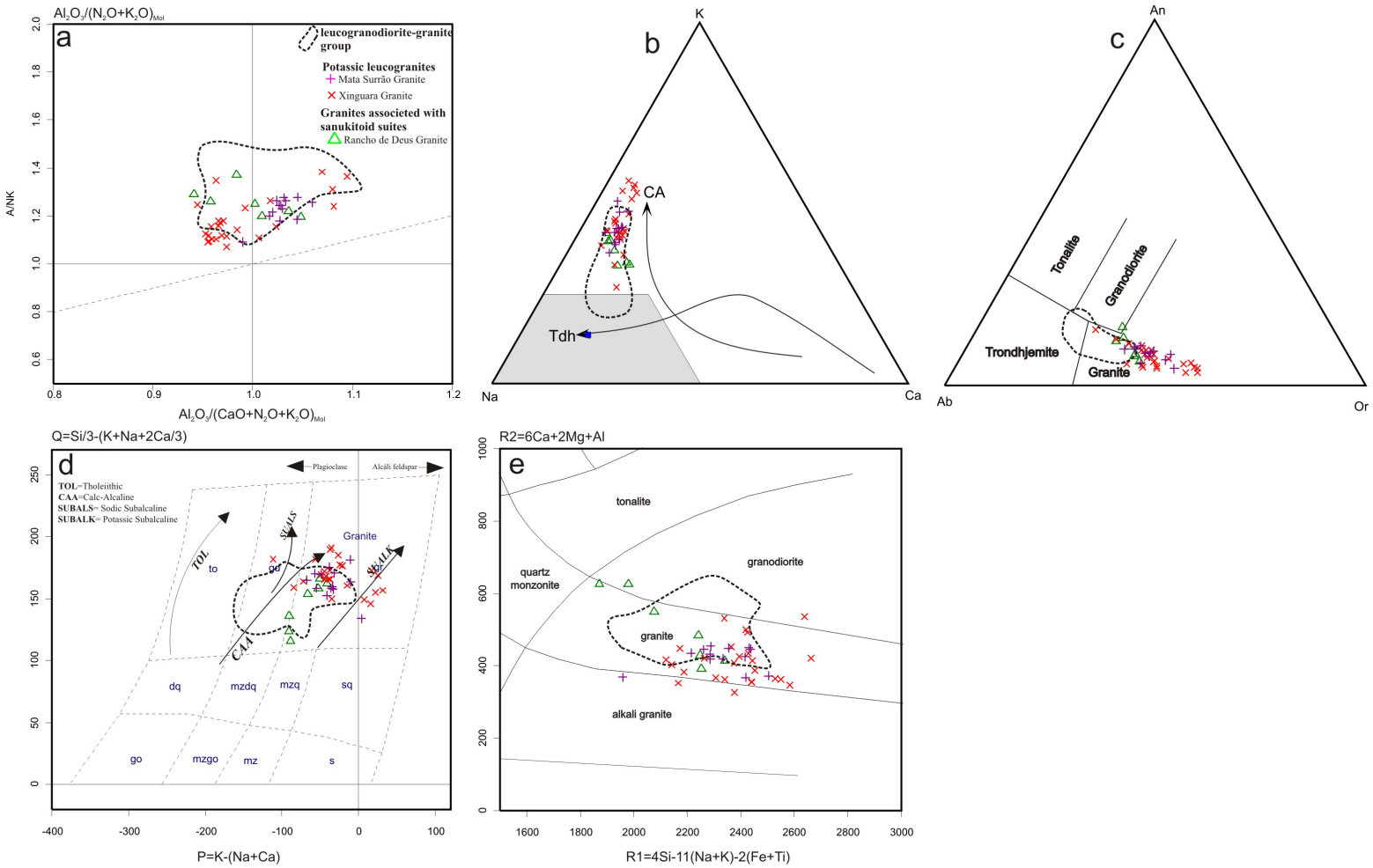

Figure 6 - Geochemical plot showing the distribuition of the samples of the Archean granite suites of the Rio Maria granite-greenstone terrane. (a) Al_2O_3/ (CaO + Na_2O + K_2O)]mol vs. [Al_2O_3/(K_2O + Na_2O)]mol diagram (Shand, 1950); (b) K–Na–Ca plots. Trends for calc-alkaline (CA) and trondhjemite (Tdh) series as defined by Barker and Arth (1976). Grey: field of Archaean TTG (Martin, 1995); (c) Normative feldspar triangle (O'Connor, 1965) with fields from Barker (1979); (d) P-Q diagram from Debon and Le fort (1988); (e) R1-R2 plot. R1-R2 are cationic parametrs of de la Roche (1980).

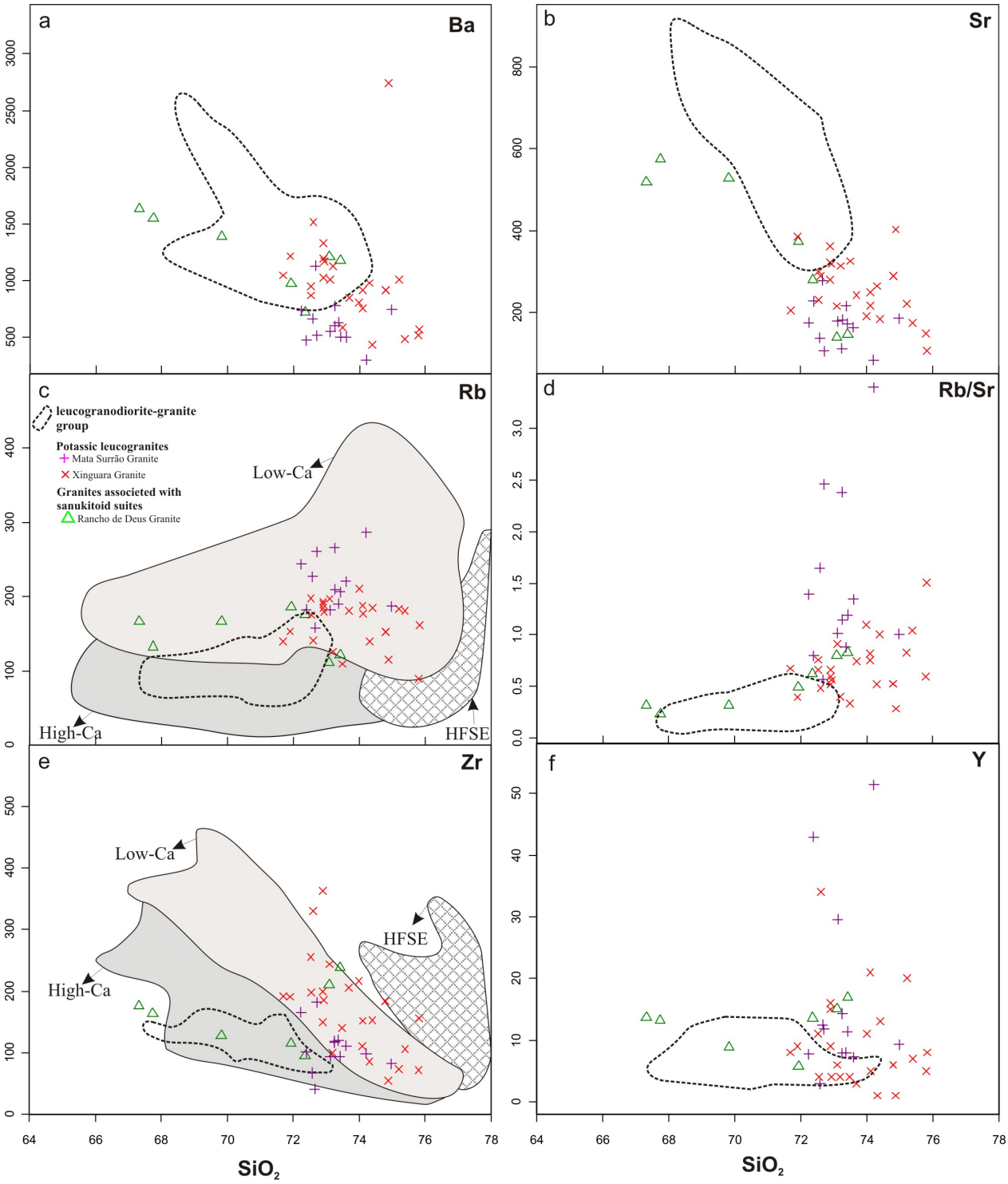

Figure 7 - Harker plots for selected trace elements and elemental ratios for Archean granite suites. The fields for High-Ca, Low-Ca and High-HFSE granites of Yilgarn craton (Champion and Sheraton, 1997) are plotted in c and e for comparison.

and Rb, whereas those of the Xinguara granite are enriched in Fe_2O_{3t}, Ba, and Sr compared to the Mata Surrão granite (Figs. 5 and 7).

The high-K_2O contents of these granites could suggest an alkaline affinity. However, they have extremely low Y, Nb, and Yb, and only moderate Zr, Ti, and Rb contents (Table 4; Figs. 7c, e, f), which are not compatible with an alkaline signature for their magmas. The contents of Sr and Ba are also moderate, and both behave as compatible elements (Figs. 7 a, b). The REE patterns (Figs. 8 a, b) show enrichment in light REE and strong [Xinguara samples, $(La/ Yb)_N$ ratios mostly in the range 23 to 120] or moderate [Mata Surrão samples, $(La/ Yb)_N$ ratios in the range 5 to 60] fractionation of the heavy REE, moderate to pronounced negative Eu anomalies (Eu/Eu* varying between 0.23 and 0.79 for both granites). A concave shape of the HREE patterns is observed only in the Xinguara samples (Figs. 8a, b), suggesting that hornblende was probably an important fractionating phase during the evolution of this granite and that it was little relevant for the Mata Surrão magma fractionation.

6.2. Leucogranodiorite-granite group (LGdG)

The rocks of this group have SiO_2 contents in the range between 68.2 and 75.8 wt. %. Except for K_2O, the other oxides are negatively correlated with SiO_2 and show scattered trends (Fig. 5). These features are observed in the suite as a whole, but also in individual plutons of the Guarantã suite (Dias, 2009) or in the Grotão granodiorite (Guimarães et al. b, submitted). The Al_2O_3 and Na_2O contents are high compared with the other Archean granite groups (Figs. 5b, f) and range respectively from 13.0-16.0 wt.% (usually >14 wt.%), and 3.3 to 5.4 wt.%. MgO (0.2-1.3 wt.%; mean=0.45 wt.%), and Mg# values (mostly 0.15-0.48; mean= 0.36) are moderate to low (Fig. 5e). This granite group show moderate K_2O/Na_2O values (normally between 0.5-1; Fig. 5h and Table 5) and FeO/FeO+MgO ratios usually lower than 0.8 (Fig. 5i and Table 4).

The granitoids of this group are metaluminous to peraluminous, but rocks with excess of alumina to alkalis are dominant (Fig. 6a). They follow the calc-alkaline trend in the K–Na–Ca diagram (Fig. 6b) and correspond to medium to high-K calc-alkaline rocks (Fig. 5g; fields of Peccerillo and Taylor, 1976). The analyzed samples straddle the limit between the trondhjemite and granite fields in the Ab-An-Or diagram (Fig. 6c). The leucogranodiorite rocks of this group do not plot in the granodiorite field in this diagram in function of their low normative anorthite

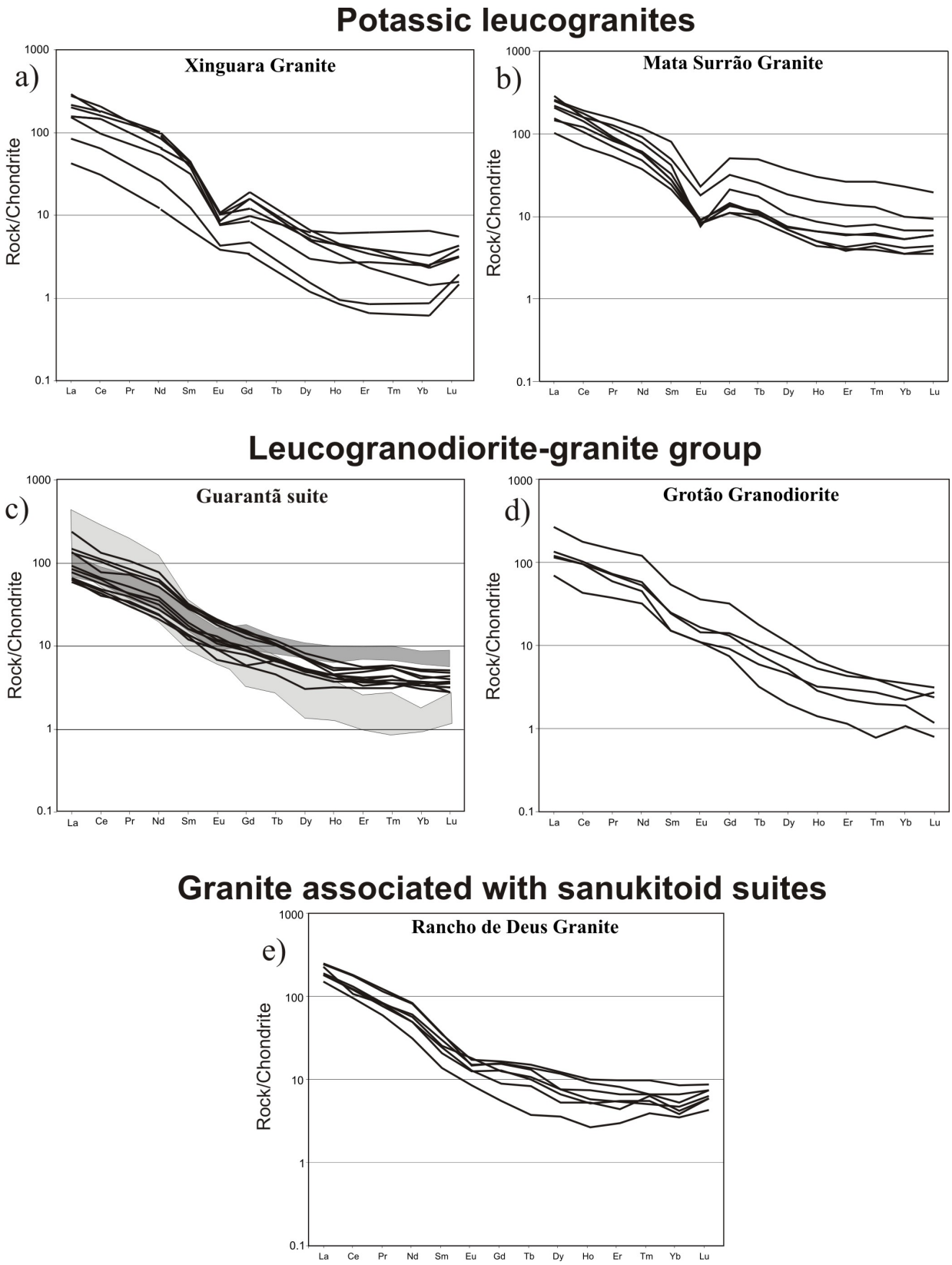

Figure 8 - REE patterns of Archean granite suites of Rio Maria granite-greenstone terrane (normalized to chondrite after Evensen et al., 1978).

content. However, they fall dominantly in the granodiorite field in the P-Q diagram (Fig 6d; fields of Debon & Le Fort 1988), which looks more suitable for the geochemical discrimination of the different Archean granite groups. In the R1-R2 diagram (De la Roche et al., 1980), the majority of samples plot in the granite field (Fig 6e).

The rocks of the *LGdG* group are enriched in Sr and Ba and impoverished in Rb (Figs. 7a, b, c) when compared to other Archean granites of the RMGGT, but have also low contents of HFSE (Zr, Y, Yb, and Nb; Figs. 7e, f; Table 4). In the granitoids of the Guarantã suite (Fig. 8c), the dominant REE patterns are enriched in LREE and show moderate to strong HREE fractionation [$(La/Yb)_N$ = 16 – 47]. However, there is a second group of samples which show higher LREE and lower HREE contents and are more strongly fractionated [$(La/Yb)_N$ = 20 – 142] than the dominant group. Finally, there is a minor third group which exhibit weakly fractionated REE patterns [$(La/Yb)_N$ = 7.8–14.4]. The patterns of the three mentioned groups have either no Eu anomaly or just small negative or positive Eu anomalies (Eu/Eu* generally between 0.70 – 1.10; Fig. 8c; Table 4). The REE patterns of the Grotão granodiorite are mostly similar to those of the dominant group of the Guarantã suite [$(La/Yb)_N$ = 31 –61; Fig. 8d], but there are also analyzed samples with a more strong fractionation of HREE [$(La/Yb)_N$ >89; Fig. 8d, Table 4]

6.3. Granites associated with sanukitoid suites (Rancho de Deus pluton)

The rocks of the Rancho de Deus granite (Dias, 2009) have SiO_2 concentration from 67.3 to 73.4 %, and vary from metaluminous to slightly peraluminous. With exception of TiO_2, K_2O, and Na_2O, the major elements decrease in an approximately linear fashion parallel to increasing SiO_2. In general, this granite group show lower Al_2O_3, CaO, and Na_2O, and higher MgO (0.3-1.5 wt %; #Mg usually >0.4) and K_2O when compared with rocks of the *LGdG* with similar silica contents (Figs. 5b, d, e, f, g). Their K_2O/Na_2O ratios show little variation and are close to 1. The FeOt/FeOt+MgO ratios are relatively low (normally <0.73) and show positive correlation with silica (Fig. 5i). These granites have low HFSE contents similar to those of the other granite groups. Their contents of Sr and Ba are similar or a little lower and those of Rb higher when compared to the *LGdG*. The REE patterns of the Rancho de Deus granite are moderately to strongly fractionated [$(La/Yb)_N$ = 28 to 59; Fig. 8e], with a discrete to moderate negative Eu anomaly (Eu/Eu* between 0.57– 0.95; Fig. 8e; Table 4).

7. Discussion

7.1. The granites of the RMGGT and their comparison with other Archean granitoids

7.1.1. Comparison between the granites and other granitoid groups of the RMGGT

The three Archean granite groups of the RMGGT can be easily distinguished from the other Archean granitoids of that terrane on the basis of their modal compositions. The TTG suites of the RMGGT are composed essentially of tonalites and trondhjemites with scarce associate granodiorites and their modal compositions are not superposed with those of the granites in the QAP plot (Fig. 3). The rocks dominant in the Rio Maria sanukitoid suite are concentrated in the granodiorite field and their modal compositions are superposed with those of the LGdG (Fig. 3). However the Rio Maria granodiorite is enriched in mafic minerals compared to the LGdG (Q-A+P-M plot, Fig. 3) and has amphibole as its main mafic phase.

The geochemical contrasts between the granitic rocks and TTG and sanukitoid suites of the RMGGT are remarkable and the different granite groups compared with TTGs and sanukitoids define in several plots (Fig. 9) clearly distinct fields. The relative enrichment in Ba and Sr of the LGdG distinguishes it from the other granitoid types (Figs. 9a, b). The potassium leucogranites have also higher silica compared to the LGdG. In the #Mg vs K/Na diagram (Fig. 9c), the #Mg values increase from the TTGs to the sanukitoids and show positive correlation with K/Na, whereas a clear decrease of #Mg from the sanukitoids to the granite groups is observed, implying a negative correlation with K/Na. The TTGs and the LGdG show similar #Mg values but they define only marginally superposed fields in function of the contrast in their K/Na ratios. In the A/CNK vs K/Na diagram (Fig. 9d), the TTGs, LGdG and potassium leucogranites plot in the transition from the metaluminous to the peraluminous fields in function of their similar A/CNK values, but they differ in their K/Na ratios that increase from the TTGs to the LGdG and attain the highest values in the potassium leucogranites group. The sanukitoids are distinguished from the other groups by their essentially metaluminous character. In the Ba vs. TiO_2 plot (Fig. 9e), the granites differ from the TTGs and sanukitoids by their lower TiO_2 contents that reflects their leucocratic nature and, in the case of the LGdG, also by the higher barium contents. The contrasts in the Eu/Eu* ratios between the different granitoid groups are also generally significant. This ratio shows a negative correlation with K/Na (Fig. 9f) decreasing from the TTGs

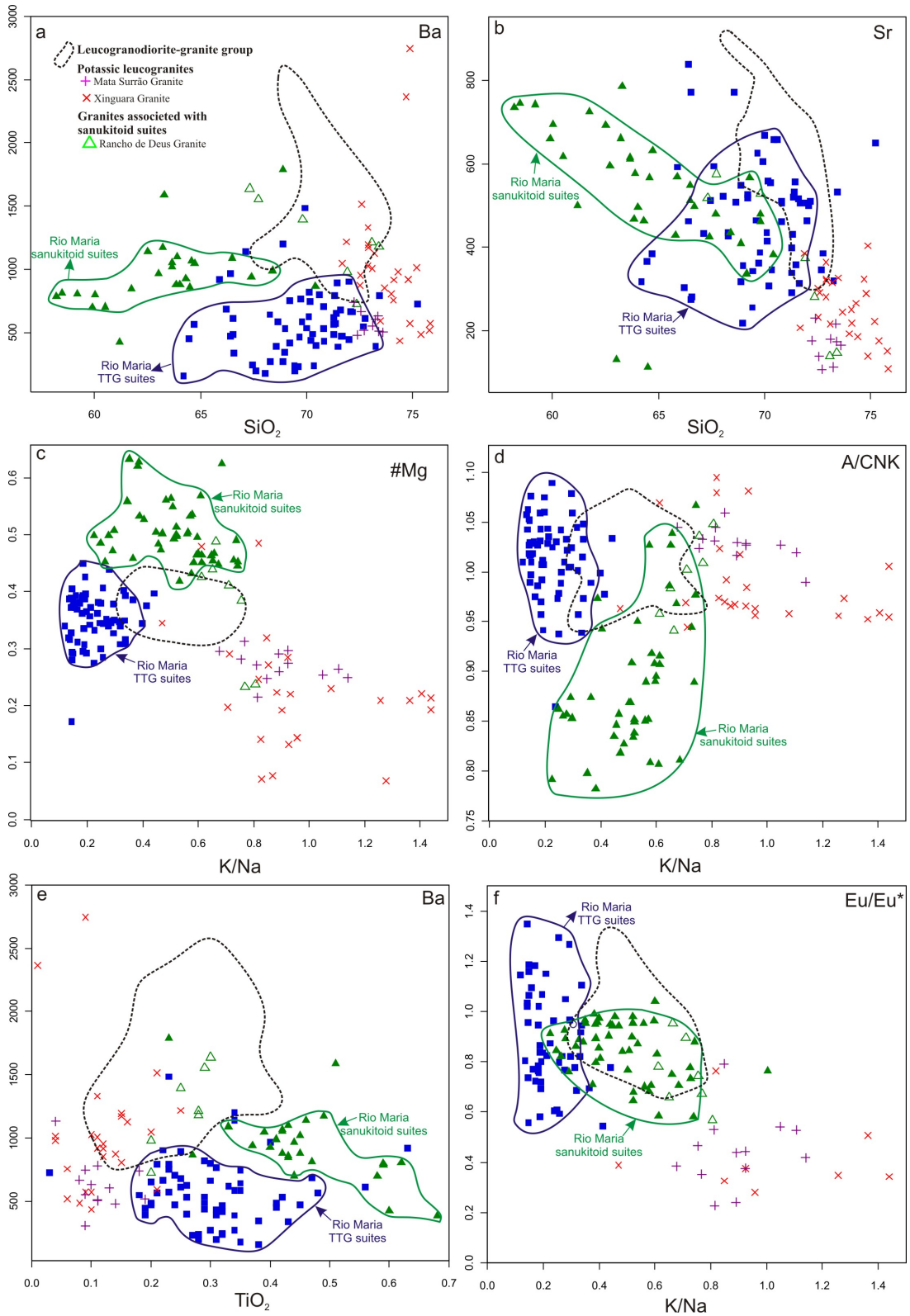

Figure 9 - Variation diagrams for the Archean granitoids of the Rio Maria granite-greenstone terrane.Mg# molecular ratio Mg/(Mg + Fe); A/CNK molecular ratio Al/(Ca+Na+K); K/Na molecular ratio; Eu/Eu*=europium anomaly calculated as [Eu/(Eu*)]=[(EuN)/((SmN+GdN)/2)].

to the potassium granites, with the sanukitoids + LGdG displaying intermediate and generally similar values. The few analyzed samples of the Rancho de Deus granite are situated in the border of the fields of the sanukitoid rocks in these geochemical diagrams (Fig. 9) or associated with the LGdG.

In terms of the REE behavior, the patterns of the Archean granites of the RMGGT (Fig. 8) are variable. Those of the LGdG (Fig. 8c, d) are similar to the patterns of the TTGs, whereas those of the Rancho de Deus granite (Fig. 8e) approach the patterns of the sanukitoid rocks. Only the patterns of the potassium leucogranites differ radically from those of the other Archean granitoids, because they show systematically accentuate negative Eu anomalies (Fig. 8a, b), which are generally absent in the other granitoids.

The geochemical data reviewed here demonstrate that both, the LGdG and the potassium granite groups, show clearly distinct characteristics when compared with the TTGs and sanukitoid rocks and that all these four groups of granitoids should have been derived from different magmas. The Rancho de Deus granite, on the other hand, show geochemical affinities with the sanukitoid series of the RMGGT, but there are also significant contrasts between the former and the dominant sanukitoid series (Oliveira et al., 2009), suggesting that it can be derived from sanukitoid magmas that were distinct in some degree from those dominant in the RMGGT.

7.1.2. Comparison between the granites of the RMGGT and similar granites of other Archean terranes

The late Archean granites of the Dharwar craton are dominantly biotite (rarely hornblende-) bearing monzo- to syenogranites or granodiorites (Moyen et al., 2003). In the Arsikere-Banawara and Chitradurga-Jampalanaikankote-Horsdurga granite suites the dominant rocks are biotite (±hornblende) monzogranites (Jayananda et al., 2006), the Arsikere granite containing also magmatic epidote (Rogers, 1988). In the Yilgarn craton, three granite groups have been distinguished (Champion and Sheraton, 1997): (1) the largely dominant is a biotite (±amphibole) granodiorite to granite (high-Ca group; equivalent at present to the transitional TTG group; cf. Champion and Smithies, 2003); (2) biotite (±fluorite) granodiorite to granite (low-Ca group); and (3) subordinate amphibole-biotite granite with minor granodiorite (high-HFSE group). In the late Archean granites of the central Wyoming province, hornblende-biotite

granodiorite and granite are also dominant (Frost et al., 2006; their Fig. 5). In his synthesis about Archean granites, Sylvester (1994) stated that the dominant rocks are granites and granodiorites.

The Archean granites of the RMGGT were compared with those of the Yilgarn craton, as characterized by Champion and Sheraton (1997), in CaO, K_2O, Rb, and Zr, versus SiO_2 diagrams (Figs. 5d, g; 7c, e). These diagrams indicate a great geochemical similarity between the high-Ca granite group of Yilgarn and the LGdG of Rio Maria. On the other hand, the potassium granite group of Rio Maria looks similar to the low-Ca granite group of Yilgarn, with the difference that the former show a more limited silica range (72 to 76 wt.%) compared to the low-Ca group of Yilgarn (68 to 76 wt.%).

The different groups of granitoids of the RMGGT were also compared with the Archean granite tipology proposed by Moyen et al. (2003) on the basis of their study in the Dharwar craton (Fig. 10). The Transitional TTG group of Yilgarn (former high-Ca granite group) was also included in these diagrams (D. Champion, written communication), as well as the fields of TTG and sanukitoid rocks of the RMGGT. In the selected plots (Fig. 10), although there is some overlap between the groups, the contrast in composition between the Archean granite groups of the RMGGT, on one hand, and the TTG and sanukitoid suites of the same terrane and also of different cratons (Moyen et al., 2003; Halla, 2005; Heilimo et al., 2010), on the other hand, is remarkable, reinforcing the evidence given above that the former are geochemically distinct from the latter series of rocks. The different plots confirm that the LGdG of Rio Maria is geochemically similar to the Transitional TTG granite group of Yilgarn with their samples plotting mostly in the fields defined by the latter (Fig. 10). The potassium granites of Rio Maria, on the other hand, are concentrated in the fields of the biotite granite (Moyen et al., 2003) and low-Ca granite groups (Champion and Sheraton, 1997). The Rancho de Deus granite samples plot in the border of the field defined by the Rio Maria sanukitoids, projecting in the direction of the biotite granite field (Fig. 10). The LGdG of Rio Maria is also partially superposed in some diagrams (Fig, 10 a, c) with the Enriched TTG group of Moyen et al. (2003) and has lower CaO and higher K_2O when compared with the GG Archean granites of the Wyoming Province (Frost et al., 2006). The GG suite of Wyoming and the LGdG of Rio Maria have in common, however, the fact that their REE patterns are similar to the TTG series of the same terranes.

It is deduced from the geochemical data that the Rio Maria potassium Archean granites are comparable with the biotite granite (Moyen et al., 2003) or low-Ca granite groups (Champion

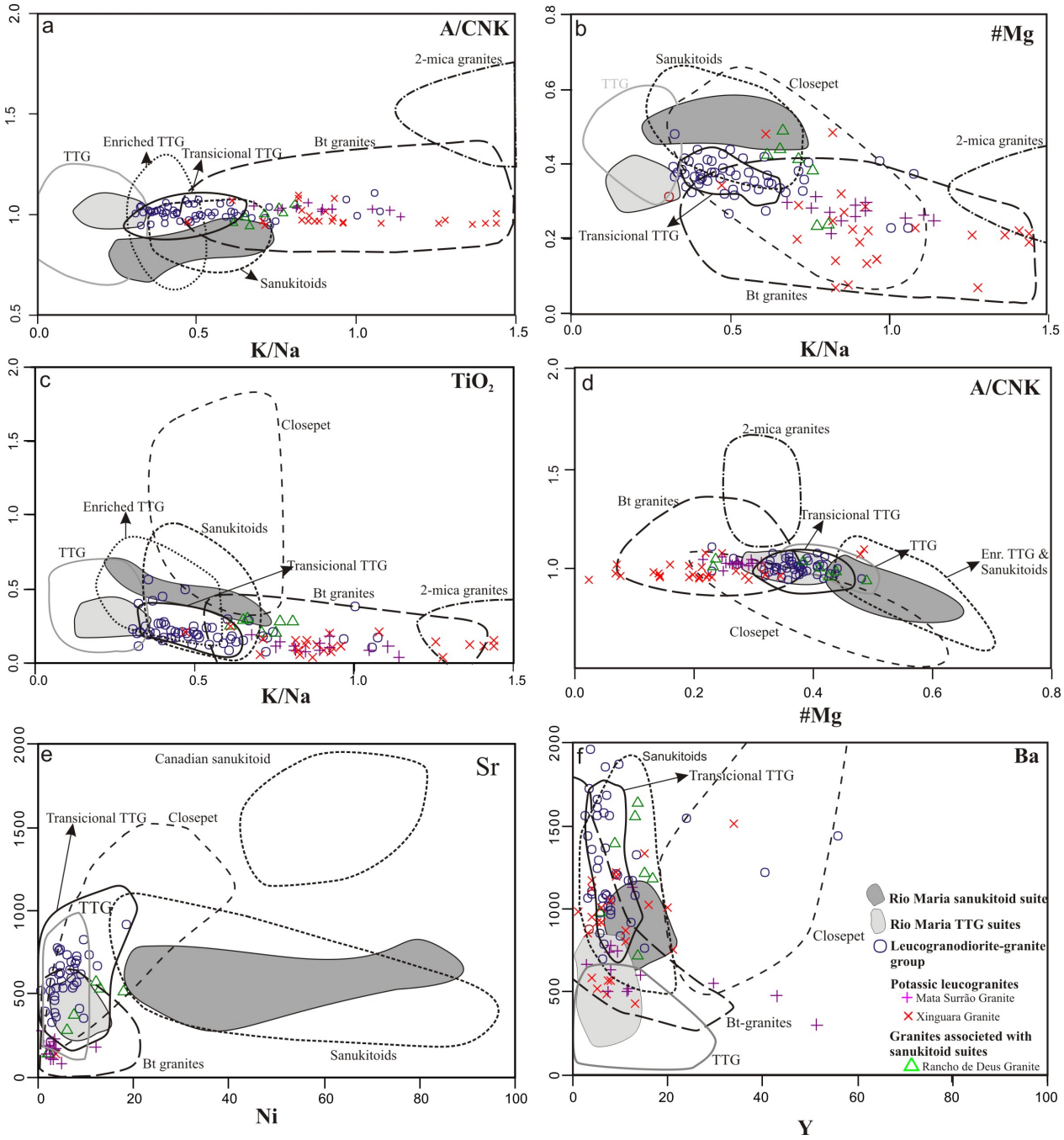

Figure 10 - (a) K/Na vs A/CNK or (b) #Mg or (c) TiO_2, (d) #Mg vs A/CNK, (e) Ni vs Sr and (f) Y vs Ba diagrams for Archean granitoids of the Rio Maria granite-greenstone terrane. Mg# molecular ratio Mg/(Mg + Fe); A/CNK molecular ratio Al/(Ca+Na+K); K/Na molecular ratio. The Archaean granitoid fields are according to the typology established by Moyen et al. (2003). The field for the Transitional TTG was designed from of the sample of the Goongarrie suite and Menangina pluton of the Yilgarn craton (D. Champion, written communication).

and Sheraton, 1997), whereas the LGdG of the RMGGT are similar to the Transitional TTG or high-Ca group of Yilgarn (Champion and Sheraton, 1997; D. Champion, written communication). Finally, the Rancho de Deus granite is geochemically akin to the evolved rocks of the sanukitoid series. There is no equivalent in the Archean granites of the RMGGT recognized so far, of the Closepet granitoid, the two-mica granite group (Moyen et al., 2003) and of the high-HFSE group of Yilgarn (Champion and Sheraton, 1997).

The Archean granite suites of the RMGGT display most of the geological, petrographic and geochemical characteristics of the Late Archaean, calc-alkaline plutons, as described by Sylvester (1989, 1994): 1) They probably represent the last magmatic events recorded in the RMGGT, but they have in contrast Mesoarchean ages (ca. 2.86 Ga); 2) They are composed dominantly of monzogranite and granodiorite and not contain primary phases more aluminous than biotite; 3) They exhibit relatively high Al_2O_3, CaO, MgO, Ba, and Sr associated with low Zr, Y, Ga, Nb, and HREE contents. In the $(A1_2O_3 + CaO)/(FeO_t + Na_2O + K_2O)$ vs. 100 $(MgO + FeOt + TiO_2)/SiO_2$ diagram (Sylvester, 1989), the samples of the LGdG and Rancho de Deus granite plot preferentially in the calc-alkaline granite field. The more evolved rocks of these groups together with the potassic leucogranites fall in the ambiguous field of the highly fractionated alkaline or calc-alkaline granites (Fig. 11), but the strong depletion in HFSE suggests a calc-alkaline better than alkaline affinity to these rocks. Moreover, Sylvester (1994) distinguished on the basis of geochemical composition the Archean calc-alkaline granites of types 1 and 2. In general, the LGdG of the RMGG have fractionated REE patterns without significant Eu anomalies and are similar to the CA1 calc-alkaline granites subgroup, whereas the potassium leucogranites and the Rancho de Deus granite are more akin to the CA2 subgroup.

7.2. Petrogenesis of the Archean granites of the RMGGT: A preliminary approach

Petrological, geochemical, and isotopic studies indicate that most Archean granitic magmas were probably originated by anatexis of crustal rocks or through more complex processes involving interaction between magmas derived from varied sources or liquids and residues from different sources (Sylvester, 1994; Leite, 2001; Champion and Smithies, 2003; Moyen et al., 2003; Frost et al., 2006; Watkins et al., 2007). The hypothesis of contribution of subducted sediments in the sources to account for the high Ba-Sr contents of some granites was

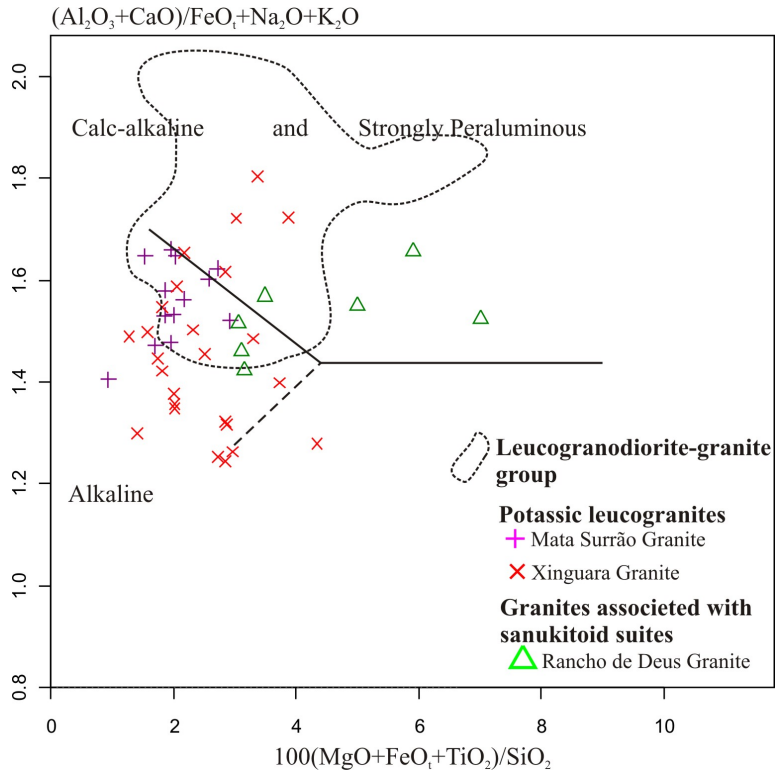

Figure 11 - Major element discrimination diagram proposed by Sylvester (1994) for Archean granite suites of the Rio Maria granite-greenstone terrane.

also considered (Champion and Sheraton, 1997; Halla et al., 2005; Champion and Smithies, 2007, and references therein).

As in most Archaean terranes, K-rich granitic plutons of the RMGGT were emplaced after the main phase of TTG magmatism, and it has often been suggested that the K-rich granitic magmas were formed by 'reworking' (partial melting) of the TTGs. Several experimental partial melting studies of metatonalites conducted under fluid-absent conditions indicate that granitic melts could be produced (Rutter and Wyllie, 1988; Skjerlie and Johnston, 1992; Singh and Johannes, 1996; Gardien et al., 1995, 2000; Patiño Douce, 2005). However, Castro (2004) and Watkins et al. (2007) argue that the late potassic granites of Archean terranes are more probably not derived from older TTG partial melting. Watkins et al. (2007) claimed additionally that the high-potassic granite magmas may contain a component derived from a highly enriched mantle (a process similar in some degree to that responsible by the origin of sanukitoid magmas). The TTG and Rio Maria sanukitoid suites constitute a major part of the basement of the Rio Maria region and are probably similar geochemically to the deep-seated Archaean rocks. Moreover, these

rocks are clearly distinct from the Archean granite groups in both their modal and chemical characteristics, and are, thus, viable protolith candidates for the granite magmas.

The SiO_2 contents of the LGdG and the potassic leucogranites of the RMGGT are partially superposed (Table 5, Fig. 5), suggesting the possibility of the derivation of the latter from the former by fractional crystallization processes. However, the bulk of geochemical data indicate that they follow two distinct trends and the contrast in Al_2O_3, K_2O, Na_2O, #Mg, Sr, Ba, Rb, Zr in both groups of rocks is particularly remarkable (Figs. 5, 7, 11). The presence of modal amphibole and the relatively high values of MgO, K_2O, #Mg, Rb, Rb/Sr, and Ni and low of Na_2O, Ba, and Sr recorded in the Rancho de Deus pluton compared to the LGdG (Figs. 5, 7, 11) suggest that the parent magmas of these two groups were also distinct. There is also no geochemical evidence favouring the derivation of the potassic granites from the Rancho de Deus granite (Figs. 5, 7, 11). It is concluded that the three granite groups derived from different magmas.

On the basis of geochemical data and modeling, Leite (2001) argue that the Xinguara granite (representative of the potassium granite group of Rio Maria) could be derived by partial melting of rocks similar to the Arco Verde tonalite, Caracol tonalite, Mariazinha tonalite and Rio Maria granodiorite. The three tonalitic units are representative of the TTGs from Rio Maria and the granodiorite of the sanukitoid suites of that terrane. Mass balance calculations for major and minor elements indicate that the four rock types have chemical compositions adequate to generate the two dominant leucogranites of the Xinguara pluton with variation in the degree of melting (20 to 30 % for the more potassic varieties; 40 to 50% for the less potassic ones; Leite, 2001, its tables 8.5 and 8.6). However, in all consistent models, the melt residue contained plagioclase (consistent with the negative Eu anomalies observed in the potassic granites), hornblende, biotite, and quartz as major mineral phases but the residue shows also significant differences depending of the assumed source: it was relatively enriched in biotite and devoid of amphibole in the case of the Arco Verde tonalite; hornblende was more abundant than biotite in the cases of the Caracol and Mariazinha tonalites and the contrary was observed in the Rio Maria granodiorite. The adjustment of these different sources was tested using REE and the best fit was obtained in the case of the Mariazinha tonalite sample. The poorest fit resulted for the Arco Verde Tonalite and the Caracol Tonalite sample which correspond to the TTG group with low $(La/Yb)_N$ ratios (in the case of the Caracol Tonalite the dominant samples with high $(La/Yb)_N$ were not modeled but a

result analogue to that of the Mariazinha tonalite could be expected because their chemical compositions and REE patterns are quite similar). The poorest fit obtained in the case of residues enriched in biotite compared to hornblende is consistent with the evidence of significant amphibole fractionation during the evolution of the Xinguara granite (Fig. 8a; cf. the concave shape of the HREE branch). However, the REE patterns of the Mata Surrão granite, the second suite representative of the potassium granite group, do not show this feature (Fig. 8b) and have higher $(La/Yb)_N$ compared to the Xinguara granite suggesting that the former could be derived from sources similar to the Arco Verde tonalite. This geochemical evidence is reinforced by the fact that the Arco Verde tonalite is the dominant TTG in the area of occurrence of the Mata Surrão granite (Fig. 1b).

The geochemical characteristics of the Rancho de Deus granite suggest that these rocks and similar granites can be generated by fractional crystallization and differentiation of sanukitoid magmas. However, the relatively higher Ba and Sr contents of the Rancho de Deus granite compared to the dominant sanukitoid granodiorites of Rio Maria indicate that the former can be derived from sanukitoid magmas enriched in the mentioned elements. A possible candidate is the Mata Geral granodiorite, a large sanukitoid pluton that occurs in proximity with the Rancho de Deus granite (Figs. 1b, 7, 11) and shows evidence of enrichment in Ba and Sr in its granitic rocks (Almeida et al., 2008).

Geochemical modelling indicates that the elevated contents of Sr and Ba in the LGdG are not compatible with their derivation directly by partial melting of TTG or sanukitoid sources. Excluding the possibility of origin of these granites directly from a mantle source, which looks improbable, it is necessary to think about complex processes involving varied crustal sources or alternatively mixed crustal and mantle sources to explain the origin of these magmas. The hypothesis of contribution of subducted sediments associated to the slab should also be considered (cf. Champion and Smithies, 2007). In fact, a possible explanation for the origin of the LGdG, the so-called transitional TTG or GG group, is beyond the goals of this paper and we want to deal with it in a paper focused only on this kind of rock. As a preliminary conclusion, it can be said that the geochemical features of these granites suggest participation of TTGs and sanukitoid rocks or liquids in their origin, but the way in which these diversified sources interacted is not clear so far.

The relatively large negative Eu anomaly observed in the potassic leucogranites is absent in the LGdG. This can be seen as evidence that the latter were formed at high pressures, within the garnet stability field (>0.8 GPa; Watkins et al., 2007), while the potassic leucogranites were originated at lower pressures, within the plagioclase stability field.

The scattered distribution of chemical compositions of samples representative of individual plutons from Archean granite suites of the RMGGT can be due either to local variations in the compositions of the sources of individual magma pulses or to variations within cogenetic granites that resulted from variable degrees of partial melting of the source rocks (Chappell, 2004; Clemens et al., 2006), rather than a reflex of fractional crystallisation on individual plutons.

7.3. The ages of the Archean granites of the RMGGT and tectonic implications

The new ages on the Archean granites presented in this paper, integrated with those previously available in the literature, demonstrate that the events responsible for granite formation in Rio Maria were concentrated around 2.87 to 2.86 Ga, during the Mesoarchean (Figs. 2, 4). As commonly observed in other Archean cratons, the main timing of granite formation succeed that of the dominant TTG magmatism, concentrated in the example of Rio Maria in between 2.98 and 2.92 Ga, with minor subordinate occurrences at 2.86 Ga (Fig. 2, and references therein). It is also worth noting that in Rio Maria, the sanukitoid suites have extremely uniform ages (ca. 2.87 Ga; Fig. 2; Oliveira et al., 2009) and were formed contemporary or a little early than the granites stricto sensu. Thus, it implies that a remarkable magmatic event marked the evolution of the RMGGT at 2.87 Ga and was responsible for the formation of diversified types of magmatic rocks, a large part of them with granitic composition. This event was probably coincident with the tectonic stabilization of the Rio Maria terrane that was not affected by the Neoarchean events registered in the Carajás Basin Archean domain to the north (Althoff et al., 2000; Souza et al., 2001; Dall'Agnol et al., 2006).

The earliest crust of Rio Maria probably did not form much earlier than the TTG suites and, hence, it should have been still quite warm at the time of the Archean granite magmas were produced. In addition, underplating in the lower crust of sanukitoids magmas at 2.87 Ga may have also contributed with heat inducing the melt of a possibly thickened crust and generation of

Archean granite magmas. The sanukitoids magmas could have ponded or underplated at the base of the crust (e.g., Gromet and Silver, 1987; Atherton and Petford, 1993), but perhaps also in hot zones within the crust (Annen et al., 2006), and were potentially able to induce partial melting at a range of crustal levels to produce granitic magmas. It is possible that the contrasts between potassium granites and LGdG traduce at least in part melting at different depths within the same broad crustal column. Melting at highest crustal level would originate the potassic leucogranites.

8. Conclusions

The modal and geochemical data demonstrate that both, the LGdG and the potassium granite groups of the RMGGT, can be easily distinguished from the TTGs and sanukitoid rocks of that terrane and that all these four groups of granitoids should have been derived from different magmas. There is a great geochemical similarity between the LGdG of Rio Maria and the high-Ca granite group (Champion and Sheraton, 1997) or Transitional TTG (Champion and Smithies 2003) of Yilgarn. On the other hand, the potassium Archean granites are comparable with the biotite granite (Moyen et al., 2003) or low-Ca granite groups (Champion and Sheraton, 1997). The Rancho de Deus granite is geochemically akin to the evolved rocks of the sanukitoid series. In general, the LGdG of the RMGG have fractionated REE patterns without significant Eu anomalies and are similar to the CA1 calc-alkaline granites subgroup, whereas the potassium leucogranites and the Rancho de Deus granite are more akin to the CA2 subgroup (Sylvester, 1994).

Geochemical modelling indicates that the Xinguara granite (potassium leucogranite group) could be derived by partial melting of rocks similar to the older TTG (Arco Verde tonalite, Caracol tonalite, Mariazinha tonalite) or sanukitoid suites (Rio Maria granodiorite) of the RMGGT. A source similar to the Arco Verde tonalite has chemical compositions adequate to generate the Mata Surrão magma. The geochemical characteristics of the Rancho de Deus granite suggest that these rocks and similar granites can be generated by fractional crystallization and differentiation of sanukitoid magmas enriched in Ba and Sr (e.g. Mata Geral granodiorite). In case of the LGdG it is necessary to think about complex processes involving varied crustal sources or alternatively mixed crustal and mantle sources to explain the origin of their magmas.

The geochronological data obtained in this study and previous studies demonstrate that the granite magmatism *stricto sensu* record in RMGGT (2.87- 2.86 Ga) succeed the main timing of TTG suites formation (2.98 - 2.92 Ga) and was originated contemporary or a little later than the sanukitoid suites of the RMGGT. Thus, it implies that a remarkable magmatic event marked the evolution of the RMGGT at 2.87 Ga and was responsible for the formation of diversified types of magmatic rocks, a large part of them with granitic composition. To explain the genesis of the Archean granite suites of the RMGGT, it should be considered that the crust of Rio Maria was probably still quite warm at the time when the granite magmas were produced. In addition, underplating in the lower crust at 2.87 Ga of sanukitoids magmas may have also contributed with heat inducing the partial melting at a range of crustal levels of a possibly thickened crust and generation of Archean granite magmas. It is possible that the contrasts between potassium leucogranites and LGdG groups traduce at least in part melting at different depths but it is clear also that more complex processes were involved in the genesis of the LGdG.

Acknowledgements

The authors are grateful to S. B. Dias and F. V. Guimarães for their contribution to the study of the Guarantã suite + Rancho de Deus granite and Grotão granodiorite, respectively. A. T. R. Ferreira, A. L. Paiva Junior, G. R. L. Feio, M. A. C. Costa, and M. A. Oliveira are acknowledged for support in geological mapping, petrographical, geochemical, and geochronological work. The authors thank to M. A. Galarza Toro for their skilful laboratory assistance for obtainment of the single zircon Pb-evaporation analyses, C. N. Lamarão for his assistance in the cathodoluminescence imaging, and E. L. Dantas, B. Lima, and S. Junges for their assistance on LA-ICP-MS analyses. The authors express special thanks to O. T. Rämö, J. Halla, E. Heilimo, M. I. Kurhila, and A. Heinonen for support during field trip in Karelia craton and for numerous discussions on Archean geology. David Champion is gratefully acknowledged for providing us with his geochemical database of the high-Ca granites from Yilgarn craton. The Brazilian Geological Survey (CPRM) is acknowledged by permission to include in this paper data generated in the GEOBRASIL Project (mapping of Marajoara sheet). This research received financial support from CNPq (R. Dall'Agnol – Grants 0550739/2001-7, 476075/2003-3, 307469/2003-4, 484524/2007-0; PRONEX – Proc. 66.2103/1998-0; J. A. C. Almeida – doctor

scholarship) and Federal University of Pará (UFPA). This paper is a contribution to the Brazilian Institute of Amazonia Geosciences (INCT program – CNPq/MCT/FAPESPA – Proc. 573733/2008-2).

Appendix A. Analytical procedures

Zircon crystals were concentrated from ca. 10 kg rock samples using conventional methods, involving combination of magnetic and gravimetric separation with handpicking techniques. Zircon dating by the single grain Pb evaporation method (Kober, 1986) was carried out at the Laboratório de Geologia Isotópica (Pará-Iso) of the UFPA, Brazil. Isotopic ratios were measured in a FINNIGAN MAT 262 mass spectrometer and data were acquired in the dynamic mode using the ion-counting system of the instrument. When the Pb signal exceeded the ion counting saturation threshold, the isotopic measurements were done in static mode on Faraday cups. For each step of evaporation, a step age is calculated from the average of the $^{207}Pb/^{206}Pb$ ratios. Common Pb corrections were made according to Stacey and Kramers (1975) and analyses with $^{206}Pb/^{204}Pb$ ratios lower than 2500 were rejected, thus minimizing the effects of common Pb correction. The age of each sample is considered confident when it was obtained using the mean of $^{207}Pb/^{206}Pb$ ratios of at least four crystals at the highest step of temperature. When different heating steps of the same grain gave similar ages, all of them were included in the age calculation. Crystals or steps showing lower ages probably reflect Pb loss after crystallization and are not included in sample age calculation. Weighted mean and errors on the ages were calculated following Gaudette et al. (1998). $^{207}Pb/^{206}Pb$ ratios were corrected for mass fractionation by a factor of 0.12±0.03 per a.m.u, given by repeated analysis of the NBS-982 standard. Analytical uncertainties are given at the 2σ level.

U–Pb LAN-ICP-MS analyses were performed in the Geochronology Laboratory of the University of Brasília and followed the analytical procedure described by Buhn et al. (2009). For these analyses, zircons from the nonmagnetic fractions were hand-picked and mounted on adhesive tape, imbedded in an epoxy-resin pellet and then polished to about half of their size. In order to investigate the internal structures of the zircon crystals prior to analysis, cathodoluminescence imaging of the zircon grains was carried out using a Mono-CL detector

attached to a scanning electron microscope (LEO 1430) at the Scanning Electron Microscopy Laboratory of the Geosciences Institute of Federal University of Pará (UFPA).

Before LA-ICP-MS analyses, mounts were cleaned with dilute (ca. 2%) HNO3. The samples were mounted in an especially adapted laser cell and loaded into a New Wave UP213 Nd:YAG laser (λ - 213 nm), linked to a Thermo Finnigan Neptune Multi-collector ICPMS. Helium was used as the carrier gas and mixed with argon before entering the ICP. The laser was run at a frequency of 10 Hz and energy of 0.4 mJ/pulse and a focused laser beam of 20–40 μm in diameter was employed depending on the sample grain size.

Two international zircon standards were analyzed throughout the U–Pb analyses. The zircon standard GJ-1 (Jackson et al., 2004) was used as the primary standard in a standard-sample bracketing method, accounting for mass bias and drift correction. The resulting correction factor for each sample analysis considers the relative position of each analysis within the sequence of four samples bracketed by two standard and two blank analyses each (Albarède et al., 2004). The UQZ was run at the start and the end of each analytical session, yielding an accuracy around 2% and a precision in the range of 1%. The errors of sample analyses were propagated by quadratic addition of the external uncertainty observed for the standards to the reproducibility and within-run precision of each unknown analysis. The instrumental set-up and further details of the analytical method applied are given by Buhn et al. (2009). The masses of $^{204,\ 206\ \text{and}\ 207}$Pb isotopes were measured with ion counters, and ^{238}U was analyzed on a Faraday cup. The signal of ^{202}Hg was monitored on an ion counter for the correction of the isobaric interference between ^{204}Hg and ^{204}Pb. The signals during ablation were taken in 40 cycles of 1s each. For data evaluation, only coherent intervals of signal response were considered. Data reduction was performed with an Excel spreadsheet, which considers blank values, zircon standards composition and errors, and error propagation. The ^{204}Pb signal intensity was calculated and corrected using a natural ^{202}Hg/^{204}Hg ratio of 4.346. A common Pb correction was applied for zircons with ^{206}Pb/^{204}Pb lower than 1000, applying a common lead composition following the Stacey and Kramers (1975) model. Plotting of U–Pb data was performed by ISOPLOT v.3 (Ludwig, 2003) and errors for isotopic ratios are presented at the 2σ level.

The 41 representative analyses showed in this work (Table 1) comprise both previously published (9 analyses from Leite, 2001; 2 analyses from Dias, 2007; 3 analyses from Guimarães et al. b, submitted; 4 analyses from Dias, 2009) and new data (23 analyses from this work). All

new analyses and those obtained by Dias (2007, 2009), Guimarães et al. (b, submitted) and in this study were performed by ICP-ES for major elements and ICP-MS for trace-elements, including the rare-earth elements, at the Acme Analytical Laboratories Ltd. in Canada. Chemical diagrams were mostly generated using the GCDkit software (Janousek et al., 2003).

References

Albarède, F., Telouk, P., Blichert-Toft, J., Boyet, M., Agranier, A., Nelson, B., 2004. Precise and accurate isotopic measurements using multiple collector ICP-MS. Geochim. Cosmochim. Acta 68, 2725–2744.

Almeida, J.A.C., Oliveira, M.A., Dall'agnol, R., Althoff, F.J., Borges, R.M.K., 2008. Relatório de mapeamento geológico na escala 1:100.000 da Folha Marajoara (SB-22-ZC V). Programa Geobrasil, CPRM – Serviço Geológico do Brasil. 147p. (In portuguese).

Almeida, J.A.C., Dall'Agnol, R., Oliveira, M.A., Macambira, M.J.B., Pimentel, M.M., Ramo, O.T., Guimarães, F.V., Leite, A.A.S., submitted. Zircon geochronology and geochemistry of the TTG suites of the Rio Maria granite-greenstone terrane: Implications for the growth of the Archean crust of Carajás Province, Brazil. Precambrian Res.

Althoff, F.J., 1996. Étude pétrologique et structurale des granitoïdes de Marajoara (Pará, Brésil): leur rôle dans l'évolution archéenne du craton Amazonien (2.7– 3.2 Ga). Ph.D thesis. Université Henri Poincaré, Nancy I, France, 296p. (in French).

Althoff, F.J., Barbey, P., Boullier, A.M., 2000. 2.8–3.0 Ga plutonism and deformation in the SE Amazonian craton: the Archean granitoids of Marajoara (Carajás Mineral province, Brazil). Precambrian Res.104, 187–206.

Annen, C., Blundy, J.D., Sparks, R.S.J., 2006. The genesis of intermediate and silicic magmas in deep crustal hot zones. J. Petrol. 47, 505–539.

Atherton, M.P., Petford, N., 1993. Generation of sodium-rich magmas from newly underplated basaltic crust. Nature 362, 144–146.

Barker, F., Arth, J.G., 1976. Generation of trondhjemite-tonalite liquids and Archean bimodal trondhjemite-basalt suites. Geology 4, 596–600.

Barros, C.E.M., Barbey, P., Boullier, A.M., 2001. Role of magma pressure, tectonic stress and crystallization progress in the emplacement of the syntectonic A-type Estrela Granite Complex (Carajás Mineral Province, Brazil). Tectonophysics, 343, 93-109.

Buhn, B., Pimentel, M.M., Matteini, M., Dantas, E.L., 2009. High spatial resolution analysis of Pb and U isotopes for geochronology by laser ablation multi-collector inductively coupled plasma mass spectrometry (LA-MC-ICP-MS). Anais Acad. Brasil. Ciências 81 (1), 1–16.

Castro A., 2004. The source of granites: inferences from the lewisian complex. Scott J. Geol. 40:49–65

Champion, D.C., Sheraton, J.W., 1997. Geochemistry and Nd isotope systematics of Archaean granites of the Eastern Goldfields, Yilgarn Craton, Australia: implications for crustal growth processes. Precambrian Res. 83, 109–132.

Champion, D.C., Smithies, R.H., 1999. Archaean granites of the Yilgarn and Pilbara cratons, Western Australia: secular changes. In: Barbarin, B. (Ed.), The Origin of Granites and Related Rocks—IVth Hutton Symposium Abstracts Doc. BRGM 290, pp. 137.

Champion, D.C., Smithies, R.H., 2003. Archaean granites. In: Blevin, P.L., Chappell, B.W., Jones, M. (Eds.), Magmas to Mineralisation: The Ishihara Symposium, pp. 19–24 (AGSO-Geoscience Australia, Record 2003/14).

Champion, D.C., Smithies, R.H., 2007. In: Van Kranendonk, M.J., Smithies, R.H., Bennett, V.C. (Eds.), Geochemistry of Paleoarchean Granites of the East Pilbara Terrane, Pilbara Craton, Western Australia: Implications for Early Archean Crustal Growth. Earth's Oldest Rocks, Developments in Precambrian Geology, vol. 15. Elsevier, Amsterdam, pp. 369–410.

Chappell, B.W., 2004. Towards a unified model for granite genesis. Transactions of the Royal Society of Edinburgh. Earth Sciences 95, 1-10.

Clemens, J.D., Yearron, L.M., Stevens, G., 2006. Barberton (South Africa) TTG magmas: Geochemical and experimental constraints on source-rock petrology, pressure of formation and tectonic setting. Precambrian Res 151, 53–78.

Condie, K.C., 1993. Chemical composition and evolution of the upper continental crust: Contrasting results from surface samples and shales. Chem.Geol. 104, 1-37.

Dall'Agnol, R., Rämö, O.T., Magalhães, M.S., Macambira, M.J.B., 1999. Petrology of the Anorogenic, Oxidised Jamon and Musa granites, Amazonian craton: implications for the genesis of Proterozoic A-type granites. Lithos, 46, 431-462.

Dall'Agnol, R., Lafon, J.M., Fraga, L.M., Scandolara, J., Barros, C.E.M., 2000. The Precambrian Evolution of the Amazonian Craton: one of the last Unknown Precambrian Terranes in the

World. In: International Geological Congress, 31. Rio de Janeiro. Abstracts. Rio de Janeiro: CPRM. K.4 (CD ROM).

Dall'Agnol, R., Teixeira, N.P., Rämö, O.T., Moura, C.A.V., Macambira, M.J.B., Oliveira, D.C., 2005. Petrogenesis of the Paleoproterozoic, rapakivi, A-type granties of the Archean Carajás Metallogenic Province, Brazil. Lithos 80, 01-129.

Dall'Agnol, R., Oliveira, M.A., Almeida, J.A.C., Althoff, F.J., Leite, A.A.S., Oliveira, D.C., Barros, C.E.M., 2006. Archean and Paleoproterozoic granitoids of the Carajás metallogenetic province, eastern Amazonian craton. In: Dall'Agnol, R., Rosa-Costa, L.T., Klein, E.L. (eds.). Symposium on Magmatism, Crustal Evolution, and Metallogenesis of the Amazonian Craton. Abstracts Volume and Field Trips Guide. Belém, PRONEX-UFPA/SBGNO, 99-150.

Davis, W.J., Fryer, B.J., King, J.E., 1994. Geochemistry and evolution of Late Archaean plutonism and its significance to the tectonic development of the Slave Craton. Precambrian res. 67, 207-241.

Debon, F. & Le Fort, P., 1988. A cationic classification of common plutonic rocks and their magmatic associations: principles, method, applications. Bull. Mineral. 111: 493-510.

De La Roche, A., Leterrier, J., Grandclaude, P., Marchal, M., 1980. A classification of volcanic and plutonic rocks using R1−R2 diagram and major elment analyses – its relationships with current nomenclature. Chem. Geol. 29, 183–210.

De Wit, M.J., 1998. On Archean granites, greenstones, craton and tectonics: does the evidence demand a verdict. Precambrian Res. 91, 181–226.

Dias, S. B., 2007. Caracterização geológica, petrografica e geoquímica de leucogranitos aflorantes na porção leste de Bannach, Sudeste do Pará. Federal University of Para. 75p. Trabalho de Conclusão de Curso. Institute of Geosciences (in Portuguese).

Dias, S. B., 2009. Caracterização geológica, petrográfica e geoquímica de granitos Arqueanos da Folha Marajoara, terreno granito-greenstone de Rio Maria, sudeste do Pará. Federal University of Para. 129p. M.Sc. Thesis. Graduated Program on Geology and Geochemistry, Institute of Geosciences (in Portuguese).

DOCEGEO., 1988. Revisão litoestratigráfica da Província Mineral de Carajás. In: Congresso Brasileiro de Geologia, 35. Belém. Anais do Congresso Brasileiro de Geologia. SBG. p. 11-54.

Duarte, K.D., 1992. Geologia e geoquímica do granito Mata Surrão (SW de Rio Maria – Pa): um exemplo de granito "stricto sensu" Arqueano. Federal University of Para. 217p. M.Sc. Thesis. Graduated Program on Geology and Geochemistry, Institute of Geosciences (in Portuguese).

Frost, C.D., Frost, B.R., Chamberlain, K.R., Hulsebosch, T.P., 1998. The Late Archean history of the Wyoming province as recorded by granitic magmatism in the Wind River Range, Wyoming. Precambrian Res. 89, 145–173.

Frost, C.D., Frost, B.R., Kirkwood, R., Chamberlain, K.R., 2006. The tonalite-trondhjemite-grandiorite (TTG) to granodiorite-granite (GG) transition in the Late Archean plutonic rocks of the central Wyoming province. Canadian J. Earth Sci. 43, 1419–1444.

Gapais, D., 1989. Shear structures within deformed granites: mechanical and thermal indicators. Geology, 17, 1144-1147.

Gardien, V., Thompson A.B., Grujic, D., Ulmer P., 1995. Experimental melting of biotite + plagioclase + quartz ± muscovite assemblages and implications for crustal melting. J. Geophys. Res.-solid Earth 100:15581–15591.

Gardien, V., Thompson, A.B., Ulmer, P., 2000. Melting of biotite + plagioclase + quartz gneisses: the role of H_2O in the stability of amphibole. J. Petrol. 41:651–666.

Gaudette, H.E., Lafon, J.M., Macambira, M.J.B., Moura, C.A.V., Scheller, T., 1998. Comparison of single filament Pb evaporation/ionization zircon ages with conventional U- Pb results: examples from the Precambrian of Brazil. J. South Am. Earth Sci. 11, 351- 363.

Goodwin, A.M., 1991. Precambrian Geology: the dynamic evolution of the continental crust. Academic Press, London, 666 pp.

Gromet, L.P., Silver, L.T., 1987. REE variations across the Peninsular Ranges Batholith: implications for batholithic petrogenesis and crustal growth in magmatic arcs. J. Petrol. 28, 75–125.

Guimarães, F.V.G., Dall'Agnol, R., Almeida, J.A.C., Oliveira, M.A., submitted a. Caracterização geológica, petrográfica e geoquímica do trondhjemito Mogno e tonalito Mariazinha, terreno granito-greenstone de Rio Maria - Pará. Rev. Bras. Geociências.

Guimarães, F.V.G., Dall'Agnol, R., Oliveira, M.A., Almeida, J.A.C., submitted b. Geologia, petrografia e geoquímica do quartzo-diorito Parazônia e granodiorito Grotão, terreno granito-greenstone de Rio Maria – Pará. Rev. Bras. Geociências.

Halla, J., 2005. Late Archean high-Mg granitoids (sanukitoids) in the Southern Karelian craton, Eastern Finland. Lithos 79, 161–178.

Heilimo, E., Halla, J., Höltta, P., 2010. Discrimination and origin of the sanukitoid series: Geochemical constraints from the Neoarchean western Karelian Province (Finland). Lithos 115, 27-39.

Hutton, D.H.W., 1988. Granite emplacement mechanism and tectonic controls: inferences from deformation studies. Transactions of the Royal Society of Edinburgh, Earth Sciences, 79, 245-255.

Jackson, S.E., Pearson, N.J., Griffin,W.L., Belousova, E.A., 2004. The application of laser ablation-inductively coupled plasma-mass spectrometry to in situ U–Pb zircon geochronology. Chem. Geol. 211, 47–69.

Janousek, V., Farrow, C.M., Erban, V., 2003. GCDkit: new PC software for interpretation of whole-rock geochemical data from igneous rocks. Godschmidt Conf. Abstr., A186.

Jayananda, M., Chardon, D., Peucat, J.-J., Capdevila, R., 2006. 2.61 Ga potassic granites and crustal reworking in the western Dharwar craton, southern India: tectonic, geochronologic and geochemical constraints, Precambrian Res. 150, 1–26.

Kober, B., 1986. Whole-grain evaporation for 207Pb/206Pb-age-investigations on single zircons using a double-filament thermal ion source. Contrib. Mineral. Petrol. 93, 482–490.

Kröner, A., Hegner, E., Wendt, J.I., Byerly, G.R., 1996. The oldest part of the Barberton granitoid-greenstone terrain, South Africa: evidence for crust formation between 3.5 and 3.7 Ga. Precambrian Res. 78, 105–124.

Hawkesworth, C.J., Kemp, A.I.S., 2006. Evolution of the continental crust, Nature 443, 811-817.

Lafon, J.M., Rodrigues, E., Duarte, K.D., 1994. Le granite Mata Surrão: un magmatisme monzogranitique contemporain des associations tonalitiques-trondhjemitiques-granodioritiques archéennes de la région de Rio Maria (Amazonie Orientale, Brésil). Comptes Rendues de la Academie de Sciences de Paris, t. 318, serie II, p. 642- 649.

Leite, A.A.S., Dall'Agnol, R., 1999. Geoquímica e aspectos petrogenéticos do Granito Xinguara, terreno granito-*greenstone* de Rio Maria – Cráton Amazônico. Rev. Bras. Geociências, 23(3), 429-436.

Leite, A.A.S., 2001. Geoquímica, petrogênese e evolução estrutural dos granitóides arqueanos da região de Xinguara, SE do Cráton Amazônico. Federal University of Para. 330p. PhD Thesis. Graduated Program on Geology and Geochemistry, Institute of Geosciences (in Portuguese).

Leite, A. A. S., Dall'Agnol, R., Macambira, M. J. B., Althoff, F. J., 2004. Geologia e geocronologia dos granitóides arqueanos da região de Xinguara (PA) e suas implicações na evolução do terreno granito-greenstone de Rio Maria. Rev. Bras. Geociências, 34, 447-458.

Le Maitre, R.W., 2002. A classification of igneous rocks and glossary of terms. 2nd Edition, London, 193 p.

Ludwig, K.R., 2003. User's Manual for Isoplot/Ex v. 3.00. A Geochronological Toolkit for Microsoft Excel. BGC Special Publication 4, Berkeley, 71 pp.

Macambira, M.J.B., Lafon, J.M., 1995. Geocronologia da Província Mineral de Carajás; Síntese dos dados e novos desafios. Boletim do Museu Paraense Emílio Goeldi, série Ciências da Terra, Belém, 7, 263-287.

Macambira, M.J.B., Lancelot, J., 1996. Time constraints for the formation of the Archean Rio Maria crust, southeastern Amazonian Craton, Brazil. International Geology Review, 38 (12), 1134-1142.

Machado, N., Lindenmayer, Z.G., Krogh, T.E., Lindenmayer, D., 1991. U-Pb geochronology of Archean magmatism and basement reactivation in the Carajás area, Amazon shield, Brazil. Precambrian Res., 49: 329-354.

Martin, H., 1994. The Archean grey gneisses and the gneisses of continental crust. In: Condie, K. C. (ed.) Developments in precambrian geology 11. Archeancrustal evolution, Amsterdam, Elsevier. p. 205-259.

Medeiros, H., 1987. Petrologia da porção leste do Maciço Granodiorítco Rio Maria, sudoeste do Pará. Federal University of Para. 187p. M.Sc. Thesis. Graduated Program on Geology and Geochemistry, Institute of Geosciences (in Portuguese).

Moyen, J.F., Martin, H., Jayananda, M., Auvray, B., 2003. Late Archaean granites: a typology based on the Dharwar Craton (India). Precambrian Res. 127, 103– 123.

Nisbet, E., 1987. The Young Earth: An Introdution to Archean Geology. Allen and Unwin, Boston, 402 pp.

Oliveira, M.A., Dall'Agnol, R., Althoff, F.J., Leite, A.A.S., 2009. Mesoarchean sanukitoid rocks of the Rio Maria Granite-Greenstone Terrane, Amazonian craton, Brazil. J. South Am. Earth Sci.. 27, 146-160.

Paterson, S.R., Vernon, R.H., Tobisch, O.T., 1989. A review of criteria for the indentification of magmatic and tectonic foliations in granitóids. Journal Structural Geology, 11(3), 349-363.

Paterson, S.R., Fowler Jr, T.K., Schmidt, K.L., Yoshinobu, A.S., Yuan, E.S., Miller, R.B., 1998. Interpreting magmatic fabric patterns in plutons. Lithos, 44, 53-82.

Patiño Douce A.E., 2005. Vapor-absent melting of tonalite at 15–32 kbar. J. Petrol. 46, 275–290.

Peccerillo, A., Taylor, S.R., 1976. Geochemistry of Eocene calc-alkaline volcanic rocks from the Kastamonu area, Northern Turkey. Contr. Mineral. Petrol. 58, 63–81.

Rolando, A.P., Macambira, M.J.B. 2003. Archean crust formation in Inajá range area, SSE of Amazonian Craton, Brazil, basead on zircon ages and Nd isotopes. *In*: South American Symposium on Isotope Geology, 4, Salvador. Expanded Abstracts. Salvador. (CD-ROM).

Rogers, J.J.W., 1988. The Arsikere granite of southern India: magmatism and metamorphism of previously depleted crust. Chem. Geol. 67, 155–163.

Rutter, M.J, Wyllie, P.J., 1988. Melting of vapour-absent tonalite at 10 kbar to simulate dehydration-melting in the deep crust. Nature 331:159–160.

Santos, J.O.S., Hartmann, L.A., Gaudette, H.E., Groves, D.I., Mcnaughton, N.J., Fletcher, I. R. 2000. A new understanding of the Provinces of the Amazon Craton based on integration of field and U-Pb and Sm-Nd geochronology. Gondwana Res., 3, 453-488.

Santos, J.S.O., Hartmann, L.A., Faria, M.S., Riker, S.R., Souza, M.M., Almeida, M.E., Mcnaughton, N.J. 2006. A compartimentação do Cráton Amazonas em províncias: avanços ocorridos no período 2000-2006. In: Simpósio de geologia da Amazônia, 9, Belém. Resumos Expandidos, Belém, SBG. (CD-ROM).

Souza, S. Z., Dall'Agnol, R., Althoff, F. J., Leite, A. A. S., Barros, C. E. M., 1996. Carajás mineral province: geological, geochronological and tectonic constrasts on the Archean evolution of the Rio Maria Granite- Greenstone Terrain and the Carajás block. In: Simp. Arch. Terr. South Amer. Plataform, Brasîlia, 1996, Extended abstracts, Brasília, SBG. p 31-32.

Souza, Z.S., Potrel, H., Lafon, J.M., Althoff, F.J., Pimentel, M.M., Dall'Agnol, R., Oliveira, C.G., 2001. Nd, Pb and Sr isotopes of the Identidade Belt, an Archaean greenstone belt of the

Rio Maria region (Carajas Province, Brazil): Implications for the Archaean geodynamic evolution of the Amazonian Craton. Precambrian Res. 109, 293–315.

Stacey, J.S., Kramers, J.D., 1975. Approximation of terrestrial lead isotope evolution by a two-stage model. Earth Planet. Sci. Lett. 26, 207–221.

Skjerlie, K.P., Johnston, A.D., 1992. Vapor-absent melting at 10 kbar of a biotite-bearing and amphibole bearing tonalitic gneiss—Implications for the generation of A-type granites. Geology 20, 263–266.

Singh, J., Johannes, W.,1996. Dehydration melting of tonalites. 2. Compositions of melts and solids. Contrib. Mineral. Petrol.125, 26–44.

Sial, A.N., Toselli, A.J., Saavedra, J., Parada, M.A., Ferreira, V.P., 1999. Emplacement, petrological and magnetic susceptibility characteristic of diverse magmatic epidote-bearing granitoid rocks in Brazil, Argentina and Chile. Lithos, 46, 367-392.

Sylvester, P.J., 1989. Post-collisional alkaline granites. J. Geol., 97, 261-280.

Sylvester, P.J. 1994. Archean granite plutons. In: Condie, K. C. (ed.) Developments in precambrian geology 11. Archean crustal evolution. Amsterdam, Elsevier. p. 261-314.

Tassinari, C.C.G., Macambira, M. 2004. A evolução tectônica do Craton Amazonico. In: Mantesso – Neto, V.; Bartorelli, A.; Carneiro, C.D.R.; Brito Neves, B.B. (Eds.), Geologia do Continente Sul Americano: Evolução da obra de Fernando Flávio Marques Almeida. São Paulo, p. 471-486.

Tullis, J. 1983. Deformation of feldspars. In: RIBBE, P.H. ed. *Feldspars Minerals*. Min. Soc. Amer. p. 297-323 (Reviews in mineralogy, 2).

Tullis, J.; Yund, R.A. 1985. Dynamic recrystallization of feldspar: A mechanism for ductile shear zone formation. Geology, 13: 238-241.

Tulloch, A., 1979. Secondary Ca–Al silicates as low-grade alteration products of granitoid biotite. Contrib. Mineral. Petrol. 69, 105–117.

Vasquez L.V., Rosa-Costa L.R., Silva C.G., Ricci P.F., Barbosa J.O., Klein E.L., Lopes E.S., Macambira E.B., Chaves C.L., Carvalho J.M., Oliveira J.G., Anjos G.C., Silva H.R. 2008. Geologia e Recursos Minerais do Estado do Pará: Sistema de Informações Geográficas – SIG : texto explicativo dos mapas Geológico e Tectônico e de Recursos Minerais do Estado do Pará. Organizadores, Vasquez M.L., Rosa-Costa L.T. Escala 1:1.000.000. Belém: CPRM.

Voll, G., 1976. Recrystallization of quartz, biotite and feldspar from Erstfeld to the Leventina Nappe, Swiss Alps, and its geological significance. Schweizerische Mineralogische und Petrographische Mitteilungen, 56, 641-647.

Watkins, J. M.,. Clemens, J. D., Treloar, P. J., 2007. Archaean TTGs as sources of younger granitic magmas: melting of sodic metatonalites at 0.6–1.2 GPa. Contrib. Mineral. Petrol., 154, 91–110

Capítulo – 4

Petrology of the leucogranodiorite-granite suites: implications for the Archean crustal evolution of the Rio Maria granite-greenstone terrane, Carajás province, Brazil.

José de Arimatéia Costa de Almeida
Roberto Dall'Agnol
Samantha Barriga Dias
Fernando Jacques Althoff

Submetido: Lithos

Dear Mr ALMEIDA,

Your submission entitled "Petrology of the Archean leucogranodiorite-granite suites: implications for the crustal evolution of the Rio Maria granite-greenstone terrane, Carajás province, Brazil." (Research Paper) has been received by Lithos.

Please note that submission of an article is understood to imply that the article is original and is not being considered for publication elsewhere. Submission also implies that all authors have approved the paper for release and are in agreement with its content.

You will be able to check on the progress of your paper by logging on to http://ees.elsevier.com/lithos/ as Author.

Your manuscript will be given a reference number in due course.

Thank you for submitting your work to this journal.

Kind regards,

Journal management

Lithos

Petrology of the Archean leucogranodiorite-granite suites: implications for the crustal evolution of the Rio Maria granite-greenstone terrane, Carajás province, Brazil.

José de Arimatéia Costa de Almeida[1,2,4] (ari@ufpa.br); Roberto Dall'Agnol[1,2] (robdal@ufpa.br); Samantha Barriga Dias[1,2] (samantha@ufpa.br); Fernando Jacques Althoff[1,3] (fjalthoff@gmail.com).

[1]Grupo de Pesquisa Petrologia de Granitóides, Instituto de Geociências (IG), Universidade Federal do Pará (UFPA), Caixa Postal 8608, CEP 66075-900, Belém, Pará, Brasil;

[2]Programa de Pós-Graduação em Geologia e Geoquímica – IG – UFPA.

[3]Curso de Geologia – Campus de Alegre – Universidade Federal do Espírito Santo.

[1,4]Faculdade de Geologia – Campus de Marabá – UFPA.

ABSTRACT

In the Mesoarchean Rio Maria granite-greenstone terrane, the leucogranodiorite-granite (LGdG) suites are mostly represented by the 2.87 Ga Guarantã suite which embraces the Trairão and Azulona granodiorite and the Guarantã granite plutons. These granites were originated around 50 m. y. after the 2.93±0.1 Ga major TTG magmatic event and were approximately coeval with the sanukitoid suites (~2.87 Ga), potassic leucogranites (~2.86 Ga) and the younger TTGs (Água Fria trondhjemite; ~2.86 Ga). The rocks of the LGdG suites are characterised by strongly fractionated REE patterns, with either no Eu anomaly or just discrete negative Eu anomalies, and show enrichment in Ba and, to a lesser degree, in Sr compared with the other Archean granitoids of the RMGGT. The LGdG have strong geochemical affinity with the high-Ca granites or Transitional TTG of the Yilgarn craton. The different models proposed to explain the origin of these granites are still controversial and apparently are not able to explain the genetic processes and evolution of the LGdG of the RMGGT.

The dual geochemical character of the LGdG suites that share some features typical of the TTGs with others more commonly observed in the sanukitoid suites, suggest a complex evolution for these granites and a possible genetic link between them and the mentioned suites. On the basis of modeling and geochemical data we deduced that the LGdG suites could be possibly derived from mixing between a granite magma, similar to the Ba- and Sr-enriched samples of the

Guarantã suite, and trondhjemitic liquids. The granite magmas participating in the mixture were originated by fractional cystallization of 35% of a sanukitoid magma of granodioritic composition leaving a residue consisting of plagioclase (46.72%), hornblende (39.05%), clinopyroxene (10.36%), magnetite (3.12%), ilmenite (0.7%) and allanite (0.06%). The large compositional variations observed in the Guarantã suite can be apparently explained by mixing in different proportions between the granite and trondhjemitic liquids. This large spectrum of variation could be yet augmented if it is admitted that fractional crystallization played a significant role in the evolution of the liquids originated by mixing processes.

Keywords: leucogranodiorite-granite suites, Mesoarchean, sanukitoids, TTGs, mixing

1. Introduction

About 70% of the rocks forming Archean cratons are tonalite-trondhjemite-granodiorite (TTG) suites and granites with subordinate sanukitoid suites (Condie, 1993). The TTGs are better known and generally correspond to the gneissic basement of preserved Archean continental crust (Barker and Arth, 1976; Barker et al., 1979; Martin et al., 2005; Moyen et al., 2007; Champion and Smithies, 2007; Almeida et al. a, submitted, Guimarães et al. a, submitted). TTGs constitute about 70 % in volume of the granitoids exposed in Archean cratons (Condie, 1993). The Archean granites received in the past relatively less attention, but this was changed as demonstrated by Sylvester (1994). Most of them were emplaced during the later evolution of the Archean craton (around 2.7-2.5 Ga; Goodwin, 1991; Sylvester, 1994), being usually intrusive in greenstone belts and TTG granitoids.

The advances in the knowledge of the Archean granites have contributed to identify important geochemical contrasts between these rocks that can be calc-alkaline, alkaline, or even strongly peraluminous rocks (Day and Weiblen, 1986; Laflech et al., 1991; Bourne and L'Heureux, 1991; Sylvester, 1994; Champion and Sheraton, 1997; Frost et al., 1998; Champion and Smithies, 2001; Moyen et al., 2003). Such diversity suggests that they are produced by contrasting petrogenetic process in various geodynamic settings.

A suite of granodiorite-granite rocks that shares some geochemical features with typical Archean TTG suites has been only recently introduced into the literature. The rocks of that suite

are characterised by strongly fractionated REE patterns with either no Eu anomaly or just small negative Eu anomalies, but when compared to TTGs *stricto sensu* have higher LILE contents, show strong enrichment in K_2O and Rb with increasing differentiation, and tend toward more siliceous composition (68%-77% SiO_2; Champion and Smithies, 2001, 2003). These rocks are widespread in many Archean terranes and are either contemporaneous (e.g., GG suites of the Wyoming Province; Frost et al., 2006) or postdate (e.g., 2.61 Ga granites of the western Dharwar craton; Jayananda et al., 2006; Pilbara craton, Champion and Smithies, 2007) true TTGs. The term "transitional TTGs" was proposed to describe a group of granites initially identified in the Pilbara and Yilgarn cratons (Champion and Smithies 2001, 2003). These rocks comprise over 60% of the granitic rocks in the Yilgarn craton and are also common in the Wyoming Province (Frost et al., 2006), Tanzania craton (Opiyo-Akech et al., 1999) and, more recently, have been described in the Dharwar craton (Jayananda et al., 2006; Sukanta et al., 2009; Prabhakar et al., 2009). Their origin and geodynamic setting are still unclear. However, Champion and Smithies (2003) claimed that the petrogenesis of the transitional TTGs requires the involvement of pre-existing crust.

2.87 Ga leucogranodiorite-granite (LGdG) associations have recently been identified in the Mesoarchean Rio Maria granite-greenstone terrane (RMGGT) in the southern part of the Archean Carajás Province (Dias, 2009; Guimarães et al. b, submitted), southeastern of the Amazonian craton. These rocks embrace the Guarantã suite, the Grotão granodiorite and similar granitic rocks (Almeida et al. b, submitted). This Archean granite group has petrographic and geochemical characteristics broadly similar to transicional TTGs (Almeida et al. b, submitted). The granitoids of the Guarantã suite are ~2.87 Ga old and were emplaced at least ca. 50 m.y after the last major peak of TTG magmatism (2.93 ± 0.1 Ga; Almeida et al. a, submitted). These granites generally preserve their textural igneous features (Althoff et al., 2000; Dias, 2009; Almeida et al. a, submitted) and are relatively well exposed in the RMGGT. In this paper, we refine the characterization of the LGdG suites of the RMGGT based on recent field work, petrography, geochronology (Almeida et al. b, submitted) and new whole rock geochemical data, with emphasis in the Guarantã suite (Dias, 2009). The results allow us to discuss the geochemical signature and petrogenesis of these rocks, which will be crucial for a better understanding of the role played by crustal reworking in their origin, as well as of the changes in geodynamic process that occurred during the stabilization of the Rio Maria crust in the final of the Mesoarchean.

2. Geological Setting

The Carajás province (Fig.1a) corresponds to the major Archean crustal segment of the Amazonian craton (Machado et al., 1991; Macambira and Lafon, 1995; Dall'Agnol et al., 2000; Rämö et al., 2002; Dall'Agnol et al., 2006). It has been included into the Central Amazonian province by Tassinari and Macambira (2004) or considered an independent tectonic province (Santos, 2003). Based on the age and nature of the supracrustal sequences, age of the magmatic and deformational events, nature of the granitoids series and tectonic setting, the Carajás province has been divided into two Archean tectonic domains (Fig.1a): the 3.0–2.86 Ga Rio Maria granite-greenstone terrane (Macambira and Lafon, 1995; Dall'Agnol et al., 2006; Vasquez et al., 2008) and the rift-related Carajás Basin dominantly composed of 2.76–2.55 Ga metavolcanic rocks, banded iron formations, and granitoids (Machado et al., 1991; Macambira and Lafon, 1995; Barros et al., 2001). The cratonization of the RMGGT occurred at the end of the Mesoarchean and that of the Carajás Basin during the Neoarchean. At around 1.88 Ga, both domains were intruded by A-type granites (Dall'Agnol et al., 2005).

The LGdG suites are exposed in the Rio Maria granite-greenstone terrane (Fig. 1b), which is composed of 2.97 to 2.9 Ga greenstone belts (Fig. 2) consisting of meta-ultramafic (komatiites), metamafic (basalts and gabbros), and intermediate to felsic metavolcanic rocks, with intercalations of metagraywackes, all grouped into the Andorinhas Supergroup (Souza et al., 2001). These rocks are intruded by a variety of Archean granitoids (Dall'Agnol et al., 2006) originated between 2.96 and 2.86 Ga (Fig. 2). The older granitoids of the RMGGT are represented by typical Archean TTG suites (Huhn et al., 1988; Althoff et al., 2000; Souza et al., 2001; Leite et al., 2004; Dall'Agnol et al., 2006; Vasquez et al., 2008; Guimarães et al., submitted a; Almeida et al. a, submitted), which exhibit major age peaks at 2.96±0.2 Ga (Mogno trondhjemite and the older rocks of the Arco Verde tonalite) and 2.93±0.1 Ga (Caracol tonalitic complex, Mariazinha tonalite, and the younger rocks of the Arco Verde tonalite; Almeida et al. a, submitted; Fig 2). Contact relationships of the TTGs and the greenstone sequences are not exposed in the field, but enclaves of rocks similar to those of the greenstone belts are found in these granitoids. After a 90 to 50 m.y., time interval, the mentioned TTG suites were intruded by several distinct granitoids emplaced between 2.87 and 2.86 Ga. These younger granitoids are represented by: (1) The Rio Maria sanukitoid suite (~2.87 Ga; Oliveira et al., 2009; Figs. 1b, 2)

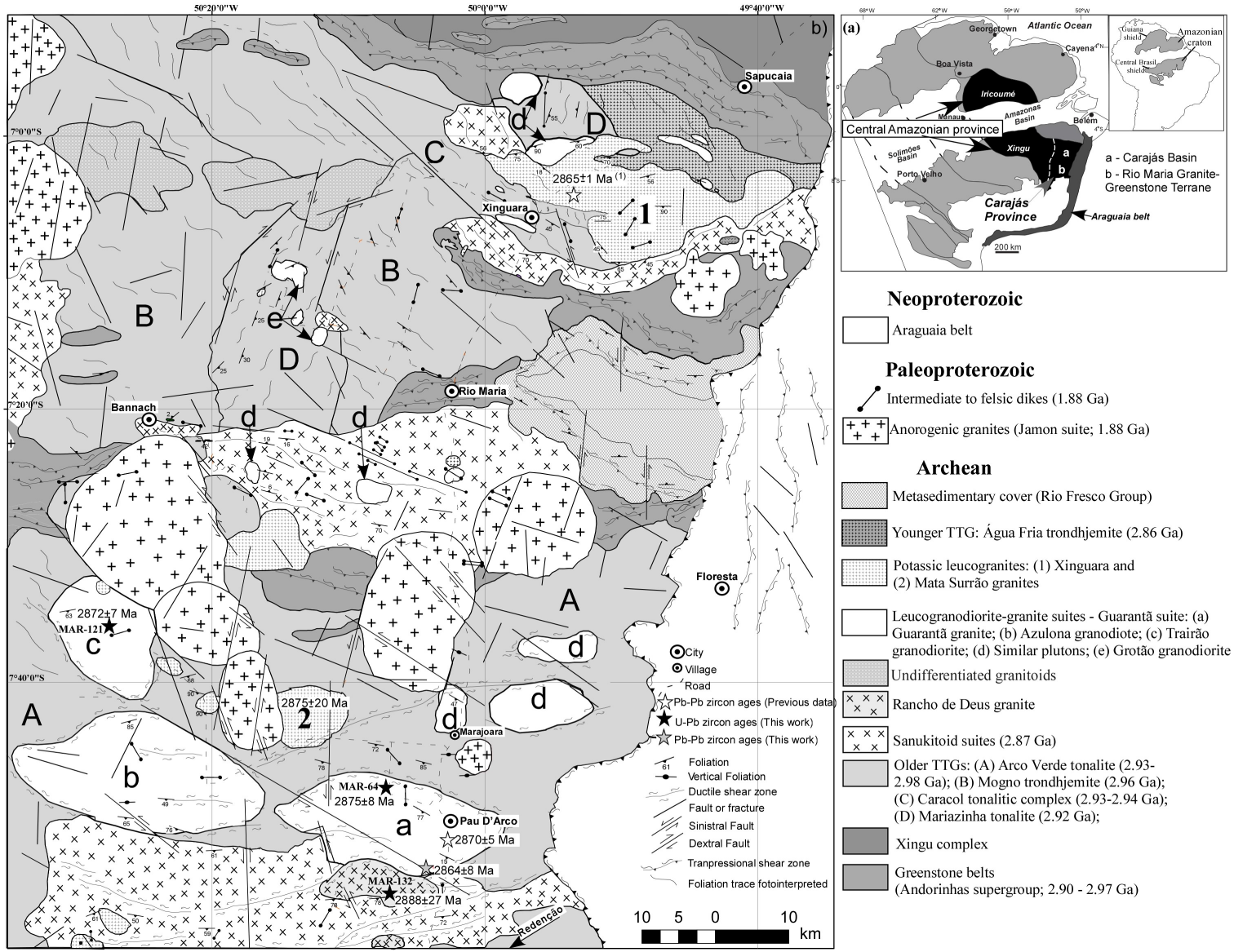

Figure 1 - (a) - Location of the studied area in the Amazonian craton. (b) Geological map of the Rio Maria granite-greenstone terrane.

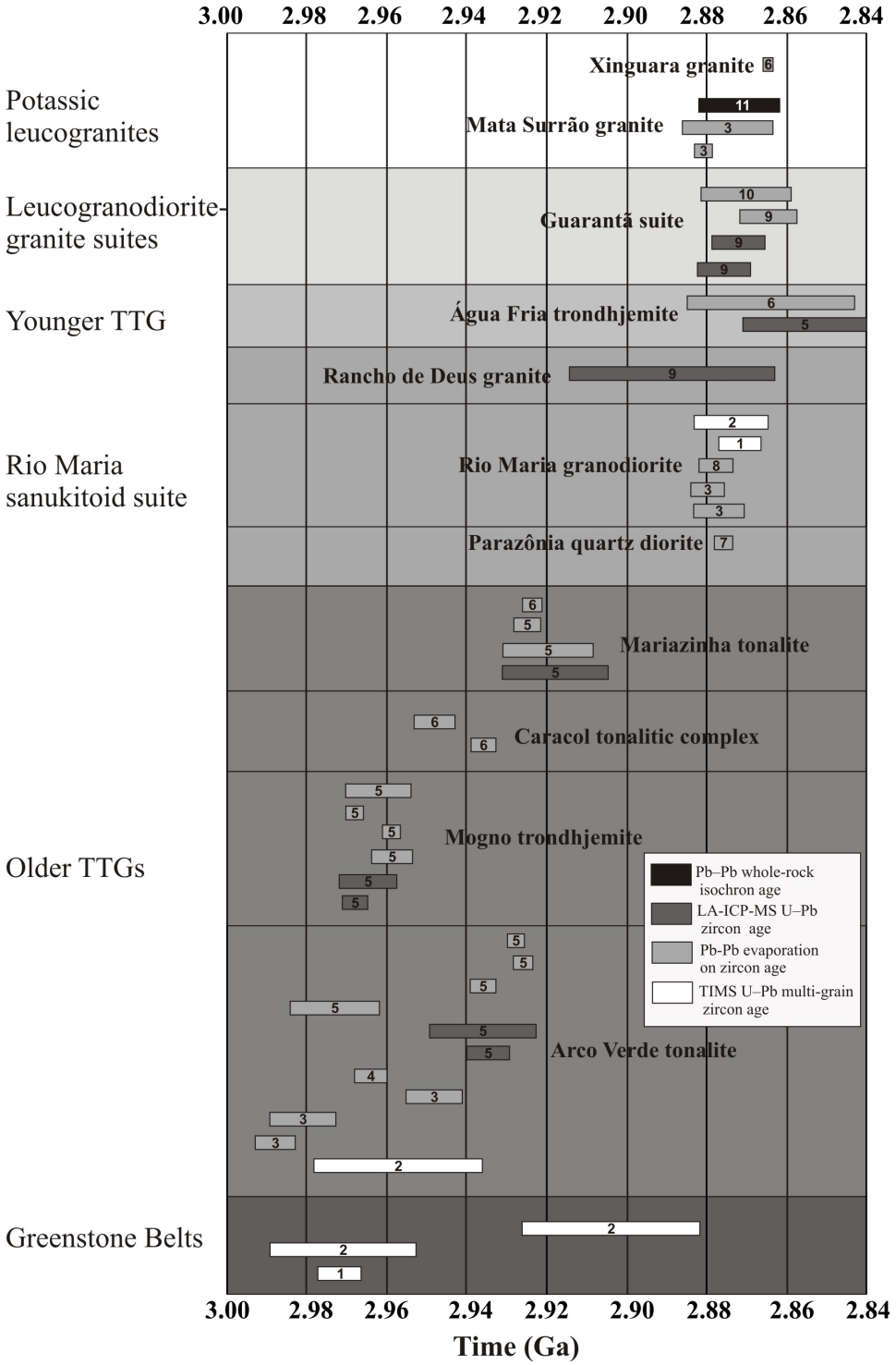

Figure 2 - Geochonological overview of the previous available data for Archean units of the Rio Maria granite-greenstone terrane. Data Source: (1) Pimentel & Machado (1994), (2) Macambira (1992), (3) Rolando & Macambira (2003), (4) Vasquez et al., (2008), (5) Almeida et al. a, submitted, (6) Leite et al., (2004), (7) Almeida (unpublished data), (8) Dall'Agnol et al., (1999), (9)Almeida et al. b submitted, (10) Althoff et al., (2000), (11) Lafon et al., (1994).

composed dominantly by granodiorites, with associated mafic and intermediate rocks, forming enclaves or, locally, small bodies. These rocks are intrusive in the greenstone belts and in the older TTG series and are intruded by the Xinguara granite and Água Fria trondhjemite (Leite et al., 2004); (2) A restricted occurrence of younger TTGs exposed only in the Xinguara area, represented by the Água Fria trondhjemite. It was dated at ca. 2.86 Ga and is intrusive in the Caracol tonalitic complex and coeval with the Xinguara potassic leucogranite (Leite et al., 2004, Almeida et al. a, submitted; Figs. 1b, 2); (3) ~2.87-2.86 Ga potassic leucomonzogranites that embrace the Xinguara (Leite et al., 2004) and Mata Surrão (Duarte, 1992) plutons (Almeida et al. b, submitted; Figs. 1b, 2) and (4) ~2.87 Ga leucogranodiorites and leucogranites (Althoff et al., 2000; Dias, 2009; Almeida et al. b, submitted; Figs. 1b, 2). The last shearing deformational event identified in this terrane occurred at around 2.86 Ga (Althoff et al., 2000; Souza et al., 2001; Leite, 2001) and, after it, the terrane remained stable until the emplacement of the Paleoproterozoic A-type granites and associated dikes.

3. Geologic features of the leucogranodiorite-granite (LGdG) suites

The LGdG suites are dominantly exposed in the Marajoara area (Fig. 1b), where they are represented by the Guarantã granite, Azulona granodiorite and Trairão granodiorite plutons which constitute the Guarantã suite (Dias, 2009; Almeida et al. b, submitted). Small granitic stocks found in the Bannach and Xinguara areas and the Grotão granodiorite (Guimarães et. b, submitted), exposed to the SW of Xinguara (Fig. 1b), are geochemically similar to the rocks of the Guarantã suite and were embraced in the same Archean granitoid group (Almeida et al. b, submitted; Fig. 1b). These plutons and stocks (2-20 km in diameter; Fig 1b) are normally elliptic in plant and elongated along the E-W direction. In spite of their location in the Amazonian region, these Archean granitic rocks are relatively well exposed because they occur in dominantly deforested areas and fresh samples are available.

There is no significant topographic contrast between the Guarantã suite plutons and the TTG country rocks and the boundaries of the plutons were defined using airborne gamma-ray spectrometry, field relationships and systematic sampling, followed by petrographic and geochemical studies. The granites of the Guarantã suite crosscut the Arco Verde tonalite and contain decimeter-sized, fine-grained, microdioritic or medium-grained tonalitic xenoliths

especially along the contacts between both units (Fig. 3a). On the other hand, the field relationships of the Guarantã suite with the contemporaneous sanukitoid suites were not observed. The rocks of the Guarantã suite are strongly deformed and display a widespread and well-developed E-W to WNW–ESE trending subvertical foliation associated to a subhorizontal stretching lineation (Althoff et al., 2000; Almeida et al., 2008; Dias, 2009). These structures are outlined by the preferred orientation of biotite, alkali feldspar megacrysts (Fig. 3b) and quartz ribbons (Althoff et al., 2000). The plutons of the Guarantã suite were affected by E–W trending sub-vertical metre do decametre-thick ductile shear zones, most of them located along their contacts with the Arco Verde tonalite (Fig 1b). Quartz veins, epidote+chorite veinlets and mafic dykes transect these plutons. The Grotão granodiorite was recently mapped (Guimarães et al. b, submitted). It occurs to the southeast of Xinguara as small stocks formed by quite homogeneous fine, even-grained rocks that cross-cut the Mariazinha tonalite (Fig. 1b).

LA-ICP-MS U-Pb zircon ages were recently obtained for representative rocks of the Guarantã and Trairão plutons of the Guarantã suite. The Guarantã granite yielded a U-Pb zircon age of 2875±8 Ma, while the Trairão granodiorite was dated at 2872±7 Ma (Almeida et al. b, submitted). Older inherited zircons with probable ages around 2.90 to 3.0 Ga are relatively common in the dated samples. A pluton compositionally similar to those of the Guarantã suite located close to Floresta town yielded a poorly defined Pb-evaporation age on zircon of 2930±19 Ma (Althoff et al., 2000). This age needs a more accurate determination because it could also be related to an inherited component. Whatever the interpretation of this specific case, the strong presence of inherited zircons in the Guarantã suite is apparently clear and it indicates the involvement of older crustal rocks in the magma sources of this unit.

4. Petrography

Coarse-grained pink or pinkish gray porphyritic rocks are dominant in most of the plutons of the Guarantã suite (Fig 3c), with minor equigranular, coarse- or medium-grained, or seriated, coarse- to medium-grained, or medium- to fine-grained rocks. In the porphyritic facies, the K-feldspar phenocrysts (5-20 mm) are set in a medium-grained matrix composed of quartz, plagioclase, microcline, biotite, epidote, and accessory minerals. In some samples, the K-feldspar phenocrysts show a strong preferential orientation (Fig.3b).

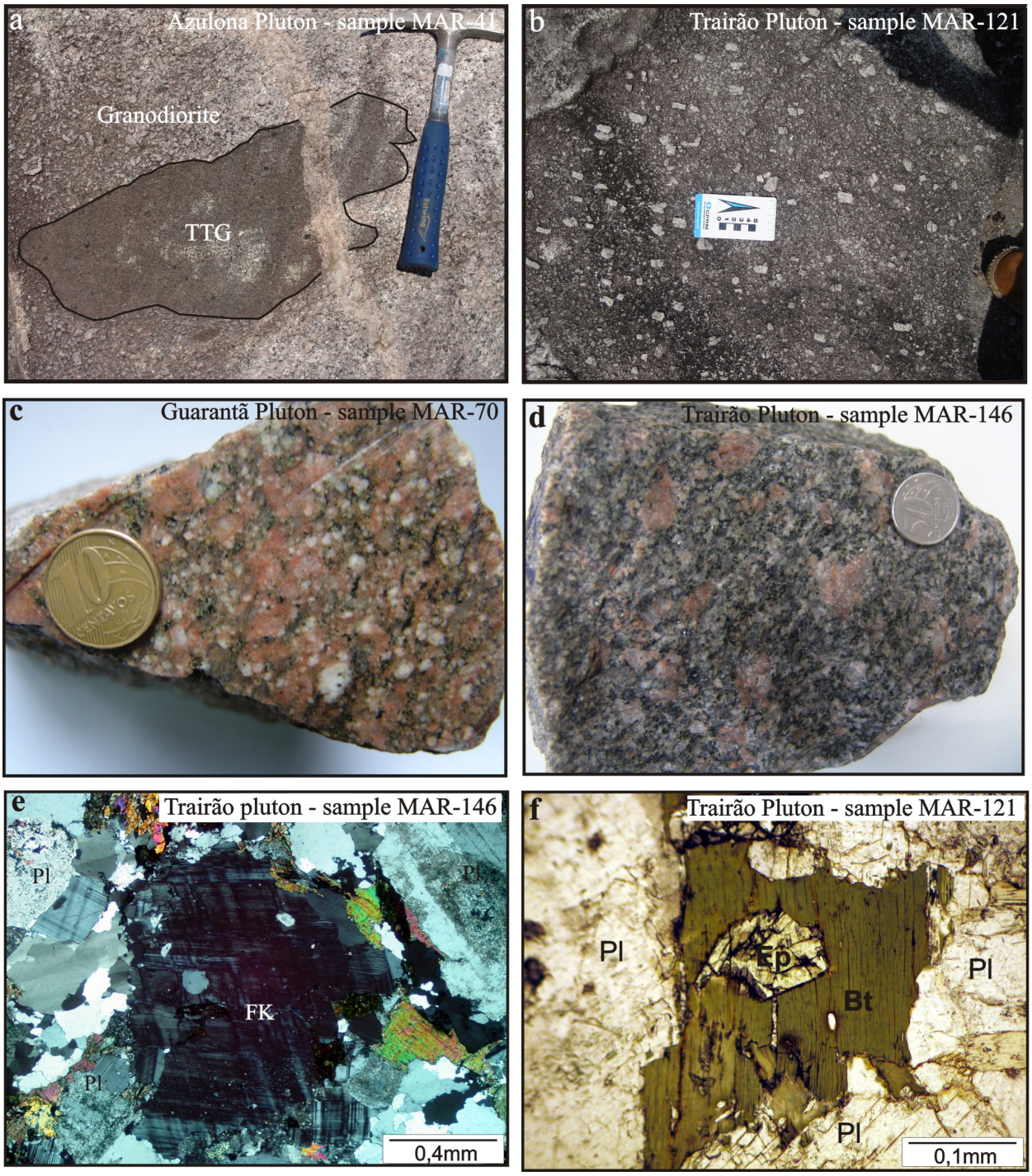

Figure 3 - Features of the Guarantã suite (a) Enclave of the Arco Verde tonalite in Azulona leucogranodiorite; (b) Oriented alkali feldspar phenocrysts defining a WNW–ESE trending subvertical foliation; (c) Hand sample of the foliated porphyritic pink monzogranite from Guarantã pluton; (d) Hand sample of the porphyritic pinkish gray granodiorite from Trairão pluton; (e) K-feldspar phenocrystal in a medium-grained equigranular matrix of quartz,

plagioclase, microcline, biotite, epidote, and accessory minerals. (f) Euhedral magmatic epidote enclosed by biotite. Source of the photos a, b, c, d, e: Dias (2009). Abbreviations: Bt = biotite; Ep= epidote; Pl=plagioclase; Qtz=quartz.

The plutons of the Guarantã suite are composed of granodiorite and monzogranite with mafic minerals content normally lower than 7 vol. % (Fig. 4). In all plutons, biotite, generally associated with magmatic epidote, is the most abundant ferromagnesian phase, and the primary accessory mineral assemblage includes zircon, apatite, allanite, titanite, and magnetite. Chlorite, zoisite, and white mica occur as secondary minerals. The earliest mineral phases in the crystallization sequence of the Guarantã rocks are apatite, zircon, magnetite, and allanite. Euhedral to subhedral sodic plagioclase crystals are the next in sequence. The biotite began to crystallize after the plagioclase and displays textural evidence of equilibrium and simultaneous crystallization with euhedral epidote. Quartz probably initiated its crystallization synchronously or a little later than biotite + epidote, whereas titanite began to crystallize after these minerals. K-feldspar is probably a little later phase forming subhedral phenocrysts that show irregular border zones (Vernon and Paterson, 2008). Chlorite, zoisite, and white mica were generated in the subsolidus stage.

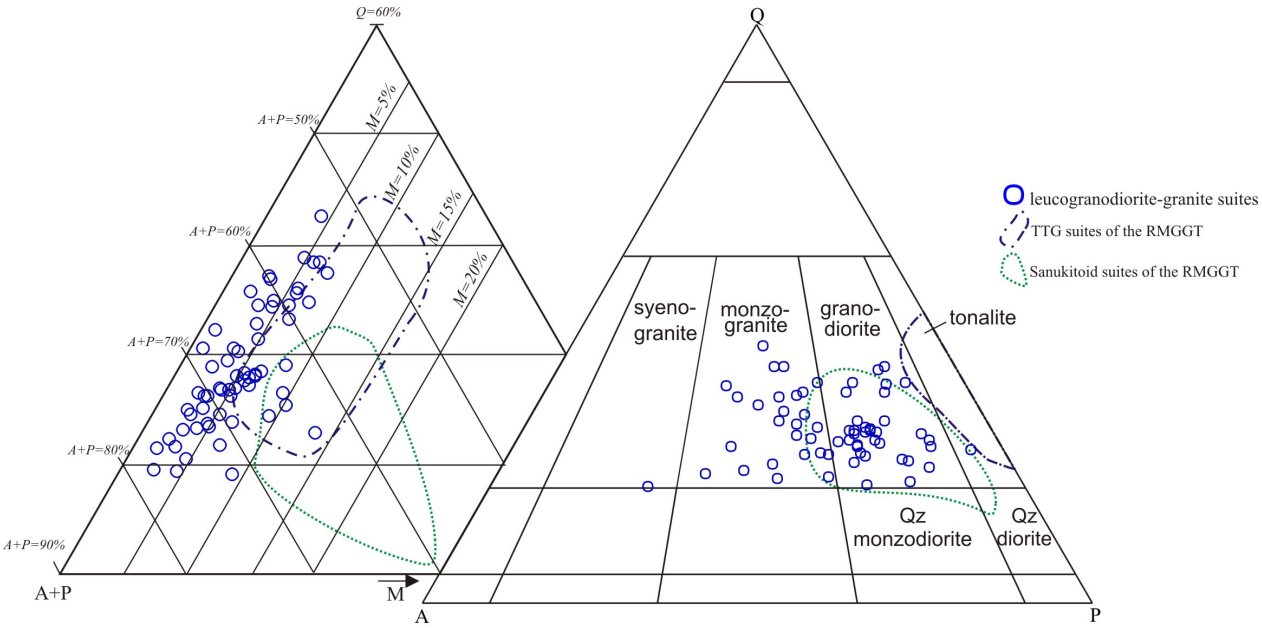

M= mafic minerals; Q=quartz; A=álcali-feldspar; P=plagioclase

Figure 4 - QAP and Q-(A+P)-M for the leucogranodiorite-granite suites of the Rio Maria granite-greenstone terrane. The field of the sanukitod and TTG suites are also plotted for comparison.

There are two textural epidote types that we consider of magmatic origin: Epidote with zoned allanite core and euhedral to subeuhedral epidote associated with and partially enclosed by biotite (Fig. 3d). Primary epidote crystals show high birefringence and microprobe chemical data are consistent with the hypothesis of their magmatic origin (25-33 mol % of pistacite component; J.A.C. Almeida, unpublished data). Magmatic epidote has been also noticed in the TTG suites (Leite, 2001; Almeida et al. a, submitted; Guimarães et al. a, submitted), Archean potassic leucogranites (Mata Surrão and Xinguara plutons; Duarte, 1992; Leite, 2001; Almeida et al. b, submitted) and in the Rio Maria sanukitoid suite (Oliveira et al., 2009) of the RMGGT.

Part of the leucogranodiorites and leucogranites that occur to the north of Xinguara and to the east of Bannach (Fig. 1b) is similar in texture to the porphyritic varieties of the Guarantã suite. On the other hand, the Grotão granodiorite, despite its similarities in mineralogy to the other granites of this group, is distinct in texture, showing typically an equigranular, fine-grained texture.

5. Geochemistry

5.1. Major Elements

Geochemical analyses of the LGdG suites of the RMGGT are listed in Table 1 and analytical procedures are described in Appendix A. These rocks span a narrow compositional range (SiO_2 contents between 68.2 and 75.8 wt %). TiO_2, Al_2O_3, Fe_2O_{3t}, MgO, and CaO decrease and K_2O and K_2O/Na_2O increase parallel to SiO_2 and most oxides show scattered trends in Harker diagrams (Fig. 5). Almost all analyzed samples show relatively high Al_2O_3 (14 to 16 wt %) and are poor in ferromagnesian elements (Fe_2O_{3t} + MgO + TiO_2 + MnO = 1.2 to 5.0 wt %). The MgO contents vary from 0.2 to 1.4 wt % (mean of 0.45 wt %) and Na_2O vary generally between 4.0 to 5.4 wt %. The Mg# values are moderate to high (mostly 0.30-0.48; mean = 0.36; Table 1) and FeO_t/FeO_t+MgO ratios are usually lower than 0.8. They typically have moderate K_2O/Na_2O values (normally between 0.5-1.0), higher than those of TTGs (Fig. 5f) and lower compared to those of the potassic leucogranites (Almeida et al. b, submitted). The LGdG rocks are metaluminous to peraluminous (Fig. 6a) and mainly consist of granodiorites and monzogranites, as shown in the R1-R2 (De La Roche et al., 1980) and Q-P (Debon and Le Fort,

Table 1 - Chemical composition of the leucogranodiorite-granite suites of the Rio Maria granite-greenstone terrane.

	Leucogranodiorite-granite suites																										
	Suite Guarantã																										
	Guarantã granite														Azulona granodiorite									Trairão granodiorite			
Element	Granodiorites				Monzogranites										Granodiorites					Monzogranites				Granodiorites		Monzogranites	
Sample	MAF-33 (1)	MAR-14A (1)	MAR-64A (1)	MAR-10A (2)	MAR-70A (2)	MAR-72A (2)	MAR-07A (2)	MAF-58 (2)	MAR-09A (2)	F77-92-29 (3)	MAR-164A (1)	F77-92-31 (5)	MAR-167 (1)	MAR-103A (1)	MAR-50A (2)	MAR-93A (1)	MAR-102 (1)	MAR-97A (1)	MAR-38A (2)	MAF-64 (2)	MAR-101A (2)	MAR-104 (2)	MAR-146 (1)	MAR-123 (1)	MAR-121 (1)	MAR-114 (1)
SiO_2	68.86	71.39	72.39	75.84	70.12	70.42	71.03	71.13	71.20	71.24	71.71	72.56	74.39	71.34	71.36	71.92	72.03	72.27	70.12	70.55	72.07	73.82	68.20	70.08	70.32	70.89
TiO_2	0.45	0.27	0.19	0.11	0.24	0.17	0.17	0.22	0.16	0.29	0.17	0.12	0.12	0.26	0.20	0.21	0.21	0.17	0.18	0.38	0.15	0.08	0.40	0.27	0.21	0.25
Al_2O_3	15.14	15.45	14.93	13.34	15.30	15.91	15.17	15.08	14.93	14.96	15.22	14.58	14.10	14.86	15.39	15.52	14.90	14.99	15.56	14.60	15.00	14.20	15.30	15.40	15.66	14.60
$Fe_2O_{3(t)}$	3.21	1.55	1.50	0.90	1.89	1.25	1.36	1.66	1.25	1.61	1.26	1.13	1.04	2.15	1.66	1.40	1.68	1.40	1.25	1.80	1.14	0.90	2.97	1.95	1.71	2.10
MnO	0.04	0.02	0.02	0.02	0.03	0.02	0.02	0.02	0.03	0.02	0.02	0.02	0.01	0.03	0.03	0.02	0.02	0.02	0.02	0.02	0.02	0.03	0.03	0.03	0.02	0.03
MgO	1.03	0.45	0.45	0.26	0.68	0.38	0.40	0.58	0.37	0.39	0.35	0.29	0.19	0.61	0.54	0.36	0.51	0.42	0.39	0.27	0.29	0.22	1.38	0.77	0.59	0.82
CaO	2.81	2.19	2.05	1.70	1.74	1.73	1.62	2.04	1.46	1.37	1.90	1.43	1.17	2.21	1.97	2.32	2.19	1.97	1.74	0.72	1.39	1.09	3.00	2.31	2.09	2.03
Na_2O	4.44	4.90	4.92	4.47	4.73	5.34	4.93	4.72	4.78	4.62	5.02	4.75	4.59	4.44	5.17	5.00	4.92	4.86	4.48	4.07	4.55	4.12	4.91	4.87	4.98	4.56
K_2O	2.68	2.87	2.64	2.19	3.85	3.55	3.85	3.05	4.46	4.72	3.24	3.94	3.43	2.76	2.51	2.73	2.46	2.98	4.86	6.20	4.51	4.54	2.41	2.91	3.31	3.44
P_2O_5	0.16	0.09	0.07	0.04	0.12	0.05	0.09	0.07	0.08	0.12	0.06	0.07	0.05	0.09	0.08	0.05	0.08	0.06	0.08	0.11	0.06	0.03	0.16	0.10	0.08	0.10
LOI	1.10	0.80	0.70	0.90	1.00	0.90	1.10	1.20	1.00	0.95	0.80	0.80	0.80	1.00	0.90	0.40	0.90	0.70	1.00	0.90	0.60	0.90	1.00	1.00	0.70	1.00
Total	99.92	99.98	99.86	99.77	99.70	99.72	99.74	99.77	99.72	100.29	99.75	99.69	99.89	99.75	99.81	99.93	99.90	99.84	99.68	99.62	99.78	99.93	99.76	99.69	99.67	99.82
Ba	1173	978	1066	1436	1873	1558	1854	1578	1547	1722	1020	1056	1081	991	964	918	785	1247	2230	1962	1363	697	1203	1170	1436	1218
Sr	554	389	650	639	830	778	757	739	630	665	534	577	366	354	643	484	567	696	767	519	571	212	919	737	725	673
Rb	78	95	70	57	94	91	103	60	121	142	81	138	76	97	59	62	96	64	173	252	170	180	74	84	78	128
Zr	132	128	96	72	147	106	107	122	112	201	82	95	71	129	91	82	100	90	98	356	101	86	137	112	92	104
Y	12.6	5.7	6.3	55.9	9.7	7.8	6.8	6.6	23.8	3.3	6.2	8.1	7.0	8.0	7.9	12.2	6.4	5.1	10.9	3.8	6.8	6.3	9.4	11.6	3.1	40.5
Hf	3.7	3.8	3.2	1.7	3.7	3.0	2.4	3.0	3.5	4.7	2.7	3.1	2.5	4.0	2.8	2.5	3.8	2.7	2.8	7.6	2.8	2.9	4.1	4.2	3.1	4.1
Nb	6.1	5.4	6.7	3.9	7.3	3.3	6.0	4.8	7.1	5.0	5.6	13.2	4.8	8.1	3.6	3.7	6.6	4.2	5.7	7.2	5.1	3.4	5.6	5.5	4.2	6.3
Ta	1.7	2.1	2.4	0.5	0.7	0.3	0.6	0.4	0.5	n.d	2.1	n.d	1.5	2.3	0.3	1.9	2.7	1.9	0.5	0.3	0.4	0.3	1.8	2.1	2.1	2.0
Ni	7.6	3.4	7.5	3.1	9.6	4.1	4.4	5.9	4.6	0.0	5.2	n.d	3.6	9.6	6.6	3.3	8.1	7.0	4.6	0.5	2.7	2.6	18.6	10.6	8.1	12.4
Cu	54.2	6.6	26.6	6.5	2.2	1.5	2.3	2.0	2.6	0.0	6.3	n.d	31.0	118.3	4.1	9.7	89.8	53.7	3.9	2.3	2.6	2.3	18.2	13.1	10.4	67.8
Th	5.0	6.9	5.0	2.4	9.7	4.3	7.3	3.2	9.7	22.3	3.0	15.4	4.7	5.9	2.5	4.2	3.3	2.3	2.7	35.8	8.3	16.5	5.0	5.1	4.6	7.6
Zn	47	39	46	26	48	42	37	36	46	n.d	31	n.d	47	39	41	38	46	36	29	50	31	32	52	40	28	43
Ga	20	21	21	15	19	20	19	18	20	21	20	25	17	20	21	16	24	21	19	19	20	18	20	19	19	20
La	56.80	25.70	18.00	75.10	35.00	23.90	21.70	18.10	29.40	62.45	14.00	20.17	22.60	26.60	15.70	28.00	15.00	15.70	15.90	104.10	18.10	14.90	31.60	32.10	13.00	27.50
Ce	80.70	46.20	32.90	65.60	68.20	36.80	40.10	34.20	54.40	113.50	26.10	38.94	26.00	46.10	29.80	46.40	28.00	28.70	34.30	177.80	46.80	24.60	63.80	47.60	29.50	44.20
Pr	10.07	4.79	3.54	17.88	8.07	4.91	4.88	4.13	6.70	10.80	2.88	4.01	3.85	4.41	3.71	5.26	3.15	3.16	4.78	19.00	4.04	3.27	7.18	6.84	2.51	5.73
Nd	36.00	17.00	12.30	74.30	29.30	19.50	18.00	16.30	23.80	33.20	9.70	14.84	11.50	13.50	12.70	16.90	11.00	10.00	18.30	57.90	15.80	11.30	27.40	23.90	8.10	20.00
Sm	4.90	2.40	1.90	13.97	4.74	2.94	2.94	2.70	4.06	3.99	2.00	2.45	1.60	2.00	2.44	2.80	2.10	1.90	3.75	5.60	2.33	1.85	4.50	4.30	1.30	4.00
Eu	1.22	0.67	0.53	3.87	1.17	0.74	0.69	0.62	0.94	1.00	0.40	0.76	0.60	0.51	0.67	0.72	0.53	0.50	0.83	1.19	0.61	0.53	1.04	1.11	0.38	1.07
Gd	2.98	1.66	1.29	13.45	3.16	2.03	2.03	1.79	3.62	2.41	1.17	1.78	1.36	1.25	1.85	1.83	1.21	1.06	2.69	2.42	1.61	1.59	2.58	2.90	0.71	3.56
Tb	0.44	0.22	0.25	1.96	0.40	0.26	0.25	0.26	0.48	0.20	0.17	0.24	0.19	0.22	0.27	0.30	0.25	0.25	0.38	0.23	0.22	0.22	0.38	0.39	0.12	0.60
Dy	2.07	1.09	0.95	10.36	1.86	1.41	1.33	1.28	2.71	0.86	0.78	1.34	0.68	1.19	1.34	1.83	1.24	0.92	2.08	0.91	1.16	1.16	1.78	1.82	0.51	3.87
Ho	0.38	0.17	0.16	2.11	0.31	0.27	0.23	0.23	0.55	0.11	0.18	0.25	0.11	0.26	0.25	0.35	0.25	0.16	0.37	0.09	0.21	0.21	0.26	0.29	0.13	0.88
Er	0.92	0.43	0.60	5.07	0.88	0.67	0.64	0.60	1.58	0.28	0.52	0.56	0.44	0.72	0.69	1.14	0.66	0.52	1.11	0.24	0.59	0.62	0.81	0.89	0.36	3.17
Tm	0.15	0.07	0.08	0.73	0.15	0.10	0.11	0.09	0.25	0.03	0.08	0.09	0.07	0.11	0.11	0.18	0.09	0.06	0.19	0.05	0.09	0.10	0.14	0.14	0.08	0.47
Yb	0.88	0.47	0.63	3.82	0.85	0.57	0.57	0.52	1.46	0.20	0.63	0.61	0.30	0.72	0.57	1.00	0.56	0.26	1.14	0.23	0.58	0.63	0.74	0.69	0.43	2.53
Lu	0.13	0.05	0.08	0.50	0.12	0.08	0.09	0.07	0.22	0.03	0.07	0.10	0.07	0.09	0.08	0.14	0.08	0.07	0.15	0.04	0.09	0.09	0.10	0.11	0.06	0.47
A/CNK	0.99	1.02	1.02	1.04	1.01	1.01	1.00	1.02	0.97	0.98	1.00	0.99	1.05	1.04	1.04	1.01	1.01	1.01	0.99	0.99	1.01	1.04	0.95	1.00	1.01	0.98
K_2O/Na_2O	0.60	0.59	0.54	0.49	0.81	0.66	0.78	0.65	0.93	1.02	0.65	0.83	0.75	0.62	0.49	0.55	0.50	0.61	1.08	1.52	0.99	1.10	0.49	0.60	0.66	0.75
$Fe_2O_{3(t)}$+MgO+ TiO_2+MnO	4.73	2.29	2.16	1.29	2.84	1.82	1.95	2.48	1.81	2.31	1.80	1.56	1.36	3.05	2.43	1.99	2.42	2.01	1.84	2.47	1.60	1.23	4.78	3.02	2.53	3.20
#Mg	0.39	0.37	0.37	0.36	0.42	0.38	0.37	0.41	0.37	0.32	0.36	0.34	0.27	0.36	0.39	0.34	0.38	0.37	0.38	0.23	0.34	0.33	0.48	0.44	0.41	0.44
Sr/Y	4.19	3.03	6.79	8.83	5.66	7.33	7.11	6.05	5.63	3.31	6.54	6.11	5.19	2.75	7.10	5.93	5.65	7.76	7.81	1.46	5.67	2.45	6.70	6.56	7.90	6.47
Rb/Sr	0.59	0.74	0.74	0.79	0.64	0.86	0.97	0.49	1.08	0.71	0.99	1.46	1.08	0.76	0.65	0.76	0.95	0.71	1.76	0.71	1.69	2.09	0.54	0.74	0.85	1.23
Rb/Ba	0.07	0.10	0.07	0.04	0.05	0.06	0.06	0.04	0.08	0.08	0.08	0.13	0.07	0.10	0.06	0.07	0.12	0.05	0.08	0.13	0.12	0.26	0.06	0.07	0.05	0.10
Ba/Sr	2.12	2.51	1.64	2.25	2.26	2.00	2.45	2.14	2.46	2.59	1.91	1.83	2.95	2.80	1.50	1.90	1.38	1.79	2.91	3.78	2.39	3.29	1.31	1.59	1.98	1.81
Rb/Y	6.17	16.67	11.17	1.02	9.71	11.68	15.15	9.06	5.09	43.03	13.03	17.10	10.86	12.14	7.49	5.07	14.94	12.51	15.90	66.34	24.96	28.63	7.82	7.22	25.13	3.15
Nb/Ta	3.59	2.57	2.79	7.80	10.43	11.00	10.00	12.00	14.20	-	2.67	-	3.20	3.52	12.00	1.95	2.44	2.21	11.40	24.00	12.75	11.33	3.11	2.62	2.00	3.15
$(La/Yb)_N$	46.30	39.22	20.49	14.10	29.54	30.08	27.31	24.97	14.44	223.98	15.94	23.84	54.04	26.50	19.76	20.08	19.21	43.31	10.00	324.66	22.38	16.96	30.63	33.37	21.69	7.80
$(Ce/Yb)_N$	25.47	27.30	14.51	4.77	22.29	17.93	19.54	18.27	10.35	157.64	11.51	17.82	24.07	17.79	14.52	12.89	13.89	30.66	8.36	214.73	22.41	10.85	23.95	19.16	19.06	4.85
Eu/Eu*	0.90	0.97	0.98	0.85	0.87	0.88	0.82	0.81	0.73	0.91	0.74	1.06	1.21	0.92	0.93	0.91	0.93	0.98	0.76	0.85	0.91	0.92	0.85	0.91	1.10	0.85
$(La/Sm)_N$	7.48	6.91	6.12	3.47	4.77	5.25	4.76	4.33	4.67	10.10	4.52	5.31	9.12	8.59	4.15	6.46	4.61	5.33	2.74	12.00	5.01	5.20	4.53	4.82	6.46	4.44
$(Gd/Er)_N$	2.61	3.11	1.73	2.14	2.89	2.44	2.55	2.40	1.85	6.91	1.81	2.58	2.49	1.40	2.16	1.29	1.48	1.64	1.95	8.12	2.20	2.07	2.57	2.62	1.59	0.90

Data Source: (1) Almeida et al., (2008); (2) Dias (2009); (3) Althoff et al., (1996); (4) Guimarães et al. (submitted b); (5) Dias (2007); (6) Leite (2001). Fe_2O_3=total iron recalculated as Fe_2O_3.LOI=loss on ignition.A/CNK: Molecular ratio (Al/Ca+Na+K).

Mg# molecular ratio Mg/(Mg + Fe). La_N, Yb_N, Sm_N, Gd_N, Eu_N:Normalized REE value (Evesen et al 1978).Eu/Eu*=europium anomaly calculated as [Eu/(Eu*)]=[(Eu_N)/((Sm_N+Gd_N)/2)].

nd: not determinated.

Table 1 – Continued

	Leucogranodiorite-granite suites																	
						Similar plutons												
	Grotão Granodiorite					Bannach area							Xinguara area					
Element	Granodiorites			Monzogranites		Monzogranites							Monzogranites					
Sample	FMR-49 [4]	FMR-69A [4]	FMR-105 [4]	FMR-59 [4]	FMR-45 [4]	MFR-14F [5]	MASF- 2A [5]	MASF- 10A [5]	MFR-04C [5]	MFR-10A [5]	MASF- 1 [5]	MASF- 7 [5]	AL-86 [6]	AL-205 [6]	AL-202 [6]	AL-75 [6]	ALF-258 [6]	AL-87 [6]
SiO2	67.57	69.61	71.02	67.89	71.67	68.87	70.19	70.31	70.46	72.63	72.73	73.14	69.44	70.40	71.60	71.80	72.90	73.91
TiO2	0.56	0.42	0.25	0.50	0.28	0.30	0.20	0.24	0.20	0.17	0.17	0.09	0.21	0.21	0.19	0.10	0.16	0.14
Al2O3	15.64	15.88	15.64	15.85	15.52	15.92	15.81	15.41	15.37	14.48	14.59	14.68	15.42	15.60	15.00	14.80	14.80	13.90
Fe2O3(t)	3.20	2.06	1.88	2.82	1.66	2.04	1.62	1.79	1.55	1.04	1.35	0.90	2.25	1.80	1.60	1.60	1.60	1.56
MnO	0.03	0.01	0.02	0.03	0.02	0.03	0.02	0.03	0.02	0.02	0.02	0.01	0.02	0.01	0.01	0.01	0.10	0.01
MgO	1.15	0.71	0.59	1.06	0.47	0.74	0.52	0.55	0.47	0.31	0.37	0.17	0.70	0.51	0.40	0.24	0.55	0.42
CaO	3.27	2.54	2.57	3.04	1.65	2.20	2.20	1.97	2.05	1.02	1.54	1.18	1.80	2.20	1.80	1.20	1.50	1.45
Na2O	4.72	4.91	4.82	4.43	5.05	4.17	4.53	4.56	5.10	3.63	4.27	4.64	4.97	4.40	4.30	3.30	3.40	4.23
K2O	2.54	2.75	2.54	3.18	3.09	3.83	3.27	3.84	3.47	5.92	3.72	4.29	3.74	3.10	3.30	5.30	5.00	4.04
P2O5	0.18	0.14	0.09	0.15	0.10	0.11	0.08	0.08	0.08	0.06	0.07	0.05	0.19	0.07	0.07	0.04	0.08	0.18
LOI	0.90	0.70	0.40	0.80	0.30	1.30	1.00	1.00	1.00	0.60	0.90	0.70	0.83	0.48	0.44	0.46	0.48	0.39
Total	99.76	99.73	99.82	99.75	99.81	99.51	99.44	99.78	99.77	99.88	99.73	99.85	99.57	98.78	98.71	98.85	100.57	100.23
Ba	1088	1324	851	1020	1103	2552	3312	1613	1563	1091	1067	1297	1211	1659	834	1081	1684	1360
Sr	599	623	539	417	670	684	705	578	518	329	459	396	861	564	424	310	525	798
Rb	78	76	57	117	110	101	92	124	91	176	94	140	126	140	142	193	121	120
Zr	146	141	118	139	157	139	120	130	93	84	84	75	168	185	134	133	220	118
Y	4.1	13.4	5.7	7.5	3.9	4.5	12.8	5.1	2.6	6.8	3.2	5.4	9.0	5.0	10.0	13.0	7.0	4.0
Hf	3.9	4.6	3.0	3.8	4.0	3.7	3.1	4.1	2.5	2.6	2.6	2.5	n.d	n.d	n.d	n.d	n.d	n.d
Nb	5.3	4.0	3.2	8.3	2.0	2.6	1.3	3.9	2.3	4.4	3.4	2.5	11.0	5.0	5.0	5.0	5.0	n.d
Ta	0.5	0.5	0.5	1.1	0.3	0.4	0.2	0.6	0.3	0.8	0.5	0.5	n.d	n.d	n.d	n.d	n.d	n.d
Ni	7.0	4.3	3.6	8.6	4.7	7.9	8.1	4.8	2.7	2.9	3.4	1.3	n.d	n.d	n.d	n.d	n.d	n.d
Cu	n.d	n.d	n.d	n.d	n.d	2.8	4.2	4.1	17.4	9.7	10.1	4.3	n.d	n.d	n.d	n.d	n.d	n.d
Th	7.2	11.4	4.2	12.1	7.1	7.1	6.9	13.7	6.4	15.6	13.2	12.3	n.d	5.0	5.0	5.0	5.0	n.d
Zn	n.d	n.d	n.d	n.d	n.d	22	19	29	32	23	18	16	n.d	n.d	n.d	n.d	n.d	n.d
Ga	20	21	19	21	21	19	18	20	18	19	19	19	17	25	29	28	24	14
La	27.40	62.70	16.50	31.90	28.20	24.40	34.30	28.00	17.60	25.50	21.60	13.10	49.58	20.12	n.d	26.97	n.d	35.22
Ce	58.70	109.40	26.30	62.80	58.50	63.20	43.60	51.20	34.00	45.50	36.40	29.60	106.90	32.16	n.d	57.68	n.d	68.84
Pr	6.70	13.63	3.58	6.97	5.64	5.29	6.52	5.38	3.45	5.83	4.14	2.77	n.d	n.d	n.d	n.d	n.d	n.d
Nd	24.70	55.50	14.90	27.00	20.90	17.30	23.10	17.40	10.60	18.50	13.20	9.30	36.58	9.07	n.d	16.42	n.d	19.55
Sm	3.83	8.20	2.32	3.74	2.31	2.40	3.40	2.60	1.50	3.10	1.80	1.50	5.04	1.45	n.d	2.68	n.d	2.60
Eu	0.96	2.09	0.63	0.83	0.63	0.70	1.32	0.68	0.46	0.60	0.44	0.45	0.72	0.35	n.d	0.38	n.d	0.65
Gd	2.70	6.60	1.86	2.91	1.53	1.52	2.63	1.67	0.66	1.94	0.99	0.88	2.63	0.92	n.d	1.71	n.d	1.47
Tb	0.29	0.66	0.22	0.37	0.12	0.20	0.46	0.20	0.10	0.33	0.12	0.18	n.d	n.d	n.d	n.d	n.d	n.d
Dy	1.32	2.81	1.18	1.83	0.50	1.02	2.08	0.88	0.36	1.31	0.57	0.88	1.24	0.48	n.d	0.77	n.d	0.59
Ho	0.16	0.37	0.18	0.30	0.08	0.16	0.39	0.16	0.07	0.20	0.10	0.16	0.22	0.07	n.d	0.14	n.d	0.10
Er	0.37	0.79	0.50	0.72	0.19	0.43	1.12	0.46	0.20	0.62	0.27	0.50	0.40	0.14	n.d	0.30	n.d	0.23
Tm	0.05	0.10	0.07	0.10	0.02	0.08	0.17	0.07	0.05	0.10	0.05	0.09	n.d	n.d	n.d	n.d	n.d	n.d
Yb	0.32	0.50	0.38	0.60	0.18	0.52	1.03	0.43	0.30	0.55	0.29	0.48	0.25	0.15	n.d	0.27	n.d	0.23
Lu	0.03	0.06	0.07	0.08	0.02	0.07	0.16	0.07	0.04	0.06	0.06	0.08	0.04	0.04	n.d	0.07	n.d	0.06
A/CNK	0.95	1.01	1.02	0.97	1.06	1.06	1.05	1.01	0.97	1.02	1.05	1.02	1.00	1.07	1.08	1.11	1.08	1.00
K2O/Na2O	0.54	0.56	0.53	0.72	0.61	0.92	0.72	0.84	0.68	1.63	0.87	0.92	0.75	0.70	0.77	1.61	1.47	0.96
$Fe_2O_{3(t)}$+MgO+ TiO_2+MnO	4.94	3.20	2.74	4.41	2.43	3.11	2.36	2.61	2.24	1.54	1.91	1.17	3.18	2.53	2.20	1.95	2.41	2.13
#Mg	0.42	0.41	0.38	0.43	0.36	0.42	0.39	0.38	0.38	0.37	0.35	0.27	0.38	0.36	0.33	0.23	0.41	0.35
Sr/Y	4.11	4.42	4.56	2.99	4.28	4.90	5.88	4.44	5.54	3.90	5.46	5.30	5.13	3.05	3.16	2.33	2.39	6.76
Rb/Sr	0.54	0.54	0.49	0.84	0.70	0.72	0.76	0.95	0.97	2.09	1.12	1.87	0.75	0.76	1.06	1.45	0.55	1.02
Rb/Ba	0.07	0.06	0.07	0.11	0.10	0.04	0.03	0.08	0.06	0.16	0.09	0.11	0.10	0.08	0.17	0.18	0.07	0.09
Ba/Sr	1.82	2.13	1.58	2.45	1.65	3.73	4.70	2.79	3.02	3.32	2.32	3.28	1.41	2.94	1.97	3.49	3.21	1.70
Rb/Y	19.10	5.63	10.07	15.56	28.15	22.33	7.16	24.25	34.88	25.87	29.34	25.89	14.00	28.00	14.20	14.85	17.29	30.00
Nb/Ta	10.60	8.00	6.40	7.55	6.67	6.50	6.50	6.50	7.67	5.50	6.80	5.00	-	-	-	-	-	-
(La/Yb)N	61.42	89.95	31.15	38.14	112.38	33.66	23.89	46.71	42.08	33.26	53.43	19.58	142.25	99.53	-	71.65	-	112.28
(Ce/Yb)N	50.95	60.78	19.23	29.07	90.28	33.76	11.76	33.07	31.48	22.98	34.87	17.13	118.78	61.61	-	59.34	-	84.99
Eu/Eu*	0.87	0.84	0.90	0.74	0.96	1.05	1.30	0.93	1.22	0.70	0.91	1.10	0.54	0.87	-	0.50	-	0.92
(La/Sm)N	4.62	4.94	4.59	5.51	7.88	6.56	6.51	6.95	7.57	5.31	7.75	5.64	6.35	8.96	-	6.51	-	8.76
(Gd/Er)N	5.88	6.73	3.00	3.25	6.49	2.85	1.89	2.92	2.66	2.52	2.95	1.42	5.30	5.24	-	4.67	-	5.21

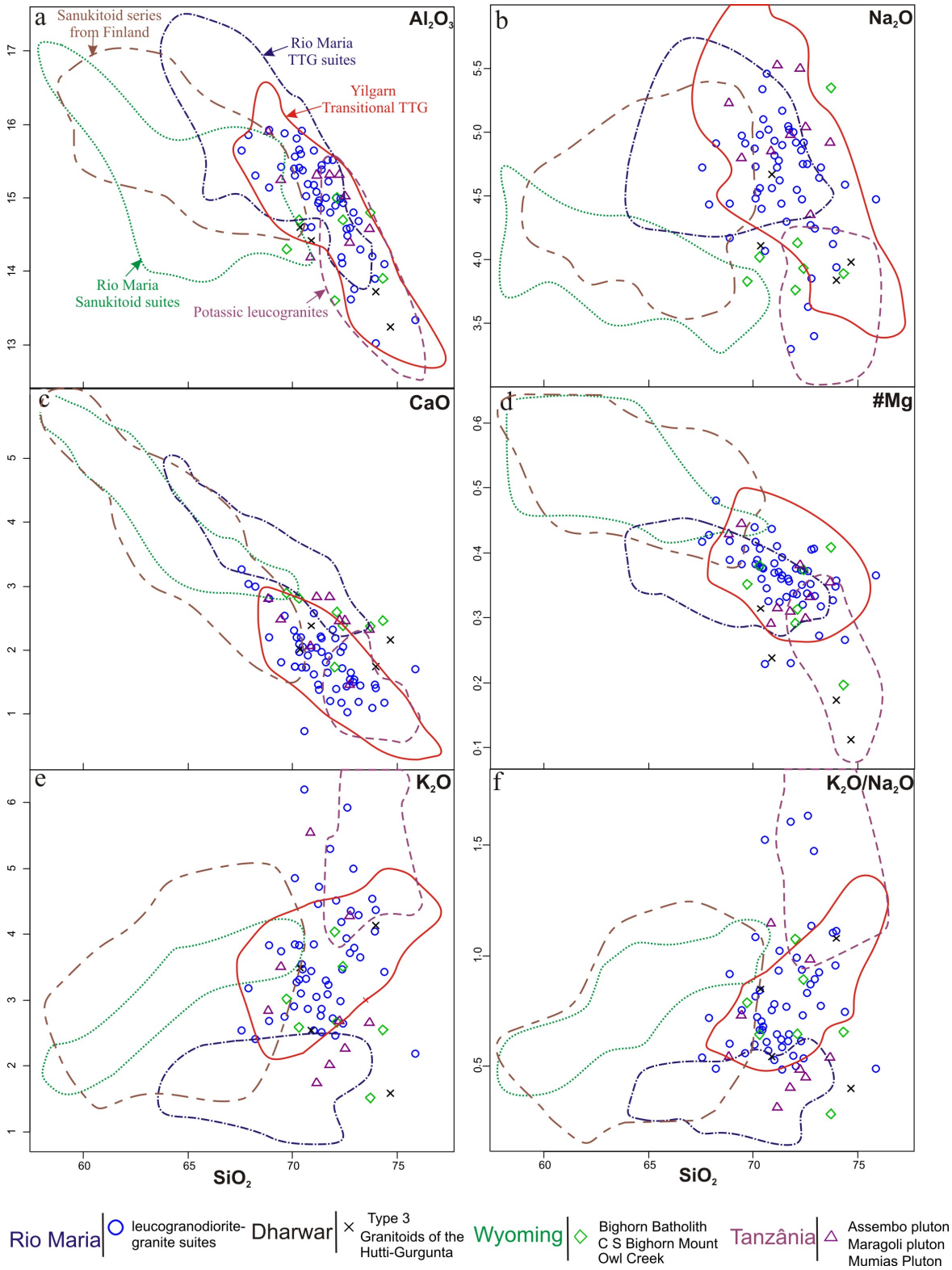

Figure 5 - Major element Harker diagrams (%wt) for leucogranodiorite-granite suites from Rio Maria granite-greenstone terrane, Granite-Granodiorite suite from Wyoming province (Frost et al., 2006) and Transitional TTGs from Dharwar craton (Jayananda et al., 2006; Prabhakar et al.,

2009). The fields for Rio Maria sanukitoid suites, TTG suites and Potassic leucogranites from Rio Maria granite-greenstone terrane, Transitional TTGs (Goongarrie suites and Menangina, Barr Smith and Union Jack plutons) from Yilgarn craton and sanukitoid series from Finland (Heilimo et al., 2009) are also plotted for comparison.

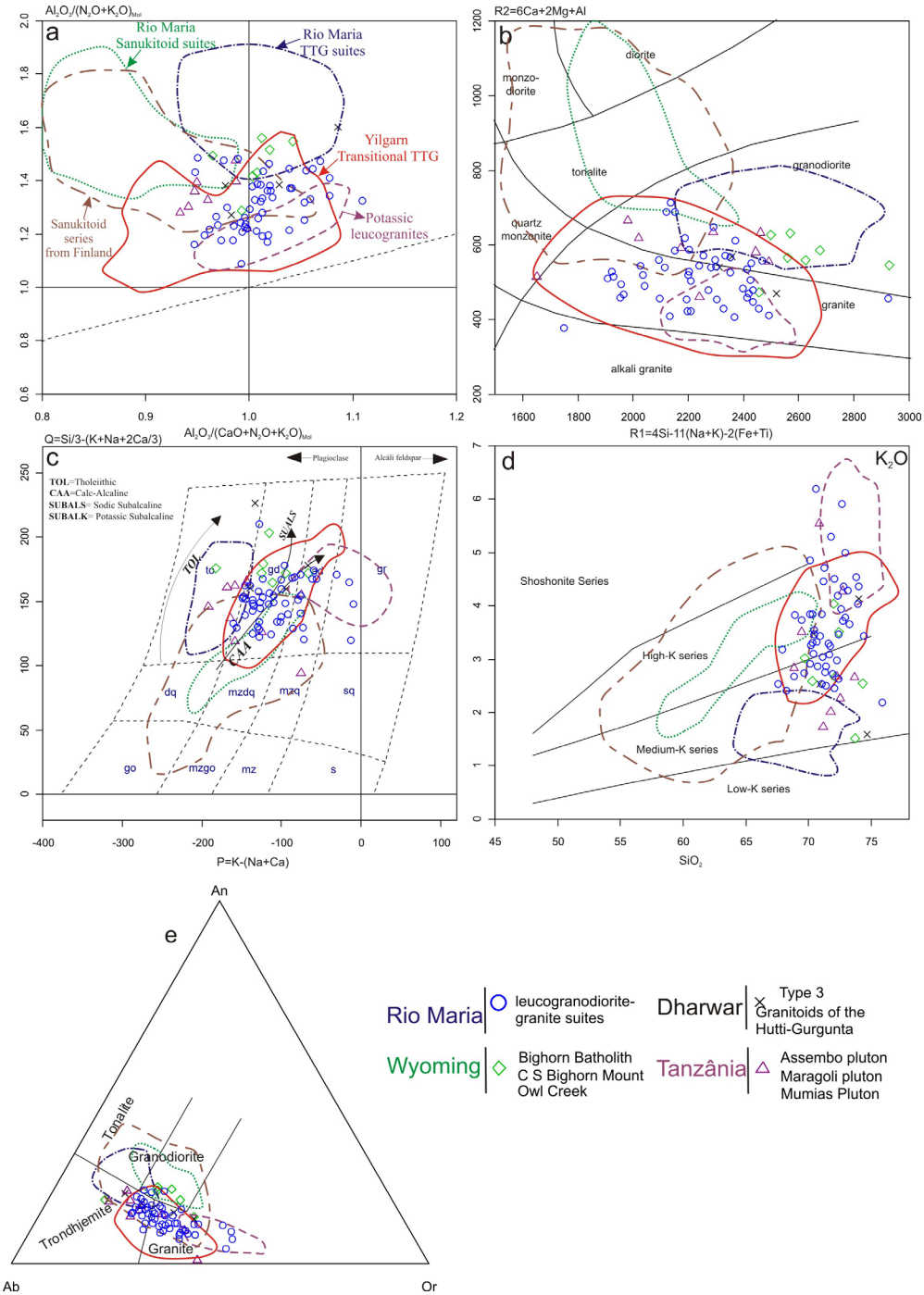

Figure 6 - Geochemical plot showing the distribuition of the samples of the leucogranodiorite granite suites from Rio Maria granite-greenstone terrane, Menangina granites from Yilgarn

craton (D. Champion, written communication), Granite-Granodiorite suite from Wyoming province (Frost et al., 2006) and Transitional TTGs from Dharwar craton (Jayananda et al., 2006, Prabhakar et al., 2009). (a) Al2O3/ (CaO + Na2O + K2O)]mol vs. [Al2O3/(K2O + Na2O)]mol diagram (Shand, 1950); (b) R1-R2 plot. R1-R2 are cationic parametrs of De La Roche (1980); (c) P-Q diagram from Debon and Le fort (1988) (d) Silica-potassium diagram (Peccerillo and Taylor, 1976); (e) Normative feldspar triangle (O'Connor, 1965).The fields for Rio Maria sanukitoid suites, TTG suites and Potassic leucogranites from Rio Maria granite-greenstone terrane, Transitional TTGs (Goongarrie suites, Barr Smith and Union Jack plutons) from Yilgarn craton and sanukitoid series from Finland (Heilimo et al., 2009) are also plotted for comparison.

1988) classification diagrams (Figs. 6 b, c). These rocks plot in the medium to high-K fields of calc-alkaline series in the K_2O vs. SiO_2 diagram (Fig. 6d; fields of Peccerillo and Taylor, 1976) and in the trondhjemite and granite fields in the An-Ab-Or normative diagram (Fig. 6e; fields of Barker, 1979).

5.2. Trace Elements

The trace elements of the LGdG suites show a considerable spread in Harker diagrams (Fig. 7). The Ba and Sr contents are variable but generally high (697-1962 and 212-861 ppm, respectively; Table 1; Figs. 7a, b), whereas those of Rb are low to moderate (57-193 ppm, generally <130; Fig. 7c). The Rb/Sr ratios are low, generally < 0.5 (Fig. 7d). These granites are depleted in HFSE [Zr (71-201 ppm, generally <140 ppm; Fig. 7e); Hf (2.4-4.7 ppm), Y (2.6 -15.1 ppm; Fig. 7f), Nb (1.3-11 ppm) and Ta (0.2-2.7)], when compared to A-type or alkaline granites (Whalen et al., 1987; Eby, 1992; Sylvester, 1994). Their Zr contents tend to be lower than those found in similar Archean granites and also than those of the TTGs of Rio Maria (Fig. 7e).

In general, they show LREE enrichment and HREE depletion, resulting in rather fractionated REE patterns. In the Guarantã suite, three main types of granites have been distinguished on the basis of their REE patterns (Fig. 8a, b, c; Table 1): *High La/Yb granites* – This group is marked by high $(La/Yb)_N$ ratios (20-224, normally >42), either absence of Eu anomaly or just a small negative or positive Eu anomaly (Eu/Eu* = 0.85-1.22) and concave shape

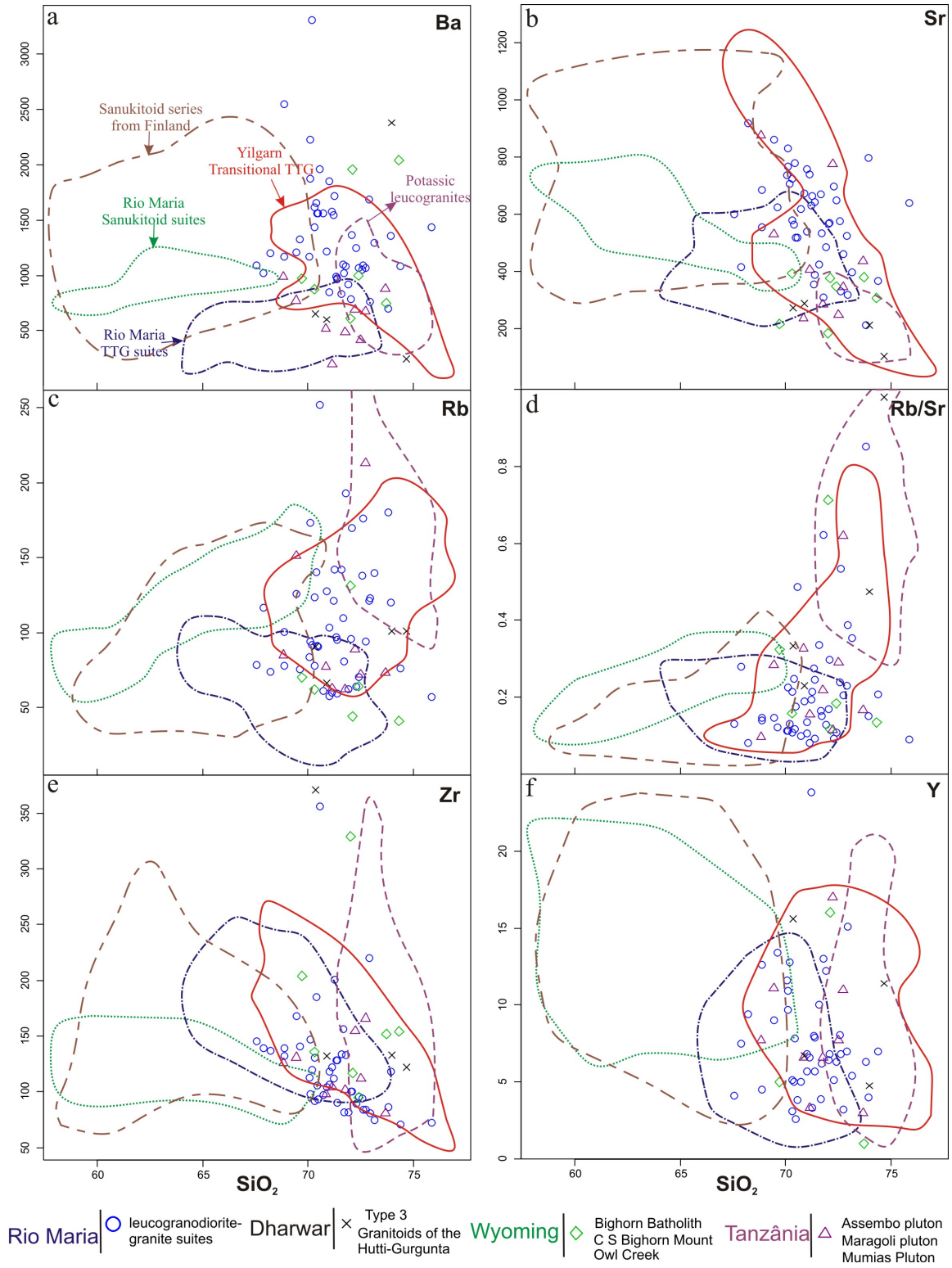

Figure 7 - Harker plots for selected trace elements and elemental ratios for leucogranodiorite-granite suites from Rio Maria granite-greenstone terrane, Granite-Granodiorite suite from Wyoming province (Frost et al., 2006) and Transitional TTGs from Dharwar craton (Jayananda et

al., 2006; Prabhakar et al., 2009). The fields for Rio Maria sanukitoid, TTG suites and potassic leucogranites from Rio Maria granite-greenstone terrane, Transitional TTGs (Goongarrie suites and Menangina, Barr Smith and Union Jack plutons) from Yilgarn craton and sanukitoid series from Finland (Heilimo et al., 2009) are also plotted for comparison.

of the HREE patterns; *Medium La/Yb granites* – This group is dominant and their rocks display lesser fractionated REE patterns [Fig. 8b; 16 < $(La/Yb)_N$ < 46] and absent or discrete Eu anomalies (0.70-1.06); *Low La/Yb granites* - The third granite group is characterized by flat HREE patterns [8 < $(La/Yb)_N$ < 24; generally<14] and the presence of a discrete negative Eu anomaly (Eu/Eu*= 0.68 – 0.91; with an isolated sample showing 1.30). The REE pattern dominant in the Grotão granodiorite is similar to those of the medium La/Yb granites of the Guarantã suite.

The *Low La/Yb granites* have higher Y and lower Sr contents compared to the other kind of granites (Figs. 9a, b). The concave shape of the HREE patterns shown by the samples of the *high La/Yb group* suggests that hornblende was probably an important fractionating phase during the evolution of these rocks.

The REE patterns and the, La/Yb, Sr/Y, and Y behavior in the Guarantã suite is similar to those described in the Arco Verde tonalite (Fig. 9a, b), the TTG unit that is the major country rock of the plutons of that suite (Fig. 1b). This indicates a possible genetic link between these granites and TTG suites.

6. Comparison between the LGdG suites and Archean granitoids

6.1. Comparison between the LGdG suites and the TTG and sanukitoid suites of the RMGGT

The LGdG suites constitute less than 10% in volume of the granitoids exposed in Rio Maria granite-greenstone terrane (Fig. 1b) and they were originated around 50 m.y. after the last major TTG magmatic event (2.93±0.1 Ga; Almeida et al. a, submitted) recorded in Rio Maria region. The mentioned granites are approximately contemporaneous with the sanukitoid suites, potassic leucogranites and the Água Fria trondhjemite (Almeida et al. a, b, submitted). In general, the LGdG suites define plutons and stocks attaining a maximum of ~20 km in their major

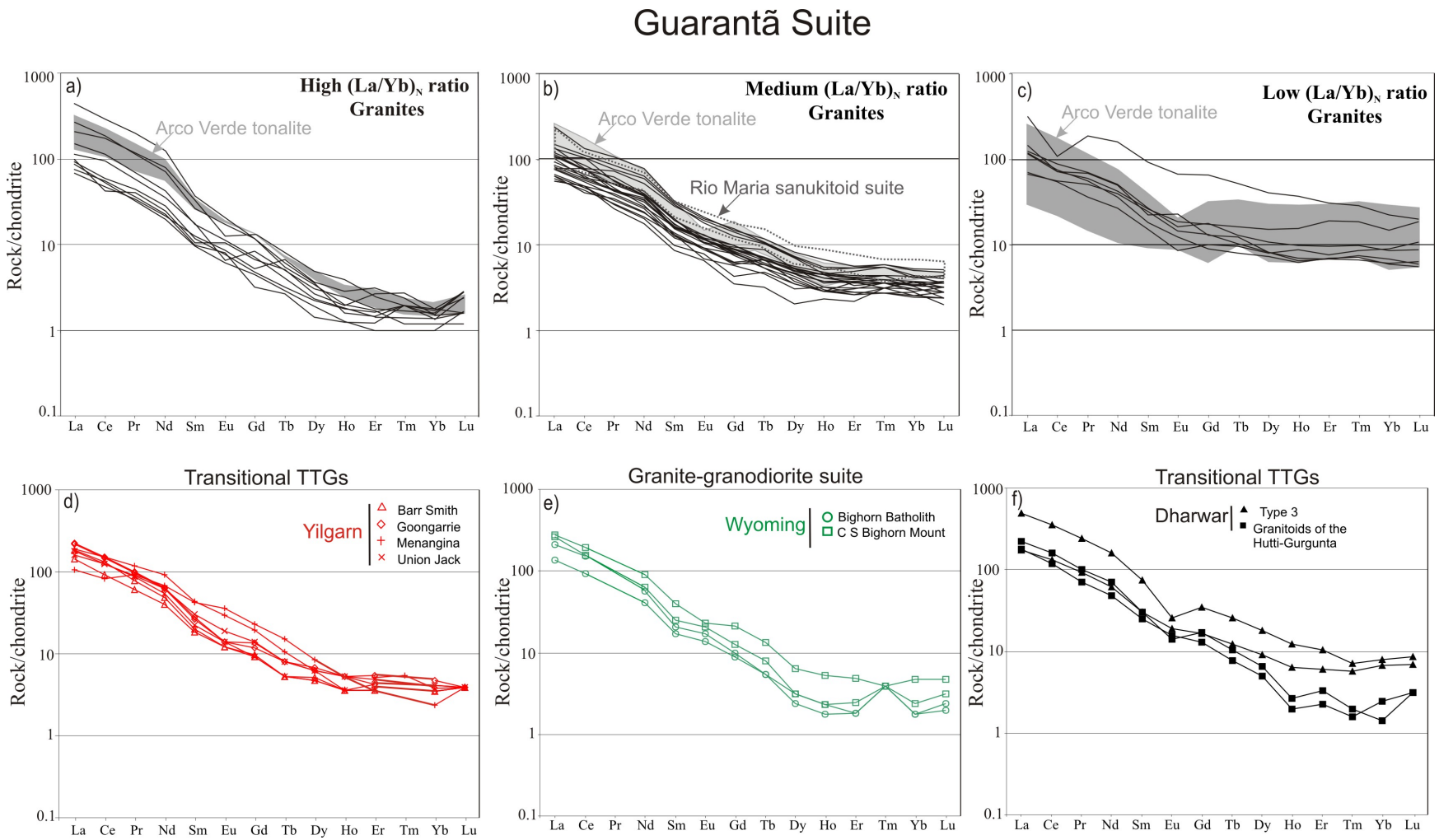

Figure 8 - Chondrite normalised (Evensen et al., 1978) REE patterns for (a, b, c) Guarantã suite of the Rio Maria granite-greenstone terrane, (d) Transitional TTGs from Yilgarn craton (D. Champion, written communication), (e) Granite-granodiorite suite from Wyoming province (Frost et al., 2006) and (f) Transitional TTGs from Dharwar craton (Jayananda et al., 2006, Prabhakar et al., 2009).

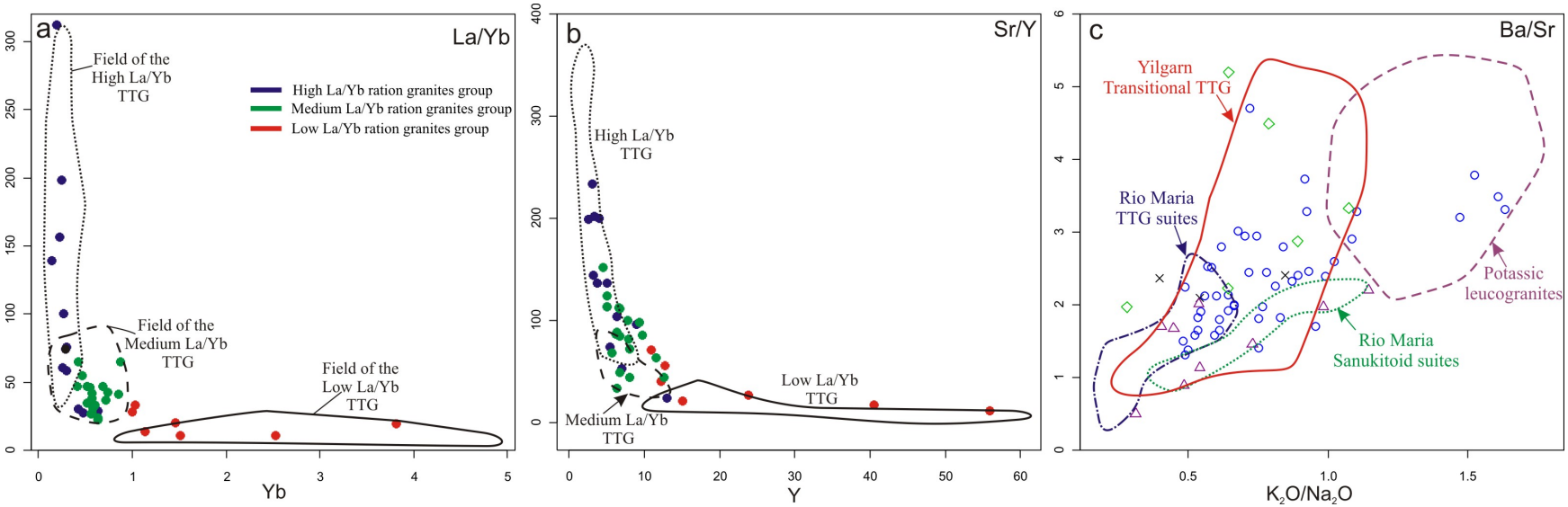

Figure 9 - a) La/Yb vs Yb and Sr/Y vs Ydiagrams used to discriminate the different groups of leucogranodiorite-granite suites from of RMGGT. The field for theTTGs granitoids with high, medium and low La/Yb rations also are plotted for comparison; c) K2O vs Ba/Sr diagram showing the distribution of the samples of the leucogranodiorite-granite suites from Rio Maria granite-greenstone terrane, Menangina granites from Yilgarn craton (D. Champion, written communication), Granite-Granodiorite suite from Wyoming province (Frost et al., 2006) and Transitional TTGs from Dharwar craton (Jayananda et al., 2006, Prabhakar et al., 2009). The fields for Rio Maria sanukitoid suites and TTG suites from Rio Maria granite-greenstone terrane and Transitional TTGs (Goongarrie suites, Barr Smith and Union Jack plutons) from Yilgarn craton are also plotted for comparison.

dimension, whereas the Rio Maria TTG and sanukitoid suites form large batholiths or sheeted complexes (Souza et al., 1992), locally with associated plutons and stocks (Fig. 1b). The porphyritic monzogranite to granodiorite, dominant in the Guarantã suite, and the fine-even-grained Grotão granodiorite differ of the equigranular, medium-grained samples of the Rio Maria TTG suites not only in textural aspects, but especially by the presence of K-feldspar as a major mineral phase. The former granites are also clearly distinct from the granodiorites largely dominant in the sanukitoid suites, because the latter are relatively enriched in mafic minerals (generally 10 to 20 volume % of mafic modal content) and have hornblende as a major phase.

The geochemical differences between the LGdG suites and the Rio Maria TTG and sanukitoid suites are remarkable. They have been discussed in detail by Almeida et al. (b, submitted) and can be observed in several geochemical plots (Figs. 5, 7). Our goal here is just to put in evidence some geochemical similarities which exist between the mentioned Archean rocks and the LGdG suites that suggest possible genetic links between these granite magmas and TTG or sanukitoid sources. The rocks of the LGdG suites show enrichment in LILE, especially in K_2O, Ba, Sr, and Rb, and impoverishment in CaO, Fe_2O_3t, and Zr compared with the TTGs of Rio Maria (Figs. 5, 7); they are, on the other hand, enriched in Al_2O_3 and Na_2O and impoverished in MgO and display higher values of A/CNK and lower of #Mg compared to the sanukitoid suites of Rio Maria (Table 1; Fig. 5). The LGdG suites are also generally enriched in Ba and, to a lesser degree, in Sr compared with the sanukitoid rocks (Figs. 7a, b). However, there is geochemical evidence that some granodiorites and the Rancho de Deus associated granite of the sanukitoid suite that occur in the Marajoara area, near the domain of the Guarantã suite (Fig. 1b), and local samples from the Xinguara area, are also relatively enriched in Ba (cf. the Ba/Sr vs. K_2O/Na_2O diagram; Fig. 9c). It is also evident that the K_2O/Na_2O ratios of the LGdG suites are similar to those of the sanukitoids and higher than those of the TTGs.

Despite the contrast in terms of the LILE, the LGdG suites share also some common features with the Rio Maria TTG rocks, such as the relatively high Al_2O_3 and Na_2O (Table 1; Figs. 5a, b), the low Yb and Y (Fig. 7f) contents and the behavior of the REE. In fact, the three distinct REE patterns identified in the granites of the Guarantã suite (Fig. 8) were also observed in the Rio Maria TTG suites (Almeida et al. a, submitted). The high, medium and low La/Yb ratio granites define REE patterns that are similar, respectively, to those of the high, medium and low La/Yb TTG groups of the Arco Verde tonalite (Fig. 8; Fig. 9a), the unit which is the country rock

of the mentioned granites (Fig. 1b). In both units, the rocks of the three groups distinguished on the basis of REE behavior are not temporally or spatially distinct, and could not be individualized in the geological maps. In the Arco Verde tonalite, the low La/Yb group is dominant (Fig. 8c), whereas in the Guarantã suite the medium La/Yb group is more abundant (Fig. 8b). The medium La/Yb REE pattern is also found in the Mogno trondhjemite and in the Mariazinha tonalite, which are exposed to the north of the area of occurrence of the Guarantã suite, but the dominant REE pattern in those units is that of the high La/Yb group (Almeida et al. a, submitted; Guimarães et al. a, submitted). On the other hand, the REE patterns of the intermediate and granodioritic rocks of the sanukitoid suites are almost uniform and similar in its broad characteristics to the REE pattern dominant in the rocks of the Guarantã suite (Fig. 8b). There is also a reasonable correspondence between the three TTG geochemical groups and their equivalent in the Guarantã suite in terms of La/Yb vs Yb and Sr/Y vs. Y (Figs. 9 a, b)

At first glance, the broad similarities between the REE patterns of the LGdG suites and those of the TTGs and sanukitoids of Rio Maria could suggest a possible genetic link between the granites and those rocks or, alternatively, fractionation during magmatic differentiation or retention in the residues of melting of their magma sources of similar phases. These hypotheses will be evaluated in the following.

6.2. LGdG suites vs. transitional TTG or GG

The geochemical characteristics of the granitoids from the Guarantã suite are compared with a large data set of the transitional TTG from Yilgarn craton (Barr Smith, Goongarrie, Menangina and Union Jack units; D. Champion, written communication), and some representative samples of the high-K granodiorite-granite suite (GG suite; Frost et al., 2006), Neoarchean granitoids from Tanzânia craton (Margoli, Mumias, Asembo plutons; Opiyo-Akech et al., 1999) and similar granites from the Dharwar craton (Arsikere-Banavara and Chitradurga-Jampalnaikankote-Hosdurga suites, Jayananda et al., 2006; Granitoids of the Hutti-Gurgunta area, Prabhakar et al., 2009). The strong geochemical similarity between the Guarantã suite rocks and the Transitional TTG of the Yilgarn craton is remarkable. The analyzed samples of the Guarantã suite are systematically concentrated in the fields defined by the Yilgarn granites in the different plots considered and this is true for major and trace elements (Figs. 5, 6, 7). The only

significant geochemical contrast observed is the zirconium contents that tend to be lower in the Guarantã granites compared to those of Yilgarn. On the other hand, the granites of Tanzânia, Wyoming, and, in a lesser degree, Dharwar show significant differences when compared with the Guarantã and Yilgarn granites (the former are dominantly granodiorites that are more calcic and poorer in K_2O, Ba, Sr, and Rb compared to the latter; cf. Figs. 5, 6, 7, 9c). The REE patterns of representative samples of Yilgarn (Fig. 8d) are also coincident with that of the medium La/Yb group dominant in the Guarantã suite, whereas those of Wyoming GG suite (Fig. 8e) are more similar to those of the high La/Yb group. The transitional TTGs of Dharwar (Fig. 8f) and the Archean granites of Tanzania display variable REE patterns that reproduce the three distinct patterns of the Guarantã suite.

Despite the clear geochemical differences between the LGdG suites and the sanukitoids of the RMGGT, we have decided to compare also the Guarantã suite with the sanukitoid series of the Karelian province (Heilimo et al., 2010), because those rocks are also relatively enriched in Ba and Sr. In spite of the similar range in Ba and Sr observed in both granitoid types (Figs. 7a, b), the sanukitoid series from Karelian province comprise dominantly metaluminous diorites, tonalites, and granodiorites, and have lower SiO_2 (<70%) and higher #Mg (Fig. 5d), Ni, and Cr contents than the LGdG suites. It is concluded that the high Ba-Sr sanukitoids of Karelia (Halla, 2005; Heilimo et al., 2010) are not similar in their broad geochemical characteristics to the Guarantã suite and to the LGdG of the RMGGT in general.

7. Discussion

7.1. Petrogenesis of the LGdG suites

7.1.1. Magmatic differentiation or partial melting of TTG

In most Archaean terranes, granitic plutons were emplaced after the main phase of TTG magmatism, and it has often been suggested that the granitic magmas were formed by 'reworking' (partial melting) of the TTG rocks (Sylvester, 1994; Althoff et al., 2000; Leite, 2001; Moyen et al., 2003; Almeida et al. b, submitted). Several experimental studies conducted under fluid-absent conditions indicate that partial melting of metatonalites could produce granitic melts

(Rutter and Wyllie, 1988; Skjerlie and Johnston, 1992; Singh and Johannes, 1996; Gardien et al., 1995, 2000; Castro, 2004; Patiño Douce, 2005; Watkins et al., 2007). The TTG suites constitute a major part of the basement of the Rio Maria region and are probably similar geochemically to the deep-seated Archaean rocks. Moreover, these rocks are clearly distinct from the Archean granite suites in both their modal and chemical characteristics, and are, thus, viable protolith candidates for their magmas. However, mass balance calculations done by us indicate that the protoliths of the melts that formed those granites, besides other identified geochemical inadequacies, should have contents of Sr and Ba more elevated than those found in the TTG suites.

On the other hand, geochemical data do not favour a linking by fractional crystallization between the rocks from LGdG suites and the Archean TTGs (Figs. 5, 6, 7). Moreover, in the case of origin of the LGdG magma by partial melting of TTG sources, it should be expected that the resulting magma would present a significant negative europium anomaly, similar to that shown by the potassic leucogranites (Sylvester, 1994; Davis et al., 1994; Almeida et al. b, submitted), due to the extremely probable retention of plagioclase in the melting residue. The absence of this feature in the REE patterns of the LGdG suites suggests that the hypothesis of the origin of their magmas only by melting of TTG sources is unlike. It is concluded that homogeneous sources composed of TTG suites of the RMGGT are unsuitable sources for the LGdG suites.

7.1.2. Mixing between sanukitoids magmas and high-K leucogranite melts

Several studies have suggested that late Archean granites could result of interaction between mantle-derived magmas and crustal melts (Jayananda et al., 1995; Evans and Hanson, 1997; Berger and Rollinson, 1997; Moyen et al., 2001). Oliveira et al. (submitted) argue that the ~2.87 Ga Rio Maria sanukitoid magmas derived from partial melting of a mantle source that was previously transformed by assimilation of trondhjemitic melts generated in a subduction zone. Independent of their origin, the emplacement of the Rio Maria sanukitoid suite was closely coeval with that of the potassic leucogranites, interpreted as crustal anatectic magmas (cf. Leite, 2001, Almeida et al. b, submitted), and LGdG suites. Thus, it is important to evaluate the role of the sanukitoid magmas in the petrogenesis of the LGdG suites. A possible model to explain the genesis of LGdG suites would be one involving the interaction between sanukitoid and potassic leucogranitic magmas. However, the geochemical data show that the Na_2O, K_2O, Ba, and Sr

contents of the LGdG do not fit with a mixing or mingling evolution trend and, hence, are not compatible with the mentioned hypothesis (Figs, 5, 6, 7).

7.1.3. Interaction between mantle-derived magmas and TTG continental crust

López et al. (2005) argue that voluminous granodioritic batholiths could be produced by interaction between mantle-derived hydrous mafic magmas (sanukitoid-like magmas) and tonalitic crust. In their model, K-rich mantle-derived magmas released H_2O and K_2O to the continental crust thus recycling tonalites into granodiorites. Testing this model to the RMGGT, we verify that granodiorites are largely dominant in the sanukitoid suites and there is little evidence of input in the crust of large volume of mafic magmas akin to the sanukitoid series (Oliveira et al., 2009; submitted). The proposed model did not also explain the high Ba and Sr contents, a remarkable geochemical feature of the leucogranodiorites and leucogranites. However, attempting to adapt this hypothesis, we can wonder if the emplacement and crystallization of the LILE-rich sanukitoid magmas in the Rio Maria continental crust would not be able to induce a gradual transfer of H_2O and K_2O, together with other LILE (e.g. Sr and Ba) to the host tonalites, thus enriching these rocks in K_2O, Sr, and Ba (resulting in rocks similar to the LGdG suites), but preserving some geochemical features of the TTGs (e.g. high Al_2O_3 and Na_2O, low Yb and Y contents and REE signature). López et al. (2005) claim that new granite batholiths could be generated in this way, but this is not entirely demonstrated, because the diffusion in crystallized rocks is a slow process even at relatively high temperatures (Cherniak and Watson, 1992; Liang et al., 1996; Van Orman et al., 2002) and this process is probable only applicable to local changes in composition from tonalites to granodiorites.

7.1.4. The restite model

The restite model invokes that the geochemical variation observed in granitic suites can be explained by variable separation of melt and refractory restite components of the parent magma (Chappell et al., 1987; Chappell and Stephens, 1988; Chappell, 1996; Champion and Sheraton, 1997). If partial melting takes place and the amount of melt exceeds the critical melt fraction, the magma moves as a mixture of restite and melt with limited separation (Van der

Molen and Paterson, 1979). In this condition the magma may later fractionate restite from melt to produce a range of rock composition. Thus, the composition of the more mafic granites can approach those of their source rocks (Chappell, 2004).

As mentioned before, there is some geochemical resemblance between the LGdG suites and the TTG suites of the RMGGT, suggesting a genetic relationship between these granitoids. In addition, the age (~2.93 Ga) of inherited zircon in samples from those granites lie in the range of the ages of the dominant TTG suites (2.98 – 2.92 Ga), suggesting that an older crust was involved in formation of the granite magmas. These aspects could be seen as evidence of a partial restitic origin for the latter. However, low degree of melting of TTGs should produce magmas similar in composition to the potassic leucogranites and distinct of the LGdG suites (cf. Champion and Sheraton, 1997; Almeida et al. b, submitted). Moreover, even these magmas should have lower Ba and Sr contents compared to the LGdG suites. The addition of restite to the melt, whatever its relative proportion, will not change the melt geochemical signature in the expected trend and is unable to give to the resulting magmas the characteristics observed in the LGdG suites.

7.1.5. Partial melting of mafic lithologies

Previous studies have shown that TTG liquids in equilibrium with garnet could be produced at pressures of 1 GPa and above (Sen and Dunn, 1994; Wolf and Wyllie, 1994; Rapp and Watson, 1995; Winther, 1996; Moyen and Stevens, 2006) and that pressure is the determinant parameter for garnet or plagioclase equilibrium in mafic assemblages. The geochemical features observed in LGdG suites suggest a severe HREE-depletion in most of these granites probably due to the presence of residual garnet and possibly amphibole in their magma sources, whereas the less fractionated REE patterns of the remainder leucogranites could be explained by a garnet-depleted residual assemblage. However, the Sr, Ba, and K_2O contents of the LGdG suites are too high and inconsistent with the derivation of their magmas solely from a mafic source. With different arguments, a similar conclusion was reached by Champion and Sheraton (1997) that discarded a mafic source to explain the origin of the Yilgarn high-Ca or Transitional TTG granites. Moreover, as also mentioned by Champion and Sheraton (1997), it is also unlikely that the inherited zircons found in the Rio Maria leucogranites would be derived

from a mafic source. It does seem obvious, that a purely mafic protolith looks not suitable for the genesis of the LGdG magmas.

7.1.6. Input of LILE-enriched component

Champion and Smithies (2007) had also pointed out that the LILE-enrichment in Transitional TTG does not reflect fractional crystallisation of the TTG magmas and cannot be produced by melting of purely basaltic precursors. Thus, they suggested that an additional component must be involved. They have evaluated different hypothesis to account for the nature of this additional component and its influence in the origin of Transitional TTG magmas, in general: 1) slab-melting with assimilation of subducted sediments (e.g., Plank, 2005); 2) crustal contamination, especially MASH-type processes (Hildreth and Moorbath, 1988); and 3) enriched crustal sources (e.g., intermediate to felsic metavolcanic rocks associated with greenstone belts). Champion and Smithies (2007) concluded that intermediate volcanic rocks differentiated from basaltic precursors could be a suitable source for the Transitional TTG from the Pilbara craton. Moyen et al. (2007) adopted a similar hypothesis to explain the origin of K-enriched granitoids associated with TTGs in the Barberton granite greenstone terrane. The crustal contamination model was evaluated above and the other two will be discussed in the following.

The slab-melting with assimilation of subducted sediments has been proposed for parts of some modern arcs (e.g., Elliot et al., 1997; Class et al., 2000; Pearce et al., 2005), and has been recently assumed to be effective in the petrogenesis of the high Ba-Sr plutons from the Northern Highlands Terrane of the British Caledonain Province (Fowler et al., 2008). Halla (2005) also argued that subducted sediments should play a role in the origin of Archean sanukitoid magmas.

In the RMGGT, as observed in the Pilbara craton transitional TTG (Champion and Smithies, 2007), there are geochemical contrasts between the three groups of LGdG suites that indicate significant variations in depth of magma generation with the influence of garnet in the melting residue increasing from the low-(La/Yb) to the high-(La/Yb) groups. Accepting the hypothesis of origin at different depths for the granitic magmas, the model of their derivation from a subducted slab that could have associated sediments will not be suitable (cf. also Champion and Smithies, 2007). A possible variation in the angle of the subducted slab could possibly explain the mentioned geochemical contrasts but it looks unlikely in the case of the

RMGGT because the LGdG suites have similar ages and occur in the same domain (Fig. 1b), being almost certainly generated by similar processes in a same tectonic setting.

The supracrustal pile of the greenstone belts from the RMGGT contains locally in its higher stratigraphic units felsic to intermediate rocks with intercalations of metagraywackes (Huhn et al., 1988) or metadacites (Souza and Dall'Agnol, 1996; Souza et al., 1997), showing that those greenstone belts are not a perfectly homogeneous pile of metabasalts. However, the partial melting of the greenstone belts involving only mafic to intermediate and dacitic rocks was probably unsuitable to generate LGdG magmas, because the mentioned rocks should be geochemically akin to their plutonic equivalents. Only a significant contribution of metagraywackes, interlayered with the metavolcanic rocks, would be possibly able to yield melts with geochemical characteristics similar to TTG melts, but more enriched in potassium and LILE. We have tested by mass balance calculations a model of derivation of the LGdG magmas from a mixed source involving 80% of tholeiite (metabasalt of the RMGGT; Souza et al., 1997) and 20% of Archean metagraywacke (Condie, 1993, Appendix F) and the results were inconsistent. Moreover, in the RMGGT, the limited distribution of metagraywackes in the greenstone belts and the scarcity of these rocks in the principal domain of the LGdG are noteworthy (Fig. 1b), making the hypothesis of a determinant influence of metasedimentary rocks in the origin of granitic magmas largely speculative and difficult to apply to the RMGGT.

Champion and Smithies (2007) have also argued that subduction processes were not directly involved in the origin of the Transitional TTG and similar granites and that the geochemical variations observed in the latter were due to crustal melting at different depths.

7.1.7. An alternative model for the origin of the LGdG suites

The different models proposed to explain the origin of the transitional TTG and similar granites are apparently not able to explain the genetic processes and evolution of the Guarantã suite, the larger suite of LGdG of the RMGGT. The geochemical variation observed in the whole Guarantã suite and in each of its individual plutons (Guarantã, Azulona and Trairão; Fig. 1b) could not be explained by a simple magmatic differentiation process involving fractional crystallization or partial melting and point to a complex magmatic evolution for the entire suite

(Figs. 5, 6, 7). Moreover, the geochemical analogies presented by the Guarantã suite and, at the same time, the TTG and sanukitoid suites are puzzling, especially if the contrasts in petrological evolution between the latter suites are considered (Smithies and Champion, 2000; Moyen et al., 2001; Martin et al., 2005; Halla, 2005; Lobach-Zhuchenko et al., 2005; Heilimo et al., 2010).

Taking this in mind, we have decided to test an alternative model to explain the origin of the Guarantã suite magmas assuming as a premise that TTG and sanukitoid magmas should be involved in their origin in order to explain the ambiguous geochemical character of the Guarantã granites. We have realized that some of the more evolved granites associated with the sanukitoid suites, i.e. the Rancho de Deus granites and the higher silica samples of the Rio Maria suite in the Marajoara area, are relatively enriched in Ba and, in lesser degree, Sr, compared to the dominant sanukitoid rocks of Rio Maria (Oliveira et al., 2009; Almeida et al. b, submitted). Thus, we have decided to test by mass balance calculations a possible link by fractional crystallization processes between a typical granodiorite of the sanukitoid suite (sample MFR-114; Oliveira et al., 2009, their Table 3) and one of the more Ba and Sr-enriched samples of the Guarantã suite (MAR-70; Table 1). The results indicate that 35% of fractionation of hornblende, plagioclase, clinopyroxene, magnetite, and ilmenite would be able to generate a liquid that fits the composition of the Guarantã monzogranite with high Ba and Sr content. The adjustment is good for major and minor elements (R^2=0.276) and also for selected trace elements, if a little fraction of allanite is added to the fractionated minerals (Table 2; Fig. 10). This suggests that the samples of the Guarantã granite with the highest contents of Ba and Sr could be derived from the sanukitoid granodiorite by fractional crystallization.

In a second step, it was tested by mass balance calculation the hypothesis of origin of the Guarantã granites by mixing between granite liquids enriched in Ba and Sr and a trondhjemitic liquid represented by the Agua Fria trondhjemite (Younger TTG formed at ~2.86 Ga and approximately coeval with the sanukitoid and Guarantã suites). Four monzogranitic samples with high Ba and Sr contents of the Guarantã suite were chosen for tests (MAR-38, MAR-07A, MAR-70A, MAR-72; Table 1), together with the sample AM-01 of the Agua Fria trondhjemite. Mixing in different proportions between the granite and trondhjemitic liquids were apparently able to explain the large compositional variations observed in the Guarantã suite (Fig.11). This is particularly true if we consider that more than one trondhjemitic liquid could be involved in the origin of the Guarantã liquids. Assuming that liquids of granitic and trondhjemitic composition

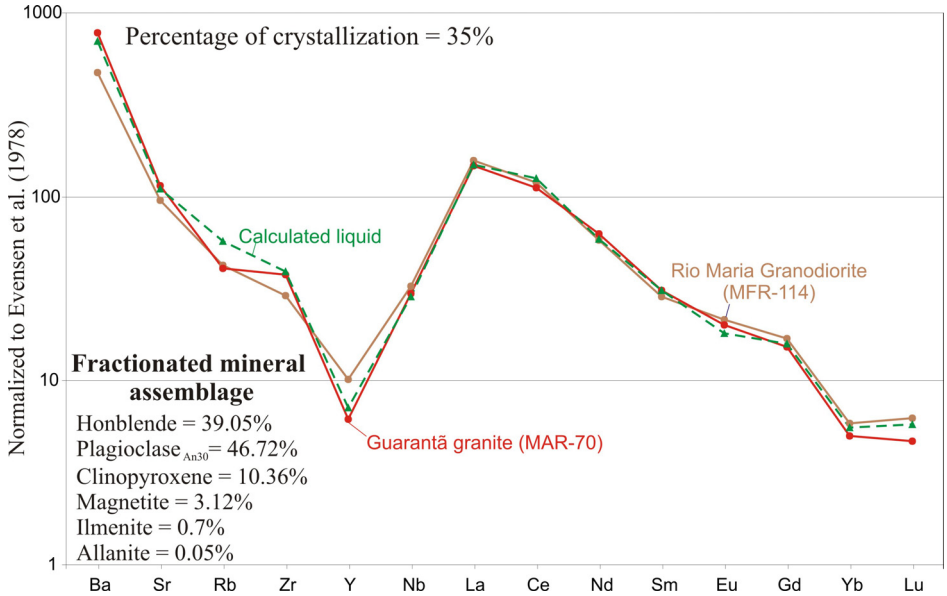

Figure 10 - A trace element model for the fractional crystallisation of the Rio Maria Granodiorite.

Table 2 - Modelling major and trace element compositions, fractionated mineral assemblages for differetiation of the Rio Maria Granodiorite.

	Rio Maria Granodiorite	**Residue**	**Calcutated magma**	**Guarantã Granite**
Elements	MFR-114		FC= 35% R^2= 0.276	MAR-70A
SiO_2 (wt%)	63.93	51.19	70.92	71.04
TiO_2	0.47	1.01	0.18	0.24
Al_2O_3	15.57	15.32	15.44	15.50
Fe_2O_3	5.46	11.76	2.03	2.07
MgO	2.67	6.42	0.66	0.69
CaO	4.50	9.39	1.76	1.76
Na_2O	4.40	4.61	4.92	4.79
K_2O	3.00	0.31	4.1	3.90
Ba (ppm)	1139		1697	1873
Sr	692		798	830
Rb	98		133	94
Zr	113		151	147
Y	16		11	10
Nb	8		7	7
La	37.30		35.51	35.00
Ce	72.80		76.82	68.20
Nd	27.20		27.53	29.30
Sm	4.40		4.76	4.74
Eu	1.25		1.05	1.17
Gd	3.47		3.26	3.16
Yb	1.00		0.95	0.85
Lu	0.16		0.15	0.12
Fractionated mineral assemblage				
Hornblende	39.05			
Plagioclase $_{An30}$	46.72			
Clinopyroxene	10.36			
Magnetite	3.12			
Ilmenite	0.7			
Allanite	0.05			

R^2= Sum of the squared residuals.
FC = percentage of crystallization.

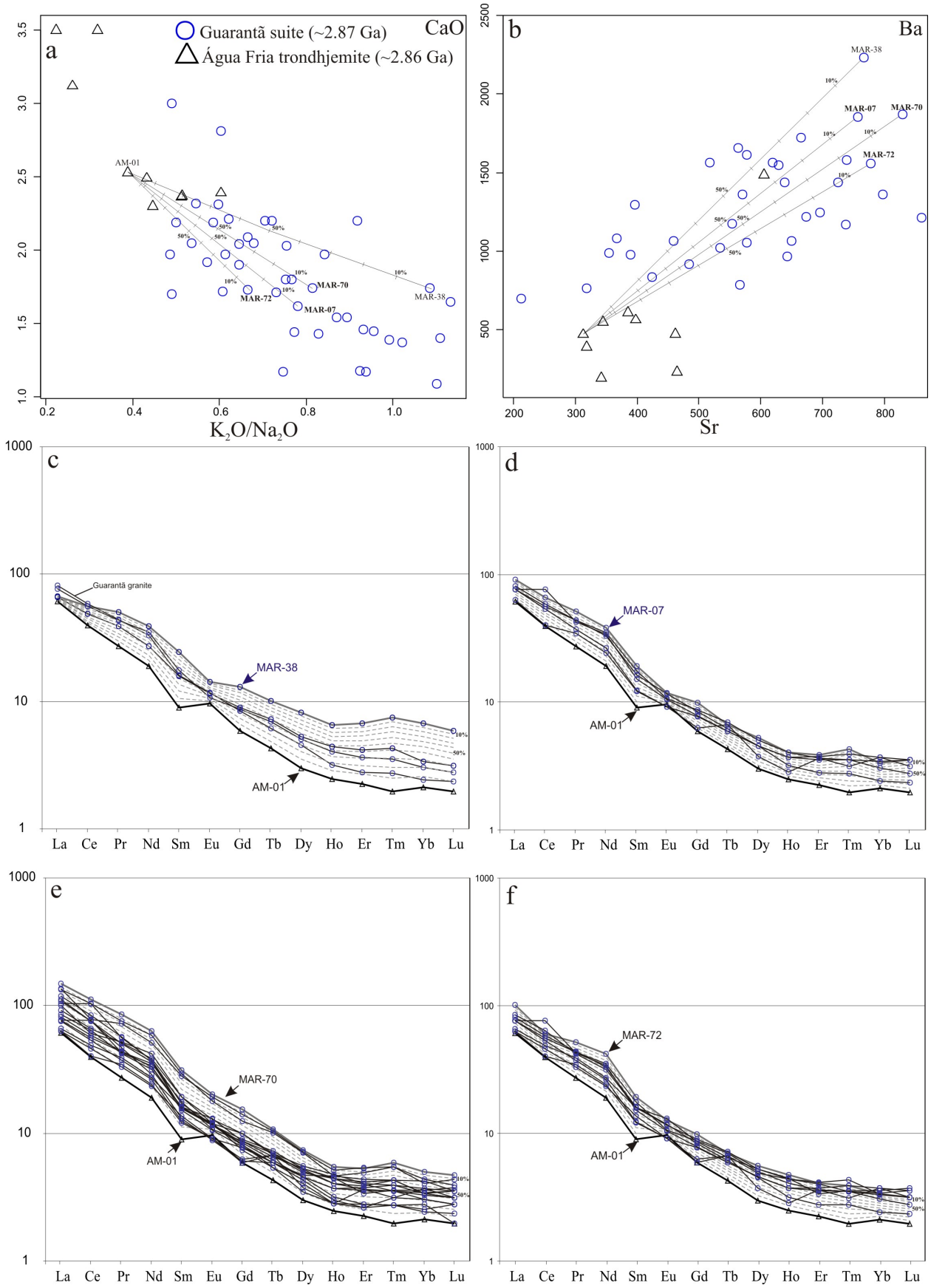
a
CaO
Guarantã suite (~2.87 Ga)
Água Fria trondhjemite (~2.86 Ga)
AM-01
MAR-70
MAR-72
MAR-07
MAR-38
K2O/Na2O
b
Ba
Sr
c
Guarantã granite
MAR-38
AM-01
d
MAR-07
AM-01
e
MAR-70
AM-01
f
MAR-72
AM-01
La Ce Pr Nd Sm Eu Gd Tb Dy Ho Er Tm Yb Lu

Figure 11 - Diagrams showing the result of the mixing between the Ba-Sr enriched granitic (MAR-38, MAR-07, MAR-70 and MAR-72) from Guarantã suite and trondhjemitic members (AM-01): a) K2O/Na2O vs CaO; b) Sr vs Ba. The tick marks along the evolutionary paths indicate the compositions of the calculated mixtures; (c to f) REE patterns. The gray and black thick lines represent the Ba-Sr enriched granitic and trondhjemitic members, respectively. The gray dotted lines represent the compositions of the calculated mixtures and the thin solid lines the composition of some samples of the Guarantã suite. Chondrite normalizing values after Evensen et al. (1978).

showing small compositional contrasts were responsible for the origin of the magmas forming each one of the plutons of the Guarantã suite (Fig. 1b) and that those magmas could result from different degrees of mixing between the two original liquids, a large spectrum of variation of final granitic liquids could be expected. This spectrum could be yet augmented if we consider the hypothesis of fractional crystallization of the liquids originated by mixing processes. The liquids with larger contribution of granite in the mixing will have compositions relatively enriched in K_2O, Sr, and Ba and will be impoverished in CaO (Figs. 11 a,b), compared to those where the percentage of trondhjemitic liquid was more significant.

We have also tested this model for REE and the results are shown in figure 11 c, d, e, f. The variation in REE patterns in function of the mixing of different proportions of the granite and trondhjemite liquids are compatible with the compositions of most Guarantã granite samples. The distribution of these samples in the REE plots for different granite compositions suggests that the participation of the granite and trondhjemite liquids could vary significantly for each specific case considered.

The proposed model is favoured by the fact that the sanukitoid suites of the Marajoara area, where the Guarantã suite and the largest plutons of LGdG suites are exposed (Fig. 1b), are enriched in silica, Ba, and Sr compared to the sanukitoid of other areas of the RMGGT (Almeida et al., 2008; Oliveira et al., 2009). It implies to admit that trondhjemitic liquids were also generated in this area at ca. 2.87 Ga. These liquids should be largely or entirely consumed by the mixing processes with the evolved sanukitoid granite magmas explaining the absence of a preserved register of trondhjemitic rocks derived from them in the Marajoara area, so far.

The generation of these trondhjemitic liquids could be due to the partial melting of the base of thickened metavolcanic piles caused by the ascension from the mantle and underplate in the crust of sanukitoid magmas (Almeida et al. a, submitted). This genetic model could possibly be also applied for the Karelian granite greenstone terrain (Halla, 2005; Lobach-Zhuchenko et al., 2005; Käpyaho et al., 2006; Halla et al., 2009; Heilimo et al., 2010), the Dharwar craton (Peucat et al., 1993; Jayananda et al., 2000; Moyen et al., 2003) and Yilgarn craton (Cassidy et al., 1991, Champion and Sheraton, 1997; Champion and Smithies, 2001) where coeval TTG and sanukitoid rocks have been recognized. Its pertinence to the Pilbara (Smithies and Champion, 2007) and to the Superior province of Canada (Stern and Hanson, 1991; Stevenson et al., 1999) is less clear.

8. Conclusions

The geochemical variation observed in the Guarantã suite could not be explained by a simple magmatic differentiation process involving fractional crystallization or partial melting and point to a complex magmatic evolution for the entire suite. Moreover, the geochemical analogies presented by the Guarantã suite and, at the same time, the TTG and sanukitoid suites are puzzling, especially if the contrasts in petrological evolution between the latter suites are considered. On the other hand, the broad compositional overlap between the LGdG suites of the RMGGT and the transitional TTG and similar granites is remarkable and point to similar processes to explain their origin. However, the origin of these granites remains controversial and the different proposed models are apparently not suitable for the Guarantã suite.

Thus, we have developed an alternative model to explain the origin of the Guarantã suite magmas assuming as a premise that TTG and sanukitoid magmas should be involved in their origin in order to explain the ambiguous geochemical character of the Guarantã granites. On the basis of modelling and geochemical data, we suggest that the LGdG suites were derived from mixing between a granite magma, similar in composition to the Ba- and Sr-enriched samples of the Guarantã suite, and trondhjemitic liquids. The granite magmas participating in the mixture were originated by fractional cystallization of 35% of a sanukitoid magma of granodioritic composition. The dominant fractionated mineral phases were plagioclase and, hornblende, with subordinate, clinopyroxene, magnetite, ilmenite, and allanite. The large compositional variations observed in the Guarantã suite would resulted of the mixing in different proportions between the

granite and trondhjemitic liquids. This large spectrum of variation would be yet augmented if admitted that fractional crystallization played a significant role in evolution of the liquids originated by mixing processes.

Acknowledgements

M. A. Oliveira, A. T. R. Ferreira, A. L. Paiva Junior, and M. A. C. Costa are acknowledged for support in geological mapping, petrographical, and geochemical work. The authors express special thanks to David Champion for providing us with a geochemical database of the high-Ca granites from the Yilgarn craton. The Brazilian Geological Survey, CPRM, is acknowledged for permission to include in this paper data generated in the GEOBRASIL Project (mapping of Marajoara sheet). The authors express special thanks to O. T. Rämö, J. Halla, E. Heilimo, M. I. Kurhila, and A. Heinonen for support during field trip in Karelia craton and for numerous discussions on Archean geology. This research received financial support from CNPq (R. Dall'Agnol – Grants 0550739/2001-7, 476075/2003-3, 307469/2003-4, 484524/2007-0; PRONEX – Proc. 66.2103/1998-0, J. A. C. Almeida – doctor scholarship), FAPESPA (S. B. Dias, master scolarship), and Federal University of Pará (UFPA). This paper is a contribution to the Brazilian Institute of Amazonia Geosciences (INCT program – CNPq/MCT/FAPESPA – Proc. 573733/2008-2).

Appendix A. Analytical procedures

The 44 chemical analyses used in this work comprise both previously published data (2 analyses from Althoff, 1996; 6 analyses from Leite, 2001; 7 analyses from Dias, 2007; 5 analyses from Guimarães et al. b, submitted; 11 analyses from Dias, 2009;) and new chemical data (13 analyses from this work). All the new analyses made in this work and those obtained by Dias (2007, 2009), Guimarães et al. (b, submitted) were performed by ICP-ES for major elements and ICP-MS for trace-elements, including the rare-earth elements, at the Acme Analytical Laboratories Ltd. in Canada. The chemical analyses obtained by Althoff (1996) were done at the Centre de Recherches Petrographiques et Geochimiques (CRPG-CNRS, France); the major and

minor elements and Sc were analyzed using ICP-ES and all other trace elements, including the rare-earth elements were analyzed by ICP-MS. Chemical diagrams were mostly generated using the GCDkit software (Janousek et al., 2003).

References

Almeida, J.A.C., Dall'Agnol, R., Oliveira, M.A., Macambira, M.J.B., Pimentel, M.M., Rämö, O.T., Guimarães, F.V., Leite, A.A.S., submitted a. Zircon geochronology and geochemistry of the TTG suites of the Rio Maria granite-greenstone terrane: Implications for the growth of the Archean crust of Carajás Province, Brazil. Precambrian Res.

Almeida, J.A.C., Dall'Agnol, R., Leite, A.A.S. submitted b. Geochemistry and zircon geochronology of the Archean granite suites of the Rio Maria Granite-Greenstone terrane, Carajás Province, Brazil. J. South Amer. Earth Sci.

Althoff, F.J., Barbey, P., Boullier, A.M., 2000. 2.8–3.0 Ga plutonism and deformation in the SE Amazonian craton: the Archean granitoids of Marajoara (Carajás Mineral province, Brazil). Precambrian Res. 104, 187–206.

Barker, F., Arth, J.G., 1976. Generation of trondhjemite-tonalite liquids and Archean bimodal trondhjemite-basalt suites. Geology 4, 596–600.

Barker, F., 1979. Trondhjemite: a definition, environment and hypotheses of origin. In: Barker, F. (Ed.), Trondhjemites, Dacites and Related Rocks. Elsevier, Amsterdam, pp. l–12.

Barros, C.E.M., Barbey, P., Boullier, A.M., 2001. Role of magma pressure, tectonic stress and crystallization progress in the emplacement of the syntectonic A-type Estrela Granite Complex (Carajás Mineral Province, Brazil). Tectonophysics, 343, 93-109.

Berger, M., Rollinson, H.R., 1997. Isotopic and geochemical evidence for crust–mantle interaction during Late Archaean crustal growth. Geochim. Cosmochim. Acta 61, 4809–4829.

Bourne, J.H., L'Heureux, M., 1991. The petrography and geochemistry of the Clericy pluton: an ultrapotassic pyroxenitesyenite suite of Late Archaean age from the Abitibi region, Quebec. Precambrian Res. 52, 37–51.

Cassidy, K.F., Barley, M.E., Groves, D.I., Perring, C.S., Hallberg, J.A., 1991. An overview of the nature, distribution and inferred tectonic setting of granitoids of the late- Archaean Norseman-Wiluna Belt. Precambrian Res. 51, 51-83.

Castro A., 2004. The source of granites: inferences from the Lewisian complex. Scott J. Geol. 40:49–65

Champion, D.C., Sheraton, J.W., 1997. Geochemistry and Nd isotope systematics of Archaean granites of the Eastern Goldfields, Yilgarn Craton, Australia: implications for crustal growth processes. Precambrian Res. 83, 109–132.

Champion, D.C., Smithies, R.H., 2001. Archaean granites of the Yilgarn and Pilbara cratons, Western Australia. In: Cassidy, K.F., Dunphy, J.M., Van Kranendonk, M.J. (Eds.), Proceedings of the Fourth International Archaean Symposium. Perth, Australia, pp. 134–136 (AGSO-Geoscience Australia, Record 2001/37).

Champion, D.C., Smithies, R.H., 2003. Archaean granites. In: Blevin, P.L., Chappell, B.W., Jones, M. (Eds.), Magmas to Mineralisation: The Ishihara Symposium, pp. 19–24 (AGSO-Geoscience Australia, Record 2003/14).

Champion, D.C., Smithies, R.H., 2007. In: Van Kranendonk, M.J., Smithies, R.H., Bennett, V.C. (Eds.), Geochemistry of Paleoarchean Granites of the East Pilbara Terrane, Pilbara Craton, Western Australia: Implications for Early Archean Crustal Growth. Earth's Oldest Rocks, Developments in Precambrian Geology, vol. 15. Elsevier, Amsterdam, pp. 369–410.

Chappell, B.W., Stephens,W.E., 1988. Origin of infracrustal (I-type) granite magmas. Transactions of the Royal Society of Edinburgh: Earth Sciences 79, 71–86.

Chappell, B.W., White, A.J.R. & Wyborn, D., 1987. The importance of residual source material (restite) in granite petrogenesis. J. Petrology 28, 1111–38.

Chappell, B. W., 1996. Compositional variation within granite suites of the Lachlan Fold Belt: its causes and implications for the physical state of granite magma. Transactions of the Royal Society of Edinburgh: Earth Sciences 87, 159–70.

Chappell, B.W., 2004. Towards a unified model for granite genesis. Transactions of the Royal Society of Edinburgh. Earth Sciences 95, 1-10.

Class, C., Miller, D.M., Goldstein, S.L., Langmuir, C.H., 2000. Distinguishing melt and fluid subduction components in Umnak Volcanics, Aleutian Arc. Geochemistry Geophysics Geosystems 1, paper number 1999GC000010.

Cherniak D. J. and Watson E. B., 1992. A study of strontium diffusion in K-feldspar, Na–K feldspar and anorthite using Rutherford backscattering spectroscopy. Earth and Plan. Sci. Letters 113, 411–425.

Condie, K.C., 1993. Chemical composition and evolution of the upper continental crust: Contrasting results from surface samples and shales. Chem. Geol. 104, 1-37.

Dall'Agnol, R., Lafon, J.M., Fraga, L.M., Scandolara, J., Barros, C.E.M., 2000. The Precambrian Evolution of the Amazonian Craton: one of the last Unknown Precambrian Terranes in the World. In: International Geological Congress, 31. Rio de Janeiro. Abstracts. Rio de Janeiro: CPRM. K.4 (CD ROM).

Dall'Agnol, R., Teixeira, N.P., Rämö, O.T., Moura, C.A.V., Macambira, M.J.B., Oliveira, D.C., 2005. Petrogenesis of the Paleoproterozoic, rapakivi, A-type granties of the Archean Carajás Metallogenic Province, Brazil. Lithos 80, 01-129.

Dall'Agnol, R., Oliveira, M.A., Almeida, J.A.C., Althoff, F.J., Leite, A.A.S., Oliveira, D.C. & Barros, C.E.M., 2006. Archean and Paleoproterozoic granitoids of the Carajás metallogenetic province, eastern Amazonian craton. In: Dall'Agnol, R., Rosa-Costa, L.T., Klein, E.L. (eds.). Symposium on Magmatism, Crustal Evolution, and Metallogenesis of the Amazonian Craton. Abstracts Volume and Field Trips Guide. Belém, PRONEX-UFPA/SBGNO, 99-150.

Day, W.C., Weiblen, P.W., 1986. Origin of Late Archaean granite: geochemical evidence from the Vermilion granitic complex of Northern Minnesota. Contrib. Miner. Petrol. 93, 283–296.

Davis, W.J., Fryer, B.J., King, J.E., 1994. Geochemistry and evolution of Late Archaean plutonism and its significance to the tectonic development of the Slave Craton. Precambrian Res. 67, 207-241.

Dey, S., Ray, A.K., Chaki, A., 2009. Geochemistry of granitoids of Bilgi area, northern part of eastern Dharwar craton, southern India – Example of Transitional TTGs derived from depleted source. J. geol. soc. India, 73, 854-870.

Dias, S. B., 2009. Caracterização geológica, petrográfica e geoquímica de granitos Arqueanos da Folha Marajoara, terreno granito-greenstone de Rio Maria, sudeste do Pará. Federal University of Para. 129p. M.Sc. Thesis. Graduated Program on Geology and Geochemistry, Institute of Geosciences (in Portuguese).

Duarte, K.D., 1992. Geologia e geoquímica do granito Mata Surrão (SW de Rio Maria – PA): um exemplo de granito "stricto sensu" Arqueano. Federal University of Para. 217p. M.Sc. Thesis. Graduated Program on Geology and Geochemistry, Institute of Geosciences (in Portuguese).

Elliot, T.T., Plank, T., Zindler, A., White, W., Bourdon, B., 1997. Element transport from slab to volcanic front at the Mariana arc. J. Geophysical Res. 102, 14991–15019.

Evans, O.C., Hanson, G.H., 1997. Late- to post-Archaean granitoids of the S.W. Superior Province: derivation through direct mantle melting. In: De Witt, M.J., Ashwall, L.D. (Eds.), Greenstone Belts. Oxford Univ. Press, pp. 280– 295.

Frost, C.D., Frost, B.R., Chamberlain, K.R., Hulsebosch, T.P., 1998. The Late Archean history of the Wyoming province as recorded by granitic magmatism in the Wind River Range, Wyoming. Precambrian Res. 89, 145–173.

Frost, C.D., Frost, B.R., Kirkwood, R., Chamberlain, K.R., 2006. The tonalite-trondhjemite-granodiorite (TTG) to granodiorite-granite (GG) transition in the Late Archean plutonic rocks of the central Wyoming province. Can. J. Earth Sci. 43, 1419–1444.

Gardien, V, Thompson A. B, Grujic, D, Ulmer P., 1995. Experimental melting of biotite + plagioclase + quartz ± muscovite assemblages and implications for crustal melting. J Geophys Res-solid Earth 100, 15581–15591.

Gardien, V, Thompson, A. B, Ulmer, P., 2000. Melting of biotite + plagioclase + quartz gneisses: the role of H2O in the stability of amphibole. J. Petrology. 41, 651–666

Goodwin, A.M., 1991. Precambrian Geology: the dynamic evolution of the continental crust. Academic Press, London, 666 pp.

Guimarães, F.V.G., Dall'Agnol, R., Almeida, J.A.C., Oliveira, M.A., submitted a. Caracterização geológica, petrográfica e geoquímica do trondhjemito Mogno e tonalito Mariazinha, Terreno Granito-Greenstone de Rio Maria - Pará. Rev. Bras. Geociências

Guimarães, F.V.G., Dall'Agnol, R., Oliveira, M.A., Almeida, J.A.C., submitted b. Geologia, petrografia e geoquímica do quartzo-diorito Parazônia e granodiorito Grotão, Terreno Granito-Greenstone de Rio Maria – Pará. Rev. Bras. Geociências.

Halla, J., 2005. Late Archean high-Mg granitoids (sanukitoids) in the Southern Karelian craton, Eastern Finland. Lithos 79, 161–178.

Halla, J., van Hunen, J., Heilimo, E., Hölttä P., 2009. Geochemical and numerical constraints on Neoarchean plate tectonics. Precambrian Res. 179, 155–162.

Heilimo, E., Halla, J., Höltta, P., 2010. Discrimination and origin of the sanukitoid series: Geochemical constraints from the Neoarchean western Karelian Province (Finland). Lithos 115, 27-39.

Hildreth, W., Moorbath, S., 1988. Crustal contributions to arc magmatism in the Andes of Central Chile. Contr. Miner. Petrol. 98, 455–489.

Huhn, S.R.B., Santos, A.B.S., Amaral, A.F., Ledsham, E.J., Gouveia, J.L., Martins, L.B.P., Montalvão, R.M.G., Costa, V.G. 1988. O terreno granito-greenstone da região de Rio Maria - Sul do Pará. In: Congresso Brasileiro de Geologia, 35., Belém. Anais do congresso Brasileiro de Geologia. Belém, SBG. v. 3, p. 1438-1453.

Jayananda, M., Martin, H., Peucat, J.J., Mahabaleswar, B., 1995. Late Archaean crust–mantle interactions: geochemistry of LREE-enriched mantle derived magmas. example of the Closepet Batholith, Southern India. Contrib. Mineral. Petrol. 199, 314–329.

Jayananda, M., Moyen, J.-F., Martin, H., Peucat, J.-J., Auvray, B., Mahabaleswar, B., 2000. Late Archaean (2550–2520Ma) juvenile magmatism in the Eastern Dharwar craton, southern India: constraints from geochronology, Nd–Sr isotopes and whole rock geochemistry. Precambrian Res. 99, 225– 254.

Jayananda, M., Chardon, D., Peucat, J.-J., Capdevila, R., 2006. 2.61 Ga potassic granites and crustal reworking in the western Dharwar craton, southern India: tectonic, geochronologic and geochemical constraints. Precambrian Res. 150, 1–26.

Käpyaho, A. Mänttäri, I., Huhma, H., 2006. Growth of Archaean crust in the Kuhmo district, Eastern Finland: U−Pb and Sm−Nd isotope constraints on plutonic rocks. Precambrian Res. 146, 95–119.

Laflèche, M.R., Dupuy, C., Dostal, J., 1991. Archaean orogenic ultrapotassic magmatism: an example from the southern Abitibi greenstone belt. Precambrian Res. 52, 71–96.

Leite, A.A.S., 2001. Geoquímica, petrogênese e evolução estrutural dos granitóides arqueanos da região de Xinguara, SE do Cráton Amazônico. Federal University of Para. 330p. PhD Thesis. Graduated Program on Geology and Geochemistry, Institute of Geosciences (in Portuguese).

Leite, A.A.S., Dall'Agnol, R., Macambira, M.J.B., Althoff, F.J., 2004. Geologia e geocronologia dos granitóides arqueanos da região de Xinguara (PA) e suas implicações na evolução do terreno granito-greenstone de Rio Maria. Rev. Bras. Geociências 34, 447-458.

Liang Y., Richter F.M., Watson E.B., 1996. Diffusion in silicate melts: II. Multicomponent diffusion in $CaO–Al_2O_3–SiO_2$ at 1,500 C and 1 GPa. Geochim. Cosmochim. Acta 60, 5021–5035.

Lobach-Zhuchenko, S.B., Rollinson, H.R., Chekulaev, V.P., Arestova, N.A., Kovalenko, A.V., Ivanikov, V.V., Guseva, N.S., Sergeev, S.A., Matukov, D.I., Jarvis, K.E., 2005. The

Archaean sanukitoid series of the Baltic Shield: geological setting, geochemical characteristics and implication for their origin. Lithos 79, 107–128.

López, S., Castro, A. García-Casco, A., 2005. Production of granodiorite melt by interaction between hydrous mafic magma and tonalitic crust. Experimental constraints and implications for the generation of Archaean TTG complexes. Lithos, 79, 229–250.

Macambira, M.J.B., Lafon, J.M., 1995. Geocronologia da Província Mineral de Carajás; Síntese dos dados e novos desafios. Boletim do Museu Paraense Emílio Goeldi, série Ciências da Terra, Belém, 7, 263-287.

Macambira, M.J.B., Lancelot, J., 1996. Time constraints for the formation of the Archean Rio Maria crust, southeastern Amazonian Craton, Brazil. Intern. Geol. Review, 38 (12), 1134-1142.

Machado, N., Lindenmayer, Z.G., Krogh, T.E., Lindenmayer, D., 1991. U-Pb geochronology of Archean magmatism and basement reactivation in the Carajás area, Amazon shield, Brazil. Precambrian Res. 49: 329-354.

Martin, H., Smithies, R.H., Rapp, R., Moyen, J.-F., Champion, D., 2005. An overview of adakite, tonalite-trondhjemite-granodiorite (TTG) and sanukitoid: relationships and some implications for crustal evolution. Lithos 79, 1–24.

Moyen, J.-F., Martin, H., Jayananda, M., 2001. Multi-elements geochemical modelling during Late Archaean crustal growth: the Closepet Granite (South India). Precambrian Res. 112, 87–105.

Moyen, J.F., Martin, H., Jayananda, M., Auvray, B., 2003. Late Archaean granites: a typology based on the Dharwar Craton (India). Precambrian Res. 127, 103– 123.

Moyen, J.-F., Stevens, G., 2006. Experimental constraints on TTG petrogenesis: implications for Archean geodynamics. In: Benn, K., Mareschal, J.-C., Condie, K.C. (Eds.), Archean geodynamics and environments. monographs. AGU, pp. 149–178.

Moyen, J.-F., Stevens, G., Kisters, A.F.M., Belcher, R.W., 2007. TTG plutons of the Barberton granitoid-greenstone terrain, South Africa. In: Van Kranendonk, M.J., Smithies, R.H., Bennet, V. (Eds.), Earth's Oldest rocks. Developments in Precambrian geology. Elsevier, pp. 606–668.

Oliveira, M.A., Dall'Agnol, R., Althoff, F.J., Leite, A.A.S. 2009. Mesoarchean sanukitoid rocks of the Rio Maria Granite-Greenstone Terrane, Amazonian craton, Brazil. J. South Amer. Earth Sci. 27, 146-160.

Oliveira, M.A., Dall'Agnol, R., Almeida J.A.C. submitted. Petrology of the Mesoarchean Rio Maria Suite: Implications for the genesis of Sanukitoid Rocks. Lithos.

Opiyo-Akech, N., Tarney, J., Hoshino, M., 1999. Petrology and geochemistry of granites from the Archaean terrain north of Lake Victoria, western Kenya. J. African Earth Sci., 29 (2), 263-300.

Patiño Douce A.E., 2005. Vapor-absent melting of tonalite at 15–32 kbar. J Petrol 46, 275–290.

Pearce, J.A., Stern, R.J., Bloomer, S.H., Fryer, P., 2005. Geochemical mapping of the Mariana arc-basin system: Implications for the nature and distribution of subduction components. Geochemistry, Geophysics, Geosystems 6 (7).

Peucat, J.-J., Mahabaleswar, M., Jayananda, M., 1993. Age of younger tonalitic magmatism and granulite metamorphism in the amphibolite-granulite transition zone of southern India (Krishnagiri area): comparison with older Peninsular gneisses of Gorur-Hassan area. J. Metam. Geol. 11, 879–888.

Plank, T., 2005. Constraints from thorium/lanthanum on sediment recycling at subduction zones and the evolution of continents. J. Petrol. 46, 921–9

Prabhakar, B.C., Jayananda, M., Shareef, M., Kano, T., 2009. Petrology and geochemistry of Late Archean granitoids in the northern part of Eastern Dharwar, southern India: Implications for transitional geodynamic setting. J. Geol. Soc. India, 74, 299-317.

Rämö, O.T., Dall'Agnol, R., Macambira, M.J.B., Leite, A.A.S., Oliveira, D.C., 2002. 1.88 Ga oxidized A-type granites of the Rio Maria region, eastern Amazonian craton, Brazil: Positively anorogenic! J. Geology 110, 603-610.

Rapp, R.P., Watson, E.B., 1995. Dehydration melting of metabasalt at 8–32 kbar implications for continental growth and crust–mantle recycling. J. Petrol. 36, 891– 931.

Rutter M.J, Wyllie P.J. 1988. Melting of vapour-absent tonalite at 10 kbar to simulate dehydration-melting in the deep crust. Nature 331:159–160

Santos, J.O.S., 2003. Geotectônica dos Escudos das Guianas e Brasil-Central. In: L. A. Bizzi, C. Schobbenhaus, R. M. Vidotti e J. H. Gonçalves (eds.). Geologia, Tectônica e Recursos Minerais do Brasil. CPRM, Brasília, 169-195 (In portuguese).

Sen, C., Dunn, T., 1994. Experimental modal metasomatism of a spinel lherzolite and the production of amphibole-bearing peridotite. Contrib. Miner. Petrol. 119, 422–432.

Souza, Z.S., Luiz, J.G., Cruz, J.C.R., Paiva, R.N. 1992. Geometria de "greenstone belts" Arqueanos da região de Rio Maria (sudeste do Pará, Brasil), a partir de interpretação gravimétrica. Rev. Bras. Geociências, 22, 198-203.

Souza, Z.S., Potrel, H., Lafon, J.M., Althoff, F.J., Pimentel, M.M., Dall'Agnol, R., Oliveira, C.G., 2001. Nd, Pb and Sr isotopes of the Identidade Belt, an Archaean greenstone belt of the Rio Maria region (Carajas Province, Brazil): Implications for the Archaean geodynamic evolution of the Amazonian Craton. Precambrian Res. 109, 293–315.

Souza, Z. S., Dall'Agnol, R. 1996. Vulcanismo dacítico cálcio-alcalino Mesoarqueano no¨greenstone belt¨ Identidade, sudeste do Pará, Brasil. Geoch. Brasiliensis, 10, 225-240.

Souza, Z.S., Dall'Agnol, R., Oliveira, C.G.; Huhn, S.R.B. 1997. Geochemistry and petrogenesis of metavolcanic rocks from Archean greenstone belts: Rio Maria region (Southeast Pará, Brazil). Rev. Bras. Geociências, 27(2): 169-180.

Stern, R.A., Hanson, G.N., 1991. Archaean high-Mg granodiorites: a derivative of light rare earth enriched monzodiorite of mantle origin. J. Petrol. 32, 201–238.

Stevenson, R., Henry, P., Gariépy, C., 1999. Assimilationfractional crystallization origin of Archaean sanukitoid suites: Western Superior Province, Canada. Precambrian Res. 96, 83–99.

Skjerlie, K.P., Johnston, A.D., 1992. Vapor-absent melting at 10 kbar of a biotite-bearing and amphibole bearing tonalitic gneiss—Implications for the generation of A-type granites. Geology 20, 263–266.

Singh, J., JohannesW., 1996. Dehydration melting of tonalites. 2. Compositions of melts and solids. Contrib. Mineral. Petrol.125, 26–44.

Smithies, R.H., Champion, D.C., 2000. The Archaean high-Mg diorite suite: links to tonalite–trondhjemite–granodiorite magmatism and implications for early Archaean crustal growth. J. Petrol. 41 (12), 1653– 1671.

Sylvester, P.J. 1994. Archean granite plutons. In: Condie, K. C. (ed.) Developments in precambrian geology 11. Archean crustal evolution. Amsterdam, Elsevier. p. 261-314.

Tassinari, C.C.G., Macambira, M. 2004. A evolução tectônica do Craton Amazonico. In: Mantesso – Neto, V.; Bartorelli, A.; Carneiro, C.D.R.; Brito Neves, B.B. (Eds.), Geologia do

Continente Sul Americano: Evolução da obra de Fernando Flávio Marques Almeida. São Paulo, p. 471-486.

Van der Molen, I. & Paterson, M. S. 1979. Experimental deformation of partially melted granite. Contrib. Miner. Petrol. 70, 299–318.

Van Orman J. A., Grove T. L., and Shimizu N. 2002. Diffusive fractionation of trace elements during production and transport of melt in Earth's upper mantle. Earth Planet. Sci. Lett. 198, 93–112.

Vasquez L.V., Rosa-Costa L.R., Silva C.G., Ricci P.F., Barbosa J.O., Klein E.L., Lopes E.S., Macambira E.B., Chaves C.L., Carvalho J.M., Oliveira J.G., Anjos G.C., Silva H.R. 2008. Geologia e Recursos Minerais do Estado do Pará: Sistema de Informações Geográficas – SIG : texto explicativo dos mapas Geológico e Tectônico e de Recursos Minerais do Estado do Pará. Organizadores, Vasquez M.L., Rosa-Costa L.T. Escala 1:1.000.000. Belém: CPRM.

Watkins, J.M., Clemens, J.D., Treloar, P.J., 2007. Archaean TTGs as sources of younger granitic magmas: melting of sodic metatonalites at 0.6–1.2 GPa. Contrib. Mineral. Petrol., 154, 91–110

Wolf, M.B., Wyllie, P.J., 1994. Dehydration-melting of amphibolite at 10 kbar: the effects of temperature and time. Contrib. Mineral. Petrol. 115, 369– 383.

Winther, K.T., 1996. An experimentally based model for the origin of tonalitic and trondhjemitic melts. Chem. Geol. 127, 43–59.

Capítulo – 5

Conclusões e Considerações Finais

CONCLUSÕES E CONSIDERAÇÕES FINAIS

Os granitóides das suites tonalíticas-trondhjemíticas-granodioríticas (TTG) e as associações de leucogranitos calcico-alcalino arqueanos, apresentam vastas ocorrências no Terreno Granito-*Greenstone* de Rio Maria. O mapeamento geológico em área chaves e estudos petrográficos e geoquímicos, aliados ao refinamento dos dados geocronológicos utilizando os métodos de datação Pb-Pb por evaporação e U-Pb por LA-ICP-MS em zircão, permitiram inferir que o Terreno Granito-*Greenstone* de Rio Maria foi afetado pelo menos por três eventos magmáticos de composição TTG durante o Mesoarqueano. O primeiro evento apresenta idade de 2,96±0,2 Ga e é representado pelo Trondhjemito Mogno e pelas rochas mais antigas do Tonalito Arco Verde. O segundo evento de geração de granitóides TTG ocorreu em 2,93±0,1 Ga e engloba o Complexo Tonalítico Caracol, Tonalito Mariazinha e as rochas mais jovens do Tonalito Arco Verde. O último evento de magmatismo TTG registrado no TGGRM ocorreu em 2,86±0,1 Ga e é representado pelo Trondhjemito Água Fria, de distribuição areal muito restrita. Este trabalho revelou que a idade do Trondhjemito Mogno é significativamente maior do que anteriormente admitida, reduzindo a importância do magmatismo TTG de idade de 2,87 Ga no TGGRM, além disso, permitiu o reconhecimento de uma nova unidade de granitóides TTG nos domínios previamente estabelecidos para o Trondhjemito Mogno, esta unidade foi aqui denominada de Tonalito Mariazinha. Os dados geocronológicos para o Tonalito Arco Verde mostraram que esta unidade é constituída de granitóides com idades distintas, cujo suas individualizações não foram possíveis nas escalas utilizadas nos mapeamentos geológicos (1:100.000 ou 1:50.000) adotadas durante este trabalho.

Com base na assinatura geoquímica de elementos traço, em particular dos ETR, Sr, Y, Nb e Ta, as suítes TTG do TGGRM podem ser divididas em três grupos: 1) grupo com alta razão La/Yb (alta razões Sr/Y e Nb/Ta), representado dominantemente pelo Trondhjemito Mogno e Tonalito Mariazinha; 2) grupo com valor da razão La/Yb intermediário, o qual engloba o Complexo Tonalítico Caracol e o Trondhjemito Água Fria e 3) grupo com baixa razão La/Yb (baixa razões Sr/Y e Nb/Ta), dominado pelo Tonalito Arco Verde. O magma do grupo com alta razão La/Yb, foi provavelmente originado a partir da fusão de uma fonte de composição máfica, em condições de pressão relativamente elevada (≥1,5 GPa), sendo compatíveis com aquelas do campo de estabilidade da granada. O grupo com baixa razão La/Yb foi gerado a partir de um magma formado em baixas pressões (≤1,0 GPa), proveniente da fusão parcial de uma fonte

anfibolítica, tendo plagioclásio como fase residual. O grupo com razão La/Yb intermediária foi originado através da fusão de fonte máfica, porém em pressões superiores aquelas do grupo com baixa razão La/Yb e inferiores em relação ao grupo com alta razão La/Yb (~1,0-1,5 GPa), porém ainda no campo de estabilidade da granada, permitindo a presença deste mineral como fase residual. Não há nenhuma correspondência temporal entre os diferentes grupos e os três períodos de formação de magmas TTG em Rio Maria. Da mesma forma, não se observa relação direta entre estes grupos e as diferentes unidades, podendo algumas delas, como, por exemplo, o Tonalito Arco Verde, englobar granitóides com alta, intermediária e baixa razão La/Yb.

As idades dos leucogranitos arqueanos mostradas neste estudo juntamente com aquelas obtidas em trabalhos anteriores, demonstraram que o magmatismo granítico arqueano (2,87- 2,86 Ga) *stricto sensu* registrado no TGGRM, sucedeu o principal evento de geração de granitóides TTG (2,98- 2,92 Ga), sendo contemporâneo ou ligeiramente posterior à colocação da Suíte Sanukitoíde Rio Maria (~2,87 Ga). Com base em dados petrográficos e geoquímicos, três suítes de leucogranitos representante do magmatismo granítico arqueano, foram reconhecidas neste estudo: a) leucogranitos potássicos (granitos Xinguara e Mata Surrão); b) suítes compostas por leucogranodioritos e leucomonzogranitos (Suíte Guarantã, Granodiorito Grotão e granitos similares); e c) granitos associados a suíte sanukitoíde Rio Maria (Granito Rancho de Deus). Existe uma grande similaridade geoquímica entre as suítes de leucogranodioritos-leucomonzogranitos do TGGRM com os granitos alto-Ca (Champion & Sheraton, 1997) ou TTGs transicionais do Craton Yilgarn (Champion & Smithies 2001, 2003), bem como dos leucogranitos potássicos com os biotita granitos do Craton Dhawar (Moyen et al., 2003) ou granitos baixo-Ca (Champion & Sheraton, 1997).

Modelamento geoquímico indica que líquidos similares aos magmas leucogranitícos potássicos podem ser gerados a partir da fusão parcial de granitóides TTG ou de rochas granodioríticas relacionadas a suíte sanukitóide Rio Maria. No entanto, a similaridade em termos de idade, afasta a hipótese de derivação dos magmas dos leucogranitos potássicos a partir da fusão parcial das rochas da Suíte Rio Maria. As características geoquímicas do Granito Rancho de Deus, sugerem que seus magmas foram derivados a partir da cristalização fracionada e diferenciação de magmas sanukitoides enriquecidos em Ba e Sr (Granodiorito Mata Geral).

Vários modelos petrogenéticos propostos na literatura para explicar a origem das suítes de leucogranodioritos+monzogranitos foram apresentados e discutidos no capitulo 4. Considerando

que essas rochas registram tanto características geoquímicas próximas daquelas das rochas sanukitoides (enriquecimento em Ba e Sr) quanto dos granitóides TTG (alto conteúdo de Al_2O_3 e Na_2O, baixo de Yb e Y e assinatura dos ETR), um modelo alternativo envolvendo a interação entre magmas sanukitódes e trondhjemíticos [similar ao magma do Trondhjemito Água Fria (~2,86 Ga) e contemporaneo a suíte sanukitóide Rio Maria] foi sugerido neste trabalho para explicar a gênese das suítes de leucogranodioritos-leucomonzogranitos. O modelamento geoquímico apresentado no capitulo 4, revela que o fracionamento de plagioclásio (46,72%), hornblenda (39,05%), clinopiroxênio (10,36%), magnetita (3,12%), ilmenita (0,70%) e allanita (0,06%), a partir da cristalização de 35% de magmas sanukitóides de composição granodiorítica (típicos da Suíte Rio Maria) pode gerar líquidos graníticos enriquecidos em Ba e Sr comparáveis com aquele que deu origem a amostra do monzogranito Guarantã com mais alto conteúdo de Ba e Sr. Os cálculos também mostraram que a mistura em diferentes proporções desses magmas graníticos enriquecidos em Ba e Sr com magmas thondhjemíticos podem explicar a variação geoquímica observada nas amostras dos corpos da Suíte Guarantã (a unidade mais representativa suítes de leucogranodioritos-monzogranitos). Além disso, a cristalização fracionada dos líquidos oriundos da mistura pode contribuir para acentuar esta variação. Este modelo é favorecido pelo fato que na área de Marajoara, local onde aflora a Suíte Guarantã, as rochas da suíte sanukitóide são mais enriquecidas em SiO_2, Ba e Sr do que granitóides similares aflorantes em outras áreas do TGGRM (Almeida et al., 2008; Oliveira et al., 2009). Admiti-se que a gênese dos líquidos trondhjemiticos na área de Marajoara se deu contemporaneamente ao magmatismo sanukitóide (~2,87 Ga) e que tais líquidos foram largamente ou inteiramente consumidos pela mistura com os magmas graníticos evoluídos a partir de líquidos sanukitóides. Isto poderia explicar a ausência do registro de rochas trondhjemíticas com idade de 2,87 Ga na área de Marajoara.

Os dados geocronológicos e isotópicos evidenciam que a granitogênese que afetou o Terreno Granito-*Greenstone* de Rio Maria ocorreu em dois principais momentos durante o Mesoarqueano. O primeiro foi dominado pelo magmatismo TTG, havendo pelo menos dois picos de geração de granitóides TTG (2,96±0,2 e 2.93±0,1 Ga). Um modelo geodinâmico foi sugerido por este autor para explicar o contraste das assinaturas geoquímicas de elementos traços dos diferentes grupos de granitóides TTG (grupos com alta, intermediária e baixa razão La/Yb), o qual sugere que os magmas TTG foram originados em diferentes profundidades na crosta. Neste modelo, admite-se que houve a subducção de uma placa oceânica sob uma crosta oceânica

espessada tectônicamente (platô oceânico) antes de 2,98 Ga. Neste contexto, os magmas TTG com alta e intermediária razão La/Yb, poderiam ser originados a partir da fusão parcial de metabasaltos da crosta oceânica subductada, em condições de pressão relativamente mais elevada no campo de estabilidade da granada (≥1,5 GPa no caso das rochas do grupo com alta razão La/Yb e ~1,0-1,5 GPa para os granitóides do grupo com intermediária razão La/Yb). O contraste dos padrões dos ETR dos referidos grupos podem ser atribuído à variações sutis da condições de pressão ou ligeira diferenças composicionais na fonte se seus magmas. A fusão de metabasaltos localizados na base da crosta oceânica espessada, em pressões comparativamente mais baixa (≤1,0 GPa), poderiam gerar os magmas do grupo com baixa razão La/Yb. Os dados isotópicos Sm/Nd indicam que os granitóides TTG de Rio Maria derivaram de uma fonte (geoquimicamente similar aos metabasaltos do Supergrupo Andorinhas) extraída do manto durante o Mesoarqueano (3,0-2,90 Ga) e com pouco tempo de residência crustal.

Parte dos magmas TTG gerados a partir da fusão da placa oceânica subductada reagiu com a cunha do manto durante sua ascensão e foi totalmente consumida, levando ao metassomatismo do manto (Oliveira et al., 2009, Oliveira et al., submetido).

O segundo momento da granitogênese arqueana ocorreu por volta de 2,87 Ga, ou seja, 50 m.y após a formação da crosta tonalítica-trondhjemítica de Rio Maria e é caracterizada pela geração de uma diversidade de granitódes composicionalmente distintos. O ambiente geodinâmico proposto neste trabalho para este período admite que manifestações termais relacionadas a processo de *slab-break-off* ou ação de plumas mantélicas, induziram a fusão do manto metassomatizado e geração de magmas sanukitóides. A ascensão desses magmas aqueceu a crosta de Rio Maria e possivelmente induziu a fusão de metabasaltos localizados na base da crosta, originando o magma parental do Trondhjemito Água Fria. A fusão da crosta tonalitíca-trondhjemítica, em mais baixa profundidade, fora do campo de estabilidade da granada, pode ter gerado os líquidos dos leucogranitos potássicos. Neste contexto, como visto anteriormente, líquidos graníticos enriquecidos em Ba e Sr produto da diferenciação de magmas sanukitóides provavelmente interagiram através de diferentes graus de mistura com magmas trondhjemíticos e produziram os granitóides das suítes de leucogranodioritos-monzogranitos.

REFERÊNCIAS

ALMEIDA, J.A.C.; DALL'AGNOL, R.; OLIVEIRA, D.C. 2006. Geologia, Petrografia e Geoquímica do Granito Anorogênico Bannach, Terreno Granito-*Greenstone* de Rio Maria, Pará. *Revista Brasileira de Geociências*, **36**: 282-295.

ALMEIDA, J.A.C.; OLIVEIRA, M.A.; DALL'AGNOL, R.; ALTHOFF, F. J.; BORGES, R. M. K. 2008. *Geologia da Folha Marajoara (SB-22-ZC V) - Programa Geobrasil*. Belém, CPRM – Serviço Geológico do Brasil. 147p. (Relatório técnico).

ALTHOFF, F. J., 1996. Étude *pétrologique et structurale des granitoïdes de Marajoara (Pará, Brésil): leur rôle dans l'évolution archéenne du craton Amazonien (2.7– 3.2 Ga)*. Université Henri Poincaré, Nancy I, France. 296p. (Tese de Doutorado).

ALTHOFF, F. J., BARBEY, P., BOULLIER, A. M. 2000. *2.8–3.0 Ga plutonism and deformation in the SE Amazonian craton: the Archean granitoids of Marajoara (Carajás Mineral province, Brazil)*. Precambrian Research, **104**: 187–206.

ARAÚJO, O.J.B.; MACAMBIRA, E.M.B.; VALE, A.G.; OLIVEIRA, J.R.; SILVA NETO, C. S.; COSTA, E.J.S.; SANTOS, A.; PENA FILHO, J.I.C.; NEVES, A.P.; JORGE JOÃO, X.S.; COSTA, J.B.S. 1994. *Primeira integração das investigações geológicas do Programa Grande Carajás na região SSE do Estado do Pará*. In: SIMPÓSIO DE GEOLOGIA DA AMAZÔNIA, 4, Belém. Boletim de Resumos Expandidos... SBG p. 299-301.

AVELAR, V. G.; LAFON, J. M.; CORREIA JR., F. C.; MACAMBIRA, E. M. B. 1999. *O magmatismo arqueano da região de Tucumã – Provínica Mineral de Carajás: Novos dados geocronológicos*. Revista Brasileira de Geociências, **29**(4): 453-460.

AVELAR, V.G. 2002. *Geocronologia Pb-Pb em zircão e Sm-Nd em rocha total da porção centronorte do Estado do Amapá – Brasil: Implicações para a evolução geodinâmica do setor oriental do Escudo das Guianas*. Universidade Federal do Pará, Instituto de Geociências, Programa de Pós-Graduação em Geologia e Geoquímica. 213 p. (Tese de Doutorado).

BARKER, F.; ARTH, J.G. 1976. *Generation of trondhjemitic-tonalitic liquids and Archaean bimodal trondhjemite-basalt suites.* Geology, **4**: 596-600.

BARKER, F. 1979. *Trondhjemites: definition, environment and hypotheses of origin. In: BARKER, F. Ed. Trondhjemites, dacites and related rocks*. Amsterdam, Elsevier, p.1-12.

BARROS, C.E.M., MACAMBIRA, M.J.B., BARBEY, P., SCHELLER, T., 2004. *Dados isotópicos Pb-Pb em zircão (evaporação) e Sm-Nd do Complexo Granítico Estrela, Província Mineral de Carajás, Brasil: Implicações petrológicas e tectônicas.* Revista Brasileira de Geociências, **34**: 531-538.

BARTON, M.D. & HANSON, R.B. 1989. *Magmatism and the development of low-pressure metamorphic belts: implications from the western United States and thermal modelling*. Bulletin of the Geological Society of America, **101**: 1051-1065.

CASSIDY, K.F.; BARLEY, M.E.; GROVES, D.I.; PERRNG, C.S.; HALLBERG, J.A. 1991. *An overview of the nature, distribution and inferred tectonic setting of granitoids in the Late Archean Norseman-Wiluna Belt*. Precambrian Research, **51**: 51-83.

CHAMPION, D.C. & SHERATON, J.W. 1997. *Geochemistry and Nd isotope systematics of Archean granites of the Eastern Goldfields, Yilgarn Craton, Australia: implications for crustal growth processes*. Precambrian Research. **83**: 109–132.

CHAMPION, D.C. & SMITHIES, R.H. 1999. Archaean granites of the Yilgarn and Pilbara cratons, Western Australia: secular changes. In: BARBARIN, B. (Ed.), *The Origin of Granites and Related Rocks*—IVth Hutton Symposium Abstracts Doc. BRGM 290, pp. 137.

CHAMPION, D.C. & SMITHIES, R.H. 2001. Archean granites of the Yilgarn and Pilbara cratons, Western Australia. In: CASSIDY, K.F., DUNPHY, J.M., VAN KRANENDONK, M.J. (Eds.), *Proceedings of the Fourth International Archaean Symposium*. Perth, Australia, pp. 134–136 (AGSO-Geoscience Australia, Record 2001/37).

CHAMPION, D. C. & SMITHIES, R. H. 2003. Archaean granites. In: BLEVIN, P.L., CHAPPELL, B.W., JONES, M. (Eds.), *Magmas to Mineralisation: The Ishihara Symposium*, pp. 19–24 (AGSO-Geoscience Australia, Record 2003/14).

CHAMPION, D. C. & SMITHIES, R. H., 2007. Geochemistry of Paleoarchean Granites of the East Pilbara Terrane, Pilbara Craton, Western Australia: Implications for Early Archean Crustal Growth. In: Van Kranendonk, M.J., Smithies, R.H., Bennett, V.C. (Eds.). *Earth's Oldest Rocks.* Developments in Precambrian Geology, vol. 15. Amsterdam, Elsevier pp. 369–410.

CHOUKROUNE, P.; BOUHALLIER, H.; ARNDT, N. T. 1995. Soft lithosphere during periods of Archaean crustal growth or crustal reworking. In: COWARD, M.P.; RIES, A.C. (Eds), 1995. *Early precambrian Processes*. Geological Society of London, Special Publication, **95**:67-86.

CHOUKROUNE, P.; LUDDEN, J.N.; CHARDON, D.; CALVERT, A.J.; BOUHALLIER, H. 1997. Archean crustal growth and tectonics processes: a comparison of the Superior Province, Canada and the Dharwar Craton, India. In: BURG, J.P., FORD, M. (Eds.), *Orogeny Through Time*, vol. 121. Geological Society Special Publish, London, pp. 63-98.

CONDIE, K.C. & HUNTER, D.R. 1976. Trace elements geochemistry of Archean granitic rocks from Barberton region, South Africa. *Earth and Planetary Science Letters*, **29**: 389-400.

CONDIE, K. C. 1993. Chemical composition and evolution of the upper continental crust: Contrasting results from surface samples and shales. *Chemical Geology*, 1**04**: 1-37.

CONDIE, K. C. 2005. TTGs and adakites: are they both slab melts?. Lithos **80**: 33-44.

COSTA, C.M.A. 2009. *Petrografia e geoquímica de rochas tonalíticas-trondhjemíticas-granodioríticas da faixa central da Folha Marajoara, sudeste do Pará*. Universidade Federal do Pará. Instituto de Geociências. Curso de Graduação em Geologia. 69 p. (Trabalho de Conclusão de Curso)

CPRM (Serviço Geológico do Brasil). 2004. *Mapa Geológico do Brasil (41 mapas)*. Escala 1:1000.000. Programa Levantamentos Geológicos Básicos do Brasil. Brasília, CPRM-MME. (em CD-ROM).

DALL'AGNOL, R.; SOUZA, Z. S.; ALTHOFF, F. J.; MACAMBIRA, M. J. B.; LEITE, A. A. S. 1996. Geologia e geoquímica do terreno granito-"greenstone" de Rio Maria, Província Mineral de Carajás, sudeste do Cráton Amazônico. In: SYMPOSIUM ON ARCHEAN TERRANES OF THE SOUTH AMERICA PLATFORM, Brasília. Extend Abstracts... p. 29-30.

DALL'AGNOL, R.; SOUZA, Z. S.; ALTHOFF, F. J.; BARROS, C. E. M.; LEITE, A. A. S.; JORGE JOÃO, X. S. 1997. General aspects of the granitogenesis of the Carajás metallogenic province. In: INTERNATIONAL SYMPOSIUM ON GRANITES AND ASSOCIATED MINERALIZATIONS, 2. Excursions Guide... Salvador, p. 135-161.

DALL'AGNOL, R.; LAFON, J. M.; FRAGA, L. M.; SCANDOLARA, J.; BARROS, C. E. M. 2000. The Precambrian Evolution of the Amazonian Craton: one of the last Unknown Precambrian Terranes in the World. In: INTERNATIONAL GEOLOGICAL CONGRESS, 31. Rio de Janeiro. Abstracts. Rio de Janeiro: CPRM. (CD ROM). K.4

DALL'AGNOL, R.; OLIVEIRA, M.A.; ALMEIDA, J.A.C.; ALTHOFF, F.J.; LEITE, A.A.S.; OLIVEIRA, D.C.; BARROS, C.E.M. 2006. Archean and Paleoproterozoic granitoids of the Carajás metallogenic province, eastern Amazonian craton. In: DALL'AGNOL, R.; ROSA-COSTA, L.T.; KLEIN, E.L. (eds.). *Symposium on Magmatism, Crustal Evolution, and Metallogenesis of the Amazonian Craton.* Abstracts Volume and Field Trips Guide. Belém, PRONEX-UFPA/SBG-NO, 150p.

DAVIS, W. J.; FRYER, B. J.; KING, J. E. 1994. Geochemistry and evolution of late Archean plutonism and its significance to the tectonic development of the Slave Craton. *Precambrian Research*. **67**: 207-241.

DE WIT, M. J., 1998. On Archean granites, greenstones, craton and tectonics: does the evidence demand a verdict. *Precambrian Research*. **91**: 181–226.

DIAS, S. B. 2009. Caracterização geológica, petrográfica e geoquímica de granitos Arqueanos da Folha Marajoara, terreno granito-greenstone de Rio Maria, sudeste do Pará. Universidade Federal do Pará, Instituto de Geociências, Programa de Pós-Graduação em Geologia e Geoquímica. 129 p. (Dissertação de Mestrado).

DOCEGEO (Rio Doce Geologia e Mineração - Distrito Amazônia) 1988. Revisão litoestratigráfica da Província Mineral de Carajás, Pará. In: CONGRESSO BRASILEIRO DE GEOLOGIA, 35, Belém. Anexos..., vol. Província Mineral de Carajás - Litoestratigrafia e Principais Depósitos Minerais. p. 11-54.

DUARTE, K.D.; PEREIRA, E.D.; DALL'AGNOL, R.; LAFON, J.M. 1991. Geologia e geocronologia do Granito Mata Surrão - sudoeste de Rio Maria (Pa). In: SIMPÓSIO DE GEOLOGIA DA AMAZÔNIA, 3, Belém. Anais... SBG, p. 7-20.

DUARTE, K. D. 1992. Geologia e geoquímica do Granito Mata Surrão (SW de Rio Maria – Pa): um exemplo de granito "stricto sensu" Arqueano. Universidade Federal do Pará, Instituto de Geociências, Programa de Pós-Graduação em Geologia e Geoquímica. 217 p. (Dissertação de Mestrado).

FEIO, G. R. L. 2009. Magmatismo granitóide arqueano da região de Canaã dos Carajás: implicações para a evolução crustal da Província Carajás. Universidade Federal do Pará, Instituto de Geociências, Programa de Pós-Graduação em Geologia e Geoquímica. 97 p. (Exame de Qualificação).

FROST, C.D.; FROST, B.R.; CHAMBERLAIN, K.R.; HULSEBOSCH, T.P. 1998. The Late Archean history of the Wyoming province as recorded by granitic magmatism in the Wind River Range, Wyoming. *Precambrian Research*. **89**: 145–173.

FROST, C. D., FROST, B. R., KIRKWOOD, R., CHAMBERLAIN, K. R., 2006. The tonalite-trondhjemite-grandiorite (TTG) to granodiorite-granite (GG) transition in the Late Archean plutonic rocks of the central Wyoming province. Canadian Journal of Earth Sciences, **43**: 1419–1444.

GOODWIN, A. M., 1991. *Precambrian Geology: the dynamic evolution of the continental crust*. Academic Press, London, 666 pp.

GUIMARÃES, F. V. 2007. Mapeamento Geológico e Petrografia de granitóide Tonalítico-Trondhjemítico da Região a Leste de Bannach, Terreno Granito-Greenstone de Rio Maria - PA. Universidade Federal do Pará, Instituto de Geociências, Curso de Graduação em Geologia. 46 p. (Trabalho de Conclusão de Curso).

HARKER, A. 1965. *The natural history of igneous rocks*. New York. Macmillan, 384p.

HUHN, S.R.B.; SANTOS, A.B.S.; AMARAL, A.F.; LEDSHAM, E.J.; GOUVEIA, J.L.; MARTINS, L.B.P.; MONTALVÃO, R.M.G.; COSTA, V.G. 1988. O terreno granito-greenstone da região de Rio Maria-sul do Pará. In: CONGRESSO BRASILEIRO DE GEOLOGIA, 35, Belém. Anais... SBG. v.3, p. 1438-1453.

HUHN, S. B.; MACAMBIRA, M. J. B.; DALL'AGNOL, R. 1999. Geologia e geocronologia Pb/Pb do Granito Alcalino Planalto, Região da Serra do Rabo, Carajás-Pa. In: SIMPÓSIO DE GEOLOGIA DA AMAZÔNIA, 6, Manaus. Boletim de Resumos Expandidos... SBG. p. 463-466.

JAYANANDA, M., CHARDON, D., PEUCAT, J.-J., CAPDEVILA, R., 2006. 2.61 Ga potassic granites and crustal reworking in the western Dharwar craton, southern India: tectonic, geochronologic and geochemical constraints, Precambrian Research, **150**: 1–26.

KÄPYAHO, A. MÄNTTÄRI, I., HUHMA, H., 2006. Growth of Archaean crust in the Kuhmo district, Eastern Finland: U−Pb and Sm−Nd isotope constraints on plutonic rocks. Precambrian Research. **146**: 95–119.

KRÖNER, A. 1991. Tectonic evolution in the Archean and Proterozoic. *Tectonophysics*, **87**:393-410.

KRÖNER, A.; LAYER, P.W. 1992. Crust formation and plate motion in the early Archean. *Science,* **256**: 1405-1410.

VAN KRANENDONK, M. J.; SMITHIES, R. H.; HICKMAN, A. H.; CHAMPION, D. C. 2007. Paleoarchean development of a continental nucleus: the east Pilbara terrane of the Pilbara craton, western Australia. In: VAN KRANENDONK, M.J., SMITHIES, R.H., BENNET, V. (Eds.), *Earth's Oldest rocks*. Developments in Precambrian geology. Elsevier, pp. 307–337.

LAFON, J.M.; RODRIGUES, E.; DUARTE, K.D. 1994. Le granite Mata Surrão: un magmatisme monzogranitique contemporain des associations tonalitiques-trondhjemitiques-granodioritiques archéennes de la région de Rio Maria (Amazonie Orientale, Brésil). p. 642-649.

LAMARÃO, C.N.; DALL'AGNOL, R.; PIMENTEL, M.M., 2005. Nd isotopic composition of Paleoproterozoic volcanic and granitoid rocks of Vila Riozinho: implications for the crustal evolution of the Tapajós gold province, Amazonian craton. *Journal of South American Earth Sciences.***18**: 277-292.

LE MAITRE, R. W. 2002. *A classification of igneous rocks and glossary of terms*. 2nd Edition , London, 193 p.

LEITE, A. A. S. 1995. *Geologia e geoquímica do Batólito Granítico Arqueano Xinguara, sudeste do Estado do Pará.* Universidade Federal do Pará, Instituto de Geociências, Programa de Pós-Graduação em Geologia e Geoquímica. 209 p. (Dissertação de Mestrado).

LEITE, A. A. S. & DALL'AGNOL, R., 1999. Geoquímica e aspectos petrogenéticos do Granito Xinguara, Terreno Granito-*Greenstone* de Rio Maria-Cráton Amazônico. *Revista Brasileira de Geociências*. **23**: 429-436.

LEITE, A. A. S. & DALL'AGNOL, R. 1997. Geologia e petrografia do maciço granítico Arqueano Xinguara e de suas encaixantes - SE do Pará. *Boletim do Museu Paraense Emílio Goeldi* - Série Ciência da Terra. **9**: 43-81.

LEITE, A.A.S. 2001. *Geoquímica, petrogênese e evolução estrutural dos granitóides arqueanos da região de Xinguara, SE do Cráton Amazônico*. Universidade Federal do Pará, Instituto de Geociências, Programa de Pós-Graduação em Geologia e Geoquímica, 490p. (Tese de Doutorado).

LEITE, A.A.S., DALL'AGNOL, R., MACAMBIRA, M.J.B., ALTHOFF, F.J., 2004. Geologia e Geocronologia dos granitóides arqueanos da região de Xinguara–PA e suas implicações na evolução do Terreno Granito-Greenstone de Rio Maria, Cráton Amazônico. *Revista Brasileira de Geociências* **34** (4), 447-458.

LOBACH-ZHUCHENKO, S.B.; ROLLINSON, H.; CHEKULAEV, V.P.; ARESTOVA, N.A.; KOVALENKO, A.V.; IVANIKOV, V.V.; GUSEVA, N.S., SERGEEV, S.A.; MATUKOV, D.I.; JARVIS, K.E. 2005. The archaean sanukitoid series of the baltic shield—geological setting, geochemical characteristics and implications for their origin. *Lithos* **79**: 107– 128.

LOBATO, L. M., ROSIÈRE, C. A., SILVA, R. C. F., ZUCCHETTI, M., BAARS, F. J., SEDANE, J. C. S., JAVIER RIOS, F., PIMENTEL, M., MENDES, G. E., MONTEIRO, A. M., 2006. A mineralização hidrotermal de ferro da Província Mineral de Carajás – controle estrutural e contexto na evolução metalogenética da província. 72p. *Caracterização de Depósitos Minerais em Distritos Mineiros da Amazônia*. Capítulo II, DNPM, CT-Mineral / FINEP, ADIMB. (CD-ROM.).

LOWE, D. R & BYERLY, G. R., 2007. An overview of the geology of the Barberton greenstone belt and vicinity: implications for early crustal development. In: VAN KRANENDONK, M.J., SMITHIES, R.H., BENNET, V. (Eds.), *Earth's Oldest rocks*. Developments in Precambrian geology. Elsevier, pp. 481–526.

MACAMBIRA, M. J. B. 1992. Chronologie *U/Pb, Rb/Sr, K/Ar et croissance de la croûte continentale dans L'Amazonie du sud-est; exemple de la région de Rio Maria, Province de Carajas, Brésil*. Université Montpellier II - France. 212 p. (Tese de Doutorado).

MACAMBIRA, M. J. B. & LAFON, J. M. 1995. Geocronologia da Província Mineral de Carajás; síntese dos dados e novos desafios. *Boletim do Museu Paraense Emílio Goeldi, série Ciências da Terra*, **7**: 263-288.

MACAMBIRA, M. J. B.; LANCELOT, J. R. 1996. Time constraints for the formation of the Archean Rio Maria crust, southeastern Amazonian Craton, Brazil. *International Geology Review,* 38: 1134-1142.

MACAMBIRA, M.J.B.; COSTA, J.B.S.; ALTHOFF, F.J.; LAFON, J.-M.; MELO, J. C. V.; SANTOS, A. 2000. New geochronological data for the Rio Maria TTG terrane; implications for the time constraints of the Caraja´s Province, Brazil. In: 31st INTERNATIONAL GEOLOGICAL CONGRESS, Rio de Janeiro, CD-ROM.

MACHADO, N.; LINDENMAYER, Z.; KROGH, T. E.; LINDENMAYER, D. 1991. U/Pb geochronology of Archean magmatism and basement reactivation in the Carajás Área, Amazon Shield, Brazil. *Precambrian Research,* **49**: 329-354.

MARTIN, H. 1986. Effect of steeper Archean geothermal gradient on geochemistry of subduction – zone magma. *Geology,* **14**:753-756.

MARTIN, H. 1993. The mechanisms of petrogenesis of the Archaean continental crust - comparison with modern processes. *Lithos,* 30: 373-388.

MARTIN, H. 1994. The Archean grey gneisses and the gneisses of continental crust. In: CONDIE, K. C. (ed.) *Archean crustal evolution*. Developments in precambrian geology 11. Amsterdam, Elsevier. p. 205-259.

MARTIN, H. & MOYEN, J.-F., 2002. Secular changes in TTG composition as markers of the progressive cooling of the Earth. *Geology* **30** (4), 319– 322

MARTIN, H., SMITHIES, R.H., RAPP, R., MOYEN, J.-F., CHAMPION, D., 2005. An overview of adakite, tonalite-trondhjemite-granodiorite (TTG) and sanukitoid: relationships and some implications for crustal evolution. *Lithos* **79**: 1–24.

MEDEIROS, H. 1987. *Petrologia da porção leste do Maciço Granodiorítico Rio Maria, sudoeste do Pará*. Universidade Federal do Pará, Instituto de Geociências, Programa de Pós-Graduação em Geologia e Geoquímica. 187 p. (Dissertação de Mestrado).

MEDEIROS, H. & DALL'AGNOL, R. 1988. Petrologia da porção leste do Batólito Granodiorítico Rio Maria, sudeste do Pará. In: CONGRESSO BRASILEIRO DE GEOLOGIA, 35, Belém. Anais... SBG. v 3, p.1488-1499.

MEIRELLES, M.R. & DARDENNE, M.A. 1991. Vulcanismo basáltico de afinidade shoshonítica em ambiente de arco Arqueano, Grupo Grão-Pará, Serra dos Carajás, Estado do Pará. In: CONGRESSO BRASILEIRO DE GEOLOGIA, 33, Rio de Janeiro. Anais... SBG, v. 5: 2164-2174.

MOYEN, J.F.; MARTIN, H.; JAYANANDA, M.; AUVRAY, B. 2003. Late Archaean granites: a typology based on the Dharwar Craton (India). *Precambrian Research*, **127**: 103– 123.

MOYEN, J.-F.; STEVENS, G.; KISTERS, A.F.M.; BELCHER, R.W. 2007. TTG plutons of the Barberton granitoid-greenstone terrain, South Africa. In: VAN KRANENDONK, M.J., SMITHIES, R.H., BENNET, V. (Eds.), *Earth's Oldest rocks*. Developments in Precambrian geology. Elsevier, pp. 606–668.

OLIVEIRA, M. A., 2005. *Geologia, Petrografia e Geoquímica do Granodiorito Sanukitóide Arqueano Rio Maria e Rochas Máficas Associadas, Leste de Bannach-PA*. Universidade Federal do Pará, Instituto de Geociências, Programa de Pós-Graduação em Geologia e Geoquímica. 151 p. (Dissertação de Mestrado).

OLIVEIRA, M. A., DALL'AGNOL, R., ALTHOFF, F. J., 2006. Petrografia e Geoquímica do Granodiorito Rio Maria da região de Bannach e comparações com as demais ocorrências no terreno Granito-Greenstone de Rio Maria-Pará. *Revista Brasileira de Geociências,* **36** (2), 313-326.

OLIVEIRA, M.A., DALL'AGNOL, R., ALTHOFF, F.J., LEITE, A.A.S. 2009. Mesoarchean sanukitoid rocks of the Rio Maria Granite-Greenstone Terrane, Amazonian craton, Brazil. Journal of South American Earth Sciences, **27**:146-160.

PIMENTEL, M.M. & MACHADO, N. 1994. Geocronologia U-Pb dos terrenos granito-*greenstone* de Rio Maria, Pará. In: CONGR. BRAS. GEOL., 38., São Paulo, 1994, Boletim de Resumos Expandidos, Camboriú, SBG, 1: 390-391.

RAGLAND, P. C., 1989. *Basic analytical Petrology*. 2. New York,Oxford University Press.

RIDLEY, J. R. 1992. The termal causes and effects of voluminous, late Archaen: terrains, processes and metallogeny. *Geology Dept. & University Extension*, The University of Western Australia Publications, **22**: 275-285.

ROLANDO, A. P. & MACAMBIRA, M. J. B., 2002. Geocronologia dos granitóides arqueanos da região da Serra do Inajá, novas evidências sobre a formação da crosta continental no sudeste do Cráton Amazônico, SSE Pará. In: CONGRESSO BRASILEIRO DE GEOLOGIA, 41. *Anais do Congresso Brasileiro de Geologia*. João Pessoa, 2002. SBG. p. 525.

ROLANDO, A. P. & MACAMBIRA, M. J. B. 2003. Archean crust formation in Inajá range area, SSE of Amazonian Craton, Brazil, basead on zircon ages and Nd isotopes. In: South American Symposium on Isotope Geology, 4, Salvador. *Expanded Abstracts*. Salvador: CD-ROM.

ROLLINSON, H., 1993. *Using geochemical data: evaluation, presentation, interpretation*. 344p.

ROSA-COSTA, L.T; RICCI, P.S.F.; LAFON, J.M.; VASQUEZ, M.L.; CARVALHO, J.M.A.;KLEIN, E.L.; MACAMBIRA, E.M.B. 2003. Geology and geochronology of archean andpaleoproterozoic domains of the southeastern Amapá and northwestern Pará, Brazil – southeastern Guyana Shield. *Géologie de la France*, **2-3-4**:101-120.

ROSA-COSTA, L. T., 2006. *Geocronologia $^{207}Pb/^{206}Pb$, Sm-Nd, U-Th-Pb e ^{40}Ar-^{39}Ar do segmento sudeste do Escudo das Guianas: Evolução crustal e termocronologia do evento Transamazônico.* Universidade Federal do Pará, Instituto de Geociências, Programa de Pós-Graduação em Geologia e Geoquímica. 226 p. (Tese de Doutorado).

ROSA COSTA, L.T; LAFON, J.M. DELOR, C. 2006. Zircon geochronology and Sm–Nd isotopic study: Further constraints for the Archean and Paleoproterozoic geodynamical evolution of the southeastern Guiana Shield, north of Amazonian Craton, Brazil, *Gondwana Research*, **10**: 277–300.

SANTOS, A & PENA FILHO, J.IC. 2000. Programa de levantamentos geológicos básicos do Brasil, Região de Xinguara, folha Xinguara (SB-22-Z-C), Estado do Pará. Texto explicativo, Brasília, DNPM/CPRM. 120p.

SARDINHA, A.S.; BARROS, C.E.M.; KRYMSKY, R. 2006. Geology, geochemistry, and U–Pb geochronology of the Archean (2.74 Ga) Serra do Rabo granite stocks, Carajás Metallogenetic Province, northern Brazil. Journal South American Earth Sciences, **20**: 327–339.

SILVA, M.G.; TEIXEIRA, J.B.G; PIMENTEL, M.M.; VASCONCELOS, P.M.; ARIELO, A.; ROCHA, W.J.S.F. 2006. Geologia e mineralização de Fe-Cu-Au do alvo GT46 (Igarapé Cinzento), Carajás. 60p. *Caracterização de Depósitos Minerais em Distritos Mineiros da Amazônia*. Capítulo III. DNPM, CT-Mineral / FINEP, ADIMB (CD-ROM).

SMITHIES, R.H., 2000. The Archean tonalite–tondhjemite–granodiorite (TTG) series is not an analogue of Cenozoic adakite. *Earth and Planetary Science Letters* **182**: 115– 125.

SMITHIES, R. H. & CHAMPION, D. C., 2000. The Archean high-Mg diorite suite: links to tonalite–trondhjemite–granodiorite magmatism and implications for early Archaean crustal growth. Journal of Petrology. **41** (12):1653– 1671.

SMITHIES, R.H.; CHAMPION, D.C.; CASSIDY, K. F., 2003. Formation of Earth's early Archean continental crust. *Precambrian Research*, **127** (1–3): 89– 101.

SOUZA, Z. S.; MEDEIROS, H.; ALTHOFF, F. J.; DALL'AGNOL, R. 1990. Geologia do terreno granito-greenstone Arqueano da região de Rio Maria, sudeste do Pará. In: SBG, CONGRESSO BRASILEIRO DE GEOLOGIA, 36, Natal. Anais... V.6: 2913-2928.

SOUZA, Z. S., 1994. *Geologia e petrogênese do Greenstone Belt Identidade: implicações sobre a evolução geodinâmica do Terreno Granito- "Greenstone" de Rio Maria, SE do Pará.* Universidade Federal do Pará, Instituto de Geociências, Programa de Pós-Graduação em Geologia e Geoquímica. 2. v. (Tese de Doutorado).

SOUZA, S. Z., DALL'AGNOL, R., ALTHOFF, F. J., LEITE, A. A. S.; BARROS, C. E. M. 1996. Carajás mineral province: geological, geochronological and tectonic constrasts on the Archean evolution of the Rio Maria Granite-Greenstone Terrain and the Carajás block. In: SYMPOSIUM ON ARCHEAN TERRANES OF SOUTH AMERICA PLATFORM, Brasília, 1996, Extended abstracts... SBG. p. 31-32.

SOUZA, Z.S.; POTREL, H.; LAFON, J.M.; ALTHOFF, F.J.; PIMENTEL, M.M.; DALL'AGNOL, R.; OLIVEIRA, C.G. 2001. Nd, Pb and Sr isotopes of the Identidade Belt, an Archaean greenstone belt of the Rio Maria region (Carajas Province, Brazil): Implications for the Archaean geodynamic evolution of the Amazonian Craton. Precambrian Research,**109**: 293–315.

STERN, R.A.; HANSON, G; SHIREY, S.B. 1989. Petrogenesis of mantle-derived, LILE-enriched Archean monzodiorites and trachyandesites (sanukitoids) in southwestern Superior Province. *Canadian Journal Earth Scinces*, **26**: 1688-1712.

STERN, A. L. & HANSON, G. 1991. Archean high-Mg granodiorite: a derivate of light rare earth element-enriched monzodiorite of mantle origin. *Journal of Petrology*, **32**: 201-238.

STEVENSON, R., HENRY, P., GARIÉPY, C., 1999. Assimilation-fractional crystallization origin of Archaean sanukitoid suites: Western Superior Province, Canadá. *Precambrian Research.* **96**: 83-99.

STRECKEISEN, A. 1976. To each plutonic rock its proper name. *Earth Science Reviews*, 12:1-33.

SYLVESTER, P. J. 1994. Archean granite plutons. In: CONDIE, K. C. (ed.). *Archean crustal evolution*. Developments in precambrian geology 11. Amsterdam, Elsevier. p. 261-314.

TASSINARI, C.C.G. & MACAMBIRA, M. 2004. A evolução tectônica do Cráton Amazônico. In: MANTESSO – NETO, V.; BARTORELLI, A.; CARNEIRO, C. D. R.; BRITO NEVES, B. B. (Eds.), *Geologia do Continente Sul Americano: Evolução da obra de Fernando Flávio Marques Almeida.* São Paulo, p. 471-486.

TEIXEIRA, J. B. G. & EGGLER, D. H. 1994. Petrology, geochemistry, and tectonic setting of Archean basaltic and dioritic rocks from the N4 iron deposit, Serra dos Carajás, Pará, Brazil. *Acta Geologica Leopoldensia,* **17**: 71-114.

TEIXEIRA, N.P.; BETTENCOURT, J.S.; MOURA, C.A.V.; DALL'AGNOL, R.; MACAMBIRA, E.M.B. 2002. Archean crustal sources for Paleoproterozoic tin-mineralized granites in the Carajás Province, SSE Pará, Brazil: Pb–Pb geochronology and Nd isotope geochemistry. *Precambrian Research* **119**: 257–275.

VASQUEZ, M. L. 2006. *Geocronologia em zircão, monazita e granada e isotópos de nd das associações litológicas da porção oeste do Domínio Bacajá: Evolução crustal da porção meridional da Província Maroni-Itacaiúnas – sudeste do Cráton Amazônico*. Universidade Federal do Pará, Instituto de Geociências, Programa de Pós-Graduação em Geologia e Geoquímica. 212p. (Tese de Doutorado).

VASQUEZ L. V.; ROSA-COSTA L. R.; SILVA C. G.; RICCI P. F.; BARBOSA J.O.; KLEIN E. L.; LOPES E.S.; MACAMBIRA E.B.; CHAVES C.L.; CARVALHO J.M.; OLIVEIRA J.G.; ANJOS G.C.; SILVA H. R. 2008. Geologia e Recursos Minerais do Estado do Pará: Sistema de Informações Geográficas – SIG: texto explicativo dos mapas Geológico e Tectônico e de Recursos Minerais do Estado do Pará. Organizadores, Vasquez M. L., Rosa-Costa L. T. Escala 1:1.000.000. Belém: CPRM.

WINDLEY, B.F., 1995. *The Evolving Continents*. Third ed. JOHN WILEY & SONS, CHICHESTER, 526 p.